Mechanism of Resistance to Oestrogen Deprivation in Breast Cancer

Cindy M. Staka MSc.

A thesis presented for the degree of Doctor of Philosophy
at
Cardiff University

April 2006

Tenovus Centre for Cancer Research
Welsh School of Pharmacy
Redwood Building
King Edward VII Avenue
Cardiff
CF10 3XF

ProQuest LLC
789 East Eisenhower Parkway
P.O. Box 1346
Ann Arbor, MI 48106-1346

DECLARATION

This work has not previously been accepted in substance for any degree and is not being concurrently submitted in candidature for any degree.

Signed _____ (candidate)

Date 11.14.06

STATEMENT 1

This thesis is the result of my own investigations, except where otherwise stated. Other sources are acknowledged by footnotes giving explicit references. A bibliography is appended.

Signed _____ (candidate)

Date 11.14.06

STATEMENT 2

I hereby give consent for my thesis, if accepted, to be available for photocopying and for inter-library loan, and for the title and summary to be made available to outside organisations.

Signed _____ (candidate)

Date 11.14.06

~Table of Contents~

~Dedication~

I would like to dedicate this thesis to three very courageous women....

Mrs. Sally Leach
~ Since the day I got the news of your diagnosis, you have been on my mind. As a scientist, I have always believed that knowing and hearing the people that are living with this disease keeps everything in perspective and very real. You have known me my entire life, and you know me well enough to see why this dedication includes you. I am sorry that the road you are on is rough, however I also know that your faith will give you the strength to get through it. I pray that you and every other woman that has to experience this disease as tough as it gets, can find a peaceful moment each day to just be. With all of your memories of my mother you keep a wonderful part of me still alive. Thank you. ~

Mrs. Beverley McClelland
~ I am aware that you might find this dedication a bit strange, although I hope that you accept it as a token of appreciation. I have included you for two reasons. First, I do not pretend to know what you have gone through, I am sure that it has not been easy. I admire your courage and your ability to continue life as a mother and wife. I have seen the disease take everything from families leaving feelings of helplessness, confusion and isolation. Second, Richard, has been one of the most valuable assets to the success of my PhD. His knowledge of the subject and his ability to share that knowledge has always been appreciated by myself as well as by fellow colleagues. There is a unique something that Richard has and it is beyond him being a good scientist or him simply having an interest in research, that something is you. Extensive research is continued in breast cancer because each life is worth it, more important your life is worth it, and that is what gives research meaning, that keeps it real. ~

Mrs. Louise Staka
~ While you struggled to find answers why or muster the faith that breast cancer would not defeat you, I sat relatively helpless. We can always do better in retrospect, however I have to believe that I did the best I could for you during that time. I knew nothing about the disease other than it was slowly taking my mother, my best friend. I like to think that together through the process we learned about living. I am not sure I will ever fully understand the wealth of knowledge you gained or the emotion you felt during the experience. Through it all, I discovered life is a journey full of wonderful people and circumstance, unfortunately time is the uncontrollable element that influences the overall impact. I have found the ability to listen and actually hear what is being said, to give without haste or expectation, and most important I have chosen to enjoy the process. I will continue to discover and absorb as I progress through my journey, with you on my mind and forever in my heart. With this project I was given the opportunity to learn a sliver of

breast cancer biology and to work under the guidance of people I admire and respect. It is my passion that will continue to drive me and my hope that this is the first of many contributions I make towards the understanding and treatment of breast cancer. It was your journey that fueled my desire to actively make a difference, and it is people like you who have made the sacrifices, which have contributed to the research of the disease. ~

~ When the hour is upon us, and our beauty surely gone, no you will not be forgotten, and you will not be alone, no you will not be alone. ~ *Rob Thomas*

~Acknowledgments~

I would like to express my sincere thanks to…

Prof. Robert Nicholson and Dr. Julia Gee

~ Being apart of your research group, under your supervision, was an honour and a true pleasure. Thank you for sharing your knowledge and your valuable guidance. Also thank you for your belief in my practical ability throughout this project. I look forward to a future of continued success and friendship. ~

Robert Staka, Walli Staka, Susan Staka, and Marcie Murphy

~ From the beginning to the very end you gave me support, encouragement, and your love. Your belief in me is what gives me the freedom to enjoy my passion. Here and far beyond this journey, you are forever with me. ~

Chris French

~ Undeniably your friendship, support and love were a huge part of this process. You listened without judgment or bias therefore able to give a fresh perception that was often needed. Ultimately you gave this experience much more meaning. ~

Dr. Frances Boyns and Mr. Grant Edwards

~ There are simply no words that can explain how I feel about your kindness. Frankie you are clearly an asset to research science, however it is your sheer determination that I admire and your friendship that I am so humbled to have. The two of you made an unforgettable contribution to my chapter on 'Wales', and for that I thank you from the best part of my heart. ~

Miss Victoria Shaw, Mr. Alastair Wilson, Mr. David Britton, and Mr. Ian Lewis

~ From the laughs to the tears, the four of you were there. A wise person once said to me if taking on a PhD was an easy feat, then everyone would be doing it. As each of you know it is not easy, however with people like you involved in the process, the tough days were tolerable and relatively few. Best wishes and always remember to enjoy the process. ~

Mr. Richard McClelland, Mrs. Pauline Finlay, Mrs. Lynne Farrow, Dr. Maureen Harper, Dr. Kathy Taylor, Dr. Steve Hiscox, Dr Helen Jones, Dr. Martin Giles, Dr. Ian Hutcheson, Mrs. Carol Dutkowski, Ms. Denise Barrow

~ You have each contributed to my learning and appreciation of research science. I am grateful for the knowledge you have shared, and truly admire the contributions you have made toward the understanding of breast cancer. ~

Miss Sue Kyme, Miss Michelle James, Mrs. Sara Davies, Mr. Chris Smith, Mrs. Xiaoling Hu, Miss Lucy Green, Mr. Huw Mottram, Mr. Dean Routledge

~ I know that students come and go, I am sorry that I am yet another one. Each one of you, I am truly grateful for. From your practical knowledge to your hands on help, you were appreciated every step of the way. Most important to me was your genuine friendship and support, thank you. ~

~Publications~

Staka C.M., Gee J.M.W. & Nicholson R.I. (2003) Mechanisms of resistance to oestrogen deprivation in breast cancer. *European Journal of Biochemistry*, **270**:(s1), pg 122 Abstract 535.

Nicholson R.I., Staka C., Boyns F., Hutcheson I.R. & Gee J.M.W. (2004) Growth factor-driven mechanisms associated with resistance to estrogen deprivation in breast cancer: new opportunities for therapy. *Endocrine-Related Cancer*, **11**:623-641.

Staka C.M., Gee J.M.W. & Nicholson R.I. (2005) Potential of growth factor signaling kinases/ERα crosstalk to undermine the effects of estrogen deprivation in vitro. *Proc. Amer. Assoc. Cancer Res. 2005*, **46**:Abstract 3668.

Staka C.M., Nicholson R.I. & Gee J.M.W. (2005) Acquired resistance to oestrogen deprivation: role for growth factor signalling kinases/ER cross-talk revealed in new MCF-7X model. *Endocrine-Related Cancer*, **12**:S85-S97.

~Summary~

Oestrogen deprivation strategies, notably aromatase inhibitors, are of increasing value in hormone sensitive breast cancer. Unfortunately, however, oestrogen deprivation, like all other antihormones, is subject to acquisition of resistance. Further understanding of resistance is required to design approaches to effectively treat this state. This project aimed to delineate and target the underlying autocrine signalling mechanisms promoting this resistant phenotype, using a unique severely oestrogen and growth factor deprived *in vitro* breast cancer model, MCF-7X.

The MCF-7X model revealed breast cancer cells are readily able to survive oestrogen deprivation, but are not oestrogen hypersensitive and lack input from classical growth factor receptors under conditions of parallel exogenous growth factor deprivation, contrasting previous models derived in the presence of stripped serum. However, there was a retained importance of oestrogen receptor (ERα) signalling, supporting use of the pure anti-oestrogen faslodex, which reduces ERα level, AF-1 phosphorylation at serine 118 (via an unknown kinase) and ERα-regulated transcriptional activity in MCF-7X cells. Furthermore, intracellular kinase signalling, primarily PI3K/AKT, contributed in MCF-7X cells, again driving transcriptional and growth-promoting activity of ERα, in this instance via ERα serine 167 phosphorylation. Critically, individual/dual targeting with faslodex and/or PI3K inhibition, while initially partially inhibitory of ERα phosphorylation and growth, ultimately supported emergence of resistance. This was invariably associated with gain of the growth factor receptors EGFR/HER2 and IGF1R and kinase-promoted re-activation of ERα phosphorylation/function. However, triple treatment using faslodex, PI3K and MAPK blockade to completely eliminate ERα phosphorylation substantially improved anti-tumour response and prevented resistance. Clearly, intelligent design of combination treatments of faslodex with targeted therapies to totally deplete ERα activity is needed to maximally inhibit oestrogen deprivation resistance. In contrast, the project showed sequential use of such agents may translate into poorer prognosis, since faslodex resistant cells were more aggressive (potentially driven by HER2).

~Abbreviation List~

ABCSG	Austrian Breast and Colorectal Cancer Study Group
AF-1	Activation Function-1
AF-2	Activation Function-2
aFGF	Acidic Fibroblast Growth Factor
AH	Anti-hormonal
AI	Aromatase Inhibitor
AIB1	Amplified in Breast Cancer 1
AP-1	Activator Protein-1
APES	3-Aminopropyltriethoxysilane
ATAC	Arimidex, Tamoxifen Alone or in Combination
bFGF	Basic Fibroblast Growth Factor
BIG-FEMTA	Breast International Group- Femara Tamoxifen
Bis	Bis-indolylmaleimide
bp	Base Pairs
BRCA-1or -2	Breast Cancer -1 or -2
BSA	Bovine Serum Albumin
CA	Chloroform Acetone
cAMP	Cyclic AMP
CDK	Cyclin-Dependent Kinase
CMF	Cyclophosphamide, Methotrexate and 5'Fluorouracil
CoA	Co-Activator
CRE	cAMP Response Element
CREB	cAMP Response Element Binding Protein
CYP450	Cytochrome P450
DAB	3,3'-Diaminobenzidene Tetrahydrochloride
DBD	DNA-Binding Domain
DCIS	Ductal Carcinoma *In Situ*
DFS	Disease-Free Survival
DHEA	Dehydroepiandrosterone
DHEA-S	Dehydroepiandrosterone Sulphate
DMSO	Dimethyl Sulphoxide
DRIP	Vitamin D Receptor Interacting Protein
DTT	Dithiothreitol

E_1	Oestrone
E_2	Oestradiol
EBCTCG	Early Breast Cancer Trialists' Collaborative Group
EGF	Epidermal Growth Factor
EGFR	Epidermal Growth Factor Receptor
EORTC	European Organisation for the Research and Treatment of Cancer
ER	Oestrogen Receptor
ERE	Oestrogen Response Element
FAS	Faslodex (Fulvestrant)
FCS	Fetal Calf Serum
FGF	Fibroblast Growth Factor
FGFR	Fibroblast Growth Factor Receptor
FS	Formal Saline
FSH	Follicle-Stimulating Hormone
GAM	Goat Anti-Mouse
GPCR	G-Protein-Coupled Receptor
H_2O	Water
H&E	Haematoxylin and Eosin
HAT	Histone Acetyl-Transferase
HDAC	Histone Deactylase
HER2	neu/erbB-2 Receptor
HRP	Horse Radish Peroxidase
HRT	Hormone Replacement Therapy
IGF	Insulin-like Growth Factor
IGFR	Insulin-like Growth Factor Receptor
IGFBP	IGF-Binding Protein
IL	Interleukin
IMPACT	Immediate Preoperative Arimidex Compared with Tamoxifen
IR	Insulin Receptor
IRS-1 or -2	Insulin Receptor Substrate -1 or -2
kDa	Kilo Dalton
LBD	Ligand Binding Domain
LCIS	Lobular Carcinoma *In Situ*
LH	Luteinising Hormone
LHRH	Luteinising Hormone Releasing Hormone

LTED	Long-Term Oestrogen Deprived
LY	LY294002 (PI3 Kinase Inhibitor)
MA	Methanol Acetone
MAPK	Mitogen Activated Protein Kinase
M-MLV	Moloney Murine Leukemia Virus
mTOR	Mammalian Target of Rapamycin
MVA	Methanol Vanadate Acetone
NAT	North American Trial
NGS	Normal Goat Serum
NHS	Normal Human Serum
OSM	Oncostatin M
PAP	Peroxidase Anti-Peroxidase
PBS	Phosphate Buffered Saline
PBS-T	Phosphate Buffered Saline + Tween 20
PCR	Polymerase Chain Reaction
PD	PD98059 (MEK1 Inhibitor)
PDGF	Platelet-Derived Growth Factor
PDGFR	Platelet-Derived Growth Factor Receptor
PDK-1	Phosphoinositide-Dependent Protein Kinase-1
pFS	Phenol Formal Saline
PFV	Paraformaldehyde Vanadate
PGE_2	Prostaglandin E_2
PI3K	Phosphatidylinositol-3-OH Kinase
PKA	Protein Kinase A
PKC	Protein Kinase C
PR	Progesterone Receptor
PROACT	Pre-Operative Arimidex Compared to Tamoxifen
RSK	p90 Ribosomal S6 Kinase
SDS	Sodium Dodecyl Sulphate
SERD	Selective Oestrogen-Receptor Down-Regulator
SERM	Selective Oestrogen-Receptor Modulator
SFCS	Charcoal-Stripped Fetal Calf Serum
Shc	Src Homology 2- Domain Containing Adaptor Protein
SMCC	SRB and Mediator-Protein-Containing Complex
SOFEA	Study of Faslodex versus Exemestane with/without Arimidex

Sp-1	Specificity Protein-1
SRC	Steroid Receptor Coactivator
S6K1	p70 Ribosomal S6 Kinase 1
TARGET	Tamoxifen and Arimidex Randomised Group Efficacy and Tolerability
TBS	Tris-Buffered Saline
TBS-T	TBS + Tween 20
Tf	Transferrin
TFIIH	Transcription Factor IIH
TfR	Transferrin Receptor
TGFα	Transforming Growth Factor- alpha
TGFβ	Transforming Growth Factor- beta
TIF	Transcriptional Intermediary Factor-2
TNFα	Tumour Necrosis Factor- alpha
TNM	Tumour Size, Lymph Node Involvement, and Distant Metastases
TRAP	Thyroid-Hormone-Receptor-Associated Protein
TTP	Time To Progression
TTR	Time To Recurrence
VEGF	Vascular Endothelial Growth Factor
VEGFR	Vascular Endothelial Growth Factor Receptor
ZEBRA	Zoladex Early Breast Cancer Research Association

CHAPTER 1

∞ *INTRODUCTION* ∞

1.1 BREAST CANCER

1.1.1 Statistics and Risk Factors

Breast cancer is the most common form of cancer among women in almost all of Europe and North America, contributing to an estimate of 1 in 7 women developing the disease. The incidence of *in situ* breast cancer has increased almost 5-fold since the 1970's, this is somewhat attributed to the development and use of widespread mammography screening (Ernster and Barclay, 1997). The American Cancer Society (American Cancer Society, 2005-2006) estimates for 2005, there will be 212,930 new breast cancer cases in the US, of which 1,690 will be men and 211,240 will be women. Sadly, the estimate of deaths is set at 40,870 (460 men and 40,410 women), with various circumstances and factors having adverse bearing on outcome (e.g. lack of optimal health care, late detection). The prognosis of breast cancer is largely dependent upon the disease stage at diagnosis. A patient presenting with early breast cancer, where the tumour is confined to the breast (+/- axillary lymph nodes), can exhibit up to a 98% 5-year survival rate. Conversely, a patient presenting with advanced breast cancer, distant metastases and multiple lymph node involvement has an estimated 26% 5-year survival rate (American Cancer Society, 2005-2006). Therefore it is important that there is early detection, and further understanding of more aggressive phenotypes to ultimately extend patients' quality of life and survival.

Anyone can develop cancer, and breast cancer is no exception to the rule. Although bias is toward the postmenopausal woman, the disease does have the potential to affect a small number of premenopausal women and an even fewer number of men (the focus throughout this thesis is on female breast cancer). An individuals' risk of developing breast cancer is multi-factorial, which is why it is necessary for both basic researchers and clinicians to provide insight into this disease. Endocrine status and hormonal involvement, in particular oestrogens, play a predominant role in the development of breast cancer as discovered by Beatson (1896) over a century ago. There is a prevailing theory postulating that oestrogens enhance the rate of cell division yielding a mechanism of carcinogenesis which contributes to the promotion and progression of breast cancer (Preston-Martin *et al.*, 1993). Increased rate of cell proliferation means less time for DNA repair, therefore creating an environment that is more susceptible to gene damage (Jefcoate *et al.*, 2000). Clearly oestrogen-induced proliferation has an important role in carcinogenesis however a controversial hypothesis suggests a indirect and/or direct genotoxicity originating from oestrogen

metabolites, in particular the 4-hydroxy catechol metabolite, are also likely to make important contributions (Yager, 2000). Mechanistically cytochrome p450 1B1 catalyses the hydroxylation of oestradiol, to 4-hydroxy oestradiol, which is converted to the 3,4 oestradiol quinine leading to the destabilisation of the glycosidyl bond which links guanine and adenine to the DNA backbone (Santen *et al.*, 2004b). This process forms DNA point mutations that serve as potential initiators of neoplastic transformation.

It must be stated that the increased risk associated with hormone environment is not constant throughout an individuals' life. There are events that contribute to the increased risk of breast cancer which are a part of life's natural progression, such as early menarche (before the age of twelve, Kampert *et al.*, 1988), late age at first pregnancy (after the age of thirty, White, 1987) and delayed menopause (over the age of 45, Gomes *et al.*, 1995). The unifying consequence of these temporal events is prolonged exposure of the breast to endogenous oestrogens. Parallel information on exogenous oestrogen exposure has come from studies which have shown that hormone replacement therapy (HRT) related to duration, promotes a small but significant increase in the risk of breast cancer (1.35-fold increase, Collaborative Group on Hormonal Factors in Breast Cancer, 1997). Recent data (5.2 year follow-up and termination of the study) of the Womens' Health Initiative Study reports that the short-term HRT combination of oestrogen plus progestin also increases the risk of breast cancer. Moreover the cancers that were diagnosed were at a more advanced stage (25.4% vs. 16.0% respectively) compared to the placebo group (Chlebowski *et al.*, 2003).

Also associated with a greater risk of breast cancer are generally postmenopausal individuals who suffer from obesity (Huang *et al.*, 1997; Magnusson *et al.*, 1998) where oestrogen production is more significant (discussed in 1.2.1 Oestrogen Production). This latter relationship may again be explained by increased oestrogen availability, since the degree of obesity correlates linearly with total-body aromatase activity in adipose tissue (Jefcoate *et al.*, 2000). Obesity may not be an easy obstacle to overcome, however dietary intake, low physical activity, and alcohol consumption can be controlled. A number of beneficial dietary components present in soy, fruits and vegetables can alter circulating oestrogen levels and modify other cell signalling pathways (Clarke *et al.*, 2003). Moderate alcohol consumption has been associated

with harmful effects on circulating oestrogen levels and therefore related to an increased relative risk of developing breast cancer (Lash and Aschengrau, 2000). Although these risk factors have only been linked through circumstance and environment, these are nonetheless very important lifestyle issues that have been reported to increase the relative risk of developing the disease (Howe *et al.*, 1990; Bowlin *et al.*, 1997). Migration studies can further support the importance of diet as well as environmental influence on the development of breast cancer. Women from Asian and other developing countries that have migrated and adapted to a Western world lifestyle assume the rate of breast cancer incidence within one or two generations (Thomas and Karagas, 1987; McPherson *et al.*, 2000).

Despite breast cancer predominantly arising in women without family history, any family history (maternal or paternal) could pose a risk to a patient. The increased risk is small except in women with a first-degree relative (mother or sister) who had breast cancer, and further increased if the relative had either premenopausal or bilateral breast cancer (Ottman *et al.*, 1983). Genetically predisposed breast cancers occur at a younger age, are more likely to be bilateral, and appear in multiple family members over three or more generations (Casey, 1997). In 1990, the Breast Cancer –1 (BRCA-1) gene was discovered as the first breast cancer susceptibility gene and localised to chromosome 17q21 by linkage analysis of multiple families affected by early onset breast and ovarian cancer (Hall *et al.*, 1990). Approximately four years later, the Breast Cancer –2 (BRCA-2) gene was localised to chromosome 13q12-13 (Wooster *et al.*, 1994) and similar to BRCA-1 the inactivating mutations are scattered throughout the coding region (Wooster *et al.*, 1995). There is indication that approximately 10% of women diagnosed with breast cancer under the age of 35, harbour a BRCA-1 alteration (Langston *et al.*, 1996). Together the BRCA-1 and BRCA-2 mutations account for nearly all of the hereditary breast cancer cases, moreover, it is estimated that inherited mutations or alterations in these breast cancer susceptibility genes account for approximately 5-10% of breast cancer cases (American Cancer Society, 2005-2006).

1.1.2 Staging and Prognostic Factors

Like other cancers, breast cancer is the end result of a multistage process that involves a series of cellular and molecular changes that alter cell function (such as decreased apoptosis) and growth, ultimately causing increased cell proliferation.

Staging is performed in order to estimate prognosis, to direct an appropriate therapy to the patient and provide a standard for reporting results. The tumour size, lymph node involvement, and any associated distant metastases (TNM) are all considered when evaluating a tumour on presentation. Among patient's with breast cancer, lymph node status provides a considerable amount of precise prognostic information and is beneficial in deciding whether inclusion of cytotoxic therapy is appropriate (Fisher *et al.*, 1981). Of considerable importance is the assessment of oestrogen receptor (ER) and progesterone receptor protein levels present in the tumour. The expression level of these two hormone receptors can help predict a patients' response to hormonal manipulation. Extensive clinical and experimental literature provides evidence that, when ER is present, oestrogen is a key stimulus for growth of breast cancer cells (Buzdar and Howell, 2001; Schiff *et al.*, 2003). Patients presenting with an ER positive (ER^+) tumour phenotype are therefore appropriate for anti-hormonal (AH) treatment strategies. Current anti-hormonal strategies involve either anti-oestrogens, notably tamoxifen, or in the case of postmenopausal women oestrogen deprivation by aromatase inhibition, and LHRH agonist in premenopausal women. Unfortunately, 30% of patients present with an ER negative phenotype (Gee *et al.*, 2004) and are unaffected by systemic hormonal treatment. As such they are considered *de novo* resistant and are treated with chemotherapeutic strategies (MacGregor and Jordan, 1998). In general, ER negative tumours are associated with poor patient survival and early recurrence (Bezwoda *et al.*, 1991).

1.2 OESTROGEN AND OESTROGEN RECEPTOR SIGNALLING

1.2.1 Oestrogen Production

Endogenous levels of steroid hormones are periodic throughout the menstrual cycle, for example oestrogen levels are higher during the luteal phase compared with the follicular phase of the menstrual cycle. In addition to variations in the underlying hormonal patterns between and within a woman, there are considerable variations in menstrual cycle length (Barnett *et al.*, 2004). The primary location of oestrogen synthesis is in the ovaries (mainly production of oestradiol, E_2) in premenopausal women. Ovarian function and oestrogen synthesis is regulated by the hypothalamic pulse release of luteinizing hormone releasing hormone (LHRH), followed by the release of luteinizing hormone (LH) and follicle-stimulating hormone (FSH) by the pituitary (Ali and Coombes, 2002). Once this signal reaches the ovaries, cyclic AMP (cAMP) levels are increased. This activates the transcription factor cAMP-response

element binding protein (CREB) thereby increasing the expression of aromatase (Ali and Coombes, 2002) (see Figure 1.1, left). Aromatase is an enzyme of the cytochrome P450 (CYP) superfamily and a product of the *CYP19* gene located on chromosome 15q21.2 (Dixon, 2004). This enzyme has the sole responsibility for the conversion of the androgens, androstenedione and testosterone to oestrogens, oestrone (E_1) and oestradiol respectively (Buzdar and Howell, 2001). Although only one gene encodes for the aromatase enzyme in both reproductive and non-reproductive tissues, this gene contains at least ten different promoters (Bulun *et al.*, 2003). These promoters vary in different types of normal tissues and in breast, and the promoters are stimulated by different ligand-induced pathways (Joensuu *et al.*, 2005).

Considerably lower levels of oestradiol and oestrone are synthesized by aromatase in other normal tissues, including mesenchymal cells of adipose tissue, osteoblasts and chondrocytes in the bone, the vascular endothelium, aortic smooth muscle and many regions in the brain (Simpson and Davis, 2001). The oestrogens synthesised particularly within the bone, breast and brain seem to be only biologically active at a local tissue level in a paracrine or 'intracrine' fashion. Intracrine activity is defined by the formation of active hormones that exert their action in the same cells in which synthesis took place without release into the pericellular compartment (Labrie *et al.*, 1997). In the case of adipose tissue oestrogen production (see Figure 1.1, right), the factors with the most impact on aromatase expression are interleukin-6 (IL-6), interleukin-11 (IL-11), oncostatin M (OSM) and tumour necrosis factor-α (TNF-α). These agents act via promoter I.4 of the aromatase gene, and require glucocorticoids as co-stimulators (Simpson and Davis, 2001). In postmenopausal women, ovarian synthesis of oestrogen ceases, therefore residual oestrogen synthesis relies on the availability of circulating adrenal precursors dehydroepiandrosterone (DHEA) and DHEA sulphate (DHEA-S) as well as the level of aromatase enzyme in peripheral tissues, including adipose (Simpson *et al.*, 2000). The major aromatization pathway in postmenopausal woman is androstenedione into oestrone, which accounts for as much as 90% of the total oestrogens synthesised (Lonning *et al.*, 1990; Joensuu *et al.*, 2005).

In the breast cancer patient the breast tumour can produce factors that also stimulate aromatase expression locally (see Figure 1.1, middle). This stimulation is associated

primarily with switching of the aromatase gene promoter from I.4 to promoter II. Locally produced prostaglandin E_2 (PGE_2) activates prostaglandin E receptors on breast cancer cells, which increases cAMP levels followed by CREB transcription leading to aromatase expression (Zhao *et al.*, 1996). An increase in prostaglandin levels could be associated with the activation of the COX-2 pathway. This pathway has a number of inducible targets involved with cell growth, invasion, anti-apoptosis, angiogenesis and the HER2 pathway (Brodie *et al.*, 2001). Activating PGE_2 and thus aromatase over-expression, consequently leads to an increase in oestrogen production which then feeds back to drive further COX-2 stimulation, creating a positive loop mechanism (Goss and Strasser-Weippl, 2004). Bulun *et al.* (2003) also suggest that oestrogen-dependent breast cancer utilizes 4 promoters (II, I.3, I.7 and I.4) for aromatase expression which increases total P450 aromatase mRNA compared with normal breast (which exclusively uses promoter I.4). It has been determined that the concentration of oestradiol present in breast tumours of postmenopausal women is at least 20-fold greater than that found in the plasma (Pasqualini *et al.*, 1996). Using an aromatase inhibitor decreases the intra-tumoural levels of oestradiol and oestrone, paralleled with a loss of aromatase activity (discussed in more detail see section 1.3.3). This may suggest it is the aromatase activity of the tumour and the surrounding adipose tissue that is responsible for the high concentrations of oestrogens within tumour cells (de Jong *et al.*, 1997).

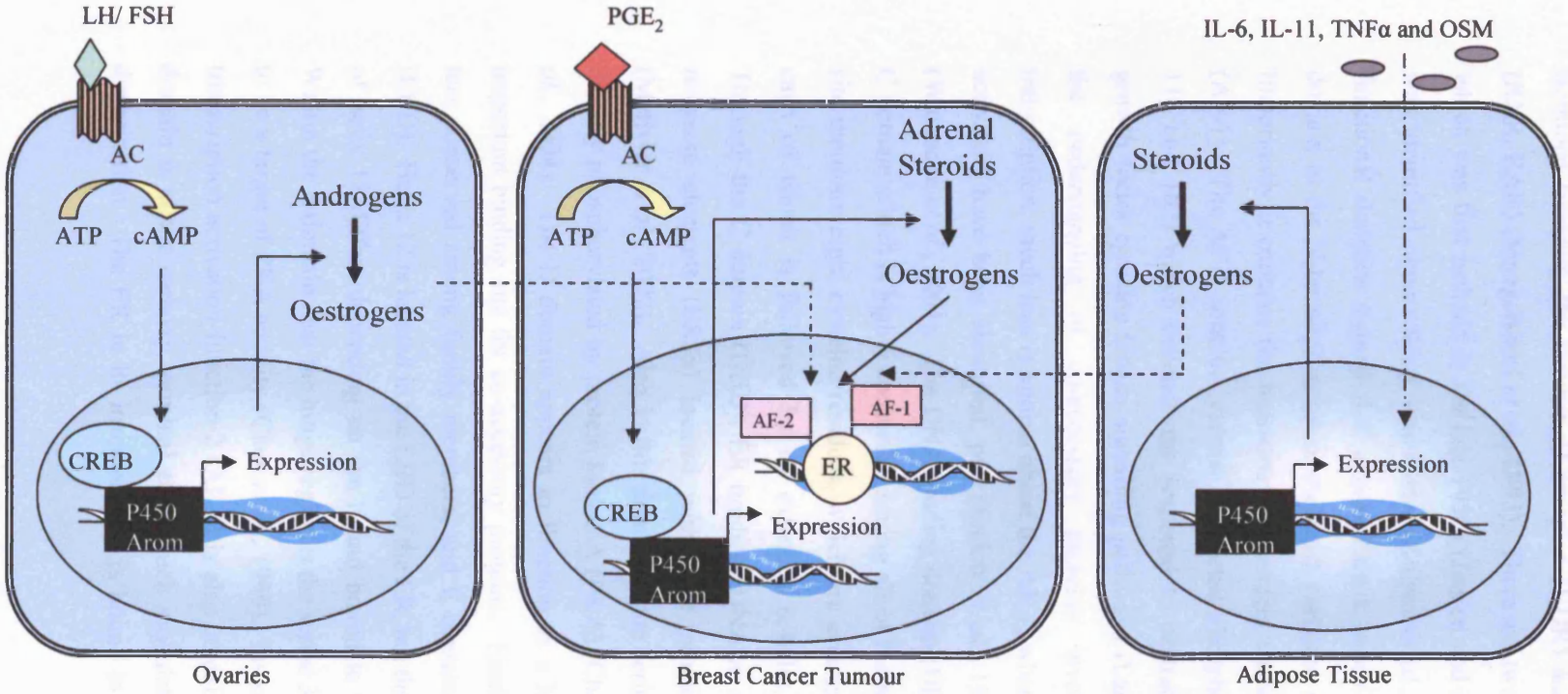

Figure 1.1 Oestrogen Production (Ali and Coombes, 2002)

Ovarian production of oestrogen (left) is regulated by the release of luteinizing hormone (LH) and follicle-stimulating hormone (FSH) by the pituitary. These molecules cause an increase in cyclic AMP (cAMP) levels which facilitates the transcription of cAMP-response element binding protein (CREB), ultimately increasing expression of aromatase. Aromatase is then responsible for the conversion of androstenedione and testosterone to oestrone and oestradiol respectively. A breast tumour (middle) can locally produce aromatase via production of prostaglandin E_2 (PGE_2) activating its receptors which increases cAMP followed by CREB transcription and aromatase expression. In adipose tissue (right) interleukin-6 (IL-6), interleukin-11 (IL-11) and tumour necrosis factor-α (TNFα) act via promoter I.4 of the aromatase gene to increase aromatase expression leading to the production of oestrogen. A pre-menopausal breast tumour therefore has oestrogen supply from the ovaries, adipose tissue as well as the tumour itself. A post-menopausal tumour is reliant on aromatase activity and oestrogen production from the surrounding adipose tissue as well as the breast tumour.

1.2.2 Structure of the Oestrogen Receptor (ER)

The ER is a member of a nuclear receptor superfamily that includes the thyroid hormone receptor, the vitamin D receptor (VDR) and the retinoic acid receptors (RXR, RAR) (Mangelsdorf *et al.*, 1995). There are two genes that encode the ER, α which was first isolated in the late 1950s (Jensen and Jacobson, 1960) and β which was identified almost thirty years later (Kuiper *et al.*, 1996). ERα is organised in functional domains termed A-F encoded by 8 exons (see Figure 1.2). The A/B domain at the N-terminal exhibits the most variation in both sequence and length. Importantly it contains the hormone–independent transcription activation function-1 (AF-1). The AF-1 contains several key serine phosphorylation sites (Ser 104, 106, 118 and 167) which enhance the response to oestradiol binding or activation of growth factor tyrosine kinase signalling pathways (Lannigan, 2003). Compared to the understanding of co-accessory proteins involved in ligand dependent transcription, much less is known about the AF-1, where only two specific AF-1 co-activators have been identified, p68 (Endoh *et al.*, 1999) and p72 RNA helicases (Watanabe *et al.*, 2001). The DNA-binding domain (DBD) is centrally located in the C domain which is highly conserved among all of the nuclear receptors. Within this site there are eight cysteine residues, which are arranged in two zinc-finger motifs, each of which is followed by an extended α-helix, forming two sub-domains. Through the C domain (DBD), ER binds to DNA as dimers, at specific oestrogen response elements (EREs) located within the promoter of E_2-responsive genes (Metivier *et al.*, 2002). Also in this domain is the serine residue 236, which can be directly phosphorylated by protein kinase A (PKA) (Chen *et al.*, 1999; Michalides *et al.*, 2004). The D domain appears to function as a hinge region, and may be an important binding site for co-accessory proteins. Finally, the E and F domains are less conserved among family members, and E contains the ligand-binding domain (LBD). Helix 12 is located in the LBD of the ER, but the composition and orientation of helix 12 differs depending on the ligand bound to the ER (Shiau *et al.*, 1998). Within the E domain near the hinge region is the serine 305 residue, which also seems to be a target of PKA activity (Chen *et al.*, 1999). Importantly, the ligand-dependent transcription activation function-2 (AF-2) is also contained in the E domain. The F domain is at the carboxy terminal end, which modulates transcriptional activation/ dimerization. The ER in its inactive state is bound to co-repressors, which recruit

histone deacetylases (HDACs) that maintain chromatin condensation (McKenna *et al.*, 1999).

ER is expressed in the brain, bone, cardiovascular system and in a number of endocrine tissues including normal breast, uterus and vagina, as well as in the pituitary and hypothalamus (Osborne *et al.*, 2004). A striking abnormal pathologic feature of many breast tumours is over-expression of ER.

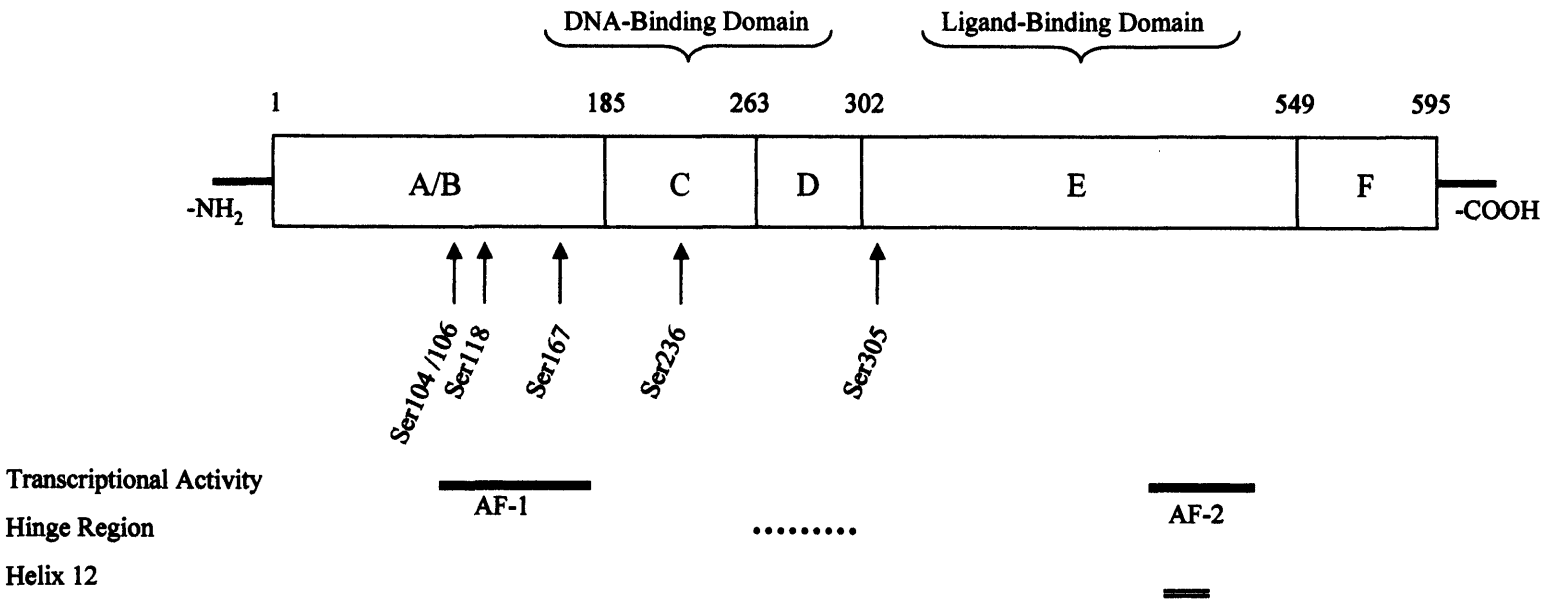

Figure 1.2 Structure of the Oestrogen Receptor

The ER has 5 domains each with specific function that lead to the complex function of the receptor. The A/B domain (N-terminus, $-NH_2$) contains the AF-1 for transcriptional activity with its key serine phosphorylation sites (104/106, 118 and 167). The DNA binding domain which importantly binds ERE sequences is located in the C domain. The D domain contains the hinge region important for dimerization and Hsp90 binding. Within the E domain is the ligand binding domain which contains helix 12 and the AF-2 for transcriptional activation. The orientation of helix 12 is dependent on the ligand bound to the ER. The F domain is the carboxy terminus (-COOH) which modulates transcriptional activity and dimerization.

1.2.3 Signalling via the Oestrogen Receptor-α (ERα)

It is now established that signalling mediated via the natural steroid hormone oestrogen through the oestrogen receptor has a mitogenic effect on many breast cancers, playing a key role in growth and development of this disease (Prall *et al.*, 1998). Unfortunately, there is not one straightforward mechanism in which oestrogen acts via oestrogen receptor to promote cell growth, proliferation and survival. The ERα is conventionally known as a nuclear receptor that, when oestradiol triggered, acts as a transcription factor promoting gene expression to drive growth. However, recent evidence suggests there is also a distinct rapid signalling mechanism not mediated by the activation of RNA or protein synthesis that has led to the discovery of receptor sub-fractions localised at the cell membrane (Simoncini and Genazzani, 2003). The nuclear and plasma membrane ERα are quite complementary and do share some overlapping features, for example both bind oestradiol and interact with signalling kinases. Furthermore, it is has been suggested that membrane ERα signalling could amplify the actions of the nuclear receptor (Levin, 2002). Each form is separated by distinct mechanisms of action, which will be discussed in detail within the following sections.

1.2.3.1 Classical/ Ligand-Dependent Genomic Signalling

In the classical or ligand dependent ERα pathway of transcriptional control, the binding of oestradiol to the ERα initiates displacement of heat shock proteins from the ERα, followed by receptor dimerization (Osborne *et al.*, 2004) (see Figure 1.3). The nuclear oestradiol/ ERα complex binds specifically to the oestrogen response elements (EREs), which are sequences situated in the regulatory regions of oestrogen sensitive genes. Transcription mediated via the ERα has direct and indirect involvement with a range of genes associated with survival, proliferation, angiogenesis, and invasion. The orchestrated concert of transcription is controlled by the AF-1 (phosphorylation at Ser118 predominately) and AF-2 domains, with the aid of co-activator (CoA) proteins. Three important classes of CoA complex are subsequently recruited. The first promotes nucleosomal remodelling required for transcriptional activation and contains steroid receptor co-activator protein-1 (SRC-1, p160), p300/CBP (CREB binding protein) and transcriptional intermediary factor-2 (TIF-2) (Metivier *et al.*, 2001). The next complex which forms a direct link to the transcriptional machinery apparatus is made up of SMCC/TRAP/DRIP (SRB and

mediator-protein- containing complex, thyroid-hormone-receptor-associated protein and vitamin-D-receptor-interacting protein) and has been implicated in activation by several nuclear receptors (Font de Mora and Brown, 2000). The third co-activator complex includes AIB1 (amplified in breast cancer-1; also known as SRC-3, RAC3, TRAM-1, pCIP and ACTR) steroid hormone receptor co-activator which binds ER and enhances the expression of cyclin D1 (Planas-Silva *et al.*, 2001). AIB1 has potential therapeutic predictive importance and has been implicated in enhancing anti-oestrogen resistance (Osborne and Schiff, 2003; Clarke *et al.*, 2003). Furthermore, this co-activator is over-expressed in approximately 50% of breast tumours (Murphy *et al.*, 2000), especially ERα positive breast cancers.

Once the CoA complex is recruited, stimulation of transcription begins via histone acetyl-transferase (HAT) activity which allows access to the transcriptional template by remodelling (or de-condensation) of the chromatin (McKenna *et al.*, 1999). Phosphorylation within the AF-1 at serine 118 and to a lesser extent serine 104/106 (Lannigan, 2003), completes the elements for the oestradiol/ERα complex to function maximally. The phosphorylation of serine 118 induced by oestradiol is mediated by CDK7, which is a cyclin kinase associated with the basal transcription factor TFIIH (Chen *et al.*, 2000; Martin *et al.*, 2003). The result of the machinery functioning properly is the transcription of oestrogen-responsive genes, such as c-myc, cyclin D, cathepsin D and transforming growth factor-α (TGF-α), all of which are known to stimulate mammary cell growth (Sun *et al.*, 2001).

1.2.3.2 Non-Classical/ Ligand-Dependent Genomic Signalling

ERs can modulate expression of target genes by indirectly interacting with further transcription factors such as AP-1 (activator protein-1) or Sp1 to facilitate expression in a tissue specific manner. Interestingly, despite some similar action at EREs, ERα and ERβ have completely different effects at AP-1 sites. ERα activates and ERβ inhibits transcription from an AP-1 site when receptors are complexed to oestradiol (Webb *et al.*, 1999). The model for ER action at AP-1 sites is complicated. It has been proposed that ERα is present at AP-1 sites through contact with co-activators (SRC1, p160) that have been recruited by Jun/Fos or Jun/Jun (Schiff *et al.*, 2003) (see Figure 1.4). There is evidence to suggest that AP-1 transcription factors control survival and apoptosis by regulating the expression and function of cell cycle

regulators, cyclin D, $p21^{cip1/waf1}$, $p19^{arf}$ and p16 (Shaulian and Karin, 2001). The difference between ER interactions at Sp1 sites versus AP-1 is ERα activates in a cell-specific manner and ERβ is nearly inactive. It has been proposed that ERα binding to Sp1 increases the binding of Sp1 to its cognate element, thereby enhancing transcription (Delaunay *et al.*, 2000).

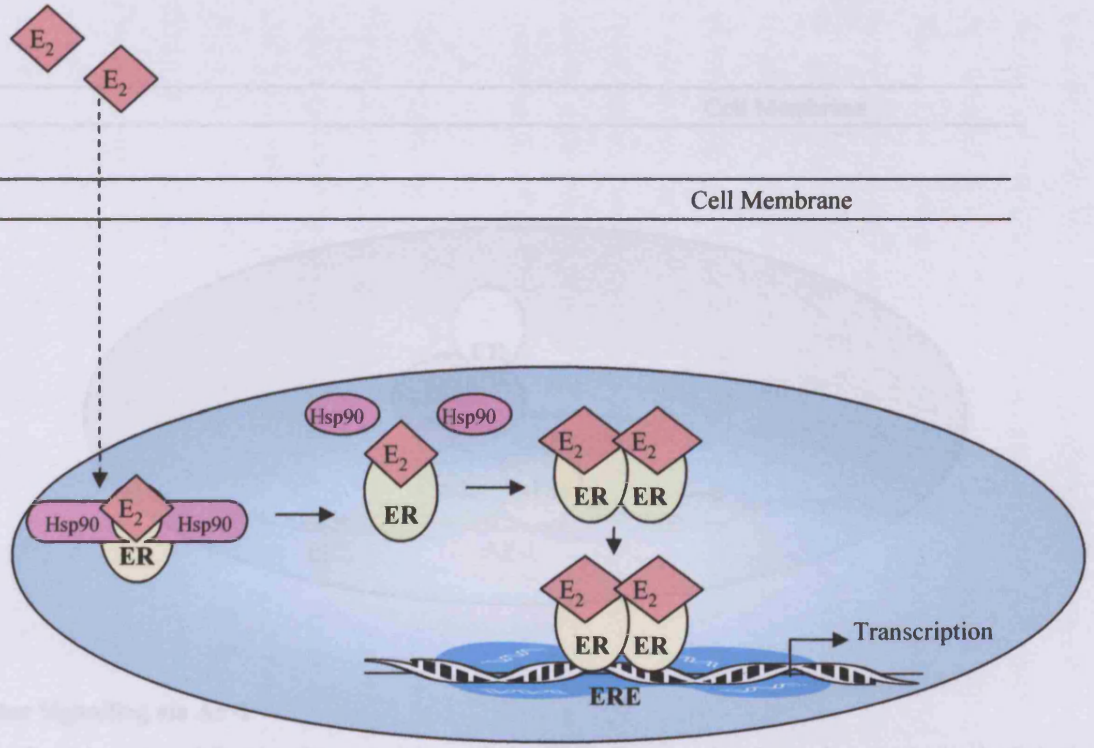

Figure 1.3 Classical/Ligand-Dependent Genomic Signalling

Oestrogen diffuses through the cell nuclear membrane binding into a hydrophobic region in the ER. There is conformational change in the ER so Helix 12 in the E domain seals the region. The Hsp90 molecules are lost and two oestrogen bound receptors dimerize leading to the binding to target sequences in the DNA of oestrogen sensitive genes, know as oestrogen response elements (ERE's). This mechanism results in the transcription of genes known to stimulate mammary cell growth.

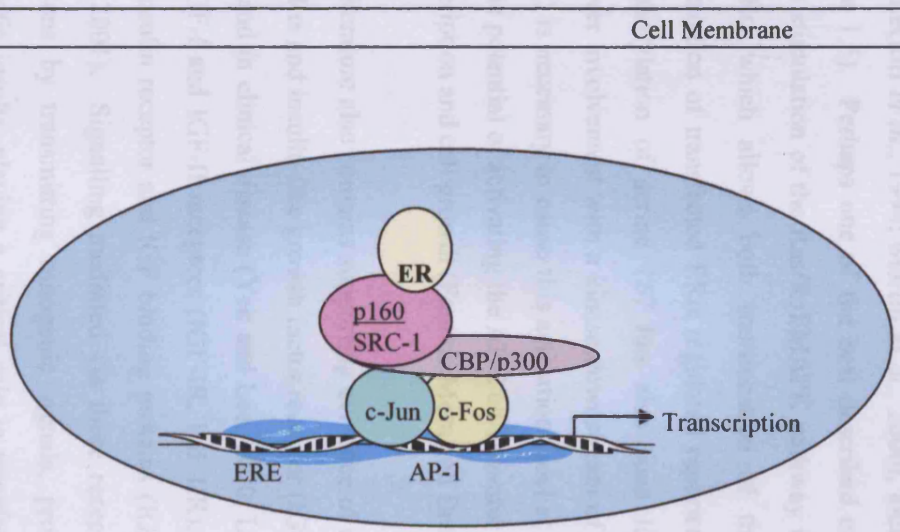

Figure 1.4 Oestrogen Receptor Signalling via AP-1

First the binding of c-Jun and c-Fos takes place following the recruitment of the CBP/p300 associated proteins which also include the p160 co-activators. The c-Jun/c-Fos heterodimer plus the co-activator complex binds to the ER triggering transcription from the AP-1 element. Transcription of genes that control survival and apoptosis occurs, such as cyclin D, $p21^{cip1/waf1}$, $p19^{arf}$ and p16.

1.2.3.3 Receptor Tyrosine Kinase Induced Oestrogen Receptor Genomic Signalling

Although in most cases both the functional domains AF-1 and AF-2 appear to act in conjunction to promote optimal transcriptional activity (Metivier *et al.*, 2001), ERα mediated transcription can also be initiated in a ligand independent manner (Ali *et al.*, 1993; Kato *et al.*, 1995; Lannigan, 2003). Crucial information has evolved describing receptor tyrosine kinase networks that are highly interactive with the ERα and breast cancer growth. Stimulation of signal transduction networks or activation of second messengers can directly phosphorylate serine residues, notably Ser 104, 106, 118 and 167 (LeGoff *et al.*, 1994; Martin *et al.*, 2000), located within the AF-1 domain (see Figure 1.5). Perhaps one of the best described examples is the epidermal growth factor stimulation of the Ras/Raf/MAPK pathway that can phosphorylate serine 118 of ERα which allows both translocation of the receptor to the nucleus and transcription of transfected ERα regulated reporter genes (Kato *et al.*, 1995). The phosphorylation of serine 167 has also been linked to EGFR/HER2 pathway; however involvement with a kinase downstream of MAPK, p90 ribosomal S6 kinase (RSK) is necessary to cause this activation (Joel *et al.*, 1998). Alternatively, MAPK has the potential of activating the AF-2 co-activator AIB-1, which also regulates gene transcription and cell growth (Font de Mora and Brown, 2000).

The literature also contains supporting evidence of cross-talk between components of the ERα and insulin-like growth factor receptor (IGFR) signalling pathway in cells *in vitro* and in clinical disease (Yee and Lee, 2000; Lee *et al.*, 2003). This consists of the IGF-I and IGF-II receptors (IGF-IR, IGF-IIR), the insulin receptor (IR), hybrid IGF/insulin receptor and IGF binding proteins (IGFBPs, six in total) (Sachdev and Yee, 2001). Signalling mediated via these receptors initiates a range of cellular functions by transmitting mitogenic signals, protecting cells from a variety of apoptotic insults, playing a critical role in transformation, regulating cell adhesion and cell motility, and inducing terminal differentiation (Yee and Lee, 2000). Key downstream signalling components include PKCδ, which seems to be linked with anchorage-independent growth and AKT/ protein kinase B (PKB), which is believed to exert an anti-apoptotic effect (Kiley *et al.*, 1999). There is strong evidence that ER Ser167 can be phosphorylated by AKT (Figure 1.5) and also casein kinase II (Arnold *et al.*, 1995; Sun *et al.*, 2001). Clearly, the tyrosine kinase receptor pathways can lead to ligand independent activation of the oestrogen receptor by direct phosphorylation

of the serine residues located in the AF-1 domain and/or by the phosphorylation of co-activators.

Within the AF-2 domain the protein kinase p21-activated kinase (Pak1), an effector of the small GTPases Cdc42 and Rac1, has been shown to directly phosphorylate Ser305 (Wang et al., 2002). The study by Wang et al. (2002) was able to show Pak-1 phosphorylates the AF-2 in the absence of oestrogen paralleled by an up regulation of MAPK activation.

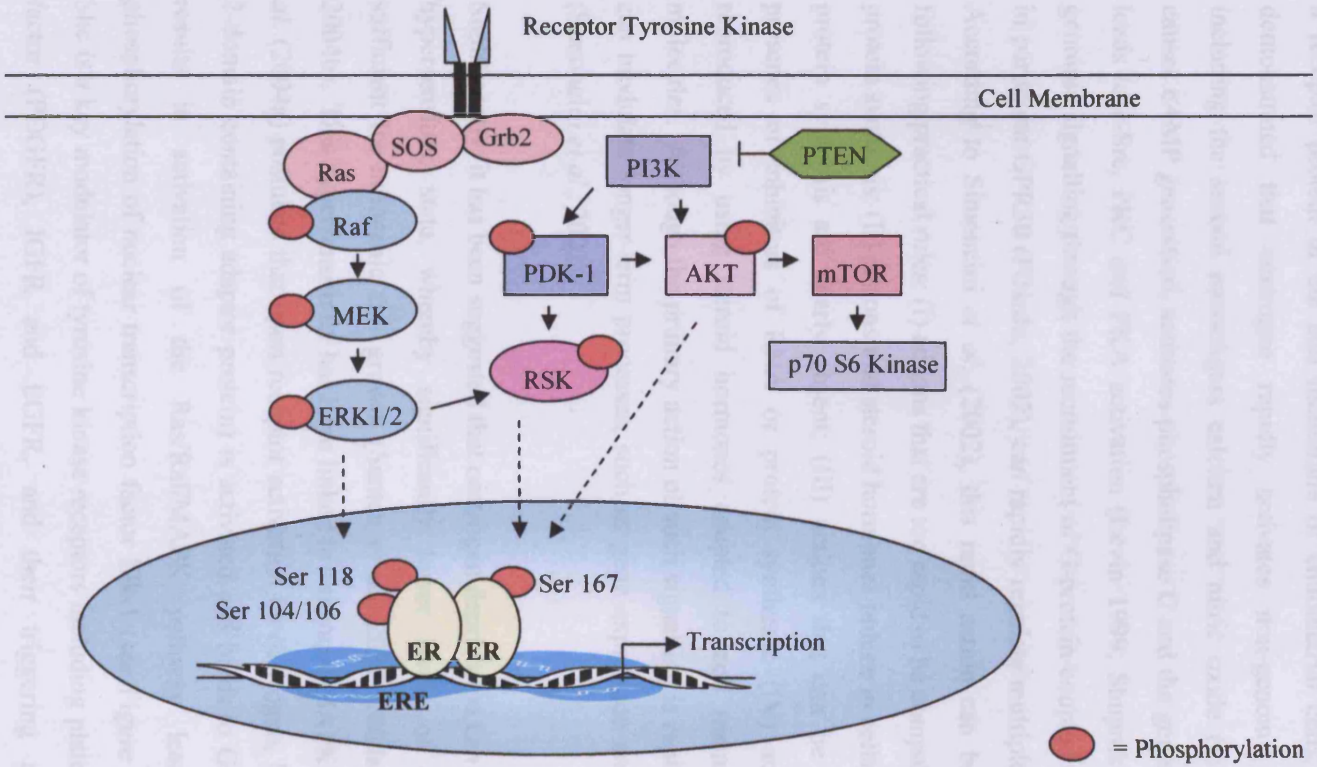

Figure 1.5 Receptor Tyrosine Kinase Induced ER Genomic Singalling

Stimulation of tyrosine kinase receptors therefore signal transduction network can lead to the phosphorylation of ER AF-1 serine residues. Ligand activation of the epidermal growth factor receptor (EGFR) results in the phosphorylation of the Ras/Raf/ERK (MAPK pathway) which can directly phosphorylate Ser118 and indirectly through RSK phosphorylate Ser167. Alternatively, ligand activation of the insulin-like growth factor receptor (IGFR) results in the phosphorylation of PI3K/AKT directly phosphorylating Ser167.

1.2.3.4 Rapid Non-Genomic Signalling via Membrane Oestrogen Receptor

The importance of functional ER associated with the plasma membrane remains somewhat controversial in breast cancer. Pietras and Szego (1977) first described the rapid generation of cyclic AMP (cAMP) in response to oestrogen which was bound to a receptor protein in the cell membrane of endometrial cells. It has also been demonstrated that oestrogen rapidly activates non-genomic signalling events including the second messengers calcium and nitric oxide (in endothelial cells), causes cAMP generation, activates phospholipase C and the generation of IP3 which leads to c-Src, PKC and PKA activation (Levin 1999; Shupnik 2004). This non-genomic signalling through the recruitment of G-protein-coupled receptors (GPCRs), in particular GPR30 (Filardo, 2002), can rapidly regulate multiple cellular functions. According to Simoncini *et al.* (2002), this rapid action can be classified by the following practical rules: (I) actions that are too rapid to be compatible with RNA and protein synthesis; (II) actions that steroid hormones induce in cells in which RNA and protein synthesis are nearly absent; (III) actions that can be reproduced in the presence of inhibitors of RNA or protein synthesis; (IV) actions that can be reproduced by using steroid hormones coupled to cell membrane-impermeable molecules. Although the primary action of such signalling is rapid, its consequences can modulate longer-term processes, such as gene expression and cell proliferation (Simoncini *et al.*, 2002).

Significantly, it has been suggested that oestrogen deprivation can cause an oestrogen hypersensitive state, whereby significantly lower levels of oestrogen become sufficient for mitogenic cell growth (Santen *et al.*, 2001, 2004a; Nicholson *et al.*, 2004b). This hypersensitivity has been linked to enhanced MAPK activity. Santen *et al.* (2004a) postulate that upon receptor activation by oestrogen, Shc (Src homology 2-domain containing adaptor protein) is activated and binds to Grb2 and Sos. This results in activation of the Ras/Raf/MAPK pathway leading to a rapid phosphorylation of nuclear transcription factor Elk-1 (see Figure 1.6). Importantly, Shc is a key modulator of tyrosine kinase receptors including platelet-derived growth factor (PDGFR), IGFR and EGFR, and their triggering actively facilitates translocation of cytoplasmic ER to the plasma membrane and thus promotes MAPK signalling (Song *et al.*, 2002; Nicholson *et al.*, 2004b). Migliaccio *et al.* (1998, 2000) have shown that an ER/Src membrane complex may also lead to the rapid activation of signalling kinases. This is supported by the Santen *et al* (2004a) studies showing

that both ER and Src are upstream of Shc and are required for its phosphorylation and subsequent MAPK activity. The ER/Src complex has also been linked physically and functionally to the p85 sub-unit of PI3K, catalyzing the synthesis of lipid mediators that act as second messengers transferring membrane signalling to intracellular protein kinases such as AKT (Castoria *et al.*, 2001; Simoncini and Genazzani, 2003).

In summary, the membrane ER signalling mechanism in breast cancer represents a relatively new aspect within the understanding of oestrogen action, most notably in its contribution to oestrogen response versus genomic mechanism. Indeed, to date ER localised to the plasma membrane has not been isolated for detailed characterisation, although localisation of the receptor in this vicinity has been reported.

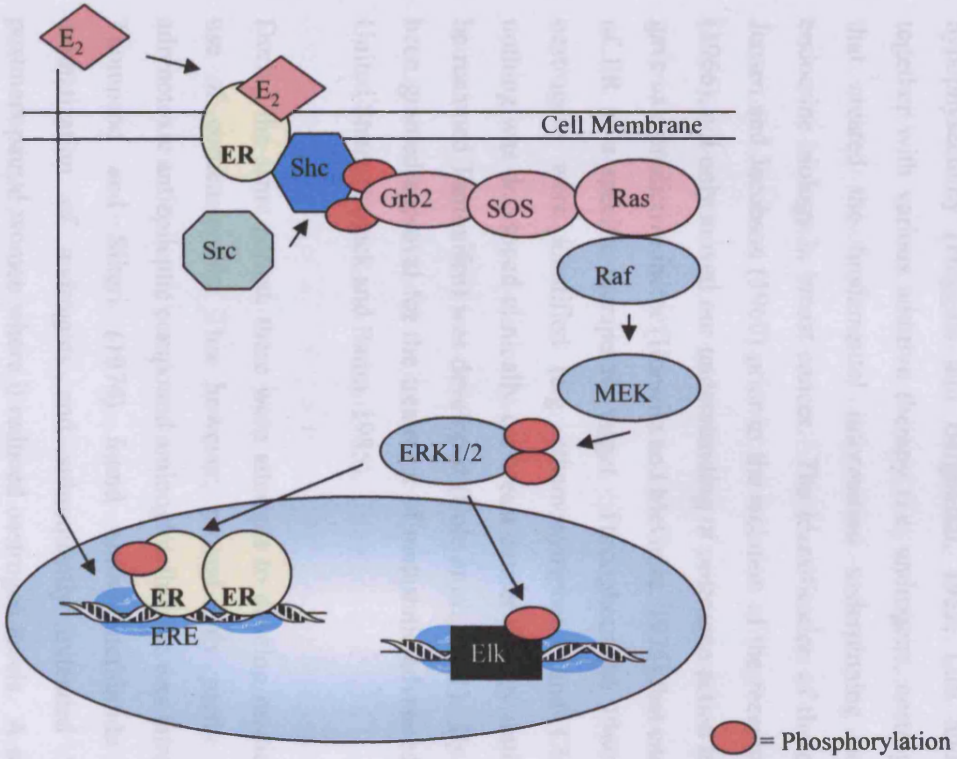

Figure 1.6 Membrane Oestrogen Receptor Signalling

The Santen et al. (2003) membrane ER suggests E_2 binds to ER near or in the cell membrane, followed by the initiation of Shc binding to the ER. Through Src kinase, Shc is phosphorylated. Then association with GRB2 and SOS leads to Ras (GDP to GTP) conversion activating Raf/MEK/ERK1/2 enhancing cell proliferation through Elk and ERE transcription.

1.3 ENDOCRINE THERAPY

The development of endocrine therapy has proved to be one of the major accomplishments in breast cancer and has resulted in much important translational research, including the discovery of the ER. It was the initial clinical discoveries with respect to Beatsons' (1896) observations of oophorectomy causing a regression of breast tumours, followed by similar clinical results caused by adrenalectomy and hypophysectomy (Huggins and Bergenstal, 1952; Luft and Olivecrona, 1953), together with various additive therapy (i.e. androgens, oestrogens and progestins), that created the fundamental information underpinning our understanding of endocrine biology in breast cancer. The identification of the oestrogen receptor by Jensen and Jacobson (1960) prior to the isolation of the receptor by Toft and Gorski (1966), not only moved our understanding of oestrogen action to a molecular level, it gave us a predictive factor (Horwitz and McGuire, 1975) that enabled the rapid screen of ER as a specific therapeutic target. Throughout the 1960s, a number of anti-oestrogens were identified (e.g. ethamoxytriphetol and Clomiphene), although nothing was developed clinically for breast cancer therapy until ICI 46,474 (later to be renamed Tamoxifen) was developed (Cole *et al.*, 1971). By 1977, tamoxifen had been granted approval for the treatment of metastatic advanced breast cancer in the United States (Cuzick and Baum, 1985).

During the same period, there were attempts to develop medical adrenalectomy by use of corticosteroids. This however, proved only partly successful until the adrenotoxic antiepileptic compound aminoglutethimide was introduced. Significantly Thompson and Siiteri (1974) found aminoglutethimide inhibited *in vitro* aromatization of androgens and subsequently extended this observation to postmenopausal women where it reduced oestrogen levels. A study by Geisler *et al.* (1997) additionally revealed treatment of postmenopausal women with aminoglutethimide decreased plasma levels of oestrone sulphate from a mean pre-treatment value of 372.4 to 50.6 pmol/l (74.5% inhibition), with plasma levels of oestrone and oestradiol being suppressed by 40.7% and 32.8% respectively. Since the 1970s endocrine therapy targeting the oestrogen receptor or inhibiting the production of oestrogen has been intensely investigated around the world, with such treatments promoting remission among patients with ER^+ tumours. Currently, tamoxifen is the mainstay of endocrine therapy in ER^+ disease, however recent advancement among oestrogen deprivation strategies, in particular the development

of third generation aromatase inhibitors which reduce circulating oestrogen levels in postmenopausal women by upwards of 95%, is set to change this situation in the Western world.

1.3.1 Anti-oestrogens

1.3.1.1 Tamoxifen- Selective Oestrogen Receptor Modulator in ER^+ Disease

It is now established that approximately 40% of breast cancer patients benefit from endocrine therapy, and most of those patients have been treated with the non-steroidal anti-oestrogen tamoxifen (Nolvadex, AstraZeneca Pharmaceuticals). The drug has been shown to be beneficial in both the adjuvant setting and in advanced ER^+ disease. Tamoxifen is deemed to be a selective oestrogen receptor modulator (SERM), because it possesses mixed agonist and antagonist properties. Positioning of helix 12 in the LBD seems to be a feature that allows discrimination between ER agonists and antagonists (Shiau *et al.*, 1998). When the ER is occupied by an agonist the proper positioning of helix 12 generates AF-2 activity and allows a surface for the recruitment of co-activators (Pearce *et al.*, 2003) thus leading to transcriptional activation. In contrast, tamoxifen does not allow the appropriate positioning of helix 12 and indeed favours the recruitment of co-repressors that inhibit transcriptional activity (Shou *et al.* 2004). Despite this reduction in AF-2, a weak activation of AF-1 does remain (Feng *et al.*, 2001) and this can promote oestrogenic actions in a tissue specific manner. Clearly the antagonistic ability of tamoxifen to block ER AF-2 driven breast cancer cell growth is beneficial, however the agonist effects are variable and have been linked to tumour flare as well as risk of uterine tumours (2-4 fold) in postmenopausal women (Early Breast Cancer Trialists' Collaborative Group, 1998). Further side effects involved with tamoxifen treatment are similar to those experienced with hormone replacement therapy, which include thromboembolic disease, endometrial cancer, pulmonary embolus and stroke (ATAC Trialists' Group, 2002).

It has been shown that almost 50% of ER positive patients treated with the anti-oestrogen tamoxifen will fail to respond despite having retained ER expression (Osborne and Fuqua, 1994; Schiff *et al.*, 2003). Furthermore, many of the remaining patients who demonstrate an initial response, which is highly variable in magnitude, eventually acquire resistance leading to tumour progression (Cheung *et al.*, 1997). The mechanisms of tamoxifen resistance have been well characterized by a number of

groups including our own at the Tenovus Centre for Cancer Research. The consensus understanding is based on the large amount of evidence suggesting a retained importance of the ER and increased signalling via several growth factor tyrosine kinase receptor pathways and their downstream signalling components, promoting resistant *in vitro/in vivo* cell growth (Gross and Yee, 2003; Nicholson *et al.*, 2001, 2004a). The inability of tamoxifen to silence ER AF-1 activity gives a tumour cell the advantage or an avenue to overcome the stress of the treatment. This activity can be promoted by growth factor receptor pathways such as EGFR/HER2 and IGFR (Nicholson and Gee, 2000; Hutcheson *et al.*, 2003; Knowlden *et al.*, 2003a) to drive tamoxifen resistant growth. A number of gene transfer studies enhancing various elements involved in growth factor signalling (see Table 1.1) have been able to demonstrate the importance of their expression to proliferation, cell survival and ultimately anti-hormone resistance, as well as to invasiveness and angiogenesis.

Table 1.0 Reference list of gene transfer studies associated with resistance.

Target Gene	Reference
IGF-II	Abdul-Wahah *et al.*, 1999; Daly *et al.*, 1991
IGF-1R	Guvakova & Surmacz, 1997, Kucab & Dunn, 2003
Heregulin-β	Tang *et al.*, 1996
EGFR	van Agthoven *et al.*, 1992; Miller *et al.*, 1994
HER2	Benz *et al.*, 1993; Liu *et al.*, 1995; Pietras *et al.*, 1995
VEGF	Guo *et al.*, 2003
Ras	Kasid *et al.*, 1985; Yu and Feig, 2002
Raf	El-Ashry *et al.*, 1997; Oh *et al.*, 2001
MAPK	Oh *et al.*, 2001
AKT	Campbell *et al.*, 2001

Moreover, to further illustrate this phenomenon without gene manipulation, there is a vast amount of both experimental and clinical evidence that indicates increased expression of EGFR (Tidow *et al.*, 2003) and HER2 (Benz *et al.*, 1993; Witters *et al.*, 1997; Dowsett, 2001; Shou *et al.*, 2004) following treatment with tamoxifen can promote endocrine resistant states. In our own tamoxifen resistant models derived from MCF-7 and T47D cells there is increased expression and activity of these two tyrosine kinase receptors with a parallel increase in activity of their downstream signalling elements MAPK and AKT (Nicholson *et al.*, 2001; Hutcheson *et al.*, 2003; Knowlden *et al.*, 2003a). A number of groups (Smith *et al.*, 1997; Webb *et al.*, 1998; Schiff *et al.*, 2003) have suggested that the agonistic properties of tamoxifen are enhanced by increased levels in co-activators such as AIB1 or SRC1. This hypothesis

is supported by the indication of increased MAPK activation, either by ER or growth factor signalling, leading to the direct phosphorylation of AIB1 which recruits p300 and HAT activity to the AIB1 complex thereby regulating gene transcription and cell growth (Font de Mora and Brown, 2000; Osborne *et al.*, 2003).

Parallel to these findings, is strong clinical evidence that suggests tumours expressing high co-activator AIB1 and HER2 have a poor outcome with anti-oestrogen treatment. In the malignant breast over-expression of HER2 occurs in 25-30% (Heldin, 2001; De Lorenzo *et al.*, 2002) of patients and has been associated with a lack of response to endocrine therapy, that translates to an increase in metastatic disease and poor survival (Hutcheson *et al.*, 2003). This supports the hypothesis that increased HER2 signalling yields increased MAPK signalling, which in turn activates ERα (primarily serine 118) and AIB1 (Osborne *et al.*, 2003).

It has also been suggested both *in vitro* (Dumont *et al.*, 1996; Kushner *et al.*, 2000) and *in vivo* (Johnston *et al.*, 1999; Schiff *et al.*, 2000) that tamoxifen may act as an agonist on AP-1 regulated genes. Increased MAPK signalling and oxidative stress can cause increased AP-1 DNA binding associated with increased c-JUN NH2 terminal kinase (JNK) activity in tamoxifen resistant breast cancer (Johnston and Dowsett, 2003). Interestingly, there is evidence that SERM induced AP-1 stimulation is more efficient with ERβ than ERα and Webb *et al.* (1999) suggested that this mechanism was totally independent of the AF-2 function of ERβ. Since ERβ has no constitutive AF-1 function, the tamoxifen (SERM)/ERβ complex appears to activate AP-1 by an AF-independent action (Kushner *et al.*, 2000).

Currently, there are several alternative SERMs being evaluated both in clinic and in the laboratory. Toremifene (Fareston, Shire US) was approved as a nonsteroidal anti-oestrogen in the treatment of metastatic breast cancer. However, there were no added benefits of toremifene over tamoxifen in comparative studies on efficacy and tolerability and its use was still associated with undesirable oestrogenic effects (e.g. increased risk of thromboembolic disease, Bross *et al.*, 2003). Raloxifene (Evista, Eli Lilly & Co) is a further class of SERM that possesses some oestrogenic activity on bone, although it has been suggested to lack the oestrogenic effects on the uterus (Clarke *et al.*, 2003). Raloxifene is currently approved for the treatment of

osteoporosis in postmenopausal women based on its ability to prevent bone degradation (Delmas *et al.*, 1997) and has some inhibitory effects on breast cancer (Cummings *et al.*, 1999).

1.3.1.2 Faslodex- Selective Oestrogen Receptor Down-regulator in ER$^+$ Disease

Faslodex (Fulvestrant, AstraZeneca Pharmaceuticals) is a 7α-alkylated analogue of oestradiol, which competitively inhibits binding of oestradiol to the oestrogen receptor (Wakeling, 1991). The binding of faslodex to the ER compromises receptor dimerization, and energy-dependent shuttling, thus not allowing nuclear localisation of the receptor (Dauvois *et al.*, 1993). The simplified mechanism of faslodex action is it binds, blocks and accelerates degradation of the ER protein, and depletes activity of both AF-1 and AF-2 on any residual ER. This leads to complete inhibition of oestrogen signalling via the ER (Osborne *et al.*, 1995). Faslodex therefore lacks the pivotal agonistic effects which limit the efficacy of tamoxifen, for example on endometrial cell growth.

The mechanisms of tamoxifen action both in treatment and resistance are reasonably understood, whereas those of faslodex are less well studied. In studies using the MCF-7 human breast cancer cell line, treatment with faslodex significantly reduces protein levels of oestrogen receptor, which is followed by suppression of the oestrogen regulated genes pS2 and cathepsin D as well as progesterone receptor (Nicholson *et al.*, 1995; McClelland *et al.*, 1996; Rajah *et al.*, 1996). It has also been demonstrated in MCF-7 tumour xenograft models that faslodex is more effective than tamoxifen at suppressing both oestrogen and progesterone receptor proteins, as well as oestrogen responsive genes pS2 and pLIV 1 (Osborne *et al.*, 1995). Significantly, faslodex shows anti-tumour activity in tamoxifen-resistant cell lines (McClelland *et al.*, 1996), confirming a lack of cross-resistance between tamoxifen and faslodex models (Hu *et al.*, 1993; Howell, 2002). This observation appears to be translated into the clinic with approximately 45% of tamoxifen-resistant breast cancer patients responding favourably to treatment with faslodex (Howell *et al.*, 2002). Despite this, acquisition of resistance is still a fundamental issue. Moreover, emerging *in vitro* studies indicate an aggressive phenotype may ultimately result from the prolonged use of faslodex, associated with loss or silenced oestrogen receptor expression (Gee *et al.*, 2004) with an increase in tumour cell motility and invasive capacity (personal communication with Dr. Steve Hiscox; Nicholson *et al.*, 2005).

1.3.2 Oestrogen Deprivation

1.3.2.1 Aromatase Inhibitors in ER^+ Postmenopausal Disease

The rationale behind targeting the synthesis of oestrogens is not new, however this strategy in breast cancer patient's has recently gained in momentum for the treatment of both pre and postmenopausal women with the availability of the effective LHRH agonists and aromatase inhibitors (AIs) targeting the pituitary/ovarian axis and the P450 aromatase enzyme respectively. According to Buzdar and Howell (2001) it is knowledge of the peripheral route of oestrogen production in postmenopausal women that led to the development of aromatase inhibitors. Simplistically, aromatase inhibitors can be divided into two types based on their mechanism of action: steroidal and non-steroidal (see Table 1.2). The steroidal aromatase inhibitors (which are considered aromatase inactivators) bind to the substrate pocket of the enzyme causing irreversible inactivation, while the non-steroidal inhibitors bind competitively and reversibly to inhibit the P450 domain of the aromatase protein (Miller, 2004).

Table 1.2 Generations of aromatase inactivators and inhibitors

	Type I: Inactivators (Steroidal)	Type II: Inhibitors (Non-Steroidal)
Generation I	Testololactone	Aminoglutethimide
Generation II	Formestane (4-hydroxyandrostenedione)	Fadrozole
Generation III	Exemestane (Aromasin, Pfizer)	Anastrozole (Arimidex, Astra Zeneca) Letrozole (Femara, Novartis)

Aminoglutethimide (a phenobarbitone) was the first clinically available aromatase inhibitor and was used extensively as a second-line treatment of advanced breast cancer (Santen *et al.*, 1978; Wells *et al.*, 1978). Unfortunately, the use of aminoglutethimide inhibited the synthesis of all steroids yielding an extreme lack of selectivity with further limitations caused by its overall toxicity. It significantly influenced adrenocorticosteroid synthesis, therefore supplementation of corticosteroids, such as hydrocortisone, was necessary (Smith and Dowsett, 2003). Aminoglutethimide was associated with high incidence of side effects including skin rash, lethargy and orthostatic hypotension. One of the first steroidal aromatase inhibitors formestane, used during the early 1990s, caused fewer side effects and produced a degree of aromatase inhibition similar to aminoglutethimide (Coombes *et*

al., 1992), but it failed to show increased clinical benefit over tamoxifen. Although fadrozole, a second-generation non-steroidal inhibitor, did demonstrate a more potent and selective inhibitory affect on aromatization than aminoglutethimide, it also influenced 11-deoxycorticosterone and aldosterone concentrations (Santen 1991; Dowsett *et al.*, 1994).

Further development of aromatase inhibitors has now given us exemestane, anastrozole and letrozole, the so-called third generation of AIs. These compounds show a high degree of selectivity for the aromatase enzyme and they have improved tolerability. They do not have the same mode of action, with anastrozole and letrozole (triazole derivatives) interfering with the heme moiety of the P450 aromatase enzyme thereby suppressing serum levels of oestrogen without affecting other steroidogenic pathways (Dixon, 2004), while exemestane is a compound structurally related to the natural substrate androstenedione which acts as a 'suicide substrate' for the aromatase enzyme. Anastrozole and letrozole have recently been evaluated in a crossover comparison study involving 12 postmenopausal women with metastatic breast cancer. The mean inhibition of whole body aromatization was 97.3% for anastrozole and >99.1% for letrozole (Geisler *et al.*, 2002). Exemestane significantly lowers circulating oestrogen concentration without affecting other enzymes involved in the steroidogenic pathway and has highly potent *in vivo* aromatase inactivation producing a >97.9% inhibition (Miller and Dixon, 2000).

Since the mid-1990s exemestane, anastrozole and letrozole have emerged as an alternative to tamoxifen in the treatment of postmenopausal women with ER^+ advanced breast cancer and show a side-effect profile related to oestrogen withdrawal. This includes hot flushes, arthralgia, and bone demineralisation (Bonneterre *et al.*, 2000). There is no association with an increase rate of vaginal discharge, vaginal bleeding, or increased risk of pathological endometrial changes, including endometrial cancer, upon treatment with aromatase inhibitors (Angelopoulos *et al.*, 2004). Importantly, aromatase inhibitors do not appear to increase the risk of thromboembolic events (Baum *et al.*, 2002), which has been one of the life-threatening side effects associated with tamoxifen treatment.

In summary, the third-generation of aromatase inhibitors/inactivators provide greater selectivity and increased suppression of oestrogens than earlier generations of

compounds (Gershanovich *et al.*, 1998). However, more information is needed to make the final judgment on which, if any of these drugs is superior and optimal duration of usage. This will emerge from comparative studies. Interestingly, there appears to be a lack of cross-resistance between the inhibitors and the inactivators of the aromatase enzyme, suggesting that patients demonstrating disease relapse on non-steroidal compounds may benefit from additional treatment using a steroidal compound (Lonning *et al.*, 2000; Dixon, 2004).

1.3.3 Aromatase Inhibitors/Inactivators versus Tamoxifen in the Clinic: In ER$^+$ Postmenopausal Disease

In 1990 the Early Breast Cancer Trialists' Collaborative Group (EBCTCG) recommended adjuvant endocrine therapy for women with breast tumours that expressed oestrogen or progesterone receptors. The overview of multiple adjuvant trials demonstrated that tamoxifen was associated with a highly significant improvement in relapse-free and overall survival of breast cancer patients. 8 years later it became general practice to treat hormone receptor-positive early breast cancer patients with 5 years of tamoxifen treatment irrespective of age, menopausal status or tumour stage (Early Breast Cancer Trialists' Collaborative Group, 1998). In postmenopausal women a number of trials are currently investigating aromatase inhibitors (AIs) as alternatives to the gold standard tamoxifen.

1.3.3.1 Aromatase Inhibitors in Advanced Breast Cancer (First-line Therapy)

A patient with advanced disease unfortunately has a poor outlook as the breast cancer has already metastasized, and in this setting systemic therapies are only offered as palliative treatments to improve quality of life and hopefully to modestly improve survival. Recently, two large phase III trials have been set up to compare the efficacy and tolerability of the third-generation aromatase inhibitor anastrozole with tamoxifen, the TARGET (Tamoxifen and Arimidex Randomized Group Efficacy and Tolerability) trial and the NAT (North American Trial) trial. Significantly, both trials have shown that when the third-generation AIs are used as first-line therapy in postmenopausal women with advanced breast cancer they are at least equivalent to tamoxifen (Sainsbury, 2004). The primary end points of the TARGET trial were time to progression (TTP), objective response (OR) and tolerability, all of which demonstrated that anastrozole is equivalent to tamoxifen (Bonneterre *et al.*, 2000). The NAT trial included postmenopausal women with ER and/or progesterone

receptor (PR) positive or receptor unknown advanced disease. Patients were randomly assigned first-line treatment with either anastrozole or tamoxifen. Both treatments were well tolerated, with a significant increase in TTP among patients who received anastrozole versus those who received tamoxifen (11.1 vs. 5.6 months) (Nabholtz *et al.*, 2000). In both trials more patients treated with tamoxifen reported vaginal bleeding in comparison with those treated with anastrozole (TARGET: 2.4% vs. 1.2%, NAT: 3.8% vs. 1.2% respectively), which may provide evidence that there is a lack of stimulation on the endometrium with anastrozole.

In a randomized phase II EORTC (European Organisation for the Research and Treatment of Cancer) study in either hormone receptor positive or unknown breast cancers (Paridaens *et al.*, 2000), the overall response rate was higher for patients receiving exemestane than tamoxifen (44.6% vs. 14.3%) (Wong and Ellis, 2004). The phase III extension of the EORTC study, evaluated after a median follow-up of 29 months, showed that exemestane significantly increased OR compared to tamoxifen (46% vs. 31%, respectively), and increased progression-free survival by approximately 4 months (exemestane 9.9 months vs. tamoxifen 5.8 months) (Paridaens *et al.*, 2004). Letrozole has similarly demonstrated an increased clinical benefit as first-line therapy versus tamoxifen in a randomized phase III trial involving 907 postmenopausal women with ER^+ and/or PR^+ or receptor unknown advanced breast cancer. Results from this trial demonstrate that letrozole (vs. tamoxifen) significantly prolonged the median TTP by 57% (9.4 months vs. 6.0 months), reduced the risk of progression by 30%, and showed that the OR rate was significantly higher in patients receiving letrozole versus tamoxifen (32% vs. 21%, respectively) (Mouridsen *et al.*, 2003).

1.3.3.2 Adjuvant Trials: Early Breast Cancer

By definition early or primary breast cancer is operable and although the disease is confined to the breast (and potentially also axillary lymph nodes), adjuvant systemic therapy is necessary to combat micrometastatic deposits. Currently, in ER^+ postmenopausal women adjuvant tamoxifen treatment is the standard treatment, administered with a potential curative aim. Emerging data from several ongoing clinical studies, including the ATAC (5 years of Arimidex and Tamoxifen Alone or in Combination) trial, the BIG FEMTA (Femara-Tamoxifen Breast International Group) trial and the MA-17 study, suggest AIs potentially offer a more effective first line

therapy in comparison to tamoxifen in postmenopausal ER^+ women with early breast cancer when used as an adjuvant to surgery. The ATAC trial included more than 9,000 postmenopausal patient's (7839 hormone receptor positive, 768 negative, 759 status unknown) who were randomly allocated to receive tamoxifen or anastrozole singly, or in combination, for a total treatment duration of five years (ATAC Trialists' Group, 2002). The 47 month update analysis (Baum *et al.*, 2003) indicated that disease-free survival (DFS) and time to recurrence (TTR) were significantly prolonged for the patients that received anastrozole alone compared to those who received tamoxifen. After evaluation of the data, it was reported anastrozole promoted a 97% inhibition of the aromatase enzyme and a 90% reduction in circulating oestrogen levels (Sainsbury, 2004). Furthermore, combination of tamoxifen and anastrozole was found to be no more effective than tamoxifen alone and less effective than anastrozole alone therefore discontinued from the trial. The recent 68 month update states anastrozole significantly reduced distant metastases and contralateral breast cancers in conjunction with the significant increase in DFS and TTR versus tamoxifen alone (ATAC Trialists' Group, 2005).

The BIG-FEMTA trial has accrued over 5100 postmenopausal women with oestrogen/progesterone receptor positive disease treated with adjuvant letrozole and/or tamoxifen for 5 years (Goss, 1999). The trial is designed to compare a continuous course of each single agent for 5 years, as well as a randomization crossover study (3 years of tamoxifen followed by 2 years of letrozole or 3 years letrozole followed by 2 years of tamoxifen). The MA-17 trial included more than 5,000 post-menopausal patients, who were randomly allocated letrozole or placebo for five years following 4-6 years of adjuvant tamoxifen therapy. At the first interim analysis (~ 2.5 years), there was a significant benefit in terms of DFS for the women who had been prescribed letrozole following tamoxifen with an estimated four-year DFS rate of 93% compared with 87% in the placebo arm (Goss *et al.*, 2003). This highly significant benefit resulted in the MA-17 trial being prematurely terminated. Further endpoints within this trial included an assessment of bone fracture incidence, bone mineral density (MA-17B), together with lipid profiles (MA-17L) (Buzdar and Howell, 2001). An assessment of these endpoints is essential in all AI trials as it was evident during the early anastrozole studies that there was an increased bone fracture risk (Wong and Ellis, 2004). Furthermore, Elisaf *et al.* (2001) have reported that aromatase inhibitors alter cholesterol and lipoprotein metabolism which could

potentially cause detrimental effects on cardiovascular health, although to date there has been no substantial indication of such problems with AIs.

1.3.3.3 Neoadjuvant Trials

The aims of neoadjuvant hormonal therapy include reduction of tumour size prior to surgery to allow less extensive surgery, the avoidance of chemotherapy, and possible cure of the disease. In addition to improving breast conserving surgery, neoadjuvant therapy can provide an opportunity to explore drug development strategies *in vivo* (Ellis, 2004). Predictive biomarker studies can be carried out over a short period of time in order to gain insight into the molecular basis of endocrine therapy and intrinsic tumour resistance (Ellis, 2004). Furthermore, neoadjuvant therapy may be able to identify promising systemic strategies for additional testing in larger adjuvant trials, and finally neoadjuvant trials can allow new combinations and sequences of anti-cancer agents to be evaluated (Freedman *et al.*, 2005). Concerns do remain in the neoadjuvant setting regarding many of the standard prognostic factors including axillary-node status which in this case is unknown at the time of initial treatment (Dixon, 2004).

There have been several randomized trials designed to make comparisons between tamoxifen and AIs in the ER^+ neoadjuvant postmenopausal setting. The PO24 trial compared 4 months of treatment with either letrozole or tamoxifen in 324 post-menopausal women with oestrogen receptor positive and/or progesterone receptor positive disease (Eiermann *et al.*, 2001). These patients were considered not eligible for breast conservation at the time of diagnosis. Following treatment, overall response rates were statistically improved in the letrozole group versus tamoxifen (55% vs. 36%). In addition 45% of the patients receiving letrozole (vs. 35% on tamoxifen) were, on completion of the study, eligible for breast conserving surgery (Eiermann *et al.*, 2001). This study included assessment of EGFR and HER2 status and it was discovered that patients whose tumours were positive for EGFR and/or HER2 had an increased response rate in the letrozole arm (88% vs. 21% in the tamoxifen arm) (Eiermann *et al.*, 2001). The IMPACT (Immediate Preoperative Arimidex Compared with Tamoxifen) trial commenced in 1997 with a target accrual of 330 patients residing in Germany and the UK. The PROACT (Pre-Operative Arimidex Compared to Tamoxifen) trial, which began in 2000 with a target accrual of 440 patients is a multicenter trial being conducted in 10 different countries. The latter

two trials involving anastrozole (Arimidex), report no significant difference in response rate compared with tamoxifen, however in both trials anastrozole was associated with more patients able to undergo breast conserving surgery versus tamoxifen (46% vs. 22% in the IMPACT trial) (Janicke, 2004). The IMPACT trial also reported that HER2 positive patient's allocated anastrozole showed a higher response rate than those receiving tamoxifen (58% vs. 22%, respectively) (Freedman *et al.*, 2005).

1.3.4 Ovarian Ablation/ Suppression in Premenopausal Women

In premenopausal woman ovarian ablation (oophorectomy or ovarian irradiation) or suppression (LHRH analogues) are two oestrogen deprivation methods that promptly reduce circulating oestrogens to postmenopausal levels in nearly all treated women. AIs are not appropriate in this setting because they block the conversion of androgens (which are produced by the adrenal glands and ovaries) into oestrogens peripherally (in adipose, muscle, brain and breast tissue), a process by which the majority of postmenopausal oestrogen is produced. Surgical ablation of the ovaries is associated with irreversible premature menopause, increased risk of coronary artery disease, osteoporosis as well as permanent infertility (Goodwin *et al.*, 1999). Ovarian chemical suppression is achieved by the administration of a LHRH analogue, such as goserelin (Zoladex, AstraZeneca Pharmaceuticals), which causes permanent internalisation of LHRH receptors in the pituitary gland due to its 100- to 200-fold higher binding affinity versus LHRH (Angelopoulos *et al.*, 2004). Although goserelin causes an initial short-lived surge in LH/FSH and oestrogen levels, it rapidly promotes a decline in the levels of these hormones (Prowell and Davidson, 2004). Goserelin is associated with menopausal symptoms and osteoporosis, however its clear advantage is its reversibility (Prowell and Davidson, 2004). This allows young women the possibility to preserve future fertility, as well as limit the effects of osteoporosis or coronary artery disease.

Important comparison data has come from the Zoladex Early Breast Cancer Research Association (ZEBRA) study which assessed the efficacy of goserelin versus the chemotherapy regime cyclophosphamide, methotrexate, and fluorouracil (CMF) as adjuvant therapy in premenopausal patients with node positive breast cancer (Jonat *et al.*, 2002). The overall survival and disease-free survival between the treatments in ER^+ patients were identical, suggesting the well-tolerated goserelin as an alternative

to the highly toxic CMF (de Haes *et al.*, 2003). In the ER negative patient population goserelin was inferior to the CMF regime (de Haes *et al.*, 2003), supporting the importance of defining ER status in order to administer the appropriate therapeutic strategy. Klijn *et al.* (2001) have shown in a meta-analysis of four randomized clinical trials, that the combination of an LHRH agonist and tamoxifen had significant survival benefit in premenopausal women with advanced breast cancer versus endocrine monotherapy. The Austrian Breast and Colorectal Cancer Study Group 5 (ABCSG) has enrolled 1,034 patients randomised to receive either 3 years of goserelin with 5 years of tamoxifen or 6 cycles of CMF. Significantly, the 6 year survival, relapse-free and local recurrence-free survival rates were all in favour of the endocrine treatments versus chemotherapy (Jakesz *et al.*, 2002).

1.3.5 Future Development Studies and Research Considerations

Despite continued improvements in our capacity to alter the hormone environment of cancer cells, unfortunately, like the anti-oestrogen tamoxifen, it is known that treatment of breast carcinoma with AIs is also associated with the development of acquired resistance and patient relapse (Johnston and Dowsett, 2003). Moreover, to date no further improvement in overall survival has been reported with these agents versus tamoxifen. Thus there is not only an urgent need to consolidate the mechanisms by which anti-oestrogens fail to adequately impede breast tumour growth, but also to begin to understand how cells can adapt to a near total removal of endogenous oestrogen supply. Fortunately, there are experimental *in vivo* and *in vitro* oestrogen deprived breast cancer models that have already contributed significant information paralleling the findings in clinical disease.

1.4 DEVELOPMENT OF THE OESTROGEN DEPRIVATION RESISTANCE MODEL

Relatively little is known about the long-term effects of aromatase inhibitors and even less is known about the resistant phenotype that is emerging in the clinic compared to the information concerning the anti-oestrogen tamoxifen. Laboratories that have notably contributed to this area of research are those of Brodie, Martin/Dowsett, Santen and the Tenovus Centre for Cancer Research. Creating an *in vitro* oestrogen deprived model that mimics clinical acquired resistance has been difficult to achieve. Previous studies at the Tenovus Centre for Cancer Research (Helena Dunne,

observations not published) have shown that the hormone sensitive MCF-7 cells are not responsive to the aromatase inhibitor anastrozole and this lack of effect concurs with the observations made by Brodie and Njara (2000). It has also been shown that hormone sensitive MCF-7 cells only poorly express the aromatase enzyme under basal growth conditions (Brodie and Njara, 2000). To overcome this experimental obstacle Brodie *et al.* (2001) developed a preclinical intra-tumoural aromatase model (MCF-7_{CA}) using the MCF-7 breast cancer cell line stably transfected with the human placental aromatase gene which could be studied both *in vitro* and *in vivo* (Yue *et al.*, 1994). The model has been used to investigate the effects of letrozole and anastrozole on tumour growth and has demonstrated their inhibitory activity (Lu *et al.*, 1998). This model was also used to investigate combination anti-oestrogen and aromatase inhibitor treatments, which did not provide greater reductions in tumour growth than either letrozole or anastrozole alone (Lu *et al.*, 1999), paralleling the recent clinical trial data from the MA-17 and the ATAC trials. In order to understand the phenomenon of acquired resistance to aromatase inhibitors, Brodies' group has cultured the MCF-7_{CA} cell line for 8 months under steroid depleted conditions, and created the sub-line UMB-1Ca. This sub-line is reported to have increased expression of ER (faslodex sensitive), HER2, and activation of AKT as well as increased invasive behaviour compared to the parental MCF-7_{CA} (Sabnis *et al.*, 2005).

In vitro models of long-term oestrogen withdrawal have been developed from endocrine responsive cell lines, including MCF-7 (Santen *et al.*, 2004a; Martin *et al.*, 2003; Jensen *et al.*, 2003). For example, the model from Santen's group was achieved by use of phenol-red-free medium containing charcoal-stripped serum, where the oestradiol concentration is reduced to 10^{-13} M. Following a growth inhibitory phase, the long-term oestrogen deprived (LTED) cells acquired resistance and resumed substantial proliferation. A unifying feature of these *in vitro* models appears to be a retained mitogenic role for the oestrogen receptor. Such models commonly express increased ER and are growth sensitive to the pure anti-oestrogen faslodex. Long-term oestrogen deprivation has also been associated with the development of hypersensitivity to extremely low residual steroid hormone levels, which appear sufficient to support tumour cell growth *in vitro* and *in vivo* (Santen *et al.*, 2004a). Thus, in such cells a 4-log lower concentration of oestradiol (10^{-14} M) has been reported to be able to stimulate the growth of the resistant cells in comparison with the parental MCF-7 cell line. In the Santen model, the aromatase enzyme is

increased in response to oestrogen deprivation in parallel with the acquisition of oestrogen hypersensitivity (Yue *et al.*, 2001; 2003), however this may not occur in invasive breast cancer and clinical endocrine resistance (de Jong *et al.*, 2003). Interestingly, Fuqua *et al.*, (2000) have demonstrated that an ERα mutation (Lys303Arg) can enable increased co-activator recruitment to the receptor, conferring hypersensitivity in the presence of reduced oestrogens. Once again the significance of this to clinical breast cancer is unknown.

However, a potentially key mitogenic contribution to resistance to oestrogen deprivation, as well as adaptive hypersensitivity, is increased growth factor signalling (Song *et al.*, 2002; Santen *et al.*, 2004a), mirrored by supportive evidence arising from other forms of anti-hormone resistance, notably anti-oestrogen resistant clinical disease and oestrogen receptor negative states, as well as acquired anti-oestrogen resistant models (Knowlden *et al.*, 2003; Nicholson *et al.*, 2004a). IGF-1R, HER2 and downstream activation of MAPK and PI3K/AKT signalling have been implicated in the acquisition of resistance to oestrogen deprivation (Santen *et al.*, 2004a; Martin *et al.*, 2003) and anti-oestrogens (Nicholson and Gee, 2000; Hutcheson *et al.*, 2003; Knowlden *et al.*, 2003a). Long-term oestrogen deprived (LTED) cells from the study of Martin *et al.* (2003) revealed elevated MAPK activity that was suggested to be due to enhanced HER2 expression. These LTED cells also express elevated levels of IGF-1R and were sensitive to pharmacological inhibition of PI3K. In the Santen *et al.* (2004a) LTED model, MAPK is again up-regulated and there is also enhanced activation of AKT, p70 S6 Kinase and 4EBP-1 (all components of the PI3K pathway). In total these data suggest anti-growth factor therapies could find a clinical role in the treatment of resistance to oestrogen deprivation. However, there remains much to learn about the biology of this resistant state. Indeed, many of the models of oestrogen deprivation employed to date have been developed in the presence of serum growth factors, with in some cases further insulin, BSA and/or transferrin supplementation. It is thus possible that the availability of exogenous growth factors in these models may force an acquired resistance mechanism involving growth factor pathways and promote oestrogen hypersensitivity.

1.5 AIMS AND OBJECTIVES

To broaden the understanding of potential mechanisms contributing to oestrogen deprived resistant cell growth, the Tenovus Centre for Cancer Research has created a unique *in vitro* model system in which ER^+ endocrine responsive breast cancer MCF-7 cells are cultured under severe oestrogen and growth factor deprived conditions to create the resistant MCF-7X sub-line. The MCF-7X model represents an autocrine model not subject to the selective pressures of the previously reported *in vitro* models of long-term oestrogen deprivation (i.e. growth factor/serum supplementation).

The aims of the thesis centre around this MCF-7X model and are as follows:

- To determine whether resistance can still arise under the severe deprivation conditions and to characterise its associated cellular features.
- To determine if oestrogen receptor signalling still contributes to growth.
- To determine if this resistant phenotype has gained oestrogen hypersensitivity.
- To determine whether there is evidence for autocrine growth factor signalling pathways contributing to growth via i) receptor/ligands ii) intracellular kinases.
- To determine whether there is cross-talk between such signalling and the oestrogen receptor.
- To determine whether the identified growth mechanisms can be specifically targeted resulting in potential treatment strategies for resistance to oestrogen deprivation. Also to determine the phenotype of any resultant resistance, and to determine and evaluate intelligent combination treatments to prevent this state.

CHAPTER 2

∞ *MATERIALS AND METHODS* ∞

2.1 MATERIALS

Table 2.1 Cell culture plastic ware/ chemicals and suppliers list

	Product	Supplier
Cell Culture Plastic	T-Flasks: 25, 75 cm^2 Dishes: 35, 60, 100, 150 mm Plates: 12, 24 well 25 ml universal containers, 15 and 50 ml Falcon tubes, 5 ml bijou tubes, pipettes (25 ml, 10 ml, 5 ml), tips (5 ml, 1 ml, 200 µl, 10 µl)	Nunc- Gibco Invitrogen Corporation Paisley, UK
Cell Culture Chemicals	PD98059	Alexis Corporation Nottingham, UK
	7α-[9(4,4,5,5,5 pentafluoropentylsulfinyl)nonyl]-oestra-1,3,5(10)-triene-3,17β-diol (Faslodex, ICI 182,780, 'Fulvestrant'), (4-3-chloro-4-fluoroanilino)-7-methoxy-6-(3-morpholinopropoxyquinazoline) (Iressa, ZD1839, 'Gefitinib')	Astra-Zeneca Pharmaceuticals Cheshire, UK
	Phenol-red free DCCM	Biological Industries Ltd. Israel
	Phenol-red RPMI 1640 medium, Phenol-red-free RPMI 1640 medium, L-glutamine, Penicillin/streptomycin, Gentamycin, Fungizone, Dulbecco's phosphate buffered saline (PBS), DCCM, Lipofectin® Reagent, Trypsin	Gibco Invitrogen Corporation Paisley, UK
	SU6656, Vascular endothelial growth factor 121 (VEGF)	Merck Biosciences Ltd. Nottingham, UK
	ADW742	Novartis Basal, Switzerland

	Fibroblast growth factor (FGF)-acidic/ basic/ 7	R&D Systems Minnesota, USA
	Herceptin (Trastuzumab)	Roche Diagnostics Mannheim, Germany
	17-β oestradiol (E_2), 4-hydroxy tamoxifen, Amphiregulin, apo-Transferrin, Bis-indoylmaleimidine (Bis), Dimethyl sulphoxide (DMSO), Epidermal growth factor (EGF), Fetal Calf Serum (FCS), Glutaraldehyde, Heregulin α/β, Insulin-like growth factor (IGF)- I/ II, LY294002 hydrochloride, Platelet derived growth factor (PDGF), Transforming growth Factor (TGF)- α/β, Wortmannin	Sigma-Aldrich Dorset, UK

Table 2.2 Product and supplier list for assays and procedures

	Product	**Supplier**
	Anti-mouse horse-radish peroxidase (HRP)-linked antibody, Anti-rabbit HRP-linked antibody, Rainbow Marker (10-250 kDa), Random Hexamers- $pd(N)_6$, dNTP Set (100mM solutions)	Amersham Biosciences UK Ltd. Buckinghamshire, UK
	Super Sensitive Concentrated Detection System (Mouse)	Biogenex California, USA
	BIOTAQ® DNA Polymerase, HyperLadder IV	Bioline Ltd. London, UK
	DC Protein Assay kit, Tris-Hydrochloride (HCl) pH 8.8, Tris-HCl pH 6.8, Thin-wall PCR tubes	BioRad Laboratories Hemel Hempsted, UK
	Rabbit polyclonal antibody specific for: total Src, phospho-Src (Y418)	BioSource International Inc. California, USA

	Rabbit polyclonal antibody specific for: total p44/42 (ERK1/2) MAP kinase, phospho-p44/42 (ERK1/2) MAP kinase (Thr202/Tyr204), phospho- PKCδ (Thr505), phospho-PDK-1 (Ser241), total AKT, phospho-AKT (Ser473) Mouse monoclonal antibody specific for: phospho-ER (Ser118, 16J4)	Cell Signalling Technology Inc. Massachusetts, USA
	Phosphorylated EGFR (Tyr1173) mouse antibody	Chemicon Europe Ltd. Hampshire, UK
	3,3'- diamoniobenzidine tetrahydrochloride (EnVision DAB), EnVision Mouse and Rabbit, Goat anti-mouse antibody (GAM), Mouse monoclonal ERα (ID5) antibody, Mouse peroxidase anti-peroxidase (PAP), Normal goat serum (NGS), Mouse monoclonal PgR (636) antibody	DAKO Ltd. Ely, UK
	Acetone, Cylindrical test tubes (12 x 75mm, 4 ml), Cell Scraper, Ethanol, Formaldehyde, Finntip Stepper (5.0 ml), Magnesium Chloride, Methanol, Whatman Filter paper (grade 3,4), Transwell® Permeable Supports (6.5 mm, 8.0 μm pore size), Xylene	Fisher Scientific Leicestershire, UK
	Autoradiography Film	Genetic Research Instrumentation Essex, UK
	Normal human serum (NHS)	Golden West Biologicals Inc. California, USA
	Rabbit polyclonal antibody specific for: total EGFR (1005)-G	Insight Biotechnology Wembley, UK

	Alexa Flour 488-conjugated anti-mouse antibody, Custom Primers, M-MLV Reverse Transcriptase, Texas Red –X phalloidin	Invitrogen Paisley, UK
	Custom Primers	MWG Biotechnology London, UK
	Rabbit polyclonal antibody specific for: total AKT, phospho-AKT (Thr308)	New England Biolabs Ltd. Hitchin, Herts.
	Polyclonal pS2 antibody, 6F11 ER antibody	Novacastra Labs. Vision Biosystems Newcastle, UK
	0.2 μm Sterile Vacuum Cap Filter	Pal Corporation Lutterworth, UK
	SuperSignal® West Femto, Dura, Pico Antibody Detection	Pierce (Perbio) Cheshire, UK
	Luciferase Assay System with Reporter Lysis Buffer, MMLV, Recombinant RNasin® Ribonuclease Inhibitor, TAQ DNA Polymerase	Promega UK Ltd. Southampton, UK
	Ehrlich Haematoxylin (10%), Eosin (1%)	Raymond A Lamb East Sussex, UK
	Western Blocking Reagent	Roche Diagnostics Mannheim, Germany
	c-Fos (4) sc-52 g, rabbit polyclonal IGF-1R antibody N-20	Santa Cruz Biotechnology California, USA
	Protran BA 85 Nitrocellulose membrane (0.45μm)	Schleicher and Schuell Dassel, Germany
	Acrylamide 30%, Agar, Aprotinin, Bovine serum albumin (BSA), 5-Bromo,4-chloro,3-indolyl β-galactopyranoside (X-gal), Bromophenol Blue, Chloroform, Dextran T-70, Dithiothreitol (DTT), Ethylenediamine tetra-acetic acid (EDTA), Ethylene glycol-bis (2-	Sigma-Aldrich Dorset, UK

	aminoethylether)-N,N,N'N'-tetra-acetic acid (EGTA), Gelatine 2%, Glycerol, Glycine, H_2O Sterile, Isopropanol, Leupeptin, Macro-disposable cuvettes (4 ml), Methyl Green, Paraplast Embedding Media, Phenol, Phenylarsine, Phenylmethylsulfonyl Fluoride (PMSF), Polaroid Black and White Print Film (Type 667), Potassium Ferricyanide, Potassium Ferrocyanide, Saponin, Sodium Chloride, Sodium Dodecyl Sulphate (SDS), Sodium Fluoride, Sodium Molybdate, Sodium Orthovanadate, Temed, Tri-reagent® Triton X-100, Trizma Base, Trizma HCl	
	Rabbit polyclonal antibody specific for: phospho- ErbB2/HER2 (Y1248)	Upstate Biotechnology Buckingham, UK
	Vectashield® Mounting Medium w/ DAPI	Vector Laboratories California, USA

2.2 CELL CULTURE

2.2.1 Routine Maintenance of MCF-7 Cells

The ER positive endocrine responsive MCF-7 human breast cancer cell line was routinely maintained in phenol-red RPMI medium supplemented with 5% (v/v) fetal calf serum (FCS), penicillin-streptomycin (100 U/ml) and fungizone (2.5 μg/ml). The cells were cultured as a monolayer in sterile T-75 cm^2 culture flasks at 37°C in a humidified 5% CO_2 atmosphere. Basal culture medium was replenished every 3-4 days. Passaging (sub-culturing) occurred at approximately 80-90% confluency. Culture medium was removed, cells were trypsinised and incubated at 37°C for 3-5 minutes. The detached cells were transferred to a sterile 25 ml universal container, while the remaining cells in the flask were washed with basal medium and transferred to the universal container. Cells were then centrifuged for 5 minutes at 1000 rpm

(168 x g). The resultant cell pellet was re-suspended and seeded into new sterile T-75 cm^2 culture flasks at split ratios of 1:10 and 1:20. Passages used for experimentation were between 12-26 and in-house mycoplasma tests were performed every 6 months by the cell culture personnel.

2.2.2 Routine Maintenance of MCF-7X Cells

The severely oestrogen and growth factor deprived MCF-7X sub-line was established within the Tenovus Centre for Cancer Research from the parental MCF-7 cell line. This resistance model system evolved after 4 months of continuous culture in phenol-red-free RPMI medium containing 5% (v/v) heat-treated (65°C for 40 min) charcoal-stripped FCS (XFCS), penicillin-streptomycin (100 U/ml), fungizone (2.5 µg/ml) and L-glutamine (400 mM). This basal culture medium was replenished every 3-4 days and passaging occurred at approximately 80-90% confluency as above (split ratios of 1:10 and 1:20). Passages used for experimentation were between 44-98 (15-28 months), and in-house mycoplasma tests were performed every 6 months by the cell culture personnel.

2.2.3 Dose Response Assays

Dose response assays were set up with two different objectives, i) to determine the optimal concentration of a test compound to be used and ii) to determine if there was a shift or alteration in sensitivity of the breast cancer cells within a dose range. The hormone sensitive MCF-7 and multiple in house anti-hormonal resistant (MCF-7X, TAM-R, FAS-R, and TAM/TKI-R, see Appendix) cell lines were utilised when new compounds were under investigation. Cells were seeded into 24-well plates (~4 x 10^4 cells/well) and allowed to adhere for 24 hours. The treatments were added in triplicate at each dose selected (see Table 2.3), replenished at day 3-4 and trypsin dispersed for Coulter (Multisizer II) whole cell counting on day 7 (experiments were performed in triplicate). The wide range of treatments and doses used are given in Table 2.3.

Table 2.3 Compounds and cell lines utilised for dose response assays

Compound	Cell Lines	Carrier	Dose Range
E_2	MCF-7 MCF-7X	Ethanol	10^{-15} M, 10^{-14} M, 10^{-13} M, 10^{-12} M, 10^{-11} M, 10^{-10} M, 10^{-9} M, 10^{-8} M, 10^{-7} M, 10^{-6} M, 10^{-5} M
Faslodex	MCF-7 MCF-7X	Ethanol	10^{-13} M, 10^{-12} M, 10^{-11} M, 10^{-10} M, 10^{-9} M, 10^{-8} M, 10^{-7} M
Transferrin	MCF-7 MCF-7X	H_2O	0.01 μM, 0.05 μM, 0.1 μM, 0.5 μM, 1.0 μM, 5.0 μM, 10.0 μM
Faslodex + Transferrin (4 μg/ml)	MCF-7 MCF-7X	Ethanol	10^{-13} M, 10^{-12} M, 10^{-11} M, 10^{-10} M, 10^{-9} M, 10^{-8} M, 10^{-7} M
PD98059	MCF-7 MCF-7X	DMSO	25 μM, 50 μM

2.2.4 Growth Stimulation Assays

The Parental MCF-7 and MCF-7X cells in log-phase growth were dispersed by trypsinisation, re-suspended in experimental medium (see Appendix) and seeded into 24-well plates (~4 x 10^4 cells/well). The cells were allowed 24 hours to adhere to the plastic before the following treatments were added (in triplicate wells):

- Control (containing carrier ethanol, DMSO or H_20)
- 17-β Oestradiol (E_2), 10^{-9} M
- EGF, 10 ng/ml
- TGF α, 10 ng/ml
- Amphiregulin, 10 ng/ml
- Heregulin α, 10 ng/ml
- Heregulin β, 10 ng/ml
- aFGF, 10 ng/ml
- bFGF, 10 ng/ml
- FGF7, 10 ng/ml
- IGF-I, 10 ng/ml
- IGF-II, 10 ng/ml
- PDGF, 10 ng/ml
- VEGF, 10 ng/ml
- Transferrin, 4 μg/ml

The experimental medium containing the various treatments was replenished every 3-4 days. The cell growth was measured by trypsin dispersion followed by Coulter whole cell counting on day 7 (experiments were performed in triplicate).

2.2.5 Growth Inhibition Assays

The parental MCF-7 and MCF-7X cells in log-phase growth were dispersed by trypsinisation, re-suspended in experimental medium and seeded into 24-well plates (~4 x 10^4 cells/well). The cells were allowed 24 hours to adhere to the plastic before the following treatments were added (in triplicate wells):

- Control (containing carrier ethanol, DMSO or H_2O) *
- Faslodex (FAS), 10^{-7} M *
- Tamoxifen, 10^{-7} M
- Gefitinib, 1 μM
- Herceptin, 100 nM
- Gefitinib/ Herceptin, 1μM/100nM
- ADW742, 1 μM
- SU6656, 1 μM
- LY294002 (LY), 5 μM *
- Wortmannin (Wortm), 1 μM
- PD98059 (PD), 25 μM *
- Bis, 0.5 μM

* +/- Transferrin, 4 μg/ml

The experimental medium containing the various treatments was replenished every 3-4 days. The cell growth was measured by trypsin dispersion followed by Coulter whole cell counting on day 7.

2.2.6 Growth Curve Assays

MCF-7 and MCF-7X cells in log-phase growth were dispersed by trypsin and re-suspended in experimental medium and seeded into 24-well plates (~4 x 10^4 cells/well). The cells were allowed 24 hours to adhere to the plastic before the following treatments were added (in triplicate wells):

- Control (containing carrier ethanol, DMSO or H_2O) *
- E_2, 10^{-9} M
- Faslodex, 10^{-7} M *
- LY294002, 5 μM *
- Wortmannin, 1 μM
- PD98059, 25 μM *
- FAS/LY, 10^{-7} M/ 5 μM
- FAS/Wortm, 10^{-7} M/ 1 μM
- LY/PD, 5 μM/ 25 μM
- Wortm/PD, 1 μM/ 25 μM
- FAS/LY/PD, 10^{-7} M/ 5 μM/ 25 μM
- FAS/Wortm/PD, 10^{-7} M/ 1 μM/ 25 μM

* +/- Transferrin, 4 μg/ml

The experimental medium containing the various treatments was replenished every 3-4 days. The cell growth was measured by trypsin dispersion followed by Coulter whole cell counting every 24 hours for 15 days.

2.2.7 Development of MCF-7X Drug-Resistant Sub-lines

The MCF-7X cell line (passage 74) was trypsin dispersed and seeded into 8 T-25 cm^2 flasks and grown to 70% confluency. The following treatments were added to each individual flask for long term culture:

- Control (basal medium)
- Faslodex, 10^{-7} M
- LY294002, 5 μM
- PD98059, 25 μM
- FAS/LY, 10^{-7} M/ 5 μM
- LY/PD, 5 μM/ 25 μM
- FAS/LY/PD, 10^{-7} M/ 5 μM/ 25 μM

Cell growth was closely monitored and medium was replenished every 3-4 days. When increased tumour cell growth became evident, the cells were trypsinised, re-suspended in medium and seeded into sterile T-25 cm^2 flasks at a split ratio of 1:2. As tumour cell growth proceeded more rapidly, the cells were passaged at a split ratio of 1:10, 1:5 and 1:2. In general the T-25 cm^2 1:5 flask was chosen for passaging, while the 1:10 and 1:2 flasks were kept for observation. Once the cells were in rapid log-phase growth (e.g. resistant to the drugs), cells were seeded into new sterile T-75 cm^2 flasks and passaged at a 1:10 split ratio. Resistant cell lines were derived from the MCF-7X cells treated with faslodex [X(FAS)], LY294002 [X(LY)], PD98059 [X(PD)], faslodex/LY294002 combined [X(FAS/LY)], and LY294002/PD98059 combined [X(LY/PD)].

2.3 RNA ANALYSIS

2.3.1 Total RNA Isolation

Cells were grown as monolayers on 100 mm culture dishes (~2.5 x 10^4 cells/dish initial seeding density) to 80% confluency. Table 2.4 describes the cell lines and treatments used prior to RNA isolation. Cell medium was replenished on day 3 or 4 and on day 7 cells were lysed with Tri-Reagent® (Sigma-Aldrich). After 5 minutes at room temperature, phase separation was achieved by adding 0.2 ml of chloroform per ml of TRI-Reagent®. Following a 10 minute incubation (at room temperature), the resulting mixture was centrifuged at 12,000 x g for 15 minutes at 4°C. The RNA remained in the aqueous phase (upper phase) which was transferred to a new tube for RNA precipitation. The aqueous phase was mixed with 0.5 ml of isopropanol per ml of TRI-Reagent® used, incubated at room temperature for 5 minutes and centrifuged at 12,000 x g for 10 minutes at 4°C. The supernatant was removed and the RNA

precipitate was washed with 1 ml of 75% ethanol. Following gentle inverting of the tube, the mixture was centrifuged at 7,500 x g for 5 minutes at 4°C. After removal of the 75% ethanol wash, the RNA was dissolved in sterile water (50 µl) and stored at –80°C.

Table 2.4 Cell lines and treatments utilised for RNA analysis

Cell Line	Medium	Treatment
MCF-7 MCF-7X	wRPMI + 5% SFCS wRPMI + 5%XFCS	Control (ethanol, DMSO)* Faslodex, 10^{-7} M* LY294002, 5 µM* PD98059, 25 µM* FAS/LY, 10^{-7} M/ 5µM* LY/PD, 5 µM/ 25 µM* FAS/LY/PD, 10^{-7} M/ 5 µM/ 25 µM* * +/- Transferrin, 4 µg/ml
X(FAS)	wRPMI + 5% XFCS + Faslodex (10^{-7} M)	N/A
X(LY)	wRPMI + 5% XFCS + LY294002 (5 µM)	N/A
X(PD)	wRPMI + 5% XFCS + PD98059 (25 µM)	N/A
X(FAS/LY)	wRPMI + 5% XFCS + FAS/LY (10^{-7} M/ 5 µM)	N/A
X(LY/PD)	wRPMI + 5% XFCS + LY/PD (5 µM/ 25 µM)	N/A

2.3.2 Measurement of Total RNA Concentration and Integrity

The concentration of the RNA isolated from each sample was measured using a spectrophotometer (CECIL 2000 series) at $A_{260/280}$, using a 1/100 dilution of RNA in sterile H_2O using the formula 40 µg RNA @ 260 nm = optical density of 1.000. The RNA integrity was validated by electrophorating 1 µg of RNA (loading buffer, see Appendix) through a 2% agarose gel in 1X tris acetate (TAE, see Appendix) buffer (80 volts for 35 minutes).

Figure 2.1 Day 7 Basal MCF-7X RNA Integrity Gel (three separate RNA samples)

2.3.3 Reverse Transcription of RNA

The RNA was reverse transcribed into matching or complementary DNA (cDNA). First, 1 µg of RNA in a total volume of 7.5 µl of sterile H_2O was added to 11 µl of RT master mix (see Appendix), this solution was then denatured at 95°C for 5 minutes in a BioRad ICycler PCR machine and cooled immediately to 4°C. While on ice the reverse transcriptase enzyme M-MLV (Moloney Murine Leukemia Virus, 200 U/µl) and the Recombinant RNasin® ribonuclease inhibitor (40 U/µl) was added to each tube of RNA being transcribed. The tubes were then placed in the PCR machine and reverse transcribed using the following parameters:

Annealing Time: 10 minutes @ 22°C

RT Extension Time: 42 minutes @ 42°C

Denaturing Time: 5 minutes @ 95°C

To verify the reverse transcription of the RNA samples, an β-Actin polymerase chain reaction (PCR) was performed. The resulting cDNA was stored at –20°C until further PCR assays were carried out.

Figure 2.2 Day 7 Basal MCF-7X Actin (204 bp) RT-PCR reaction at 25 cycles (three separate samples)

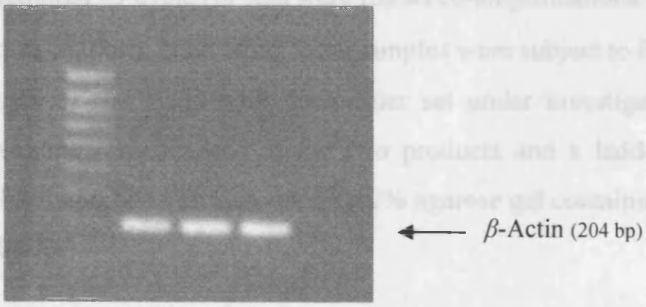

2.3.4 Polymerase Chain Reaction (PCR)

A PCR reaction master mix (see Appendix), including the target primers, was prepared based on the number of samples that were being run. The mix was aliquoted into the appropriate number of sterile tubes and 0.5 µl of sample cDNA was added to each (a negative control contained master mix and sterile H_2O only). The first cycle consists of heat denaturation to separate the double stranded DNA, annealing of the primers to their complementary sequences at a lower temperature, and extension of the annealed primers with stable DNA polymerase:

Denaturing Time: 2 minutes @ 95°C

Annealing Time: 1 minute @ 55°C

Extension and Formation of PCR Product: 10 minutes @ 72°C

This is followed by repeat cycles of heat denaturing, annealing and extension so that one cycle doubles the amount of DNA synthesized by the previous one. The annealing temperature* and cycle number** were optimised for each set of primers.

Denaturing Time: 30 seconds @ 94°C
Annealing Time: 1 minute @ 55°C*
Primer Extension: 1 minute @ 72°C
} x n cycles**

The final cycle consists of:

Denaturing Time: 1 minute @ 94°C

Annealing Time: 1 minute @ 55°C

Final Extension Time: 10 minutes @ 60°C

A complete list of primer sequences and PCR parameters is presented in Table 2.5. The primer design was carried out in-house using Basic Local Alignment Search Tool (BLAST, http://www.ncbi.nlm.nih.gov/BLAST/). Each primer set was optimised against multiple cell lines, a series of cycle numbers were evaluated, and annealing temperature was varied, to ensure quality of the final product. Primer sets that required 29 cycles or less were run as co-amplifications with β-Actin (to enable semi-quantitation), in all other cases samples were subject to PCR once with β-Actin (@ 25 cycles) and again with the primer set under investigation. The combination (1:3 volume ratio loaded) of the two products and a ladder marker (HyperLadder IV, 1000-100 bp) was then run on a 2% agarose gel containing ethidium bromide (in TAE buffer).

Table 2.5 Target primer sequences and PCR parameters

Target	Forward Sequence	Reverse Sequence	Cycles/ Annealing Temperature	Size (bp)
β-Actin	5'GGAGCAATGATCTT GATCTT-3'	5'CCTTCCTGGGCATG GAGTCCT-3'	25/ 55°C	204
AKT-1	5'ATGAGCGACGTGG CTATTGTGAGG-3'	5'GAGGCCGTCAGCC ACAGTCTGGATG-3'	29/ 55°C	329
AKT-2	5'ATGAATGAGGTGT CTGTCATCAAAGAAG GC-3'	5'TGCTTGAGGCTGTT GGCGACC-3'	29/ 55°C	314
c-fos	5'GAGATTGCCAACCT GCTGAA-3'	5'AGACGAAGGAAGA CGTGTAA-3'	32/ 55°C	483
c-myc	5'CCAAGCTCGTCTCA GAGAAG-3'	5'CAGCAGGATAGTC CTTCCGA-3'	29/ 55°C	549
c-src	5'CAGTGTCTGACTTC GACAAC-3'	5'CTCCTCTGAAACCA CAGCAT-3'	30/ 55°C	433
ER α	5'GGAGACATGAGAG CTGCCAAC-3'	5'CCAGCAGCATGTC GAAGATC-3'	25/ 55°C	432
HER2	5'CCTCTGACGTCCAT CATCTC-3'	5'ATCTTCTGCTGCCG TCGCTT-3'	35/ 55°C	98
IGF-1R	5'GAGCAGATGACAT TCCTGGG-3'	5'CCTGGACATAGAA GAACACAG-3'	26/ 55°C	287
$P21^{cip1/waf1}$	5'GTCTCAGTGTTGAG CCTTTTCC-3'	5'TCCGCTGCTAATCA AAGTGC-3'	30/ 55°C	460
PKC α	5'AGTGCACCATGGT AGAAAAGC-3'	5'TAGCTCGTCTTCAT CTTCACC-3'	34/ 55°C	494
PKC δ	5'CACCATCTTCCAGA AAGAACG-3'	5'CTTGCCATAGGTCC CGTTGTTG-3'	30/ 55°C	351
pS2	5'CATGGAGAACAAG GTGATCTG-3'	5'CAGAAGCGTGTCT GAGGTGTC-3'	25/ 55°C	336
Tf	5'CTGCACCAGGCTCT ATCCTAG-3'	5'GTACCTAACTCTGC ACAGGTG-3'	32/ 55°C	316
TfR	5'TCTGCTATGGGACT ATTGCTG-3'	5'CTGTTGCAGCCTTA CTATACG-3'	25/ 55°C	484

The PCR products were run on 2% agarose (TAE buffer) gels in the presence of ethidium bromide (5 mg/ml stock) at 80 volts for 35 minutes. The gel was then exposed to UV light to visualise bands and photographed. Using a BioRad GS-690 Imaging Densitometer each PCR photographed result was scanned.

2.4 TRANSIENT TRANSFECTION ASSAYS

2.4.1 Cell Culture and Transfection (18 hour)

The parental MCF-7 and MCF-7X cells in log-phase growth were dispersed by trypsinisation, re-suspended in experimental medium and seeded into 12-well plates (~2.5 x 10^5 cells/well). After 24 hours, the following solutions were prepared for each transfection:

A) 3 µl of Lipofectin® Reagent (Gibco Invitrogen Corp.) plus 60 µl serum free/phenol-red free DCCM medium containing L-glutamine (400 mM) per well.

B) 1.1 µg plasmid DNA, consisting of 400 ng of the reporter construct of interest* or control construct plus 700 ng carrier plasmid DNA in 60 µl serum free/phenol-red free DCCM per well.

* of either ERE or AP-1 luciferase

Oestrogen Response Element (ERE)-firefly luciferase reporter plasmid. ERE is a dual reporter construct therefore the addition of a third construct, renilla luciferase reporter plasmid (150 ng) was included. The levels of carrier were adjusted to 550 ng so that the overall DNA load was maintained.

or

Activating protein-1 luciferase reporter plasmid.

C) 5 µl DMSO diluted in 380 µl serum free/phenol-red free DCCM medium containing L-glutamine (400 mM) per well.

Solution A and B were left to equilibrate at 37°C. After 45 minutes, solution A and B were combined, gently mixed and returned to 37°C for a further 15 minutes. The A/B solution was then combined with C to produce the final transfection mixture. The cell culture medium was removed and the cell monolayers washed once with serum free/phenol-red free DCCM containing L-glutamine. The appropriate transfection mixture was added to each well and the plate was returned to incubate at 37°C for 6 hours. The transfection medium was then removed and the wells were washed with experimental medium before treatments (in triplicate) were added for 18 hours. Table 2.6 has the complete list of treatments applied to each ERE and AP-1 transient transfection assay.

Table 2.6 Transient transfection assays and treatment list

Reporter Construct		
ERE + Renilla The ERE construct is an ERE-tk-luc (firefly) reporter. Non-specific promoter transactivation (i.e. directly on the thymidine kinase promoter tk) is controlled by co-transfection into the same well with a non-ERE bearing reporter tk-luc (renilla). Thus levels of non-specific activation of this reporter are used to normalize the specific signal of ERE- driven luciferase production.	AP-1 AP-1 system differs in that transfection of parallel wells is performed using two constructs, which produce firefly luciferase a) AP-1-pTal-luc, which represents total transactivation of the reporter, b) pTal-luc, which represents only the promoter driven activity. The normalization of b) against a) gives the specific activity.	β-Galactosidase
Treatment		
Control (ethanol, DMSO) * E_2 Dose Response, 10^{-15} M- 10^{-8} M E_2, 10^{-9} M Faslodex, 10^{-7} M * LY294002, 5 μM * PD98059, 25 μM * FAS/LY, 10^{-7} M/ 5 μM * LY/PD, 5 μM/ 25 μM FAS/LY/PD, 10^{-7} M/ 5 μM/ 25μM *	Control (ethanol, DMSO) E_2, 10^{-9} M Faslodex, 10^{-7} M LY294002, 5 μM PD98059, 25 μM FAS/LY, 10^{-7} M/ 5 μM LY/PD, 5 μM/ 25 μM FAS/LY/PD, 10^{-7} M/ 5 μM/ 25μM	N/A

2.4.2 Preparation of Cell Lysates

Following 18 hours of treatment the medium was removed and the cells were washed with 1 ml PBS. The PBS was replaced with 200 μl of appropriate lysis buffer, 1X Passive Lysis Buffer (Promega, diluted from 5X stock with sterile H_2O) for dual ERE- firefly/Renilla luciferase assay, or 1X Reporter Lysis Buffer (Promega, diluted from 5X stock with sterile H_2O) for the AP-1 luciferase assay. The cells were gently scraped from the wells and transferred into 1.5 ml tubes, placed on ice (wet) until all tubes were collected. They were then stored at –80°C in order to perform a single freeze-thaw for complete lysis.

2.4.3 Luciferase Assay System

A dual-luciferase reporter assay kit (Promega UK Ltd.) was used to determine ERE-Renilla luciferase activity. To each sample luminometer tube 100 μl of assay reporter buffer was added, followed by the same volume of thawed sample lysate. This

mixture was read over 10 seconds using a Lumat LB 9507 luminometer (GC+C Wallac, UK). The tube was then removed, 100 µl of Stop and Glo® (Promega UK Ltd.) reagent was added to terminate the first phase, ERE luciferase activity, and initiate the second phase of the assay, measurement of the renilla luciferase activity. The tube was then re-placed into the luminometer for the final reading. To calculate activity the renilla reading was subtracted from the ERE reading for each individual sample. In the case of the AP-1 assay only the first step was followed, as Stop and Glo® was not required for the one reading of AP-1 luciferase activity.

2.4.4 In-situ β-*Galactosidase Fixation, Staining and Quantitation*

The β-Galactosidase transfected wells (in triplicate) were washed with 1 ml PBS prior to a 15 minute 0.5% glutaraldehyde fixation (1 ml/well, room temperature). The fixation solution was removed, the wells washed with 1 ml PBS, replaced with 1 ml of X-gal staining solution (see Appendix) and placed in incubator overnight. The percentage of transfected cells (β-Galactosidase positive stained) was used in the normalisation of each luciferase assay.

2.5 PROTEIN ANALYSIS: WESTERN BLOTTING

2.5.1 Cell Culture

Cells were seeded into 60 mm (~1 x 10^5 cells/dish) dishes and allowed to acclimatise for 24 hours. Monolayers were subsequently treated for 7 days with the agents that are listed in Table 2.7. Cell culture medium was replenished on day 3 or 4.

Table 2.7 Cell lines and treatments utilised for Western blotting

Cell Line	Medium	Treatment
MCF-7	wRPMI + 5%SFCS	Control (ethanol, DMSO) Faslodex, 10^{-7} M LY294002, 5 µM PD98059, 25 µM FAS/LY, 10^{-7} M/ 5µM
MCF-7X	wRPMI + 5%XFCS	Control (ethanol, DMSO) Faslodex, 10^{-7} M LY294002, 5 µM PD98059, 25 µM FAS/LY, 10^{-7} M/ 5µM LY/PD, 5 µM/ 25 µM FAS/LY/PD, 10^{-7} M/ 5 µM/ 25 µM
X(FAS)	wRPMI + 5% XFCS + Faslodex (10^{-7} M)	N/A

X(LY)	wRPMI + 5% XFCS + LY294002 (5 μM)	N/A
X(PD)	wRPMI + 5% XFCS + PD98059 (25 μM)	N/A
X(FAS/LY)	wRPMI + 5% XFCS + FAS/LY (10^{-7} M/ 5 μM)	N/A
X(LY/PD)	wRPMI + 5% XFCS + LY/PD (5 μM/ 25 μM)	N/A

2.5.2 Preparation of Whole Cell Lysates

At day 7, dishes of cells were washed in PBS (x 3) followed by the addition of ice cold lysis buffer (see Appendix). The cells were scraped from the dishes, transferred to sterile 1.5 ml tubes and subject to 4°C centrifugation at 13,000 rpm (14,196 x g) for 15 minutes. The supernatant was removed and stored in aliquots of 50 and 100 μl at –20°C until required for Western blotting.

2.5.3 Protein Concentration Assay

Total protein concentrations were determined using the DC BioRad protein assay (BioRad Laboratories Ltd.). According to the suppliers' recommendation, a standard curve was produced using the following dilutions of BSA (mg/ml) in lysis buffer in duplicate:

- 0
- 0.25
- 0.5
- 0.75
- 1.0
- 1.45

Protein samples were diluted 1:5 in lysis buffer to a volume of 50 μl (in duplicate). To each protein dilution 250 μl of reagent A (containing 20 μl reagent S/ 1 ml reagent A) and 2 ml of reagent B was added (see Appendix for description of reagent A,S and B). The samples were allowed to develop for 15 minutes before optical density was read at 750 nm on a spectrophotometer (CECIL 2000 series).

2.5.4 Sodium Dodecyl Sulphate (SDS)- PAGE

Electrophoresis was carried out using the Mini-Protein Slab II Electrophoresis Cell (BioRad Labs Ltd.,) and the apparatus was assembled to the manufacturers' recommendations. The separating gel (see Appendix) was poured to reach a level just below the well-forming comb, and allowed to set for 10-20 minutes. A layer of distilled H_2O was applied on top of the gel during this time to allow polymerization of the gel. The H_2O was removed and the well-forming comb was inserted before the

pouring of the stacking gel (see Appendix). Ready to use gels were then submerged in the electrophoresis tank containing 1X running buffer (see Appendix) and the combs were removed. Protein samples from total cell lysates (20-40 μg) were mixed with 10 μl Laemmli sample loading buffer (see Appendix) containing 20 mM dithiothreitol (DTT) and heat denatured (100°C) for 10 minutes. Samples were loaded, including one sample of Rainbow Marker (5 μl, 10-250 kD) onto each gel, and electrophoresis was carried out at 200 volts for 45 minutes.

2.5.5 Western Blotting

Western blotting was carried out using the Trans-Blot Electrophoretic Transfer Cell (Bio-Rad). A nitrocellulose membrane (0.45 μm), Whatman filter paper (grade 3) and sponge pads were pre-soaked in transfer buffer (see Appendix). Once the electrophoresis was complete, the separating gel was briefly soaked in transfer buffer before it and the other components of the transfer cassette were loaded together. The cassette was placed into the transfer tank (containing transfer buffer and an ice block) and was subject to electroblotting for 1 hour at a constant voltage (100V). The nitrocellulose membrane was removed from the cassette and incubated in blocking solution for 1 hour at room temperature on a rocking platform. The membrane was then probed with primary specific antibodies for target proteins (see Table 2.8). Following the primary incubation the membrane was washed in Trizma Buffered Saline (TBS-T, see Appendix) (5 x 5 minutes) prior to the addition of the secondary antibody. The antibody concentration and incubation duration for each specific target is described in Table 2.8.

Table 2.8 Western blotting antibody concentration and parameter list

Antibody	Block	Primary Antibody Concentration/ Duration	Secondary Antibody Concentration/ Duration	Film Exposure Time/ Detection System
Total- ER	Blocking Reagent	1:2000 / O/N	Anti-mouse 1:10,000 / 1 hour	30 seconds/ Femto
p-ER (Ser118)	Blocking Reagent	1:10,000 / 4 hours	Anti-mouse 1:10,000 / 1 hour	20 seconds/ Femto
Total- AKT	Blocking Reagent	1:1,000 / 4 hours	Anti-rabbit 1:10,000 / 1 hour	5 minutes/ Dura
p-AKT (Thr308)	Blocking Reagent	1:1,000 / 4 hours	Anti-rabbit 1:10,000 / 1 hour	2.5 minutes/ Dura
Total- ERK 1/2	Blocking Reagent	1:1,000 / 4 hours	Anti-rabbit 1:10,000 / 1 hour	2 minutes/ Femto
p-ERK 1/2 (Thr202/ Tyr204)	Blocking Reagent	1:1,000 / 4 hours	Anti-rabbit 1:10,000 / 1 hour	4.5 minutes/ Dura
Total- HER2	5% Marvel in TBS-T	1:1,000 / O/N	Anti-rabbit 1:10,000 / 2 hours	10 seconds/ Dura
p-HER2 (Y1248)	5% Marvel in TBS-T	1:1,000 / O/N	Anti-rabbit 1:10,000 / 2 hours	10 seconds/ Dura
Total- PKC-δ	Blocking Reagent	1:1,000 / O/N	Anti-rabbit 1:10,000 / 1 hour	30 seconds/ Dura
p-PKC-δ (Thr505)	5% Marvel in TBS-T	1:2,000 / O/N	Anti-rabbit 1:10,000 / 1 hour	1 minute/ Dura
p-PDK-1 (Ser214)	Blocking Reagent	1:4,000 / O/N	Anti-rabbit 1:10,000 / 1 hour	20 seconds/ Femto
p-p70S6K (Thr389)	Blocking Reagent	1:1,000 / O/N	Anti-rabbit 1:10,000 / 1 hour	30 seconds/ Femto
Total- Src	Blocking Reagent	1:1,000 / O/N	Anti-rabbit 1:10,000 / 1 hour	30 seconds/ Dura
p-Src (Y418)	Blocking Reagent	1:2,000 / O/N	Anti-rabbit 1:10,000 / 1 hour	30 seconds/ Femto
Total- EGFR	5% Marvel in TBS-T	1:1,000 / O/N	Anti-rabbit 1:10,000 / 2 hour	5 minutes/ Dura
Total- IGFR	Blocking Reagent	1:2,000 / 3 hours	Anti-rabbit 1:10,000 / 1 hour	5 minutes/ Dura
β-Actin	Blocking Reagent	1:10,000 / 4 hour	Anti-mouse 1:10,000 / 1 hour	5 seconds/ Dura

2.5.6 Detection and Analysis

The nitrocellulose membrane was washed in TBS-T (5 x 5 minutes) and placed into a plastic folder with a 1:1 dilution of chemiluminescent substrate (Super Signal West; Femto for strong signal enhancement, or Dura for moderate signal enhancement) for 5 minutes. The membrane was then placed into a light proof X-ray cassette and exposed to autoradiography film for various time intervals. The film was then developed using an X-ray film processor (X-ograph Imagining Systems). Using a

BioRad GS-690 Imaging Densitometer the results of each blot were scanned. Data was normalised against β-Actin expression for each blot.

2.6 PROTEIN ANALYSIS: IMMUNOCYTOCHEMISTRY

2.6.1 Cell Culture

Cells in log-phase growth were subject to trypsin dispersion, re-suspended in experimental medium and seeded onto 3-aminopropyltriethoxysilane (APES) –coated glass coverslips (~8 x 10^4 cells /coverslip) in 35 mm culture dishes. The cells were allowed 24 hours to adhere to the coverslip before treatments were added (see Table 2.9). Cell medium was replenished on day 3 or 4.

Table 2.9 Cell lines and treatments utilised for immunocytochemistry assays

Cell Line	Medium	Treatment
MCF-7	wRPMI + 5%SFCS	Control (ethanol, DMSO) E_2, 10^{-9} M Faslodex, 10^{-7} M LY294002, 5 μM Wortmannin, 1 μM PD98059, 25 μM FAS/LY, 10^{-7} M/ 5μM AG1024, 1 μM IGF-I, 10 ng/ml
MCF-7X	wRPMI + 5%XFCS	Control (ethanol, DMSO) E_2, 10^{-9} M E_2/ Faslodex, 10^{-9} M/ 10^{-7} M Faslodex, 10^{-7} M LY294002, 5 μM Wortmannin, 1 μM PD98059, 25 μM FAS/LY, 10^{-7} M/ 5μM LY/PD, 5 μM/ 25 μM FAS/LY/PD, 10^{-7} M/ 5 μM/ 25 μM
TAM-R	wRPMI + 5% SFCS + Tamoxifen (10^{-7} M)	Control (ethanol, DMSO) E_2, 10^{-9} M AG1024, 1 μM IGF-I, 10 ng/ml
X(FAS)	wRPMI + 5% XFCS + Faslodex (10^{-7} M)	N/A
X(LY)	wRPMI + 5% XFCS + LY294002 (5 μM)	N/A
X(PD)	wRPMI + 5% XFCS + PD98059 (25 μM)	N/A
X(FAS/LY)	wRPMI + 5% XFCS + FAS/LY (10^{-7} M/ 5 μM)	N/A
X(LY/PD)	wRPMI + 5% XFCS + LY/PD (5 μM/ 25 μM)	N/A

2.6.2 Coverslip Fixation

Optimal fixation immobilises the antigen, retains cellular structure while permitting antibody access to all cells and their cellular/sub-cellular compartments. Organic solvents such as alcohols and acetone remove lipids and dehydrate the cells, while precipitating protein architecture. Cross-linking reagents (such as paraformaldehyde) form intermolecular bridges, normally through a free amino acid groups, thus creating a network of linked antigens. These reagents preserve cell structure better than organic solvents, however may reduce the antigenicity of some cellular components and require a permeabilisation step to allow antibody access. Fixatives are selected based on the nature of the antigen being examined and on the properties of the antibody being used.

2.6.2.1 ERICA- (McClelland et al., *1991)*

Coverslips were removed from the 35 mm culture dishes and placed into a fixation rack. Coverslips were immersed into a 3.7% (v/v) formaldehyde (in phosphate buffered saline [PBS]) bath at room temperature for 15 minutes. They were then washed in a PBS bath at room temperature for 5 minutes, followed by 5 minutes in methanol (–10°C to –30°C) and 3 minutes in acetone (–10°C to –30°C). Finally coverslips were washed in PBS at room temperature for 5 minutes and then immersed in sucrose storage medium (SSM, see Appendix) and stored at –20°C.

2.6.2.2 Formal Saline (FS)-

Cell culture medium was removed from the 35 mm dishes and replaced with formal saline for 10 minutes. The formal saline (see Appendix) was removed and the coverslips were washed (2 x 5 minutes) in 70% ethanol followed by 2 x 5 minute washes in PBS before storage at –20°C in sucrose storage medium.

2.6.2.3 Phenol Formal Saline (pFS)- (Knowlden et al., *2005)*

Cell culture medium was removed from the 35 mm dishes and replaced with phenol formal saline (see Appendix) for 10 minutes. The phenol formal saline was removed and the coverslips were washed in 70% ethanol (3 x 5

minutes) followed by PBS washes (3 x 5 minutes) before storage at –20°C in sucrose storage medium.

2.6.2.4 Paraformaldehyde Vanadate (PFV)- (Britton et al., *2006)*

Cell culture medium was removed from the 35 mm culture dishes and replaced with 2% paraformaldehyde vanadate (see Appendix) for 20 minutes. The coverslips were subsequently washed with PBS (3 x 5 minutes) and stored in storage sucrose medium at –20°C.

2.6.2.5 Methanol Vanadate Acetone (MVA)- (Jones et al., *2004)*

Prior to fixation methanol and acetone baths were cooled to –10°C to –30°C. Cell culture medium was removed from the 35 mm culture dishes and replaced with methanol vanadate (see Appendix) for 5 minutes. The methanol vanadate was subsequently removed from the coverslips and replaced with methanol. At this time the coverslips were placed into a fixation rack, before being placed into an acetone bath for 5 minutes. The coverslips were then allowed to air dry for 30 minutes and stored dry at –80°C.

2.6.2.6 Acetone-

Coverslips were removed from the 35 mm culture dishes, placed into a fixation rack, then immersed in acetone (–10°C to –30°C) for 10 minutes. Coverslips were allowed to air dry for 30 minutes and stored dry at –80°C.

2.6.2.7 Chloroform Acetone (CA)-

Coverslips were removed from the 35 mm culture dishes and allowed to air dry for 2 hours before storing at –80°C. Prior to assay coverslips were immersed in a 1:1 chloroform/acetone solution at 4°C for 10 minutes. Coverslips were then allowed to air dry for 30 minutes before storing dry at –80°C.

2.6.2.8 Methanol Acetone (MA)-

Coverslips were removed from the 35 mm culture dishes, placed into a fixation rack and immersed into a methanol bath (–10°C to –30°C) for 5

minutes. Immediately followed by an acetone bath (−10°C to −30°C) for 5 minutes. Coverslips were then allowed to air dry for 30 minutes before storing at −80°C.

2.6.3 Immunocytochemistry

The following tables describe the immunocytochemistry assays according to which secondary detection system was utilised. Following two washes in PBS (5 minutes) and a blocking step the coverslips were incubated with a specific antibody. Coverslips were washed in PBS (3 x 3 minutes) followed by a PBS-T (phosphate buffered saline + 0.02% Tween 20) rinse before the addition of the secondary detection system. The coverslips were washed again in PBS (3 x 3 minutes) and again rinsed in PBS-T prior to the addition of the diaminobenzidine tetrahydrochloride and hydrogen peroxide (DAB) chromagen substrate. Tables 2.10 to 2.13 describe the details of each assay performed, grouped according to the secondary detection system utilised.

Table 2.10 Assays utilising the DAKO EnVision® detection system

Antibody	Fixation/ Block	Primary Antibody Concentration/ Duration	EnVision Detection Label Polymer HRP/ Duration	Chromagen DAB Duration
p-AKT (Thr308)	ERICA/ PBS-T*	1:200 (PBS)/ 120 min	Rabbit/ 60 min	10 min
p-ER (Ser118)	PFV/ PBS-T	1:400 (PBS)/ O/N	Mouse/ 120 min	6 min
p-ER (Ser167)	ERICA/ PBS-T	1:25 (PBS)/ O/N	Rabbit/ 120 min	10 min
p-IGFR (Y1316)	PFV or MVA/ PBS-T	1:200 (PBS)/ O/N	Rabbit/ 120 min	8 min
p-MAPK (Thr202/ Tyr204)	FS/ PBS-T	1:20 (PBS)/ 60 min	Rabbit/ 60 min	10 min
p-PDK-1 (Ser214)	ERICA/ PBS-T	1:50 (5%BSA/PBS)/ O/N	Rabbit/ 60 min	10 min
p-PKC-δ (Thr505)	ERICA/ PBS-T	1:20 (PBS)/ O/N	Rabbit/ 120 min	8 min
pS2	ERICA/ PBS-T	1:500 (PBS)/ 90 min	Rabbit/ 60 min	8 min
Total-IGFR	pFS/ PBS-T	1:125 (PBS)/ O/N	Rabbit/ 120 min	6 min

* PBS-T, Phosphate buffered saline + 0.02 % Tween 20.

Table 2.11 Assays utilising DAKO GAM/ PAP detection system

Antibody	Fixation/ Block	Primary Antibody Concentration/ Duration	2° Goat anti-Mouse (Z0420) Conc/ Duration	3° Mouse PAP (P0850) Conc/ Duration	Chromagen DAB Duration
Total-ER (ID5)	ERICA/ 10% NGS* in PBS	1:100 (PBS)/ 60 min	1:25 (PBS)/ 30 min	1:250 (PBS)/ 30 min	10 min
Total-ER (6F11)	ERICA/ PBS-T	1:75 (PBS)/ 90 min	1:25 (PBS)/ 30 min	1:250 (PBS)/ 30 min	10 min
p-EGFR (Tyr1173)	MA/ PBS-T	1:5 (PBS)/ O/N	1:25 (PBS)/ 30 min	1:250 (PBS)/ 30 min	10 min
PgR (636)	ERICA/ 10% NGS* in PBS	1:200 (PBS)/ 60 min	1:25 (PBS)/ 30 min	1:250 (PBS)/ 30 min	10 min
Total-PKC-δ	ERICA/ PBS-T	Pre-absorb w/ neat NHS** 30 min 1:50 (PBS)/ O/N	1:25 (PBS)/ 30 min	1:250 (PBS)/ 30 min	6 min

* NGS - normal goat serum, ** NHS - normal human serum.

Table 2.12 Assays utilising goat anti-rabbit secondary detection

Antibody	Fixation/ Block	Primary Antibody Concentration/ Duration	2° Goat anti-Rabbit Concentration/ Duration	Chromagen DAB Duration
c-fos (4)	ERICA/ 20% NHS in 0.1% BSA/PBS	1:500 (40% NHS in 5% BSA/PBS)/ O/N	1:40 (20% NHS in 0.1% BSA/PBS)/ 60 min	10 min*
Total – HER2	ERICA/ 5% NGS + 5% NHS in PBS	1:100 (5% NGS + 5% NHS in PBS)/ 60 min	1:50 (5% NGS +5% NHS in PBS)/ 60 min	6 min
p-HER2 (Y1248)	MVA/ PBS-T	1:20 (PBS)/ O/N	1:50 (0.1% BSA/PBS)/ 120 min	10 min

* An extra enhancement step is added to this assay: 0.5% copper sulphate in 0.85% sodium chloride solution, 5 min.

Table 2.13 Assays utilising the Biogenex Super Sensitive Link Label system

Antibody	Fixation/ Block	Primary Antibody Concentration/ Duration	2° Biogenex Mouse Link Conc/ Duration	3° Biogenex Mouse Label Conc/ Duration	Chromagen DAB Duration
CD71 (TfR)	pFS PBS-T	1:100 (PBS)/ 60 min	1:65 (1% BSA/PBS)/ 20 min	1:65 (1% BSA/PBS)/ 20 min	5 min DAB + 3 min Haemo-toxylin + 5 dH_2O
MIB-1	FS/ PBS-T	1:50 (PBS)/ 60 min	1:65 (1% BSA/PBS)/ 20 min	1:65 (1% BSA/PBS)/ 20 min	10 min
Total-EGFR	pFS or CA/ PBS-T	1:100 (PBS)/ O/N	1:65 (1% BSA/PBS)/ 20 min	1:65 (1% BSA/PBS)/ 20 min	10 min

2.6.4 Counterstain and Glass Slide Mounting

Following the DAB chromagen incubation, the coverslips were washed with distilled H_2O (3 x 3 minutes) and 0.5% methyl green (aqueous) solution added for 20-30 seconds to stain cell nuclei. After removal of the counterstain the coverslips were washed in distilled H_2O and air dried. The coverslips were then mounted on glass slides using a xylene soluble mountant (Depex, Sigma-Alrich), labelled appropriately and stored until immunostaining analysis.

2.6.5 Immunostaining Analysis

Assessment of the immunostaining was determined at X20/ X40 magnification on a dual viewing Olympus BH-2 light microscope by two people. Comparative areas of confluency were located and given estimates of the percentage and intensity of cells positively stained. These data were used to calculate a semi quantitative H-Score on a scale of 0-300 (McClelland *et al.*, 1991). Assays were performed in triplicate, and two areas of each coverslip were assessed.

H-Score = Σ (% of very weakly stained cells x 0.5)
+ (% of weakly stained cells x 1)
+ (% of moderately stained cells x 2)
+ (% of strongly stained cells x 3).

2.6.6 Haematoxylin & Eosin Staining

ERICA fixed coverslips were washed with PBS (3 x 3 minutes) prior to 10% Ehrlich Haematoxylin application for 10 minutes. The coverslips were then rinsed in tap H_2O for approximately 5 minutes prior to a 2½ hour application of 1% aqueous Eosin. The coverslips were washed in distilled H_2O (3 x 3 minutes), allowed to air dry then mounted onto glass slides using xylene soluble mountant.

2.7 IMMUNOFLUORESCENCE

2.7.1 Cell Culture

MCF-7 and MCF-7X cells in log-phase growth were subject to trypsin dispersion, re-suspended in experimental medium and seeded onto 0.17 mm thick coverslips (~8 x 10^4 cells /coverslip) in 35 mm culture dishes. Experimental medium was replenished on day 3 or 4 and on day 7, a portion of the coverslips was treated with E_2 (10^{-9} M) for 10 minutes prior to fixation with 3.7% (v/v) formaldehyde (in PBS) for 15 minutes. An equal portion of control and E_2 treated coverslips were permeabilised with 0.4% saponin (in 1% BSA/ PBS) for 15 minutes.

2.7.2 Total ER Assay

The fixed cells on the coverslips were blocked with 10% (v/v) normal goat serum and incubated for 1 hour with total ER (ID5, 1/20 in 1% BSA/ PBS +/- 0.4% saponin) antibody at room temperature. The secondary antibody utilized was Alexa Fluor 488-conjugated anti-mouse antibody (1/1000 in 1% BSA/ PBS +/- saponin) for 1 hour prior to 15 minute incubation in Texas Red phalloidin (6.6 μM). Coverslips were mounted on to glass slides with Vectashield mounting medium (with DAPI). Assessment of the coverslips was done on a Leica RPE automatic microscope using a X100 oil immersion lens. Fluorescent superimposed images were acquired by using a multiple band-pass filter set appropriately for DAPI (360 nm, blue), Alexa 488-fluorescein (488 nm, green) and Texas Red (594 nm, red).

2.8 MOTILITY AND INVASION

2.8.1 Insert Coating

2.8.1.1 Fibronectin Coating-

A fibronectin coating was applied to the bottom side of the Transwell® Permeable Support (6.5 mm, 8.0 μm pore size) inserts. For each insert that was being coated, a total volume of 300 μl was necessary to ensure that the bottom of the insert was properly submerged in the fibronectin solution (10 μg/ml in PBS). The fibronectin solution was aliquoted into the outer wells (grey wells, Diagram 2.1) and the inserts from the inner 12 wells were placed into the liquid. The plate was placed in an incubator at 37°C for 2 hours. Each insert was then washed in sterile PBS, placed upside down to dry and returned to the empty inner wells (white wells, Diagram 2.1).

Diagram 2.1 Transwell® Permeable Support 24-well plate

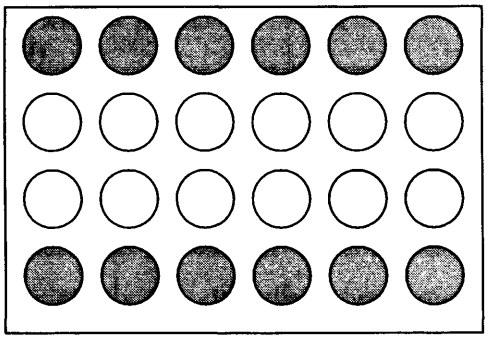

2.8.1.2 Matrigel Coating-

Matrigel coating was applied to the inside of the insert in order to form a barrier for cell invasion. Approximately 50 μg Matrigel (diluted in serum-free medium) was aliquoted on each insert utilising pre-cooled tips and allowed to set overnight at room temperature.

2.8.2 Cell Culture

MCF-7, MCF-7X and MCF-7X drug-resistant sub-lines in log-phase growth were subject to trypsin dispersion and re-suspended in appropriate experimental medium (see Table 2.14).

Table 2.14 Cell lines and treatments utilised for motility and invasion assays

Cell Line	Medium	Treatment
MCF-7	wRPMI + 5%SFCS	Control (ethanol, DMSO) Faslodex, 10^{-7} M LY294002, 5 μM PD98059, 25 μM FAS/LY, 10^{-7} M/ 5μM
MCF-7X	wRPMI + 5%XFCS	Control (ethanol, DMSO) Faslodex, 10^{-7} M LY294002, 5 μM PD98059, 25 μM FAS/LY, 10^{-7} M/ 5μM LY/PD, 5 μM/ 25 μM FAS/LY/PD, 10^{-7} M/ 5 μM/ 25 μM
X(FAS)	wRPMI + 5% XFCS + Faslodex (10^{-7} M)	N/A
X(LY)	wRPMI + 5% XFCS + LY294002 (5 μM)	N/A
X(PD)	wRPMI + 5% XFCS + PD98059 (25 μM)	N/A
X(FAS/LY)	wRPMI + 5% XFCS + FAS/LY (10^{-7} M/ 5 μM)	N/A
X(LY/PD)	wRPMI + 5% XFCS + LY/PD (5 μM/ 25 μM)	N/A

2.8.3 Motility Assay

Treatment medium (~600 μl) was placed in the appropriate inner (white) wells with the inserts in place and the plate was placed in a 37°C incubator while cells were prepared for seeding. Approximately 5 x 10^5 cells/ml were re-suspended in serum free/phenol-red-free RPMI medium containing the appropriate treatment. Each cell suspension (5 x 10^4 /well) was added to the inside of duplicate inserts. The plate was returned to incubate at 37°C for 24 hours.

The medium was removed from the inside and the bottom side of the insert washed with PBS. The cells on the bottom side were then fixed in 4% formaldehyde for 15 minutes at room temperature and then washed with PBS. After fixation the inserts were placed in the outer wells with a crystal violet solution for 15 minutes. Inserts were washed in PBS and excess stain was removed prior to air drying. Inserts were assessed by viewing at X10 on a microscope. Cell counts were taken from 5 representative fields of view on each insert.

2.8.4 Invasion Assay (Jones et al., *2004; Hiscox* et al., *2005)*

The matrigel coating was rehydrated by adding serum-free phenol-red-free RPMI (~100 µl) to each insert followed by an incubation period of 1 hour at 37°C. Approximately 5 x 10^4 cells/well in a volume of 200 µl (serum-free/phenol-red-free RPMI) containing the appropriate treatment was seeded to the upper compartment. The lower compartment was filled with 600 µl of phenol-red-free RPMI also containing the appropriate treatment.

Diagram 2.2 Transwell® Permeable Support insert

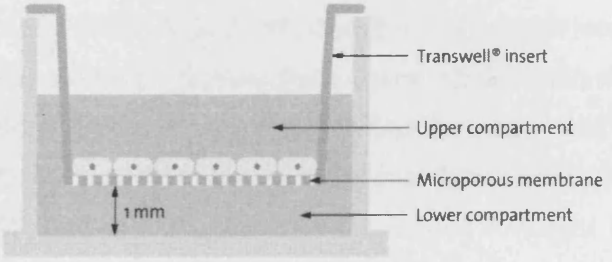

http://www.corning.com/lifesciences/technical_information/techdocs/transwell_guide.pdf

After the culture period of 72 hours, the medium was removed from the inside of the insert and its respective well. The matrigel layer on the inside of the insert was removed using a cotton bud (matrigel will stain thus making it difficult to assess). The cells on the reverse side were then fixed in 4% formaldehyde for 20 minutes at room temperature then washed with distilled H_2O. The membrane of each insert was removed using a scalpel then placed onto a glass slide containing a drop of Vectashield (mounting medium with DAPI). The membrane was then covered with a coverslip, allowed to dry and stored at 4°C in the dark until analysis. Each slide was analysed (cell counts taken from 5 representative fields of view/ slide) using a Leica microscope at DAPI wavelength (360 nm).

CHAPTER 3

∞ *RESULTS* ∞

3.1 MCF-7 to MCF-7X: THE ACQUISITION OF RESISTANCE TO OESTROGEN DEPRIVATION

As with other endocrine strategies, the acquisition of resistance remains a significant problem with aromatase inhibitors. Sadly improvement in relapse-free survival in the adjuvant setting remains modest and relapse rates in advanced disease are still measured in months rather than years (Nicholson *et al.*, 2004b). Studies focusing on this problematic development of resistance to oestrogen deprivation strategies are currently emerging, although model systems remain relatively sparse. An ER^+ long-term oestrogen deprived xenograft model has been described by Shim *et al.* (2000), while the laboratory of Brodie *et al.* (1999) describes a preclinical model system that used xenografts from the MCF-7 human breast cancer cell line stably transfected with the human placental aromatase gene ($MCF\text{-}7_{CA}$) to study both response and resistance. In addition long-term oestrogen deprived ERα positive *in vitro* models (Martin *et al.*, 2003; Santen *et al.*, 2004a) have also been developed from endocrine responsive cell lines, including MCF-7 cells (while a recent resistant model from Brodie/Sabnis has been developed from aromatase transfected cells, UMB-1Ca, Sabnis *et al.*, 2005). However, in most *in vitro* model systems to date the cell cultures have been developed and even maintained in the presence of serum growth factors with in some cases further insulin supplementation. This exogenous growth factor rich environment could feasibly force the acquired resistance mechanism and even promote oestrogen hypersensitivity, therefore masking any inherent tumour capabilities to escape control by oestrogen deprivation.

In order to decipher resistance *in vitro* to oestrogen deprivation in the absence of high levels of growth factors, phenol-red-free RPMI (wRPMI) containing 5% charcoal stripped, heat-inactivated foetal calf serum (termed XFCS medium) was utilised in our system. Importantly this approach, which depletes oestrogens and exogenous growth factors, still ensures cell viability and attachment (van der Burg *et al.*, 1988). The growth of the parental MCF-7 cell line subjected to these severely deprived conditions was inhibited by 74.3% compared to control MCF-7 cells grown in 5% charcoal stripped serum following 15 days of treatment. This initial phase of substantial growth inhibition was subsequently maintained under such conditions for 4 months. However, resistance was then acquired with proliferative activity of the resultant MCF-7X sub-line restored to that of the parental cell line prior to treatment (Figure 3.1). Later passages (44-98) of MCF-7X cells were utilised in the

experimental characterisation and functional analysis involved in this project to ensure a stable phenotype had been achieved. The MCF-7X cell model clearly demonstrates that the acquisition of resistance to oestrogen deprivation can still arise in the absence of exogenous growth factors, with input from any residual steroid hormone and presumably predominately any autocrine growth factor signalling apparently adequate.

In order to compare the visual morphology of the MCF-7 parental control versus the MCF-7X cell line, phase contrast images (Figure 3.2A) and Haematoxylin & Eosin (Figure 3.2B) stained images were obtained. The MCF-7 parental cell line was a relatively homogenous population with respect to cell size and shape. The cell nuclei were ovoid in shape containing few prominent nucleoli. These cells had a nuclear to cytoplasmic area ratio of approximately 1 : 4. In contrast, MCF-7X cells were a more heterogeneous population in size and shape with more prominent mitotic bodies. There were multiple nucleoli visible in the oestrogen deprived cells paralleled by a nuclear to cytoplasmic ratio of approximately 1.5 : 1. There was prominent attachment between MCF-7 cells when confluent, whereas the MCF-7X cells formed a loose 'cobble stone' structure where cell separation was evident (Figure 3.2A). In agreement with current literature (Sabnis *et al.*, 2005), the parental MCF-7 cells had very low levels of measured motility and invasiveness, a profile indicative of a non-aggressive phenotype. This was also noted in MCF-7X cells, and although difficult to accurately quantify, there was some suggestion of a further reduction in these features within the resistant line versus MCF-7 cells (Figure 3.3A/B).

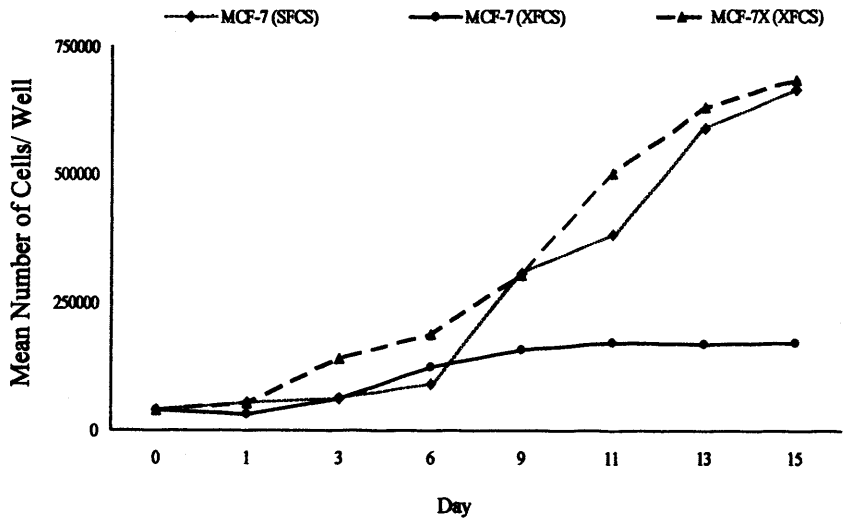

Figure 3.1 Basal MCF-7 and MCF-7X cell growth. MCF-7 cells were grown and maintained in phenol-red-free RPMI media containing 5% SFCS or XFCS for 15 days on 24-well plates. MCF-7X cells were grown and maintained in phenol-red-free media containing 5% XFCS for 15 days on 24-well plates. Triplicate wells were subject to trypsin dispersion and Coulter cell counting at each time point indicated.

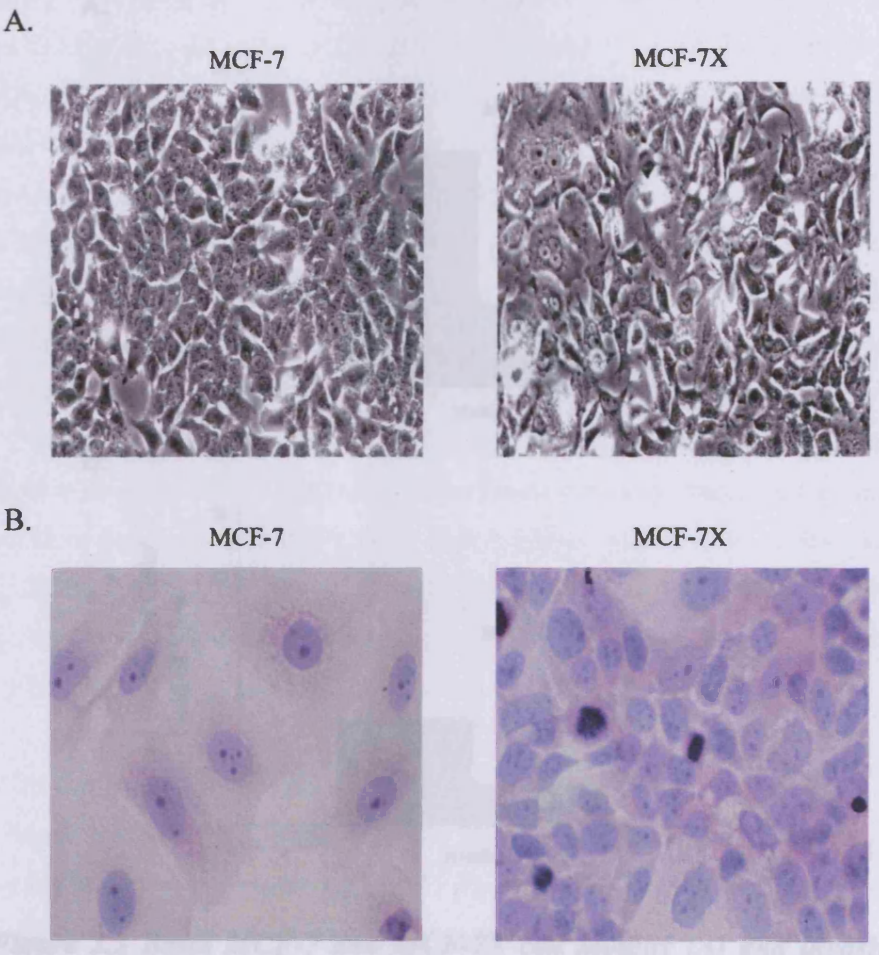

Figure 3.2 Basal MCF-7 and MCF-7X cell visual morphology by phase contrast imaging (A) and H&E staining (B). MCF-7 and MCF-7X cells were grown in phenol-red-free RPMI media containing 5% SFCS or XFCS respectively. (A) Cell phase contrast digital images were obtained during log phase growth (X20 magnification). (B) MCF-7 and MCF-7X cells were grown under the same conditions previously described for 7 days on coverslips prior to ERICA fixation. The cells were H&E stained with 10% Ehrlich Haematoxylin (10 min) followed by 1% Eosin (2½ hrs). The H&E digital images shown above are X40 magnification.

A.

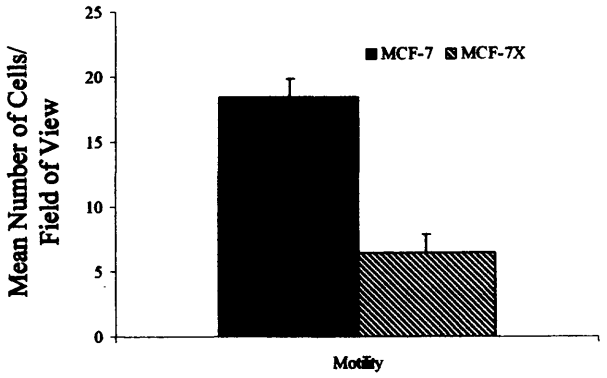

B.

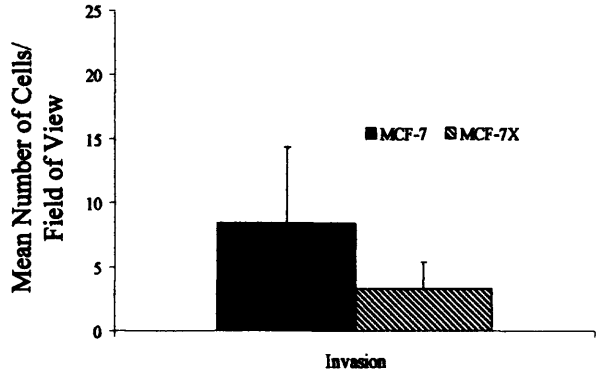

Figure 3.3 Basal MCF-7 and MCF-7X cell motility (A) and invasive capacity (B). (A) MCF-7 and MCF-7X cells were seeded onto fibronectin coated Transwell® permeable supports for 24 hours prior to formaldehyde fixation and crystal violet staining. (B) MCF-7 and MCF-7X cells were seeded onto matrigel coated Transwell® permeable supports for 72 hours prior to formaldehyde fixation and mounting on glass slides with mounting medium containing DAPI. These data represent the mean number of cells/field of view +/- SD of triplicate inserts.

3.1.1 Oestrogen Receptor (ERα) Expression

MCF-7 cells express oestrogen receptors (Horwitz *et al.*, 1978) which allow investigation of the effects of hormone and anti-hormone sensitivity. Extensive characterisation of the MCF-7X oestrogen deprived cell line versus the parental MCF-7 cells revealed considerable evidence that the oestrogen receptors are retained and functional in the resistant model. Both the MCF-7 and MCF-7X cell lines were cultured for 7 days (log-phase growth) to compare the mRNA and protein levels of ERα, employing RT-PCR, Western blotting and immunocytochemistry. These approaches revealed that, like MCF-7 cells, MCF-7X cells expressed substantial levels of ERα (Figures 3.4, 3.5 & 3.6). Moreover, a modest but significant increase in nuclear ERα was detected in MCF-7X versus the MCF-7 cells by immunocytochemistry ($p<0.001$*). This small increase was due to enhanced intensity of nuclear staining rather than an increase in the percentage of positivity (Figure 3.6). Although only a small 25.8% increase was evident in MCF-7X cells, more substantial adaptive increases in ERα expression have been commonly described for models of long-term oestrogen deprivation (3-10 fold increases, Martin *et al.*, 2003; Santen *et al.*, 2004a, Sabnis *et al.*, 2005). Of note, in MCF-7X cells the immunocytochemical staining was entirely nuclear, observations certainly suggestive that any ERα function may be predominantly genomic in these cells.

3.1.2 Classical ERα/ Genomic Signalling

To begin to assess if the nuclear ERα was transcriptionally active in the MCF-7X cell line and to evaluate comparatively versus the MCF-7 cell line, phosphorylation status of key AF-1 serine residues, 118 and 167 was first investigated by immunocytochemistry (Figure 3.7). Heterogeneous nuclear staining was apparent for Ser118ER phosphorylation in both MCF-7X and MCF-7 cells. Phosphorylated Ser167ER staining was also apparent in MCF-7 and MCF7X cells and was punctated within the nucleus. There was also cytoplasmic staining with the phospho-Ser167ER antibody, but previous antibody absorption studies in the laboratory have suggested this staining component is unwanted background and so was not quantified in this study. Nuclear ERα phosphorylation activity at serine 118 (Ser118ER) was increased by 28.6% ($p=0.037$*) in MCF-7X cells, but not significantly altered at serine 167 (Ser167ER) versus MCF-7 cells at day 7. The increase in Ser118ER was due to an increase in the percentage of cells stained positive. Basal ERα transcriptional activity was subsequently measured using luciferase ERE (oestrogen response element)

reporter gene construct assays in MCF-7X versus MCF-7 cells. There was a 5-fold increase in ERE reporter activity (Figure 3.8) in MCF-7X cells under basal growth conditions. In parallel with these reporter assays, basal expression of endogenous oestrogen regulated genes were monitored as a further indicator of ERα function. The oestrogen regulated gene pS2 was detectable in both MCF-7 and MCF-7X cells by RT-PCR (Figure 3.9) with pS2 mRNA expression significantly increased (65.5%, $p=0.017^*$) in the resistant model. Furthermore, there was a parallel increase (44.4%, $p<0.001^*$) in this cytoplasmic-localised protein expression by immunocytochemistry (Figure 3.10) at day 7. In MCF-7 cells progesterone receptor (a further oestrogen inducible gene) was heterogeneously detectable in the nuclei of approximately 30% of the cell population by immunocytochemistry but, in contrast to pS2 expression, in the MCF-7X cells there was a total loss ($p<0.001^*$) of this protein (Figure 3.11).

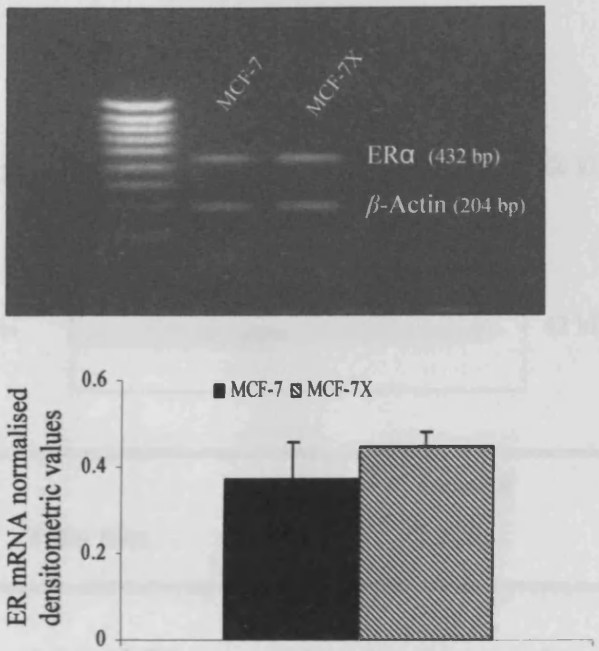

Figure 3.4 Basal MCF-7X versus MCF-7 cell mRNA expression of ERα by RT-PCR. MCF-7 and MCF-7X cells were grown on 100 mm dishes in phenol-red-free RPMI media containing 5% SFCS or XFCS respectively. Conditions were maintained for 7 days before RNA was isolated and reverse transcribed. Co-amplification RT-PCR of ERα (25 cycles/ 55°C annealing temperature, 432 bp) and β-Actin (204 bp) was performed. The RT-PCR product was run on a 2% agarose gel containing ethidium bromide, subsequently photographed, scanned and normalised to β-Actin. The digital image is representative of 3 experiments and the statistical analysis applied was an unpaired-T test (p=0.230) comparing mean ERα expression in MCF-7 (0.37 +/- 0.08) and MCF-7X (0.45 +/- 0.04) cells.

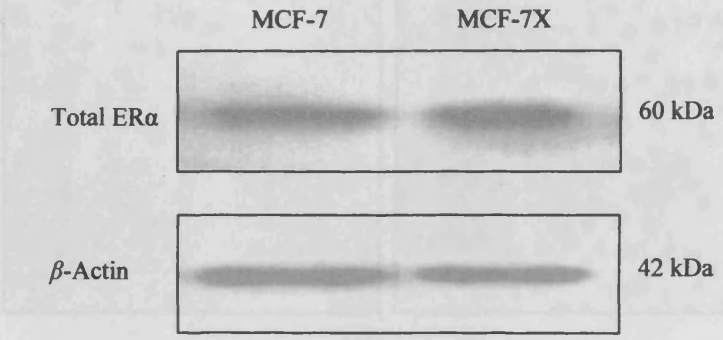

	MCF-7	MCF-7X
Total ERα	1.2 +/- 0.3	1.3 +/- 0.1

Figure 3.5 Basal MCF-7X versus MCF-7 cell expression of total ERα by Western blotting. MCF-7 and MCF-7X cells were grown on 60 mm dishes in phenol-red-free media containing 5% SFCS or XFCS respectively. Conditions were maintained for 7 days prior to whole cell lysis, SDS-PAGE (40 µg of sample protein/well) and Western blotting. The nitrocellulose membrane (0.45 µm) was probed for total ER (ID5, 60 kDa) and β-Actin (42 kDa). The developed autoradiography film was scanned using densitometric imaging for each blot probed and ERα expression was normalised to β-Actin. Data are presented as the mean (+/- SD) and the image above is representative of 3 experiments.

Total Oestrogen Receptor (ERα)

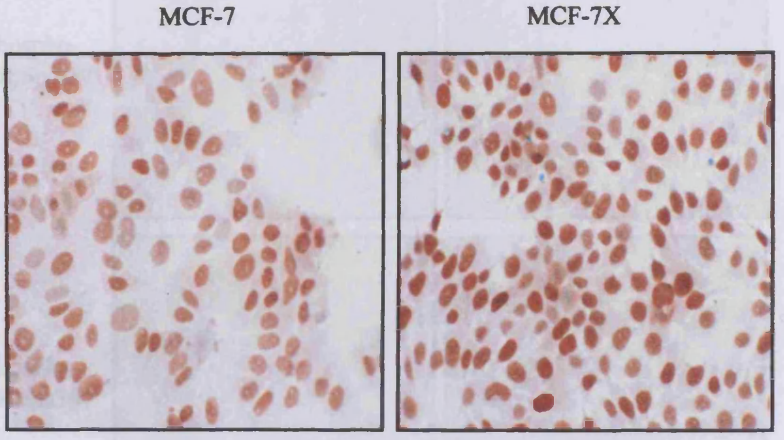

	MCF-7	MCF-7X	p-value
Total ERα			
(Nuclear)	147.0 (142.0-155.0)	185.0 (185.0-195.0)	<0.001*

Figure 3.6 Basal MCF-7X versus MCF-7 cell ERα expression by immunocytochemistry. MCF-7 and MCF-7X cells were grown on coverslips in phenol-red-free RPMI media containing 5% SFCS or XFCS respectively. Conditions were maintained for 7 days prior to ERICA fixation. The total nuclear ERα (6F11, antibody dilution 1:100) digital images shown above (X20 magnification) are representative of 3 experiments. H-Score data were obtained by dual assessment of 2 representative areas of each coverslip followed by statistical analysis (Mann-Whitney U-Test). The median H-Score and Q1-Q3 values are displayed. A p-value <0.05(*) indicates a significant difference in ERα expression between MCF-7 and MCF-7X cells.

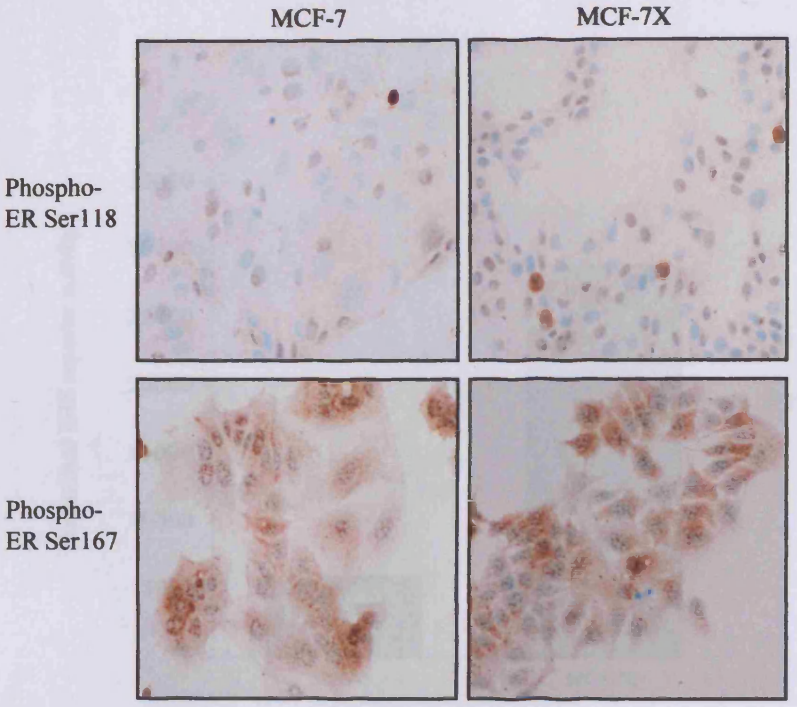

	MCF-7	MCF-7X	p-value
Phospho-ER Ser118			
(Nuclear)	70.0 (63.8-71.3)	90.0 (77.5-110.5)	0.037*
Phospho-ER Ser167			
(Nuclear)	82.5 (71.3-100.0)	50.0 (45.0-70.0)	0.170

Figure 3.7 Basal MCF-7X versus MCF-7 cell phosphorylation of ERα at Ser118 and Ser167 residues by immunocytochemistry. MCF-7 and MCF-7X cells were grown on coverslips in media containing 5% SFCS or XFCS respectively. Conditions were maintained for 7 days on coverslips prior to the appropriate fixation. The phospho-ER Ser118 (antibody dilution 1:400) assay required coverslips paraformaldehyde vanadate fixed and the phospho-ER Ser167 (1:25) assay required coverslips ERICA fixed. The digital images shown above (X20 magnification) are representative of 6 experiments. H-Score data were obtained by dual assessment of 2 representative areas of each coverslip followed by statistical analysis (Mann-Whitney U-Test). The median H-Score and Q1-Q3 values are displayed. A p-value <0.05(*) indicates a significant difference in ERα phosphorylation at Ser118/Ser167 between MCF-7 and MCF-7X cells.

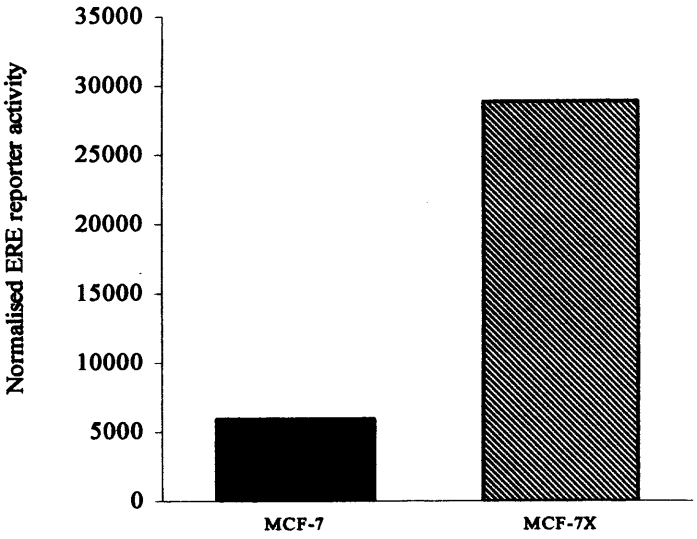

Figure 3.8 Basal MCF-7X versus MCF-7 cell comparison of ER transcriptional activity by ERE reporter assay. MCF-7 and MCF-7X cells were grown on 12-well plates in phenol-red-free RPMI media containing 5% SFCS or XFCS respectively for 24 hours. Cells were transfected in DCCM serum-free media containing transfection lipid (3 µl/well, Lipofectin), ERE reporter construct (400 ng/well), *Renilla* (150 ng/ml), and 'carrier' DNA (550 ng/well, PCRscript) After 6 hours, the transfection medium was replaced with phenol-red-free RPMI media for 18 hours. A dual-luciferase reporter assay kit was utilised for cell lysis and luminometer assessment. Illustrated above is the basal reporter activity in MCF-7X versus MCF-7 cell which has been normalised to β-Galactosidase to account for variations in transfection efficiency.

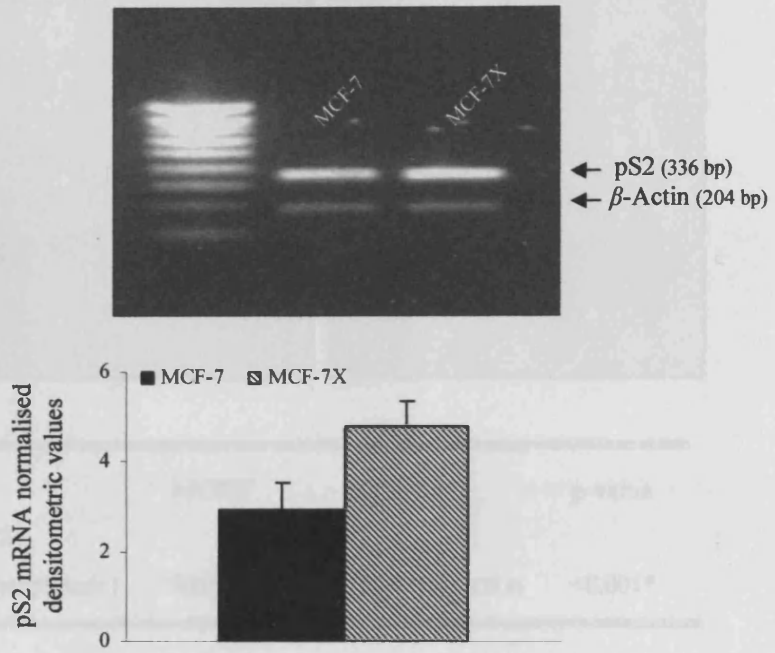

Figure 3.9 Basal MCF-7X versus MCF-7 cell mRNA expression of the endogenous oestrogen regulated gene pS2 by RT-PCR. MCF-7 and MCF-7X cells were grown on 100 mm dishes in phenol-red-free RPMI media containing 5% SFCS or XFCS respectively. Conditions were maintained for 7 days before RNA was isolated and reverse transcribed. Co-amplification RT-PCR of pS2 (25 cycles/ 55°C annealing temperature, 336 bp) and β-Actin (204 bp) was performed. The RT-PCR product was run on a 2% agarose gel containing ethidium bromide, subsequently photographed, scanned and normalised to β-Actin. The digital image is representative of 3 experiments and the statistical analysis applied was a unpaired-T test (p=0.017*) comparing mean pS2 expression in MCF-7 (2.9 +/- 0.6) and MCF-7X (4.8 +/- 0.6) cells.

pS2

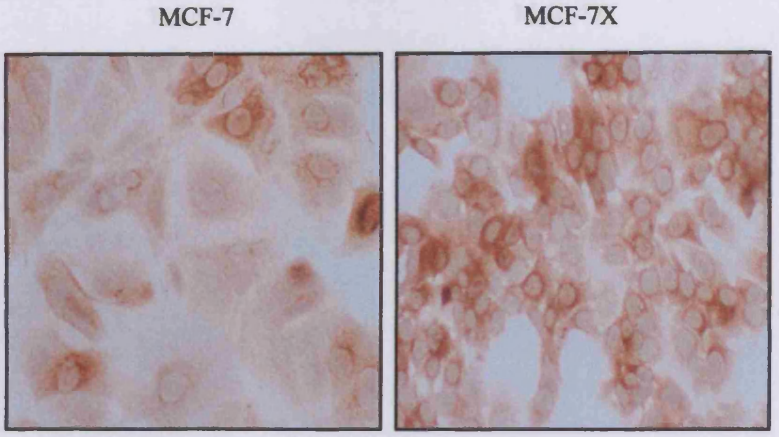

	MCF-7	MCF-7X	p-value
pS2 (Cytoplasmic)	90.0 (81.3-98.8)	130.0 (121.3-133.8)	<0.001*

Figure 3.10 Basal MCF-7X versus MCF-7 cell pS2 expression by immunocytochemistry. MCF-7 and MCF-7X cells were grown on coverslips in phenol-red-free RPMI media containing 5% SFCS or XFCS respectively. Conditions were maintained for 7 days prior to ERICA fixation. The pS2 (antibody dilution 1:500) digital images shown above (X20 magnification) are representative of 3 experiments. H-Score data were obtained by dual assessment of 2 representative areas of each coverslip followed by statistical analysis (Mann-Whitney U-Test). The median H-Score and Q1-Q3 values are displayed. A p-value <0.05(*) indicates a significant difference in pS2 expression between MCF-7 and MCF-7X cells.

Progesterone Receptor (PgR)

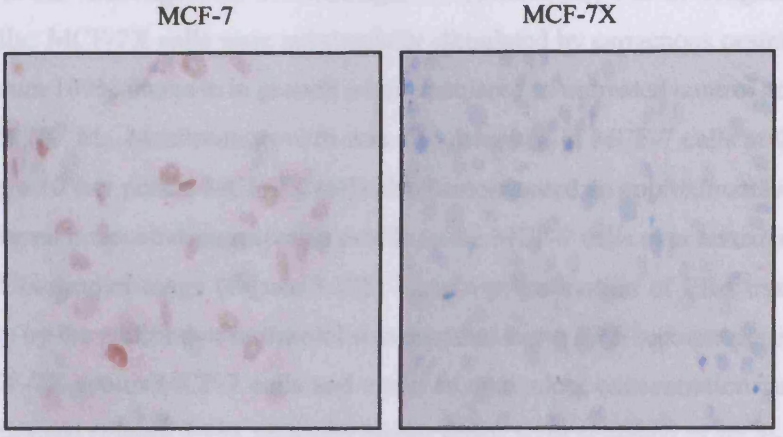

	MCF-7	MCF-7X	p-value
PgR (Nuclear)	22.5 (13.8-27.8)	0.0 (0.0-0.0)	<0.001*

Figure 3.11 Basal MCF-7X versus MCF-7 cell progesterone receptor expression by immunocytochemistry. MCF-7 and MCF-7X cells were grown on coverslips in phenol-red-free RPMI media containing 5% SFCS or XFCS respectively. Conditions were maintained for 7 days prior to ERICA fixation. The progesterone receptor (636, antibody dilution 1:200) digital images shown above (X20 magnification) are representative of 3 experiments. H-Score data were obtained by dual assessment of 2 representative areas of each coverslip followed by statistical analysis (Mann-Whitney U-Test). The median H-Score and Q1-Q3 values are displayed. A p-value <0.05(*) indicates a significant difference in progesterone receptor expression between MCF-7 and MCF-7X cells.

3.1.3 ERα Contribution: Oestrogen and Faslodex Effects

An obvious indicator of ERα function is growth sensitivity to oestrogens. A key feature under investigation by several groups in resistance to oestrogen deprivation is its apparent oestrogen hypersensitivity. In order to evaluate if this is a feature of our resistant model derived under conditions of exogenous growth factor/oestrogen deprivation, challenge with the ERα ligand oestradiol (E_2) was investigated in MCF-7X cells. MCF-7X cells were substantially stimulated by exogenous oestradiol with a maximum 100% increase in growth when compared to untreated control achieved at a dose of 10^{-9} M. Maximum growth was also achieved in MCF-7 cells at this dosage. During a 10 day period MCF-7X cells also demonstrated an approximately equivalent bell-shaped concentration response profile to the MCF-7 cells over an extensive 10^{-15}-10^{-5} M oestradiol range (Figure 3.12). Similarly, promotion of ERα transcriptional activity by the addition of oestradiol was assessed using ERE reporter gene constructs in MCF-7X versus MCF-7 cells and again an equivalent concentration curve profile was achieved (Figure 3.13), although higher levels were achieved in MCF-7X cells in relation to the stimulation achieved by oestradiol in MCF-7 cells. Collectively these data demonstrate ERα signalling is growth contributory in MCF-7X cells, but the dose response profiles indicate they are not growth hypersensitive to sub-physiological oestradiol levels. Therefore, severely depleted conditions (growth factor and oestrogen deprived) do not support oestrogen hypersensitivity in contrast to reported models where exogenous growth factors are available.

A further indication of ERα dependence is growth inhibition by the pure anti-oestrogen faslodex. MCF-7 and MCF-7X cells subject to a dose range of the pure anti-oestrogen faslodex (10^{-13}-10^{-7} M) for 7 days again demonstrated a broadly similar concentration response profile (Figure 3.14), although a large variability of response was seen in the parental cell line. MCF-7X cells were subsequently challenged with the anti-oestrogen at a significant inhibitory dose (10^{-7} M, $p<0.001$*) over a 15 day time course, with cell growth assessed every 48 hours. Faslodex significantly inhibited growth 37.2% ($p<0.001$*) at day 7, and by day 15 this inhibition was increased to 59.6% versus the untreated control ($p=0.001$*, Figure 3.15). In both MCF-7 and MCF-7X cells, faslodex treatment significantly decreased nuclear ERα (78.2%, $p=0.001$* and 63.5%, $p=0.001$* respectively) as measured by immunocytochemistry (Figure 3.16). Low levels of nuclear ERα remained subsequent to treatment in both MCF-7 and MCF-7X cells, with more occasional

cells retaining a moderate nuclear intensity in the latter cell line. A decrease in ERα (60 kDa) with faslodex was also demonstrated by Western blotting in MCF-7X cells (Figure 3.17).

Treatment with the pure anti-oestrogen resulted in a significant MCF-7X cell reduction of Ser118ER phosphorylation (13.9%, p=0.030*, Figure 3.18) although there was no effect on the phosphorylation of Ser167ER (p=0.841, Figure 3.19). This result was contrary to faslodex producing some decrease in Ser118ER phosphorylation but with a significant reduction in the phosphorylation of Ser167ER (30.3%, p=0.019*) in MCF-7 cells by immunocytochemistry (Figures 3.18 & 3.19). Faslodex partially diminished ERE reporter activity after 18 hour treatment by 32.5% (p=0.007*) in MCF-7X cells (Figure 3.20). In parallel with these inhibitory effects on ERE reporter activity, RT-PCR of faslodex treated (7 days) MCF-7X cells revealed that level of the oestrogen regulated gene pS2 mRNA (336 bp) was significantly reduced (92.2%, p=0.002*, Figure 3.21). Immunocytochemistry demonstrated a significant 44.2% reduction in cytoplasmic localised endogenous pS2 protein in MCF-7X cells (p=0.001*, Figure 3.22), a fall nearly equivalent to that revealed in MCF-7 cells (41.7%, p<0.001*).

3.1.4 Non-genomic ERα Signalling

In the long-term oestrogen deprived (LTED) model from Santen *et al.* (2003), confocal analysis displayed membrane-bound ERα in the ruffles and the peri-membrane region of the pseudopodia after short-term oestradiol treatment. However, immunofluorescence studies (Figure 3.23) performed in MCF-7X cells failed to demonstrate obvious cytoplasmic or plasma membrane recruitment of ERα either before or after short-term (10 min.) E_2 treatment, despite a prominent nuclear immunolocalisation (green). A strong level of actin polymerisation (red) was apparent by the colour merged digital images which importantly seemed to lack any evidence of co-localisation (yellow) with ERα. The lack of cytoplasmic or plasma membrane staining was also observed in the MCF-7 cells examined in this project both pre and post E_2 treatment. This suggests that ERα signalling is unlikely to occur in a predominantly non-genomic manner in the MCF-7X model, or indeed substantially in the MCF-7 parental cell line in this study.

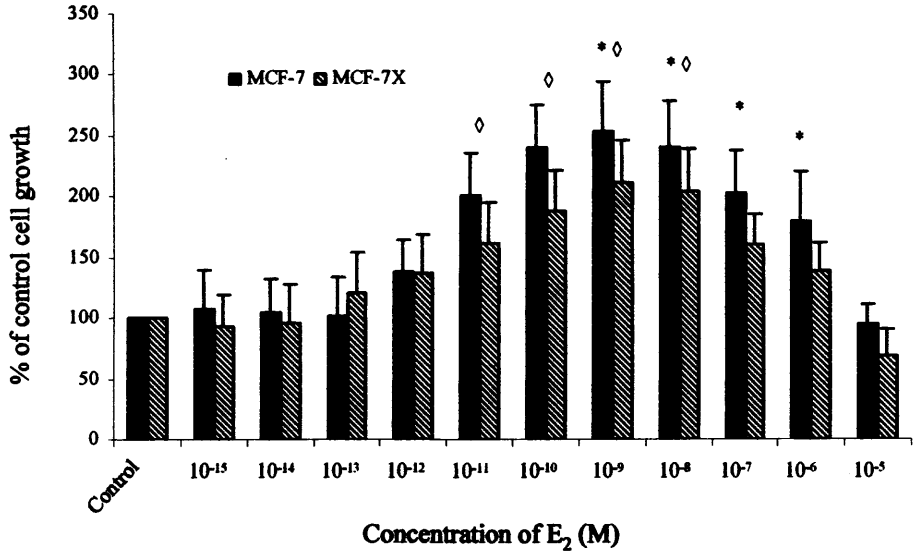

Figure 3.12 Dose Response to Oestradiol in MCF-7X versus MCF-7 cells. MCF-7 and MCF-7X cells were grown on 24-well plates in phenol-red-free RPMI media containing 5% SFCS or XFCS respectively. Cells were exposed to a dose range of 10^{-15} M to 10^{-5} M E_2 including a control (ethanol 1µl/ 10 ml). Conditions were maintained for 10 days prior to trypsin dispersion followed by Coulter counting (triplicate wells per dose). The data are displayed as the mean percentage of control cell growth +/- SD (n=4). The statistical analysis applied was an ANOVA Test followed by a Tamhane Post-Hoc Test.

* and ◊ Denotes a dose at which MCF-7 and MCF-7X cells were significantly growth promoted by oestradiol versus their respective controls at $p<0.05$.

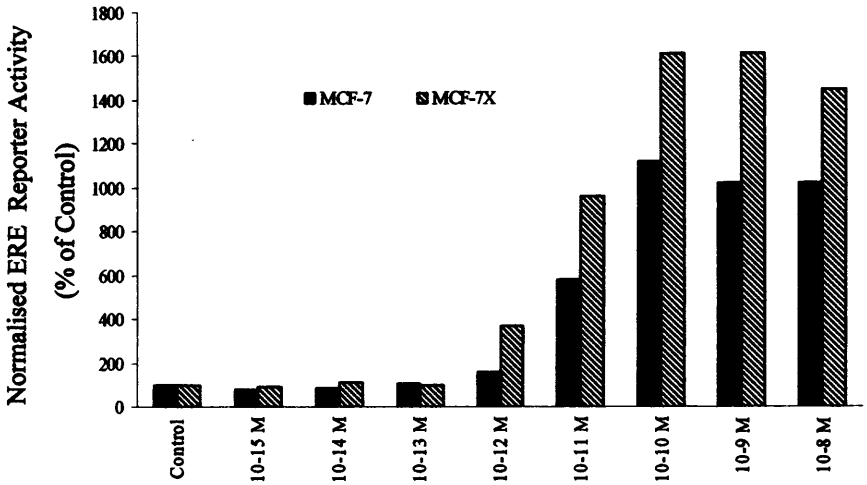

Figure 3.13 Oestrogen sensitivity of ERE transcriptional activity in MCF-7X versus MCF-7 cells. MCF-7 and MCF-7X cells were grown on 12-well plates in phenol-red-free media containing 5% SFCS or XFCS respectively for 24 hours. Cells were transfected in DCCM serum-free media containing transfection lipid (3 µl/well, Lipofectin) ERE reporter construct (400 ng/well), *Renilla* (150 ng/ml), and 'carrier' DNA (550 ng/well, PCRscript) After 6 hrs, the transfection medium was removed and phenol-red-free RPMI media containing a dose range 10^{-15} M to 10^{-8} M E_2 including a control (ethanol 1 µl/ 10 ml) was added (triplicate wells per treatment). Subsequent to 18 hour treatment incubation a dual-luciferase reporter assay kit was utilised for cell lysis and luminometer assessment (n=1). Data are displayed as a percentage of control ERE reporter activity for each cell line and has been normalised to β-Galactosidase to account for variations in transfection efficiency.

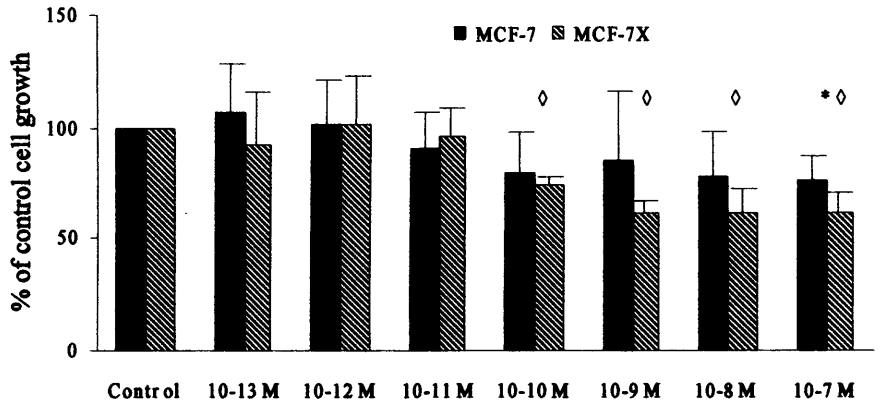

Figure 3.14 Dose response to the pure anti-oestrogen faslodex in MCF-7X versus MCF-7 cells. MCF-7 and MCF-7X cells were grown on 24-well plates in phenol-red-free RPMI media containing 5% SFCS or XFCS respectively. Cells were exposed to a dose range of 10^{-13} M to 10^{-7} M faslodex including a control (ethanol 1 µl/ 10 ml). Conditions were maintained for 10 days prior to trypsin dispersion followed by Coulter counting (triplicate wells per dose). The data are displayed as the mean percentage of cell growth +/- SD (n=3) for each cell line. The statistical analysis applied was an ANOVA Test followed by a Tamhane Post-Hoc Test.

* and ◊ Denotes a dose at which MCF-7 and MCF-7X cells were significantly growth inhibited by faslodex versus their respective controls at $p<0.05$.

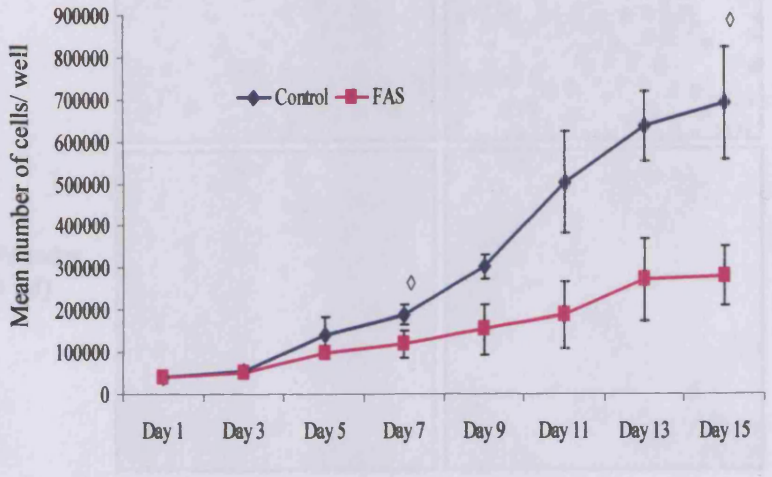

Figure 3.15 Growth of MCF-7X cells challenged with the pure anti-oestrogen faslodex. MCF-7X cells were grown on 24-well plates in phenol-red-free RPMI media containing 5% XFCS in the absence or presence of faslodex (10^{-7} M) for 15 days. At the time points indicated above, cells were subject to trypsin dispersion followed by Coulter counting (triplicate wells per time point). These data were log transformed to compare growth rate at day 7 and day 15. The statistical analysis applied was an ANOVA Test followed by a Bonferroni Post-Hoc Test. Data are displayed as the mean number of cells/well +/- SD (n=5).

◊ Denotes faslodex treatment was significantly lower at day 7 ($p<0.001$) and day 15 ($p=0.001$) versus untreated MCF-7X cells.

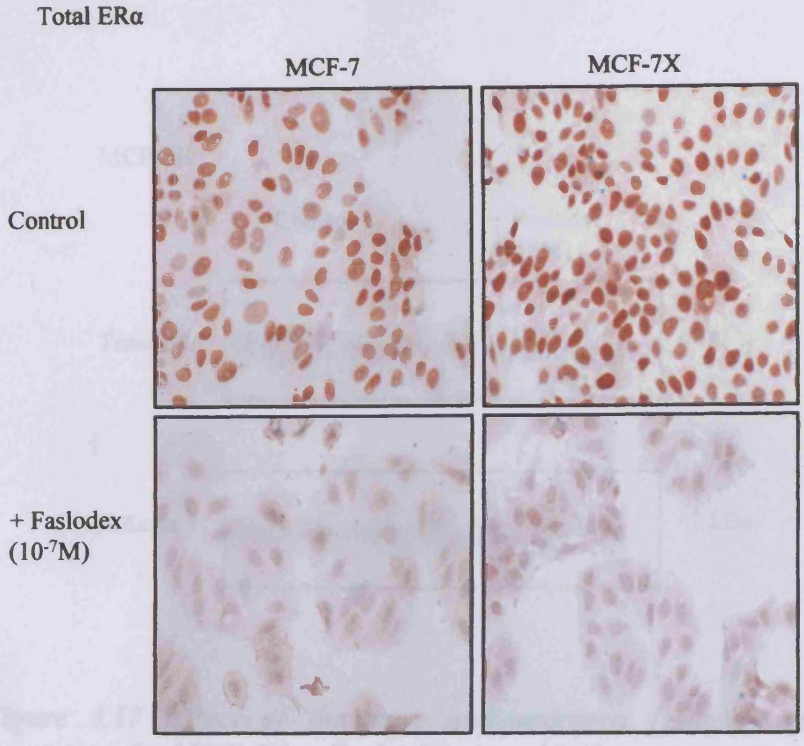

	MCF-7		MCF-7X	
Total ERα (Nuclear)				
Basal Control	147.0 (142.0-155.0)		185.0 (185.0-195.0)	
+ Faslodex (10^{-7}M)	32.0 (30.0-36.3)	p=0.001*	67.5 (60.0-71.3)	p=0.001*

Figure 3.16 Effect of the pure anti-oestrogen faslodex on ERα expression in MCF-7 and MCF-7X cells by immunocytochemistry. MCF-7 and MCF-7X cells were grown on coverslips in phenol-red-free RPMI media containing 5% SFCS or XFCS respectively in the absence or presence of faslodex (10^{-7} M). Conditions were maintained for 7 days prior to ERICA fixation. The total nuclear ERα (6F11, antibody dilution 1:100) digital images shown above (X20 magnification) are representative of 3 experiments. H-Score data were obtained by dual assessment of 2 representative areas of each coverslip followed by statistical analysis (Mann-Whitney U-Test). The median H-Score and Q1-Q3 values are displayed. A p-value <0.05(*) indicates a significant difference in ERα expression following faslodex treatment.

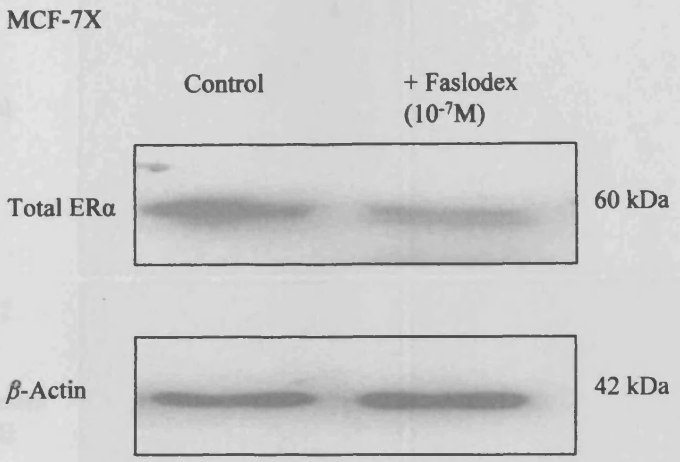

Figure 3.17 Effect of the pure anti-oestrogen faslodex on ERα expression in MCF-7X cells by Western blotting. MCF-7X cells were grown on 60 mm dishes in phenol-red-free media containing 5% XFCS in the absence and presence of faslodex (10^{-7} M). Conditions were maintained for 7 days prior to whole cell lysis, SDS-PAGE (40 µg of sample protein/well) and Western blotting. The nitrocellulose membrane (0.45 µm) was probed for total ER (ID5, 60 kDa) and β-Actin (42 kDa). The developed autoradiography film was scanned using densitometric imaging for each blot probed and ERα expression was normalised to β-Actin. Above is a representative experiment.

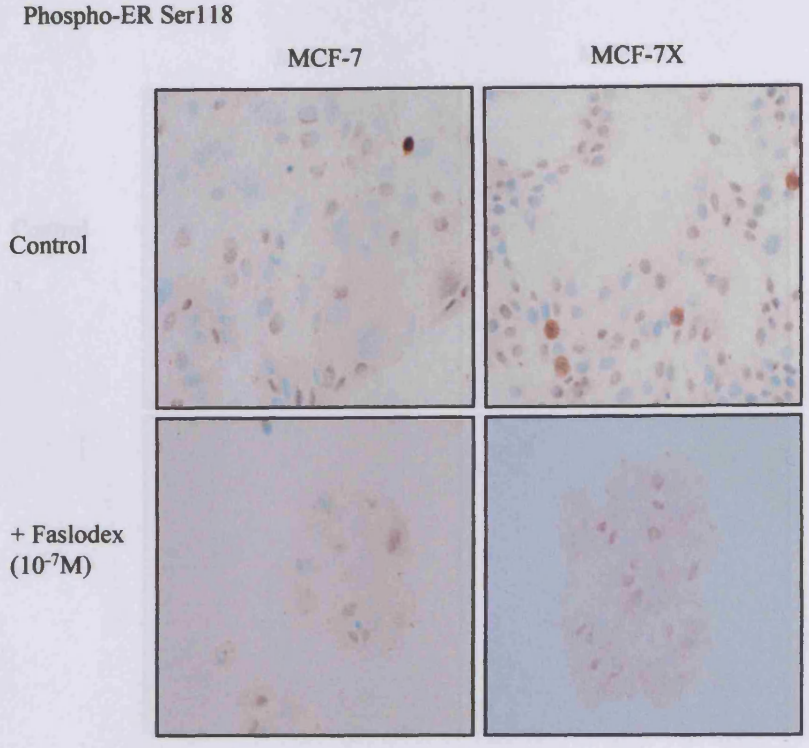

	MCF-7	MCF-7X
Phospho-ER Ser118 (Nuclear)		
Basal Control	70.0 (63.8-71.3)	90.0 (77.5-110.5)
+ Faslodex (10^{-7}M)	57.5 (50.0-70.0) p=0.080	77.5 (61.3-80.0) p=0.030*

Figure 3.18 Effect of the pure anti-oestrogen faslodex on phosphorylation of ERα at Ser118 residue in MCF-7 and MCF-7X cells by immunocytochemistry. MCF-7 and MCF-7X cells were grown on coverslips in phenol-red-free RPMI media containing 5% SFCS or XFCS respectively in the absence or presence of faslodex (10^{-7}M). Conditions were maintained for 7 days prior to paraformaldehyde vanadate fixation. The phospho-ER Ser118 (antibody dilution 1:400) digital images shown above (X20 magnification) are representative of 4 experiments. H-Score data were obtained by dual assessment of 2 representative areas of each coverslip followed by statistical analysis (Mann-Whitney U-Test). The median H-Score and Q1-Q3 values are displayed. A p-value <0.05(*) indicates a significant difference in phospho-ER Ser118 level following faslodex treatment.

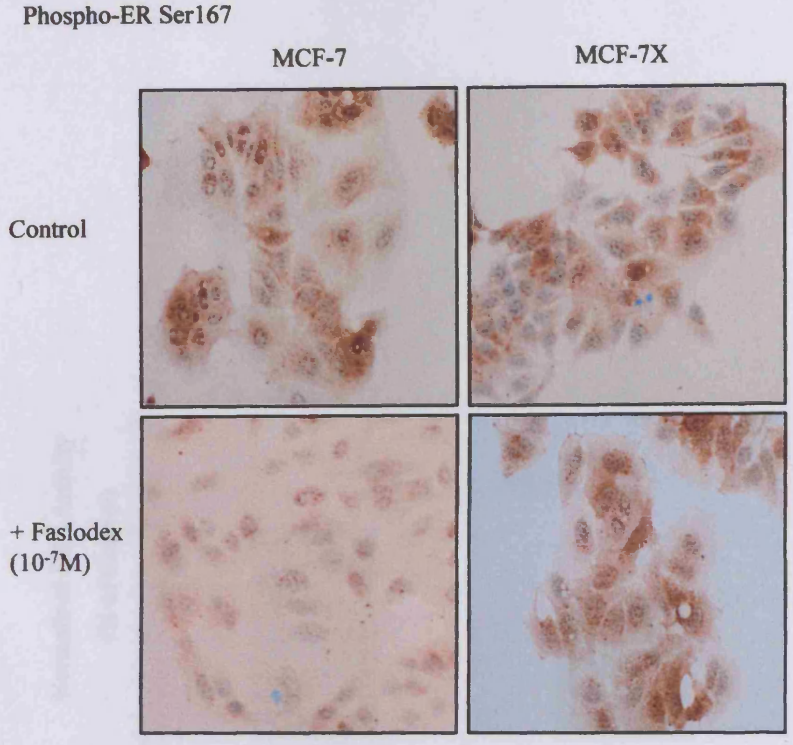

	MCF-7		MCF-7X	
Phospho-ER Ser167 (Nuclear)				
Basal Control	82.5 (71.3-100.0)		50.0 (45.0-70.0)	
+ Faslodex (10^{-7}M)	57.5 (53.8-71.3)	p=0.019*	55.0 (40.0-70.0)	p=0.841

Figure 3.19 Effect of the pure anti-oestrogen faslodex on phosphorylation of ERα at Ser167 residue in MCF-7 and MCF-7X cells by immunocytochemistry. MCF-7 and MCF-7X cells were grown on coverslips in phenol-red-free RPMI media containing 5% SFCS or XFCS respectively in the absence or presence of faslodex (10^{-7}M). Conditions were maintained for 7 days prior to ERICA fixation. The phospho-ER Ser167 (antibody dilution 1:25) digital images shown above (X20 magnification) are representative of 4 experiments. H-Score data were obtained by dual assessment of 2 representative areas of each coverslip followed by statistical analysis (Mann-Whitney U-Test). The median H-Score and Q1-Q3 values are displayed. A p-value <0.05(*) indicates a significant difference in phospho-ER Ser167 level following faslodex treatment.

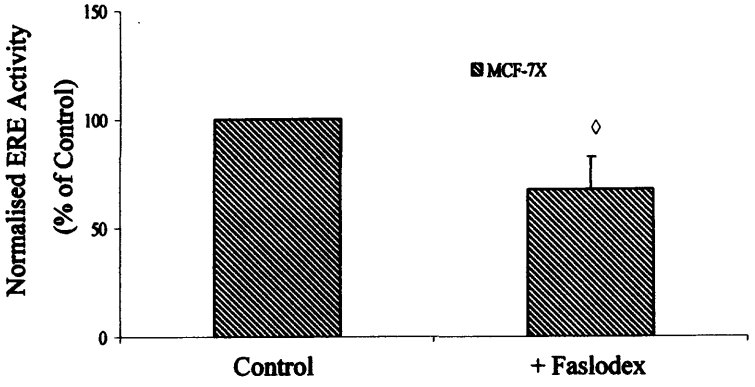

Figure 3.20 Effect of the pure anti-oestrogen faslodex on ER transcriptional activity in MCF-7X cells after 18 hour treatment. MCF-7X cells were grown on 12-well plates in phenol-red-free RPMI media containing 5% XFCS for 24 hours. Cells were transfected in DCCM serum-free media containing transfection lipid (3 µl/well, Lipofectin), ERE reporter construct (400 ng/well), *Renilla* (150 ng/ml), and 'carrier' DNA (550 ng/well, PCRscript) After 6 hours, the transfection medium was replaced with phenol-red-free RPMI media in the absence or presence of faslodex (10^{-7} M) in triplicate wells. Subsequent to 18 hour treatment incubation, a dual-luciferase reporter assay kit was utilised for cell lysis and luminometer assessment (n=3). Data are displayed as percentage of control ERE activity +/- SD (triplicate wells) and has been β-Galactosidase normalised in the absence and presence of faslodex (10^{-7} M). The statistical analysis applied was an ANOVA Test followed by a Bonferroni Post-Hoc Test.

◊ Denotes faslodex treatment (18 hrs) significantly decreased ERE activity in MCF-7X cells versus untreated control.

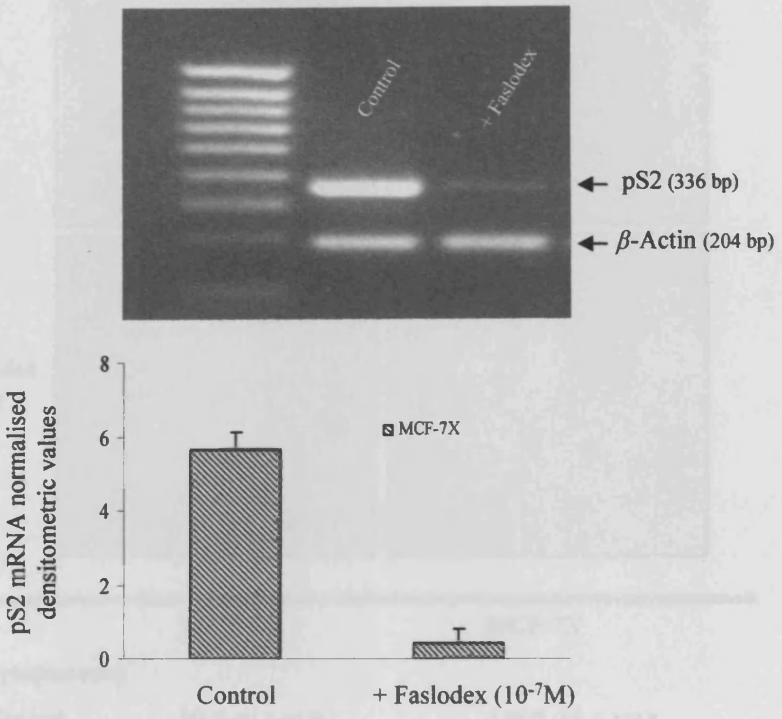

Figure 3.21 Effect of the pure anti-oestrogen faslodex on pS2 mRNA in MCF-7X cells by RT-PCR. MCF-7X cells were grown on 100 mm dishes in phenol-red-free RPMI media containing 5% XFCS in the absence or presence of faslodex (10^{-7} M). Conditions were maintained for 7 days before RNA was isolated and reverse transcribed. Co-amplification RT-PCR of pS2 (25 cycles/ 55°C annealing temperature, 336 bp) and β-Actin (204 bp) was performed. The RT-PCR product was run on a 2% agarose gel containing ethidium bromide, subsequently photographed, scanned and normalised to β-Actin. The digital image is representative of 3 experiments and the statistical analysis applied was an unpaired-T test (p=0.002*) comparing mean pS2 expression in untreated MCF-7X cells (5.7 +/- 0.4) and faslodex treated MCF-7X cells (0.4 +/- 0.3).

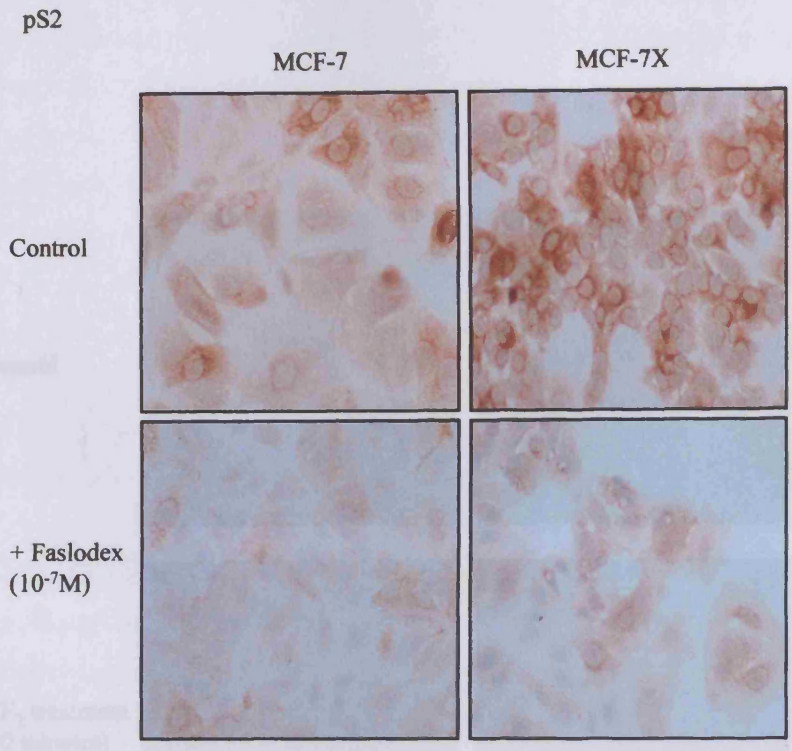

	MCF-7		MCF-7X	
pS2 (Cytoplasmic)				
Basal Control	90.0 (81.3-98.8)		130.0 (121.3-133.8	
+Faslodex (10^{-7} M)	52.5 (42.5-58.8)	p<0.001*	72.5 (58.8-80.0)	p=0.001*

Figure 3.22 Effect of the pure anti-oestrogen faslodex on pS2 expression in MCF-7 and MCF-7X cells by immunocytochemistry. MCF-7 and MCF-7X cells were grown on coverslips in phenol-red-free media containing 5% SFCS or XFCS respectively in the absence or presence of faslodex (10^{-7} M). Conditions were maintained for 7 days prior to ERICA fixation. The pS2 (antibody dilution 1:500) digital images shown above (X20 magnification) are representative of 3 experiments. H-Score data were obtained by dual assessment of 2 representative areas of each coverslip followed by statistical analysis (Mann-Whitney U-Test). The median H-Score and Q1-Q3 values are displayed. A p-value <0.05(*) indicates a significant difference in pS2 expression following faslodex treatment.

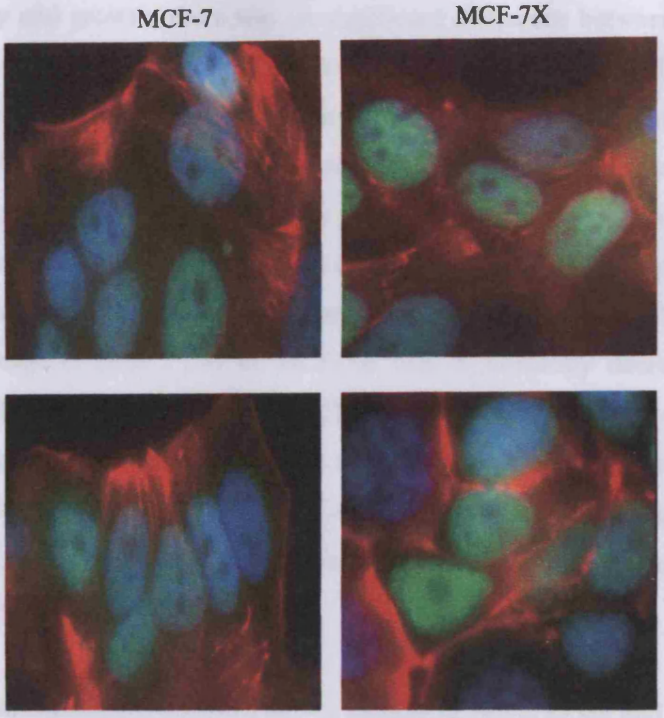

Figure 3.23 ERα localisation in oestrogen stimulated MCF-7 and MCF-7X cells by immunofluorescence. MCF-7 and MCF-7X cell were grown on coverslips in phenol-red-free RPMI media containing 5% SFCS or XFCS respectively. Conditions were maintained for 7 days prior to 10 minute E_2 (10^{-9} M) or control (ethanol, 1 µl/ 10 ml) treatment followed by 3.7% formaldehyde fixation. The ERα (ID5, antibody dilution 1:20) superimposed digital images shown above were acquired using a multiple band-pass filter on a Leica RPE automatic microscope using a X100 (magnification) oil immersion lens [DAPI (nuclear counter stain, blue, 360 nm), Alexa 488-fluorescein (ERα, green, 488 nm) and Texas Red phalloidin (actin fibers, red, 594 nm].

3.1.5 AP-1 Signalling and Cell Cycle

In order to address whether non-classical/genomic ERα signalling via AP-1 was contributory in MCF-7X cells, AP-1 transcriptional activity was measured using an AP-1 reporter assay in both MCF-7 and MCF-7X cells. Basal AP-1 reporter activity was increased 4.6 fold in MCF-7 cells compared to the oestrogen deprived MCF-7X cells (Figure 3.24). In contrast to their obvious impact on ERE reporter gene construct activity and growth, there was no significant difference between untreated control and E_2 (10^{-9} M) or faslodex (10^{-7} M) treatment in MCF-7X cells (Figure 3.25). MCF-7 cells treated with E_2 showed a small but significant reduction (11.0%, p=0.002*) in AP-1 activity while faslodex treatment had no effect versus untreated control. The protein c-fos binds to DNA by forming a stable heterodimer with the protein c-jun (Shaulian and Karin, 2001) that comprises the AP-1 transcription factor complex which targets the AP-1 response elements. RT-PCR revealed c-fos mRNA (483 bp) expression (Figure 3.26) in MCF-7X was significantly decreased with respect to the MCF-7 parental cell line (57.5%, p=0.001*). Fos protein expression was moreover significantly decreased 23.8% (p=0.004*) in MCF-7X versus MCF-7 by immunocytochemistry (Figure 3.27). Cumulatively, these data suggest non-classical/genomic ERα signalling via AP-1 interactions is not a major contributory factor for ER-promoted growth in MCF-7X.

The transcriptional regulator c-myc is a strong inducer of proliferation and its role in cell cycle control is believed to be critical to oncogenesis (Nasi *et al.*, 2001). RT-PCR of c-myc mRNA (549 bp) expression (Figure 3.28) revealed an increase in MCF-7X versus MCF-7 cells, although this did not reach significance (64.3%, p=0.087). Coller *et al.* (2000) has shown c-myc directly represses the expression of $p21^{cip1/waf1}$ during its promotion of growth. In MCF-7X cells $p21^{cip1/waf1}$ mRNA (460 bp) expression was significantly decreased 47.8% (p=0.031*) versus MCF-7 cells by RT-PCR (Figure 3.29).

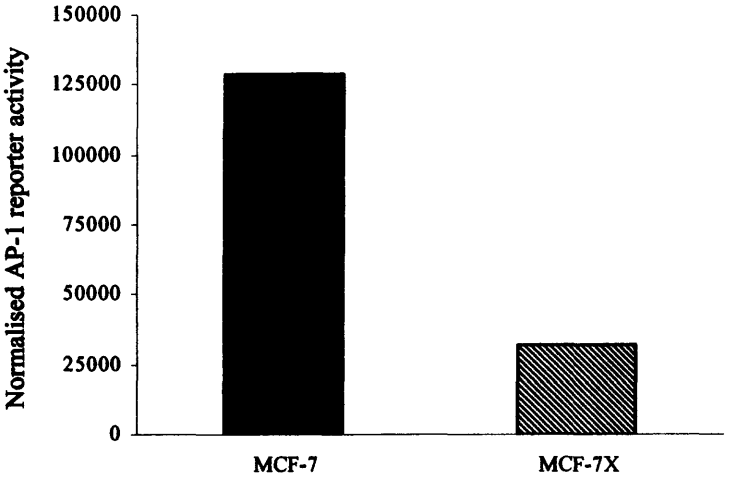

Figure 3.24 Basal MCF-7X versus MCF-7 cell comparison of AP-1 transcriptional activity. MCF-7 and MCF-7X cells were grown on 12-well plates in phenol-red-free RPMI media containing 5% SFCS or XFCS respectively for 24 hours. Cells were transfected in DCCM serum-free media containing lipid (3 µl/well, Lipofectin), AP-1-pTal reporter construct (400 ng/well), and 'carrier' DNA (700 ng/well PCRscript). Control pTal luciferase reporter constructs were included for each treatment at the same construct and 'carrier' concentrations. After 6 hours, the transfection medium was removed and phenol-red-free RPMI for 18 hours. A luciferase reporter assay kit was utilised for cell lysis and luminometer assessment. Illustrated above is basal reporter activity in MCF-7X versus MCF-7 cells which has been normalised to β-Galactosidase to account for variations in transfection efficiency.

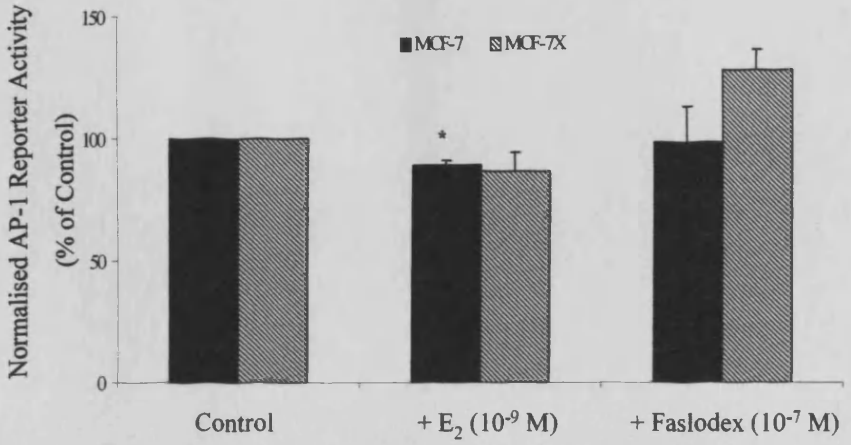

Figure 3.25 Treatment effects on AP-1 transcriptional activity in MCF-7X versus MCF-7. MCF-7 and MCF-7X cells were grown on 12-well plates in phenol-red-free RPMI media containing 5% SFCS or XFCS respectively for 24 hours. Cells were transfected in DCCM serum-free media containing lipid (3 µl/well, Lipofectin), AP-1-pTal reporter construct (400 ng/well), and 'carrier' DNA (700 ng/well PCRscript). Control pTal luciferase reporter constructs were included for each treatment at the same construct and 'carrier' concentrations. After 6 hours, the transfection medium was removed and phenol-red-free RPMI media containing E_2 (10^{-9} M), faslodex (10^{-7} M) or control (ethanol, 1µl/ 10 ml) was added (triplicate wells per treatment). Subsequent to 18 hour treatment incubation, a luciferase reporter assay kit was utilised for cell lysis and luminometer assessment (n=3). Data are displayed as a percentage of control AP-1 activity for each cell line +/- SD and has been β-Galactosidase normalised to account for variations in transfection efficiency. The statistical analysis applied was an ANOVA Test followed by a Dunnett-T Post-Hoc Test.

* Denotes E_2 treatment significantly decreased AP-1 activity in MCF-7 cells versus untreated control.

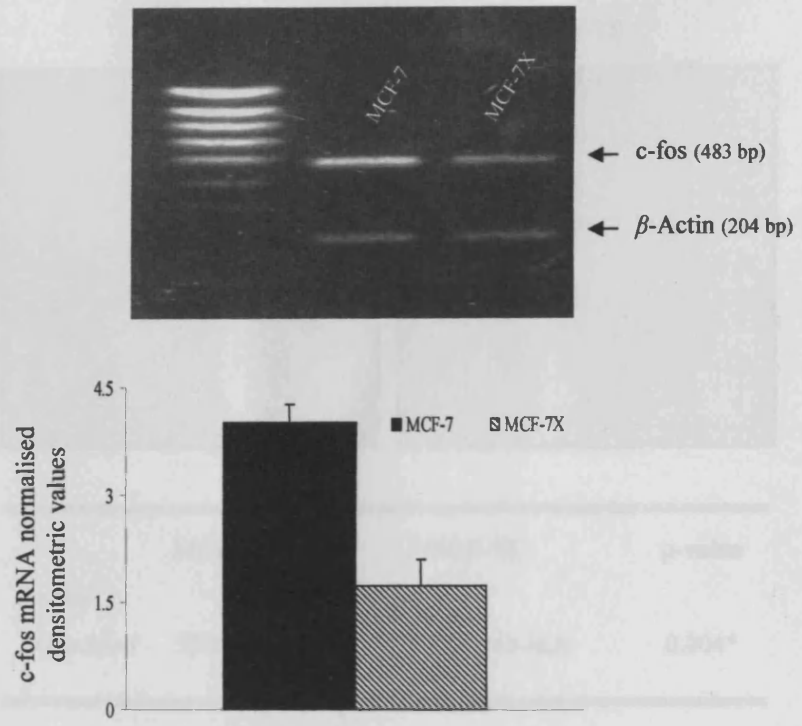

Figure 3.26 Basal MCF-7X versus MCF-7 cell mRNA expression of c-fos by RT-PCR. MCF-7 and MCF-7X cells were grown on 100 mm dishes in phenol-red-free RPMI media containing 5% SFCS or XFCS respectively. Conditions were maintained for 7 days before RNA was isolated and reverse transcribed. RT-PCR of c-fos (32 cycles/ 55°C annealing temperature, 483 bp) and β-Actin (25 cycles/ 55°C annealing temperature, 204 bp) was performed. Product from each reaction was combined and run on a 2% agarose gel containing ethidium bromide, subsequently photographed, scanned and normalised to β-Actin. The digital image above is representative of 3 experiments and the statistical analysis applied was an unpaired-T test (p=0.001*) comparing mean c-fos expression in MCF-7 (4.0 +/-0.2) and MCF-7X (1.7 +/- 0.4) cells.

c-fos

MCF-7 MCF-7X

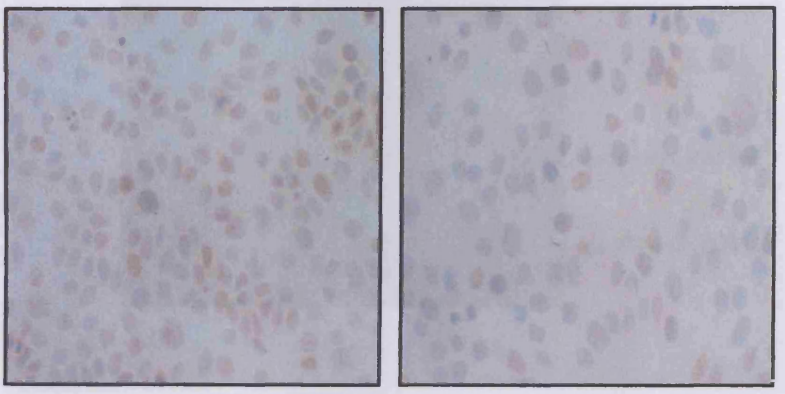

	MCF-7	MCF-7X	p-value
c-fos (Nuclear)	52.5 (48.8-61.3)	40.0 (38.0-40.3)	0.004*

Figure 3.27 Basal MCF-7X versus MCF-7 c-fos expression by immunocytochemistry. MCF-7 and MCF-7X cells were grown on coverslips in phenol-red-free RPMI containing 5% SFCS or XFCS respectively. Conditions were maintained for 7 days prior to ERICA fixation. The c-fos (antibody dilution 1:500) digital images shown above (X20 magnification) are representative of 3 experiments. H-Score data were obtained by dual assessment of 2 representative areas of each coverslip followed by statistical analysis (Mann-Whitney U-Test). The median H-Score and Q1-Q3 values are displayed. A p-value <0.05(*) indicates a significant difference in c-fos expression between MCF-7 and MCF-7X cells.

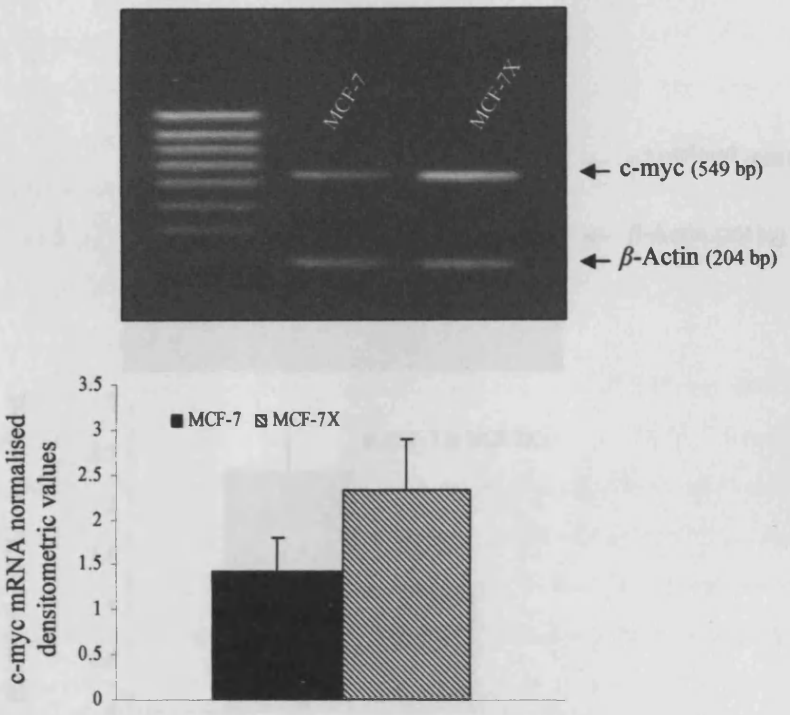

Figure 3.28 Basal MCF-7X versus MCF-7 cell mRNA expression of c-myc by RT-PCR. MCF-7 and MCF-7X cells were grown on 100 mm dishes in phenol-red-free RPMI media containing 5% SFCS or XFCS respectively. Conditions were maintained for 7 days before RNA was isolated and reverse transcribed. Co-amplification RT-PCR of c-myc (29 cycles/ 55°C annealing temperature, 549 bp) and β-Actin (204 bp) was performed. The RT-PCR product was run on a 2% agarose gel containing ethidium bromide, subsequently photographed, scanned and normalised to β-Actin. The digital image above is representative of 3 experiments and the statistical analysis applied was an unpaired-T test (p=0.087) comparing mean c-myc expression in MCF-7 (1.4 +/- 0.4) and MCF-7X (2.3 +/- 0.6) cells.

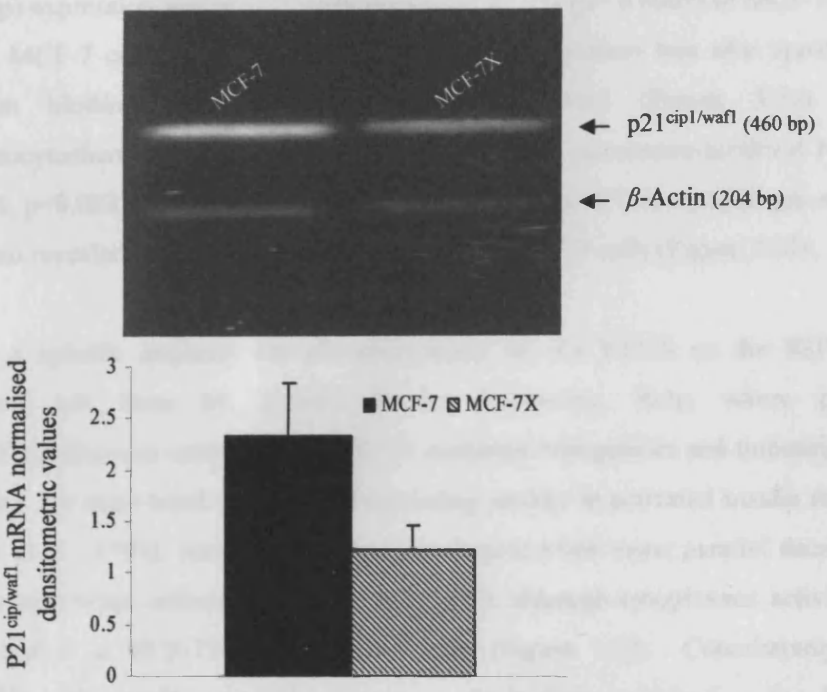

Figure 3.29 Basal MCF-7X versus MCF-7 cell mRNA expression of $p21^{cip1/waf1}$ by RT-PCR. MCF-7 and MCF-7X cells were grown on 100 mm dishes in phenol-red-free RPMI media containing 5% SFCS or XFCS respectively. Conditions were maintained for 7 days before RNA was isolated and reverse transcribed. Co-amplification RT-PCR of $p21^{cip1/waf1}$ (30 cycles/ 55°C annealing temperature, 460 bp) and β-Actin (204 bp) was performed. The RT-PCR product was run on a 2% agarose gel containing ethidium bromide, subsequently photographed, scanned and normalised to β-Actin. The digital image above is representative of 3 experiments and the statistical analysis applied was a unpaired-T test (p=0.031*) comparing mean $p21^{cip1/waf1}$ expression in MCF-7 (2.3 +/-0.5) and MCF-7X (1.2 +/- 0.2) cells.

3.2 CLASSICAL GROWTH FACTOR RECEPTOR SIGNALLING

3.2.1 Insulin-like Growth Factor Receptor (IGF-1R) Signalling

The insulin-like growth factor-1 receptor (IGF-1R) is expressed to some degree in most cell types and its signalling promotes mitogenesis, apoptosis, cell adhesion and motility as well as terminal differentiation (Valentinis and Baserga, 2001). Both the MCF-7 and MCF-7X cell lines were cultured for 7 days to assess the mRNA and protein levels of IGFR. While readily detectable in MCF-7 cells, IGF-1R mRNA (287 bp) expression was significantly decreased 87.7% ($p= 0.006$*) in MCF-7X cells versus MCF-7 cells by RT-PCR (Figure 3.30). A decrease was also apparent by Western blotting (128 kDa) at the protein level (Figure 3.31). By immunocytochemistry a substantial decline in plasma membrane-localised receptor (86.7%, $p=0.003$*) along with a decrease (64.5%, $p=0.003$*) in cytoplasmic staining was also revealed versus the prominent staining in MCF-7 cells (Figure 3.32).

Using a specific antibody for phosphorylation of site Y1316 on the IGF-1R (a generous gift from M. Rubini, Ferrara University, Italy; where pY1316 phosphorylation can contribute to IGF-1R mediated mitogenesis and tumourigenesis and does not cross-react with the corresponding moiety in activated insulin receptor, Rubini *et al.*, 1999), immunocytochemistry demonstrated some parallel decrease in plasma membrane activation (37.5%, $p=0.002$*), although cytoplasmic activity was not depleted in MCF-7X versus MCF-7 cells (Figure 3.32). Cumulatively these MCF-7X cell results possibly suggest a diminished contribution for IGF-1R signalling versus the parental cell line. In accordance with this, although when challenged with the IGF-1R inhibitor ADW742 (1 μM) a 19.5% ($p<0.001$*) decrease in MCF-7X cell growth was observed (Figure 3.33), this was inferior to the 40.3% ($p<0.001$*) growth inhibitory effect in the MCF-7 cell line, where a dominant role for IGF-1R signalling prior to endocrine therapy has previously been established (Nicholson *et al.*, 2004a). Finally there was no significant effect on MCF-7X cell growth when challenged with IGF-1R ligands IGF1 and -2 (Figure 3.34). In total, these data would suggest there is no dominant role for IGF-1R in MCF-7X growth, which is in contrast to some of the long-term oestrogen-deprived models generated in the presence of serum growth factors (Santen *et al.*, 2004a; Martin *et al.*, 2003).

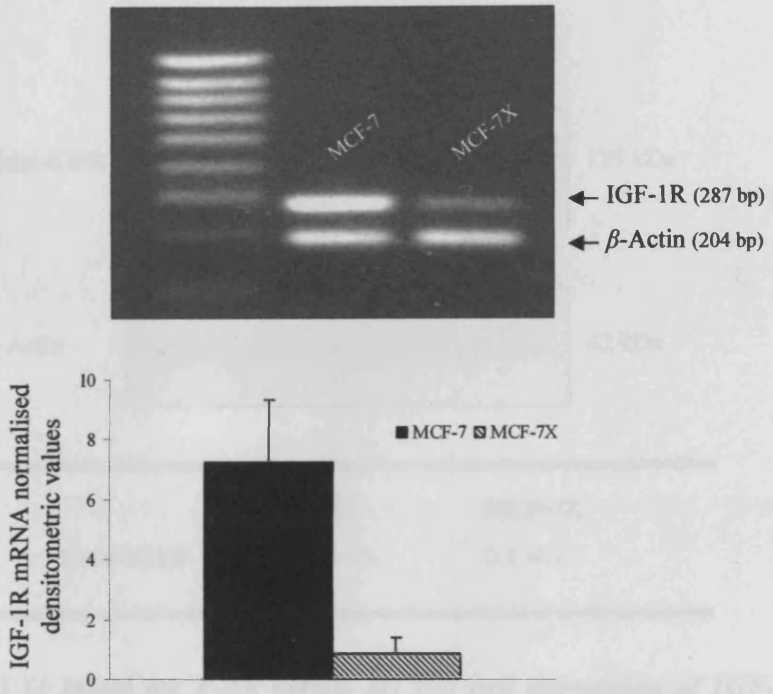

Figure 3.30 Basal MCF-7X versus MCF-7 cell mRNA expression of IGF-1R by RT-PCR. MCF-7 and MCF-7X cells were grown on 100 mm dishes in phenol-red-free RPMI media containing 5% SFCS or XFCS respectively. Conditions were maintained for 7 days before RNA was isolated and reverse transcribed. Co-amplification RT-PCR of IGF-1R (26 cycles/ 55°C annealing temperature, 287 bp) and β-Actin (204 bp) was performed. The RT-PCR product was run on a 2% agarose gel containing ethidium bromide, subsequently photographed, scanned and normalised to β-Actin. The digital image above is representative of 3 experiments and the statistical analysis applied was an unpaired-T test (p=0.006*) comparing mean IGF-1R expression in MCF-7 (7.3 +/- 2.1) and MCF-7X (0.9 +/- 0.5) cells.

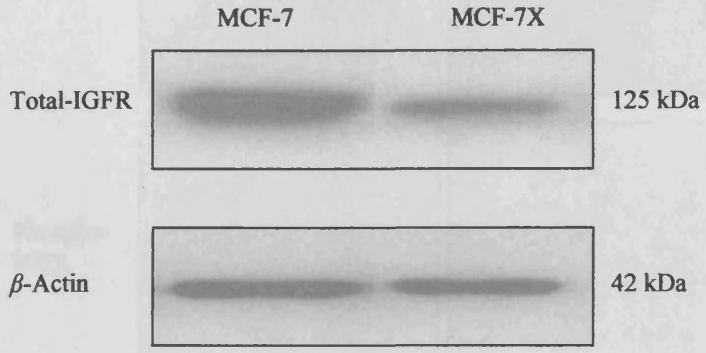

	MCF-7	MCF-7X
Total-IGFR	6.2 +/- 0.3	2.1 +/- 1.1

Figure 3.31 Basal MCF-7X versus MCF-7 cell expression of IGF-1R by Western blotting. MCF-7 and MCF-7X cells were grown on 60 mm dishes in phenol-red-free RPMI media containing 5% SFCS or XFCS respectively. Conditions were maintained for 7 days prior to whole cell lysis, SDS-PAGE (30 µg of sample protein/well) and Western blotting. The nitrocellulose membrane (0.45 µm) was probed for total IGF-1R (125 kDa) and β-Actin (42 kDa). The developed autoradiography film was scanned using densitometric imaging for each blot probed and IGF-1R expression was normalised to β-Actin. The data is presented as the mean +/- SD and the image above is representative of 3 experiments.

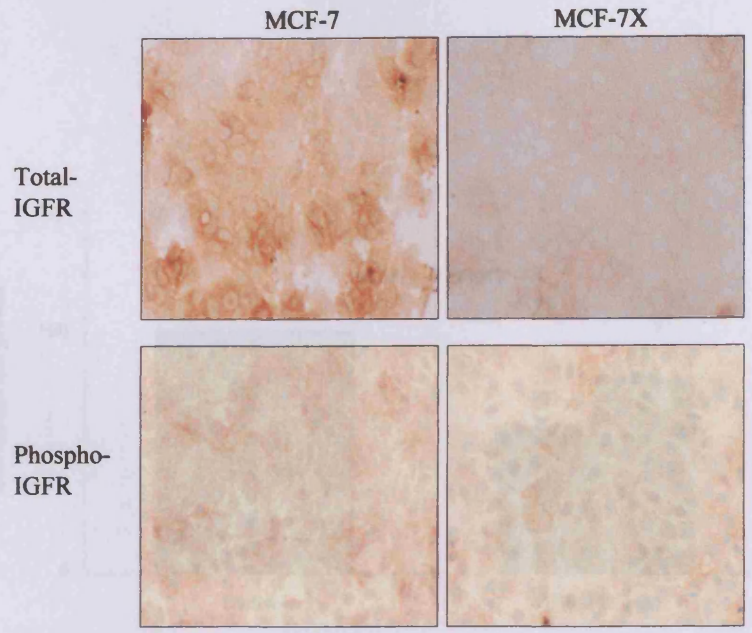

	MCF-7	MCF-7X	p-value
Total IGF-1R			
(Membrane)	75.0 (68.8-82.5)	10.0 (10.0-12.8)	0.003*
(Cytoplasmic)	155.0 (151.3-161.3)	55.0 (50.0-61.3)	0.003*
Total	230.0	65.0	
Phospho-IGFR			
(Membrane)	32.0 (28.8-36.3)	20.0 (15.0-20.0)	0.002*
(Cytoplasmic)	125.0 (120.0-125.0)	135.0 (130.0-135.0)	0.028*
Total	157.0	155.0	

Figure 3.32 Basal MCF-7X versus MCF-7 cell total and phosphorylated IGF-1R levels by immunocytochemistry. MCF-7 and MCF-7X cells were grown on coverslips in phenol-red-free RPMI media containing 5% SFCS or XFCS respectively. Conditions were maintained for 7 days prior to the appropriate fixation. The total IGF-1R (antibody dilution 1:125) and phosph-IGFR (1:150) assays required coverslips fixed in phenol formal saline and methanol vanadate acetone respectively. The digital images shown above (X20 magnification) are representative of 3 experiments. H-Score data was obtained by dual assessment of 2 representative areas on each coverslip followed by statistical analysis (Mann-Whitney U-Test). The median H-Score and Q1-Q3 values are displayed. A p-value <0.05(*) indicates a significant difference in total/phospho- IGF-1R level between MCF-7 and MCF-7X cells.

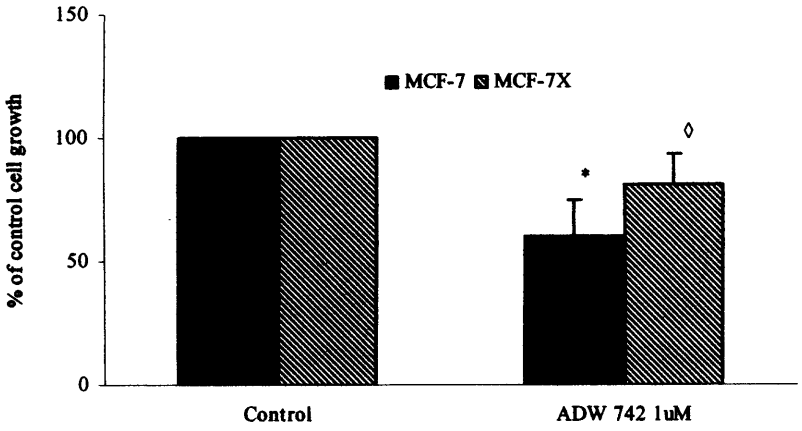

Figure 3.33 Effect of the IGF-1R inhibitor ADW 742 on the growth of MCF-7 and MCF-7X cells. MCF-7 and MCF-7X cells were grown on 24-well plates in phenol-red-free RPMI media containing 5% SFCS or XFCS respectively in the absence or presence of ADW 742 (1 μM). Conditions were maintained for 7 days prior to trypsin dispersion and Coulter counting (triplicate wells per treatment). Data are displayed as a percentage of control cell growth and include 3 experiments +/- SD. The statistical analysis applied was an ANOVA Test followed by a Tamhane Post-Hoc Test.

* and ◊ Denotes ADW 742 treatment significantly inhibited MCF-7 ($p<0.001$) and MCF-7X ($p<0.001$) cell growth versus their respective controls.

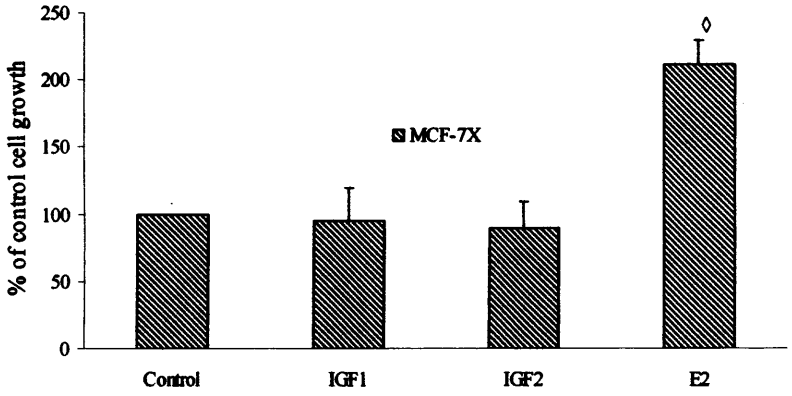

Figure 3.34 Effect of exogenous IGF ligands on the growth of MCF-7X cells. MCF-7X cells were grown on 24-well plates in phenol-red-free RPMI media containing 5% XFCS. Media was supplemented with IGF-1, -2 (10 ng/ml), E_2 (10^{-9} M) or control (ethanol 1 µl/ 10 ml). Conditions were maintained for 7 days prior to trypsin dispersion and Coulter counting (triplicate wells per treatment). Data is displayed as percentage of control cell growth and include 4 experiments +/- SD. The statistical analysis applied was an ANOVA Test followed by a Tamhane Post-Hoc Test.

◊ Denotes E_2 had a significant stimulatory effect on MCF-7X cell growth versus control ($p<0.001$).

3.2.2 Epidermal Growth Factor Receptor (EGFR)/HER2 Signalling

The over-expression of EGFR and HER2 has been found in a proportion of breast cancers and correlates with an adverse prognosis for survival. Implicated in our own acquired tamoxifen resistant cell line, there is evidence that the EGFR/HER2 pathway is involved in a cross-talk relationship with the ER that contributes to endocrine resistance (Knowlden *et al.*, 2003b). Within the MCF-7X *in vitro* model detailed investigation of EGFR and HER2 tyrosine kinase signalling pathways was performed versus the parental MCF-7 cell line. Protein expression of total EGFR (175 kDa) by Western blotting (Figure 3.35) revealed low levels in both MCF-7X cells and MCF-7 cells. While immunocytochemistry (Figure 3.36) revealed similar levels of plasma membrane EGFR expression in MCF-7X versus MCF-7 cells (p=0.866), cytoplasmic staining was significantly lower in the resistant line (65.7% fall, p=0.004*). Furthermore, while there was only a very low level of phosphorylated plasma membrane staining in both lines, again an obvious fall in cytoplasmic EGFR activity (42.9% fall, p=0.003*) using a pan-phospho-specific EGFR antibody was observed in MCF-7X cells.

RT-PCR indicated HER2 mRNA (98 bp) expression was equivalent in MCF-7X cells versus MCF-7 cells (p=0.275, Figure 3.37) with parallel Western blotting also indicating that total and phosphorylated HER2 (185 kDa) levels were similar in the two cell lines (Figure 3.38). There was similarly no significant change in expression of HER2 as detected by immunocytochemistry. However this technique did detect an apparent fall in MCF-7X cell membrane activity (33.3%, p=0.006*) versus MCF-7 cells coupled with a significant fall in cytoplasmic activity (87.1%, p=0.003*, Figure 3.39).

These EGFR/HER2 data suggest a diminished role for such signalling activity in MCF-7X versus MCF-7 cells. In agreement, there was a lack of obvious effect of inhibitors specifically targeting such signalling in MCF-7X cells (Figure 3.40). The selective EGFR tyrosine kinase inhibitor (TKI) gefitinib failed to significantly inhibit MCF-7X growth (p=0.102) using a 1 μM concentration. This has previously been demonstrated to be EGFR-selective and highly growth-inhibitory across our various anti-oestrogen resistant cell lines, versus the smaller significant effect on the parental MCF-7 cell line (32.9%, p<0.001*, Figure 3.40). Challenge with humanised HER2 directed monoclonal antibody herceptin (100 nM) also failed to exert any growth

inhibitory effect in MCF-7X cells (p=1.000) versus a modest significant effect in MCF-7 cells (21.5% fall, p=0.001*). Combination treatment was similarly ineffective in MCF-7X cells (Figure 3.40) however in MCF-7 cells the combination appeared equivalent to the significant effect of either herceptin or TKI alone (this arm of the experiment was only included once). Ligand challenge with an extensive range of peptide growth factors (10 ng/ml) for the erbB family of receptors (including HER3), notably epidermal growth factor (EGF), transforming growth factor-α (TGFα), heregulin- α, heregulin- β and amphiregulin, all failed to stimulate MCF-7X cell growth (Figure 3.41). There thus appears to be little EGFR/HER2 (and potentially HER3) signalling contribution to MCF-7X cell growth, contrasting several reported long-term oestrogen deprived cells developed in the presence of exogenous growth factors from Santen *et al.* (2004a), Martin *et al.* (2003) and Brodie *et al.* (1999).

Moreover, a range of ligands for further key growth factor receptors including fibroblast growth factors (FGFs), vascular endothelial growth factor (VEGF) and platelet derived growth factor (Figure 3.42) failed to exert any positive effect on growth in MCF-7X cells. These data cumulatively suggest no dominant role for classical growth factor receptor signalling in our long-term oestrogen deprived MCF-7X model derived in the absence of exogenous growth factors.

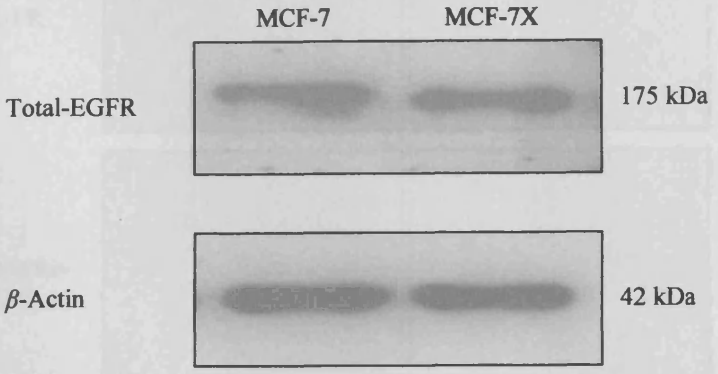

	MCF-7	MCF-7X
Total-EGFR	3.3 +/- 0.8	3.0 +/- 0.4

Figure 3.35 Basal MCF-7X versus MCF-7 cell expression of EGFR by Western blotting. MCF-7 and MCF-7X cells were grown on 60 mm dishes in phenol-red-free RPMI media containing 5% SFCS or XFCS respectively. Conditions were maintained for 7 days prior to whole cell lysis, SDS-PAGE (30 µg of sample protein/well) and Western blotting. The nitrocellulose membrane (0.45 µm) was probed for total EGFR (175 kDa) and β-Actin (42 kDa). The developed autoradiography film was scanned using densitometric imaging for each blot probed and EGFR expression was normalised to β-Actin. The data is presented as the mean +/- SD and the image above is representative of 3 experiments.

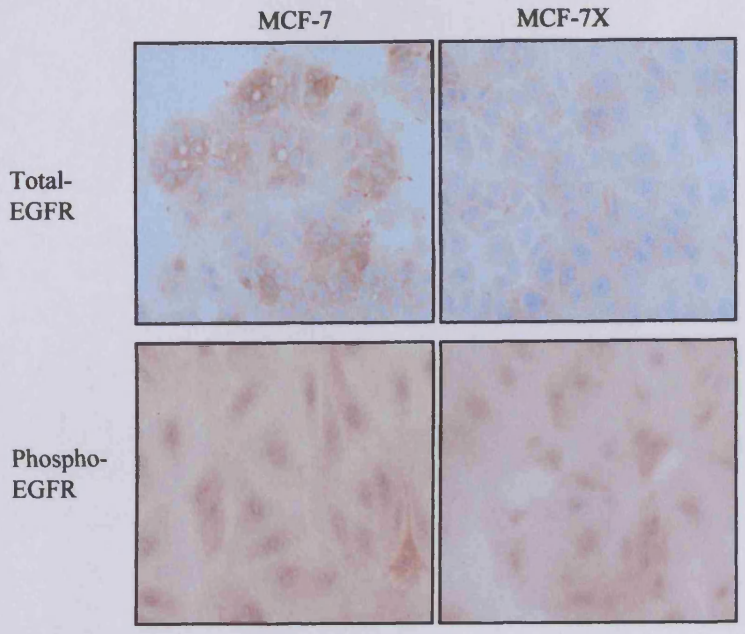

	MCF-7	MCF-7X	p-value
Total EGFR			
(Membrane)	32.5 (30.0-40.3)	35.0 (30.0-40.0)	0.866
(Cytoplasmic)	87.5 (78.8-100.0)	30.0 (28.0-35.0)	0.004*
Total	120.0	65.0	
Phospho-EGFR			
(Membrane)	3.0 (2.0-4.3)	1.5 (1.0-2.0)	0.012*
(Cytoplasmic)	70.0 (68.8-76.3)	40.0 (38.8-45.0)	0.003*
Total	73.0	41.5	

Figure 3.36 Basal MCF-7X versus MCF-7 cell total and phosphorylated EGFR levels by immunocytochemistry. MCF-7 and MCF-7X cells were grown on coverslips in phenol-red-free RPMI media containing 5% SFCS or XFCS respectively. Conditions were maintained for 7 days prior to the appropriated fixation. The total EGFR (antibody dilution 1:100) and the phospho-EGFR (1:5) assays required coverslips fixed in phenol formal saline and methanol acetone respectively. The digital images shown above (X20 magnification) are representative of 3 experiments. H-Score data were obtained by dual assessment of 2 representative areas of each coverslip followed by statistical analysis (Mann-Whitney U-Test). The median H-Score and Q1-Q3 values are displayed. A p-value <0.05(*) indicates a significant difference in total/phospho- EGFR level between MCF-7 and MCF-7X cells.

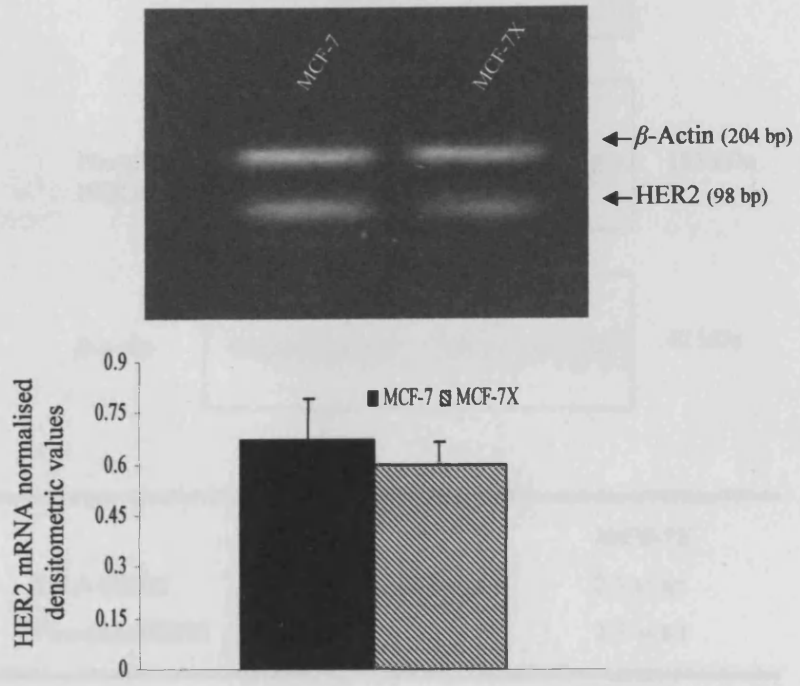

Figure 3.37 Basal MCF-7X versus MCF-7 cell mRNA expression of HER2 by RT-PCR. MCF-7 and MCF-7X cells were grown on 100 mm dishes in phenol-red-free RPMI media containing 5% SFCS or XFCS respectively. Conditions were maintained for 7 days before RNA was isolated and reverse transcribed. Individual RT-PCR of HER2 (35 cycles/ 55°C annealing temperature, 98 bp) and β-Actin (25 cycles/ 55°C annealing temperature, 204 bp) was performed. Product from each reaction was combined and run on a 2% agarose gel containing ethidium bromide, subsequently photographed, scanned and normalised to β-Actin. The digital image above is representative of 3 experiments and the statistical analysis applied was an unpaired-T test (p=0.275) comparing mean HER2 expression in MCF-7 (0.7 +/- 0.1) and MCF-7X (0.6 +/- 0.1) cells.

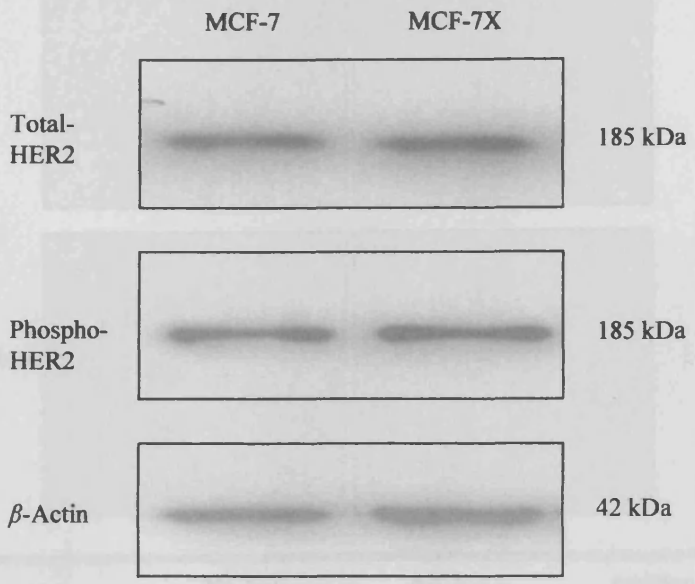

	MCF-7	MCF-7X
Total-HER2	2.6 +/- 0.3	2.3 +/- 0.5
Phospho-HER2	2.5 +/- 0.5	2.7 +/- 0.4

Figure 3.38 Basal MCF-7X versus MCF-7 cell levels of total and phosphorylated HER2 by Western blotting. MCF-7 and MCF-7X cells were grown on 60 mm dishes in phenol-red-free RPMI media containing 5% SFCS or XFCS respectively. Conditions were maintained for 7 days prior to whole cell lysis, SDS-PAGE (30 µg of sample protein/well) and Western blotting. The nitrocellulose membrane (0.45 µm) was probed for total HER2 (185 kDa), phospho-HER2 (185 kDa) and β-Actin (42 kD). The developed autoradiography film was scanned using densitometric imaging for each blot probed. Subsequently, both total and phospho-HER2 blots were normalised to β-Actin. The data is presented as the mean +/- SD and the image above is representative of 5 experiments.

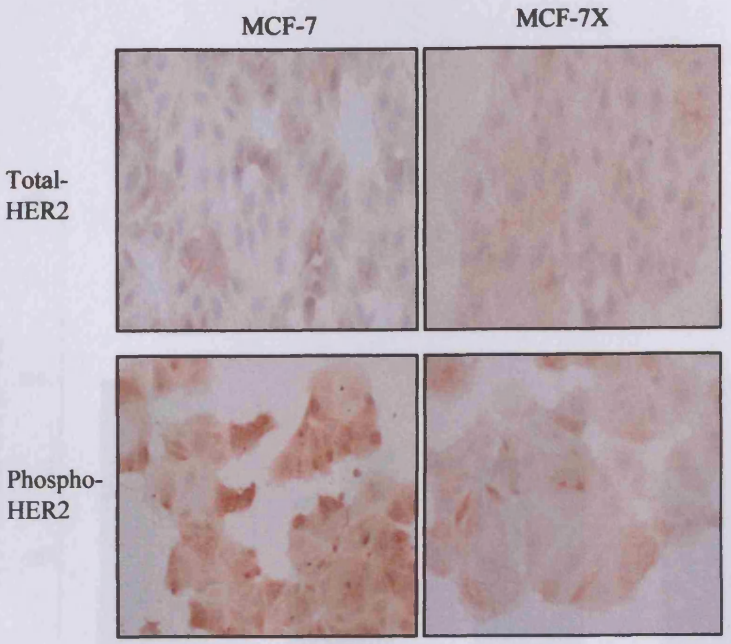

	MCF-7	MCF-7X	p-value
Total HER2			
(Membrane)	57.5 (45.0-60.0)	67.5 (51.3-78.8)	0.107
(Cytoplasmic)	30.0 (25.0-31.3)	25.0 (20.0-30.0)	0.117
Total	87.5	92.5	
Phospho-HER2			
(Membrane)	22.5 (20.0-31.5)	15.0 (13.8-16.3)	0.006*
(Cytoplasmic)	77.5 (73.8-81.3)	10.0 (10.0-15.0)	0.003*
Total	100.0	25.0	

Figure 3.39 Basal MCF-7X versus MCF-7 cell total and phosphorylated HER2 levels by immunocytochemistry. MCF-7 and MCF-7X cells were grown on coverslips in phenol-red-free RPMI media containing 5% SFCS or XFCS respectively. Conditions were maintained for 7 days prior to the appropriate fixation. The total HER2 (antibody dilution 1:100) and the phospho-HER2 (1:20) assays required coverslips fixed in ERICA and methanol vanadate acetone respectively. The digital images shown above (X20 original magnification) are representative of 3 experiments. H-Score data were obtained by dual assessment of 2 representative areas of each coverslip followed by statistical analysis (Mann-Whitney U-Test). The median H-Score and Q1-Q3 values are displayed. A p-value <0.05(*) indicates a significant difference in total/phospho- HER2 level between MCF-7 and MCF-7X cells.

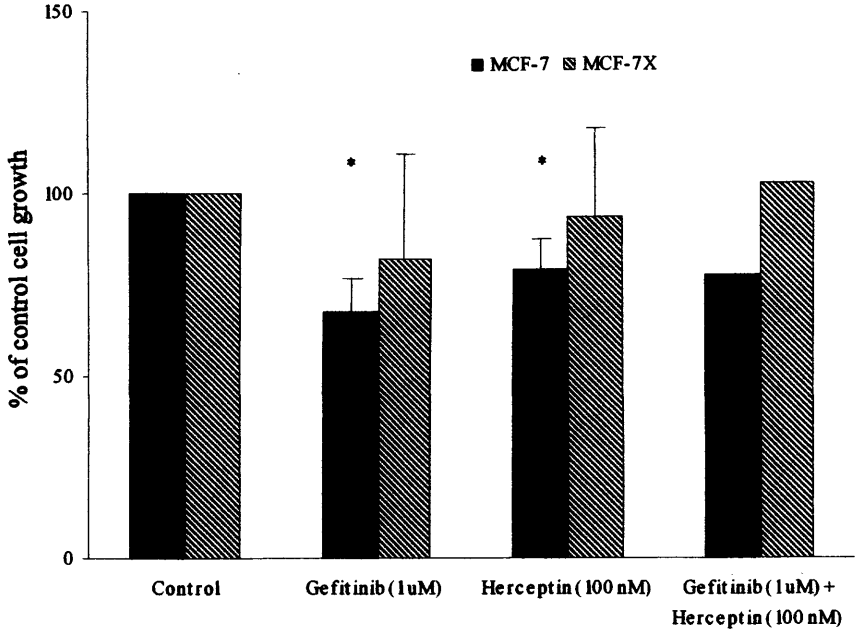

Figure 3.40 Effect of the EGFR inhibitor gefitinib and the HER2 monoclonal antibody herceptin singly and in combination on the growth of MCF-7 and MCF-7X cells. MCF-7 and MCF-7X cells were grown on 24-well plates in phenol-red-free RPMI media containing 5% SFCS or XFCS respectively in the absence and presence of gefitinib (1 μM), herceptin (100 nM) or gefitinib/herceptin co-treatement. Conditions were maintained for 7 days prior to trypsin dispersion and Coulter counting (triplicate wells per treatment). Data are displayed as a percentage of control cell growth and include 4 experiments +/- SD, with the exception of the gefitinib/herceptin combination (1 experiment only). The statistical analysis applied was an ANOVA Test followed by a Tamhane Post-Hoc Test.

* Denotes gefitinib ($p<0.001$) and herceptin ($p=0.001$) treatment significantly inhibited MCF-7 cell growth versus control.

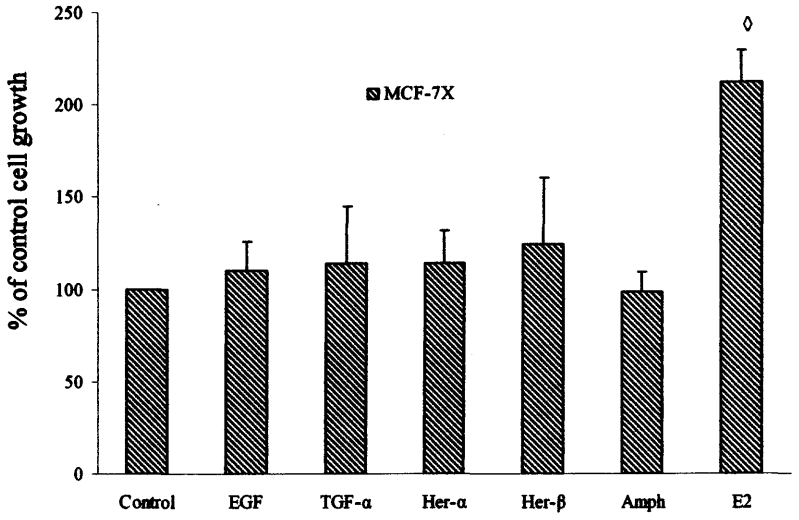

Figure 3.41 Effect of exogenous EGF-like ligands on the growth of MCF-7X cells. MCF-7X cells were grown on 24-well plates in phenol-red-free RPMI media containing 5% XFCS. Media was supplemented (10 ng/ml) with EGF, TGFα, Heregulin-α, Heregulin-β, amphiregulin, E_2 (10^{-9} M) or control (1 µl/ 10 ml). Conditions were maintained for 7 days prior to trypsin dispersion and Coulter counting (triplicate wells per treatment). Data are displayed as a percentage of control cell growth and include 4 experiments +/- SD. The statistical analysis applied was an ANOVA Test followed by a Tamhane Post-Hoc Test.

◊ Denotes E_2 had significant stimulatory effect on MCF-7X cell growth versus control ($p<0.001$).

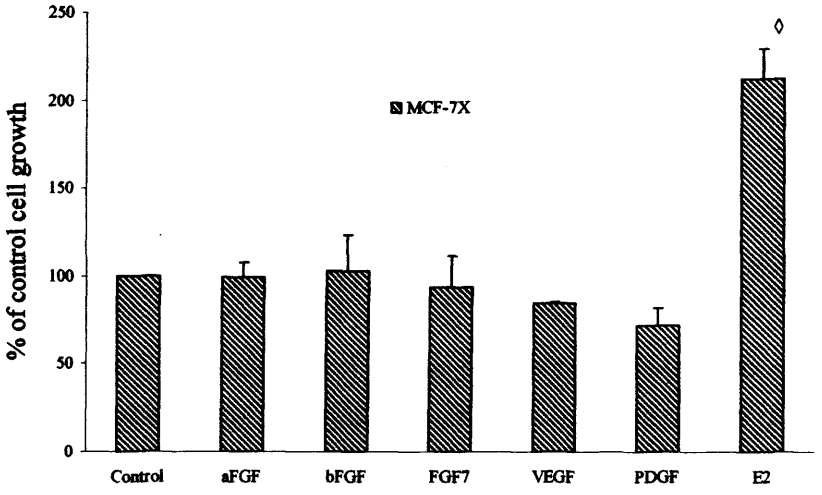

Figure 3.42 Effect of exogenous FGF, VEGF, and PDGF ligands on the growth of MCF-7X cells. MCF-7X cells were grown on 24-well plates in phenol-red-free RPMI media containing 5% XFCS. Media was supplemented (10 ng/ml) with acidic FGF, basic FGF, FGF7, VEGF, PDGF, E_2 (10^{-9} M) or control (ethanol 1 µl/ 10 ml). Conditions were maintained for 7 days prior to trypsin dispersion and Coulter counting (triplicate wells per treatment). Data are displayed as a percentage of control cell growth and include 4 experiments +/- SD. The statistical analysis applied was an ANOVA Test followed by a Tamhane Post-Hoc Test.

◊ Denotes E_2 had a significant stimulatory effect on MCF-7X cell growth versus control ($p<0.001$).

3.3 GROWTH FACTOR SIGNALLING PATHWAYS: INTRACELLULAR KINASES

3.3.1 Mitogen Activated Protein Kinase (MAPK) Signalling

An adaptive increase in the activity of ERK1/2 mitogen activated protein kinase (MAPK) and recruitment to growth has been implicated from our own studies of anti-oestrogen resistance (McClelland *et al.*, 2001; Gee *et al.*, 2003). Parallel *in vitro* and *in vivo* evidence also suggests this adaptation occurs in long-term oestrogen deprivation (Jeng *et al.*, 2000; Martin *et al.*, 2003; Santen *et al.*, 2004a). MAPK (42/44 kDa) was detectable in MCF-7X cells by Western blotting and its expression and activity was unchanged versus the parental MCF-7 cells known to exhibit quite low levels of such signalling using this detection procedure (Figure 3.43). Immunocytochemistry (Figure 3.46) revealed very little nuclear phosphorylated MAPK in either MCF-7 or MCF-7X cells, but was able to detect a significant 46.1% decrease ($p=0.002^*$) in cytoplasmic-localised phosphorylated MAPK in the resistant line attributed predominantly to a reduction in the percentage of positive staining.

Challenge with the MAP kinase kinase (MEK1) inhibitor PD98059 was able to significantly reduced MCF-7 cell growth 35.0% ($p<0.001^*$) by day 7 (Figure 3.44). In keeping with the reduced prominence of MAPK activity in MCF-7X cells, PD98059 (25 μM) was unable to substantially inhibit cell growth. Moreover growth curve studies revealed PD98059 effect measured at day 7 or day 15 could not produce a significant growth inhibitory effect (Figure 3.45, $p=1.000$). This was despite the MEK1 inhibitor after 7 days significantly depleting the cytoplasmic phosphorylated MAPK in both MCF-7 and MCF-7X cells (53.1%, $p=0.003^*$ and 70.0%, $p=0.001^*$ respectively) as detected by immunocytochemistry (Figure 3.46). Western blotting in MCF-7X cells confirmed this reduction of phosphorylated MAPK with PD98059 (Figure 3.47). Clearly, although there may be a small contribution for MAPK signalling in MCF-7 cells, this kinase does not appear to provide a dominant growth mechanism in MCF-7X cells.

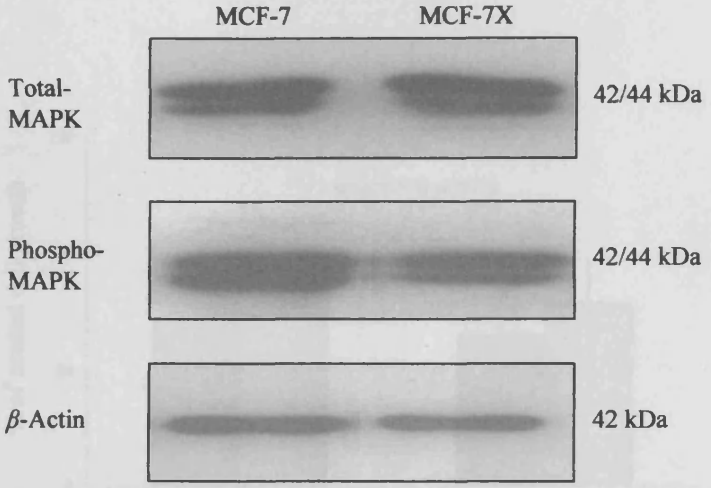

	MCF-7	MCF-7X
Total-MAPK	1.9 +/- 0.4	1.6 +/- 0.3
Phospho-MAPK	1.7 +/- 0.6	1.3 +/- 0.5

Figure 3.43 Basal MCF-7X versus MCF-7 cell levels of total and phosphorylated MAPK by Western blotting. MCF-7 and MCF-7X cells were grown on 60 mm dishes in phenol-red-free RPMI media containing 5% SFCS or XFCS respectively. Conditions were maintained for 7 days prior to whole cell lysis, SDS-PAGE (30 µg of sample protein/well) and Western blotting. The nitrocellulose membrane (0.45 µm) was probed for total MAPK (42/44 kDa), phosphorylated MAPK (42/44 kDa) and β-Actin (42 kDa). The developed autoradiography film was scanned using densitometric imaging for each blot probed. Subsequently, both total and phospho-MAPK blots were normalised to β-Actin. The data is presented as the mean +/- SD and the image above is representative of 4 experiments.

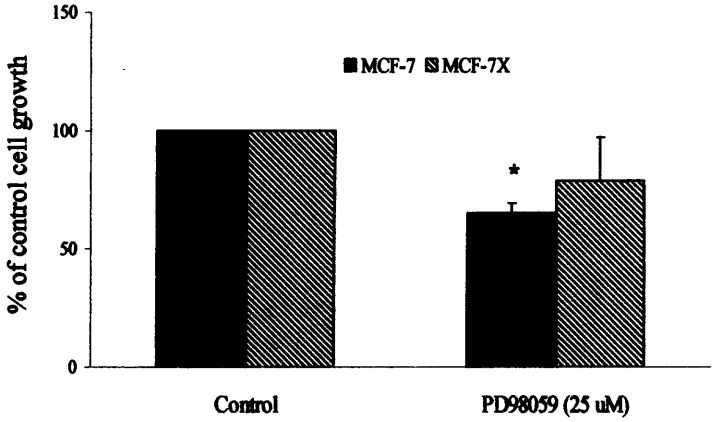

Figure 3.44 Effect of the MEK-1 inhibitor PD98059 on the growth of MCF-7 and MCF-7X cells. MCF-7 and MCF-7X cells were grown on 24-well plates in phenol-red-free RPMI media containing 5% SFCS or XFCS respectively in the absence or presence of PD98059 (25 μM). Conditions were maintained for 7 days prior to trypsin dispersion and Coulter counting (triplicate wells per treatment). Data are displayed as a percentage of control cell growth and include 5 experiments +/- SD. The statistical analysis applied was an ANOVA Test followed by a Tamhane Post-Hoc Test.

* Denotes PD98059 treatment significantly inhibited MCF-7 ($p<0.001$) cell growth versus control.

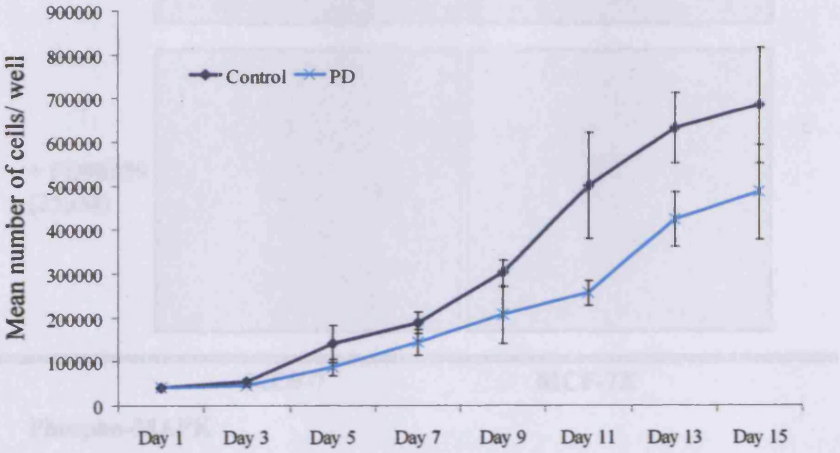

Figure 3.45 Growth of MCF-7X cells challenged with the MEK-1 inhibitor PD98059. MCF-7X cells were grown on 24-well plates in phenol-red-free RPMI media containing 5% XFCS in the absence or presence of PD98059 (25 μM) for 15 days. At the time points indicated above, cells were subject to trypsin dispersion followed by Coulter counting (triplicate wells per time point). The data were log transformed to compare growth rate at day 7 and 15. The statistical analysis applied was an ANOVA Test followed by a Bonferroni Post-Hoc Test. The data is displayed as the mean number of cells/well +/- SD (n=5).

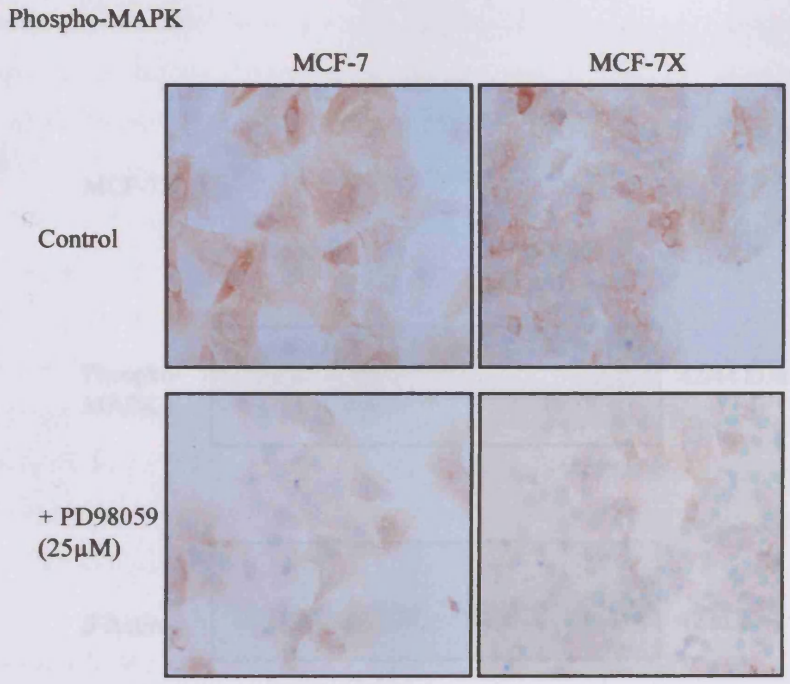

	MCF-7		MCF-7X	
Phospho-MAPK				
Basal Control				
(Cytoplasmic)	65.0 (63.8-72.5)		35.0 (35.0-48.8)	
(Nuclear)	5.0 (3.0-5.0)		3.5 (1.3-5.0)	
Total	70.0		38.5	
+ PD98059 (25 μM)				
(Cytoplasmic)	30.5 (30.0-36.3)	p=0.003*	10.5 (5.0-10.0)	p=0.001*
(Nuclear)	5.0 (3.8-5.5)	p=0.589	1.0 (1.0-1.8)	p=0.023*
Total	35.5		11.5	

Figure 3.46 Effect of the MEK-1 inhibitor PD98059 on phosphorylated MAPK level in MCF-7 and MCF-7X cells by immunocytochemistry. MCF-7 and MCF-7X cells were grown on coverslips in phenol-red-free RPMI media containing 5% SFCS or XFCS respectively in the absence or presence of PD98059 (25 μM). Conditions were maintained for 7 days prior to formal saline fixation. The phospho-MAPK (antibody dilution 1:20) digital images shown above (X20 magnification) are representative of 4 experiments. H-Score data was obtained by dual assessment of 2 representative areas of each coverslip followed by statistical analysis (Mann-Whitney U-Test). The median H-Score and Q1-Q3 values are displayed. A p-value <0.05(*) indicates a significant difference in phospho-MAPK level following PD98059 treatment.

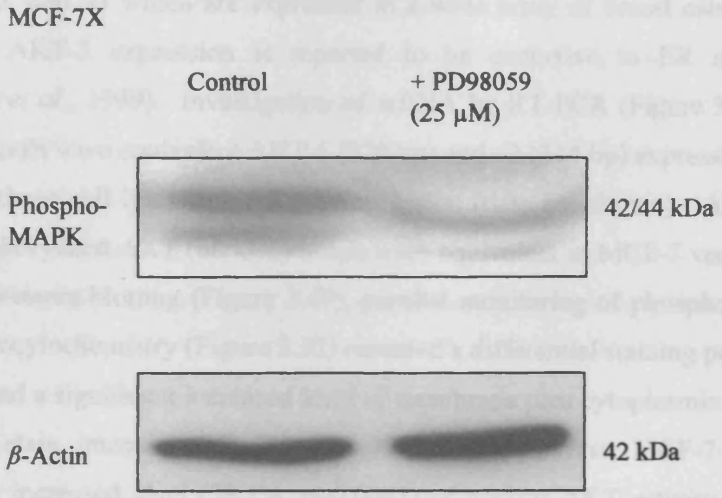

Figure 3.47 Effect of the MEK-1 inhibitor PD98059 on phosphorylated MAPK level in MCF-7X cells by Western blotting. MCF-7X cells were grown on 60 mm dishes in phenol-red-free media containing 5% XFCS in the absence and presence of PD98059 (25 μM). Conditions were maintained for 7 days prior to whole cell lysis, SDS-PAGE (40 μg of sample protein/well) and Western blotting. The nitrocellulose membrane (0.45 μm) was probed for phospho-MAPK (42/44 kDa) and β-Actin (42 kDa). The developed autoradiography film was scanned using densitometric imaging for each blot probed and phospho-MAPK level was normalised to β-Actin. Above is a representative experiment.

3.3.2 PI3K/AKT Signalling

The AKT/PKB kinase lies downstream of PI3 kinase (PI3K) and controls a number of intracellular processes that have been implicated in the genesis and/or progression of breast cancer, mainly effector molecules involved in regulating cell survival and cell cycle progression (Zinda *et al.*, 2001). Three isoforms of AKT have been identified, AKT-1, -2, and –3 which are expressed in a wide array of breast cancer cell lines. However AKT-3 expression is reported to be exclusive to ER negative cells (Nakatani *et al.*, 1999). Investigation of mRNA by RT-PCR (Figure 3.48) revealed MCF-7X cells have equivalent AKT-1 (329 bp) and –2 (314 bp) expression to MCF-7 cells and these cell lines lack AKT-3 expression (data not shown). Although, total and phosphorylated AKT (60 kDa) levels were equivalent in MCF-7 versus MCF-7X cells by Western blotting (Figure 3.49), parallel monitoring of phosphorylated AKT by immunocytochemistry (Figure 3.52) revealed a differential staining pattern. MCF-7X cells had a significant increased level of membrane plus cytoplasmic signal due to increased stain intensity (170.7%, p=0.004*). In contrast, MCF-7 cells had a significant increased level (58.1%, p=0.004*) of nuclear AKT activity compared to MCF-7X cells. This differential pattern across the two cell lines is likely to explain the equivalent overall phosphorylated AKT levels observed by Western blotting. PDK-1 (phosphoinositide-dependent protein kinase-1) is also a downstream signalling element of PI3K and immunocytochemistry (Figure 3.54) demonstrated its activity in the cytoplasm, like AKT, was also significantly increased (34.9%) in MCF-7X cells compared to MCF-7 cells (p=0.004*). This increase was predominantly due to increased staining intensity in MCF-7X.

The PI3K inhibitor LY294002 (5 μM) was superior in reducing MCF-7X cell growth 49.1% (p<0.001*) after 7 days of treatment versus a modest 21.6% (p<0.001*) inhibitory effect on MCF-7 cell growth (Figure 3.50). A growth curve subsequently monitoring the effect of LY294002 on MCF-7X cell growth revealed that the inhibitory response was further increased to 69.1% (p<0.001*) by day 15 versus the untreated control (Figure 3.51). PI3K/AKT signalling thus appears to be of increased importance to MCF-7X cell growth versus the parental line, in accordance with the increased cytoplasmic activity of AKT and PDK-1. To ensure the agent was targeting the activity of the PI3K pathway in parallel with these growth effects in MCF-7X cells, immunocytochemistry and Western blotting were employed to evaluate the status of phosphorylated AKT and PDK-1 before and after 7 day treatment.

LY294002 treatment resulted in a significant decrease of phosphorylated AKT, comprising a 66.0% (p=0.004*) decrease in membrane plus cytoplasmic activity coupled with a 32.1% (p=0.004*) decrease in nuclear activity by immunocytochemical analysis of MCF-7X cells (Figure 3.52). In contrast, there was a smaller significant decline in membrane plus cytoplasmic AKT activity alone detected with LY294002 in MCF-7 cells (17.3% fall, p=0.012*). Western blotting in MCF-7X cells confirmed an obvious reduction of phosphorylated AKT in MCF-7X cells treated with LY294002 (Figure 3.53). The activity of PDK-1 was also investigated following treatment challenge with the PI3K inhibitor LY294002 by immunocytochemistry (Figure 3.54) in MCF-7 and MCF-7X cells. The results revealed a 31.0% (p=0.004*) inhibitory effect on the cytoplasmic activity of PDK-1 in MCF-7X cells, largely due to a decreased intensity of positive staining, in contrast to the lack of inhibitory effect in MCF-7 cells. To further qualify the apparent growth contribution of PI3K signalling in MCF-7X cells, the impact of the PI3K inhibitor wortmannin (1 μM) was briefly examined in these cells. This agent partially inhibited growth 25.9% in MCF-7X cells (Figure 3.55) at 7 days, an event that was again associated with a significant depletion of AKT activity. Immunocytochemistry revealed a 31.0% (p=0.041*) reduction in membrane plus cytoplasmic activity and a 32.6% (p=0.004*) decrease in nuclear activity in MCF-7X cells (Figure 3.56). Furthermore, unlike LY294002 treatment wortmannin treatment had no effect on the phosphorylation of cytoplasmic localised PDK-1 (p=0.104, Figure 3.56).

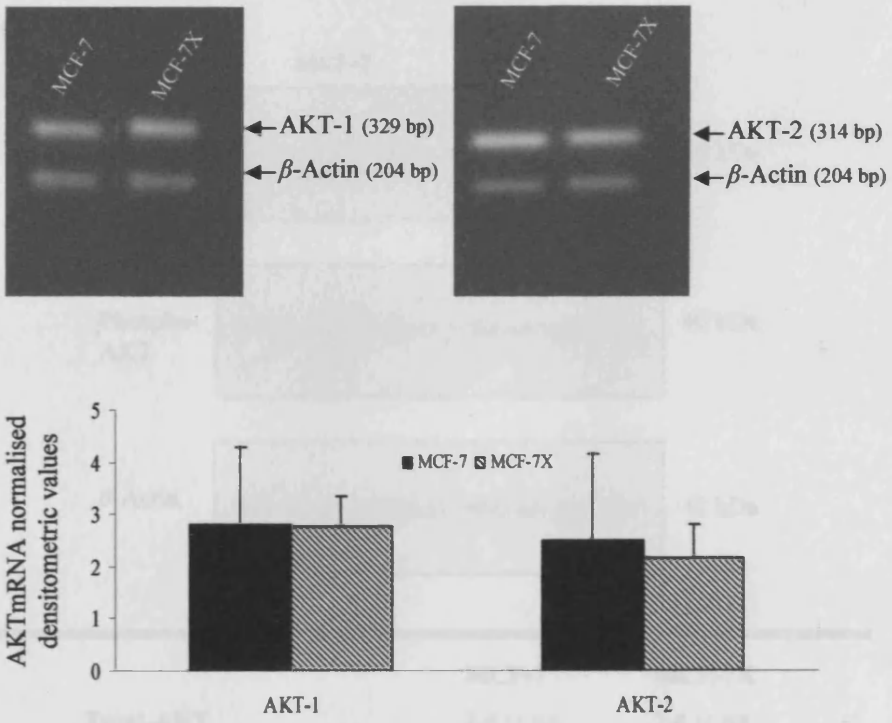

Figure 3.48 Basal MCF-7 versus MCF-7X cell mRNA expression of AKT-1 and AKT-2 by RT-PCR. MCF-7 and MCF-7X cells were grown on 100 mm dishes in phenol-red-free RPMI media containing 5% SFCS or XFCS respectively. Conditions were maintained for 7 days before RNA was isolated and reverse transcribed. Co-amplification RT-PCR of AKT-1 (29 cycles/ 55°C annealing temperature, 329 bp) and β-Actin (204 bp) was performed. Co-amplification RT-PCR of AKT-2 (29 cycles/ 55°C annealing temperature, 314 bp) and β-Actin was performed. Product from each reaction was run on a 2% agarose gel containing ethidium bromide, subsequently photographed, scanned and normalised to β-Actin. The digital images above are representative of 3 experiments (for each target sequence) and the statistical analysis applied was an unpaired-T test comparing mean AKT-1 expression (p=0.974) in MCF-7 (2.1 +/- 1.5) and MCF-7X (2.8 +/- 0.6) cells. An unpaired-T test was also applied to compare mean AKT-2 expression (p=0.758) in MCF-7 (2.5 +/- 1.7) and MCF-7X (2.2 +/- 0.6) cells.

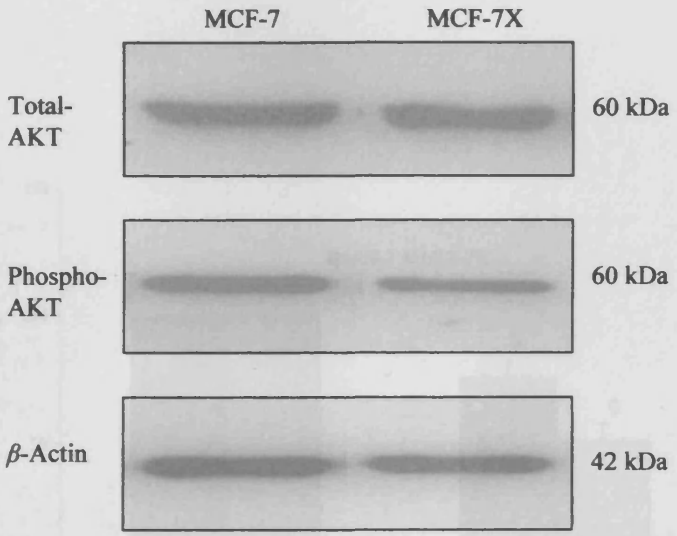

	MCF-7	MCF-7X
Total-AKT	2.4 +/- 0.6	2.4 +/- 0.8
Phospho-AKT	2.1 +/- 0.9	1.9 +/- 0.6

Figure 3.49 Basal MCF-7X versus MCF-7 cell levels of total and phosphorylated AKT by Western blotting. MCF-7 and MCF-7X cells were grown on 60 mm dishes in phenol-red-free RPMI media containing 5% SFCS or XFCS respectively. Conditions were maintained for 7 days prior to whole cell lysis, SDS-PAGE (40 µg of sample protein/well) and Western blotting. The nitrocellulose membrane (0.45 µm) was probed for total AKT (60 kDa), phosphorylated AKT (60 kDa) and β-Actin (42 kDa). The developed autoradiography film was scanned using densitometric imaging for each blot probed. Subsequently, both total and phospho-AKT blots were normalised to β-Actin. The data is presented as the mean +/- SD and the image above is representative of 4 experiments.

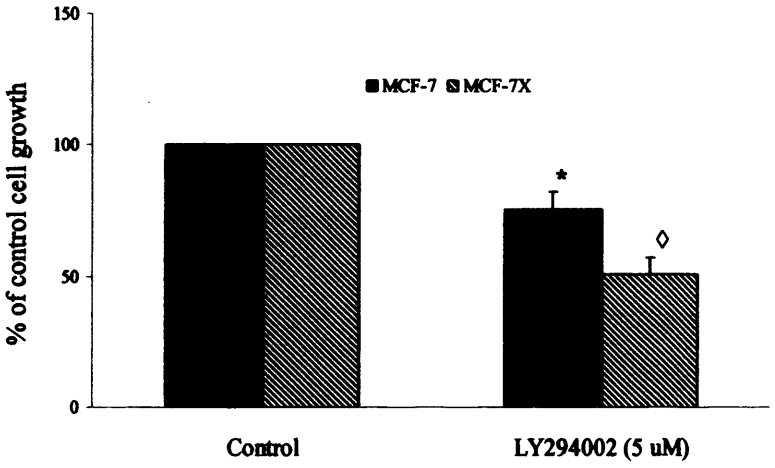

Figure 3.50 Effect of the PI3K inhibitor LY294002 on the growth of MCF-7 and MCF-7X cells. MCF-7 and MCF-7X cells were grown on 24-well plates in phenol-red-free RPMI media containing 5% SFCS or XFCS respectively in the absence or presence of LY294002 (5 μM). Conditions were maintained for 7 days prior to trypsin dispersion and Coulter counting (triplicate wells per treatment). Data are displayed as a percentage of control cell growth and include 5 experiments +/- SD. The statistical analysis applied was an ANOVA Test followed by a Tamhane Post-Hoc Test.

* and ◊ Denotes LY294002 treatment significantly inhibited MCF-7 ($p<0.001$) and MCF-7X ($p<0.001$) cell growth versus their respective controls.

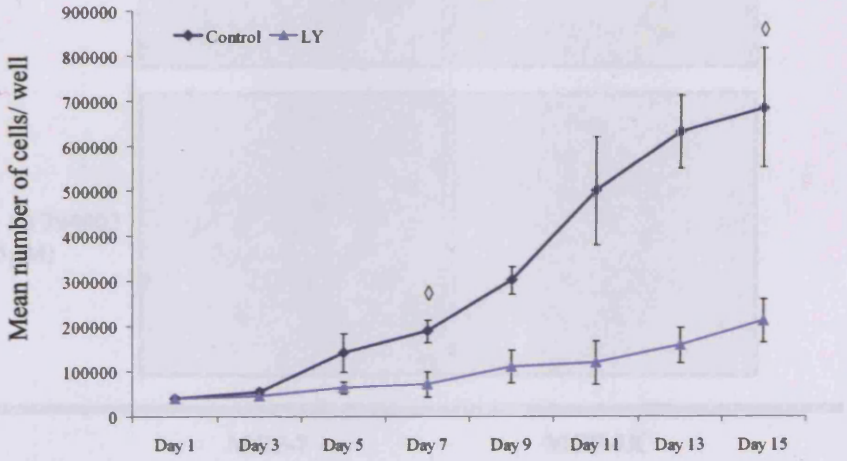

Figure 3.51 Growth of MCF-7X cells challenged with the PI3K inhibitor LY294002. MCF-7X cells were grown on 24-well plates in phenol-red-free RPMI media containing 5% XFCS in the absence or presence of the PI3K inhibitor LY294002 (5 μM) for 15 days. At the time points indicated above, cells were subject to trypsin dispersion followed by Coulter counting (triplicate wells per time point). The data was log transformed to compare growth rate at day 7 and 15. The statistical analysis applied was an ANOVA Test followed by a Bonferroni Post-Hoc Test. The data is displayed as the mean number of cells/well +/- SD (n=5).

◊ Denotes LY294002 treatment was significantly lower at day 7 ($p<0.001$) and day 15 ($p<0.001$) versus untreated MCF-7X cells.

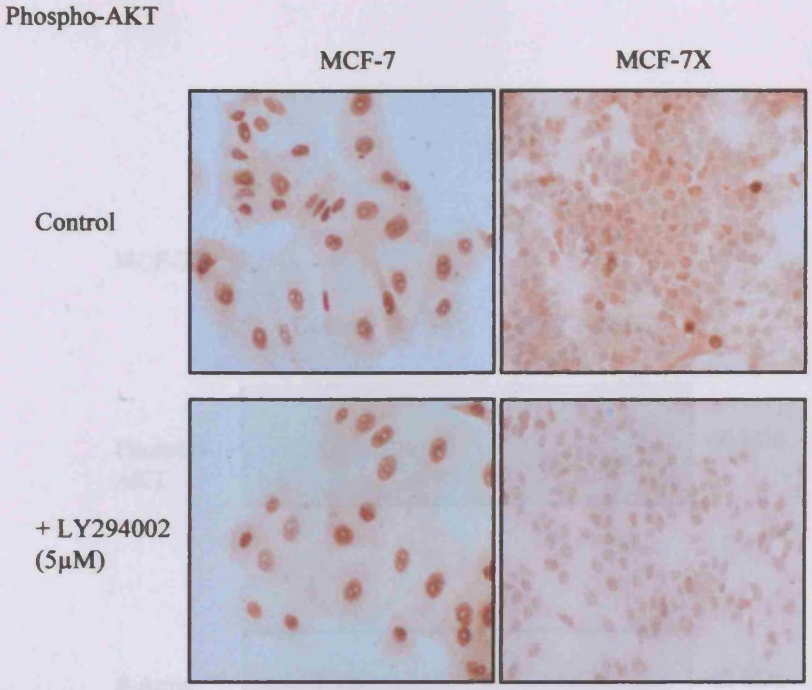

	MCF-7		MCF-7X	
Phospho-AKT				
Basal Control				
(Memb. + Cyto.)	37.5 (33.5-43.0)		101.5 (76.5-119.3)	
(Nuclear)	170.0 (157.5-181.3)		107.5 (95.0-112.5)	
Total	207.5		209.0	
+ LY294002 (5 μM)				
(Memb. + Cyto.)	31.0 (26.0-33.0)	p=0.012*	34.5 (32.0-57.0)	p=0.004*
(Nuclear)	157.5 (151.3-168.8)	p=0.197	73.0 (61.0-81.3)	p=0.004*
Total	188.5		107.5	

Figure 3.52 Effect of the PI3K inhibitor LY294002 on phosphorylated AKT level in MCF-7 and MCF-7X cells by immunocytochemistry. MCF-7 and MCF-7X cells were grown on coverslips in phenol-red-free RPMI media containing 5% SFCS or XFCS respectively in the absence or presence of LY294002 (5 μM). Conditions were maintained for 7 days prior to ERICA fixation. The phospho-AKT (antibody dilution 1:200) digital images above (MCF-7 cells X40 magnification and MCF-7X cells X20) are representative of 4 experiments. H-Score data were obtained by dual assessment of 2 representative areas of each coverslip followed by statistical analysis (Mann-Whitney U-Test). The median H-Score and Q1-Q3 values are displayed. A p-value <0.05(*) indicates a significant difference in phospho-AKT level following LY294002 treatment.

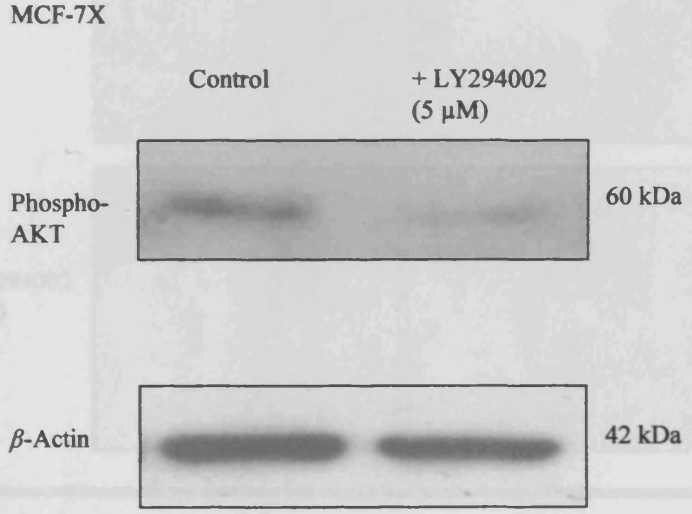

Figure 3.53 Effect of the PI3K inhibitor on phosphorylated AKT level in MCF-7X cells by Western blotting. MCF-7X cells were grown on 60 mm dishes in phenol-red-free media containing 5% XFCS in the absence and presence of LY294002 (5 μM). Conditions were maintained for 7 days prior to whole cell lysis, SDS-PAGE (40 μg of sample protein/well) and Western blotting. The nitrocellulose membrane (0.45 μm) was probed for phospho-AKT (60 kDa) and β-Actin (42 kDa). The developed autoradiography film was scanned using densitometeric imaging for each blot probed and phospho-AKT expression was normalised to β-Actin. Above is a representative experiment.

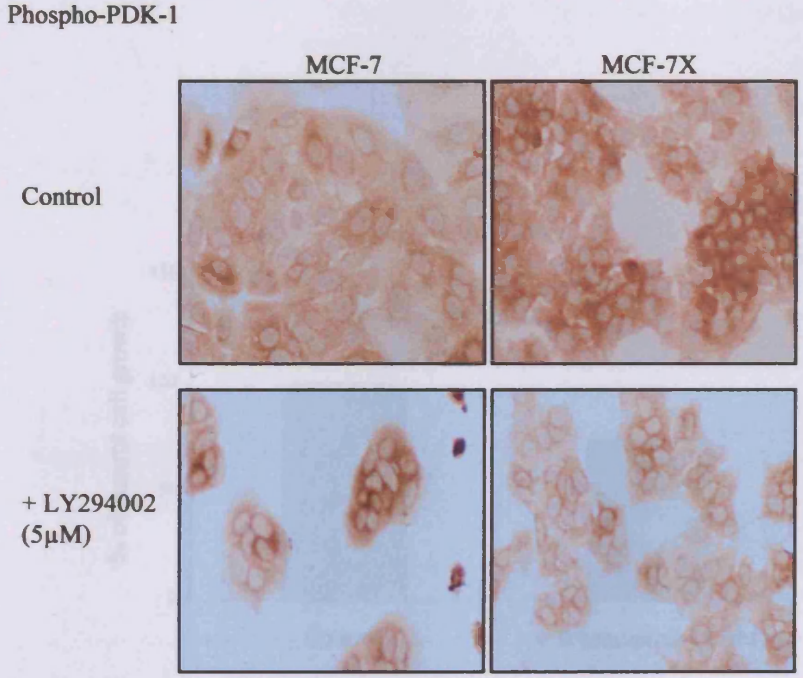

	MCF-7		MCF-7X	
Phospho-PDK-1				
Basal Control				
(Cytoplasmic)	107.5 (103.8-112.3)		145.0 (140.0-160.0)	
+ LY294002 (5 μM)				
(Cytoplasmic)	142.5 (135.3-155.0)	p=0.328	100.0 (93.8-101.3)	p=0.004*

Figure 3.54 Effect of LY294002 on phosphorylated PDK-1 level in MCF-7 and MCF-7X by immunocytochemistry. MCF-7 and MCF-7X cells were grown for 7 days on coverslips in the presence of LY294002 (5 μM) prior to ERCIA fixation. The phosphorylated PDK-1 (antibody dilution 1:50) digital images shown above (X20 magnification) are representative of 2 experiments. H-Score data were obtained by dual assessment of 3 representative areas of each coverslip followed by statistical analysis (Mann-Whitney U-Test). The median H-Score and Q1-Q3 values are displayed. A p-value <0.05(*) indicates a significant difference in phosphp-PDK-1 level following LY294002 treatment.

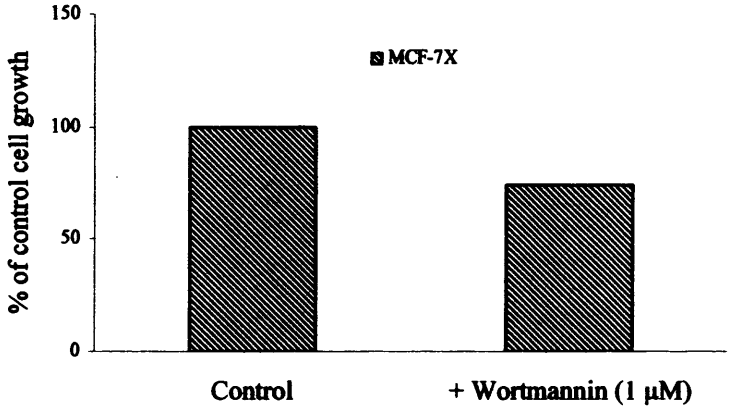

Figure 3.55 Effect of the PI3K inhibitor wortmannin on cell growth in MCF-7X cells. MCF-7X cells were grown on a 24-well plate in phenol-red-free RPMI media containing 5% XFCS in the absence or presence of wortmannin (1 μM). Conditions were maintained for 7 days prior to trypsin dispersion and Coulter counting (triplicate wells per treatment). Data are displayed as a percentage of control cell growth and include 1 experiment.

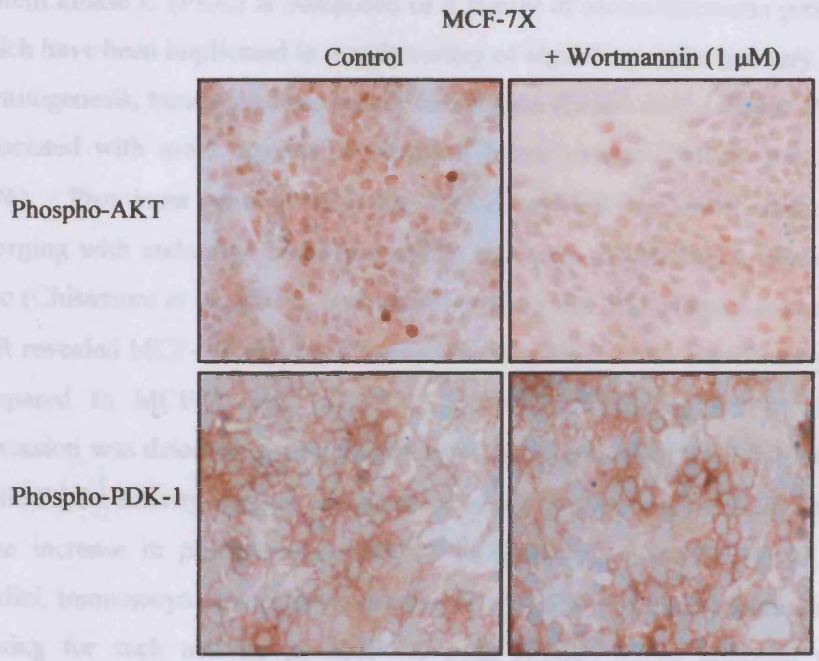

MCF-7X

Phospho-AKT			**Phospho-PDK-1**	
Basal Control			**Basal Control**	
(Memb. + Cyto.)	101.5 (76.5-119.3)		(Cytoplasmic)	145.0 (140.0-160.0)
(Nuclear)	107.5 (95.0-112.5)			
Total	209.0			
+ Wortmannin (1 μM)			**+ Wortmannin (1 μM)**	
(Memb. + Cyto.)	70.0 (68.8-72-5)	p=0.041*	(Cytoplasmic)	157.5 (148.8-166.3)
(Nuclear)	72.5 (68.8-76.3)	p=0.004*		p=0.104
Total	142.5			

Figure 3.56 Effect of the PI3K inhibitor wortmannin on phorsphorylated AKT and PDK-1 levels in MCF-7X cells by immunocytochemistry. MCF-7X cells were grown on coverslips in phenol-red-free RPMI media containing 5% XFCS in the absence or presence of wortmannin (1 μM) prior to ERICA fixation. The phospho-AKT (antibody dilution 1:200) and phospho-PDK-1 (antibody dilution 1:200) digital images shown above (X20 magnification) are representative of 2 experiments. H-Score data were obtained by dual assessment of 3 representative areas of each coverslip followed by statistical analysis (Mann-Whitney U-Test). The median H-Score and Q1-Q3 values are displayed. A p-value <0.05(*) indicates a significant difference in phospho-AKT level following wortmannin treatment in MCF-7X cells versus basal control.

3.3.3 Protein Kinase-C (PKC) α and δ

Protein kinase C (PKC) is composed of a family of serine/threonine protein kinases which have been implicated in a wide variety of signalling and regulatory events such as mitogenesis, tumourigenesis and differentiation (Blobe *et al.*, 1996). PKCs can be associated with more aggressive forms of breast cancer (Patrick and Heimbrook, 1996). Prominent among these are PKCδ and PKCα, where associations are emerging with endocrine resistance and in the latter instance with ER negativity *in vitro* (Chisamore *et al.*, 2001). Investigating these two PKC family members by RT-PCR revealed MCF-7X cell mRNA expression of PKCα was significantly decreased compared to MCF-7 cells (47.2% fall, p=0.030*, Figure 3.57), while PKCδ expression was detected at a lower and apparently equivalent level in both cell lines. While PKCα activity was not examined, Western blotting (Figure 3.58) demonstrated some increase in phosphorylated PKCδ in MCF-7X cells (57.7%, 78 kDa). In parallel, immunocytochemistry demonstrated a 37.5% (p=0.003*) increase in nuclear staining for such activity in MCF-7X cells (Figure 3.59), although there were somewhat lower levels of cytoplasmic staining (35.0, p=0.011*). It was also revealed by immunocytochemistry that total PKCδ expression was low in both cell lines, with this technique again showing significant decreases predominantly in the cytoplasmic staining in MCF-7X cells (48.7%, Figure 3.59) compared to MCF-7 cells. When challenged with the PKC inhibitor bisindolylmaleimide (Bis, 0.5 μM) there was no impact on growth suggesting that there is no substantial growth regulatory role for PKCs in MCF-7X (Figure 3.60). The contrasting MCF-7 cell growth data indicate there was some contribution for such signalling in these cells as the inhibitor was responsible for a significant 29.1% (p=0.001*) inhibitory effect at day 7.

3.3.4 Src

A number of growth factor receptor-driven responses have been functionally linked to Src, such as the activation of Shc followed by Grb2 and SOS recruitment leading to stimulation of the Ras-MAPK pathway (Blake *et al.*, 2000). Recently, steroid hormones have been implicated in the rapid activation of intracellular signalling cascades, whereby membrane associated receptors interact directly with and activate Src and other molecules such as Shc, PI3K and p130 Cas impacting on cell growth (Shupnik, 2004). RT-PCR revealed an equivalent level of mRNA expression of Src (433 bp) in MCF-7 and MCF-7X cells (Figure 3.61). While Src protein expression measured by Western blotting (Figure 3.62) paralleled the mRNA expression,

phosphorylated Src (60 kDa) was increased in MCF-7X cells with respect to MCF-7 cells. Despite this, when challenged with the specific Src inhibitor SU6656 (1.0 μM) MCF-7X cell growth was only reduced by 12.2% (p=0.011*), with a superior inhibition of 23.1% observed in MCF-7 cell (p=0.006*) after 7 days of treatment (Figure 3.63). Thus, Src signalling appears to make a diminished growth contribution in the resistant cells.

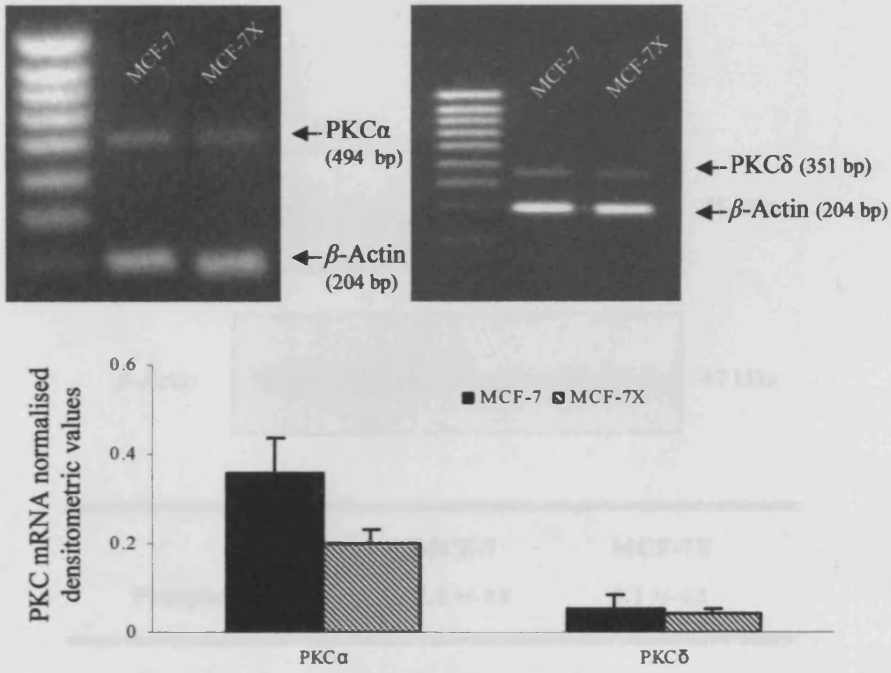

Figure 3.57 Basal MCF-7 versus MCF-7X cell mRNA expression of PKCα and PKCδ by RT-PCR. MCF-7 and MCF-7X cells were grown on 100 mm dishes in phenol-red-free RPMI media containing 5% SFCS or XFCS respectively. Conditions were maintained for 7 days before RNA was isolated and reverse transcribed. Individual RT-PCR of PKCα (34 cycles/ 55°C annealing temperature, 494 bp) and β-Actin (25 cycles/ 55°C annealing temperature, 204 bp) was performed. Product from each reaction was combined and run on a 2% agarose gel containing ethidium bromide, subsequently scanned, and normalised to β-Actin. Co-amplification RT-PCR of PKCδ (30 cycles/ 55°C annealing temperature, 351 bp) and β-Actin (204 bp) was performed. RT-PCR product was run on a 2% agarose gel containing ethidium bromide, subsequently photographed, scanned and normalised to β-Actin. The digital images above are representative of 3 experiments (for each target sequence) and the statistical analysis applied was an unpaired-T test comparing mean PKCα expression (p=0.030*) in MCF-7 (0.36 +/- 0.08) and MCF-7X (0.19 +/- 0.03) cells. An unpaired-T test was also applied to compare mean PKCδ expression (p=0.706) in MCF-7 (0.05 +/- 0.03) and MCF-7X (0.04 +/- 0.01) cells.

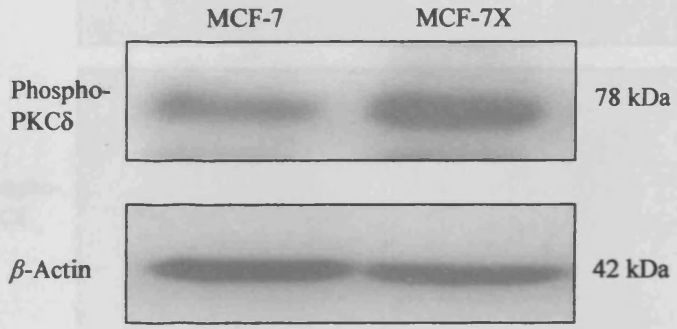

	MCF-7	MCF-7X
Phospho-PKCδ	2.6 +/- 0.8	4.1 +/- 0.5

Figure 3.58 Basal MCF-7X versus MCF-7 cell level of phosphorylated PKC-δ by Western blotting. MCF-7 and MCF-7X cells were grown on 60 mm dishes in phenol-red-free RPMI media containing 5% SFCS or XFCS respectively. Conditions were maintained for 7 days prior to whole cell lysis, SDS-PAGE (30 μg of sample protein/well) and Western blotting. The nitrocellulose membrane (0.45 μm) was probed for phosphorylated PKC-δ (78 kDa) and β-Actin (42 kDa). The developed autoradiography film was scanned using densitometric imaging for each blot probed and phospho-PKCδ level was normalised to β-Actin. The data is presented as the mean +/- SD and the image above is representative of 5 experiments.

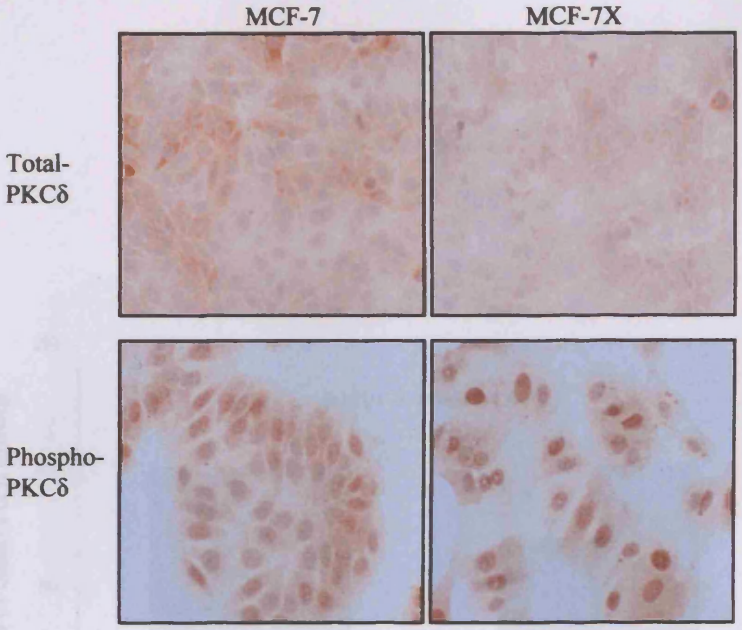

	MCF-7	MCF-7X	p-value
Total-PKC-δ			
(Cytoplasmic)	97.5 (90.0-105.0)	50.0 (45.0-60.0)	0.004*
(Nuclear)	9.0 (5.0-10.0)	2.0 (1.0-2.3)	0.003*
Total	106.5	52.0	
Phospho-PKC-δ			
(Cytoplasmic)	50.0 (35.0-51.3)	32.5 (30.0-35.0)	0.011*
(Nuclear)	80.0 (80.0-85.0)	110.0 (93.8-121.3)	0.003*
Total	130.0	142.5	

Figure 3.59 Basal MCF-7X versus MCF-7 cell total and phosphorylated PKC-δ levels by immunocytochemistry. MCF-7 and MCF-7X cells were grown on coverslips in phenol-red-free RPMI media containing 5% SFCS or XFCS respectively. Conditions were maintained for 7 days prior to the appropriate fixation. The total PKC-δ (antibody dilution 1:50) and phosphorylated PKC-δ (1:20) assays required coverslips fixed in ERICA. The digital images shown above (X40 magnification) are representative of 3 experiments. H-Score data were obtained by dual assessment of 2 representative areas of each coverslip followed by statistical analysis (Mann-Whitney U-Test). The median H-Score and Q1-Q3 values are displayed. A p-value <0.05(*) indicates a significant difference in total/phospho-PKC-δ level between MCF-7 and MCF-7X cells.

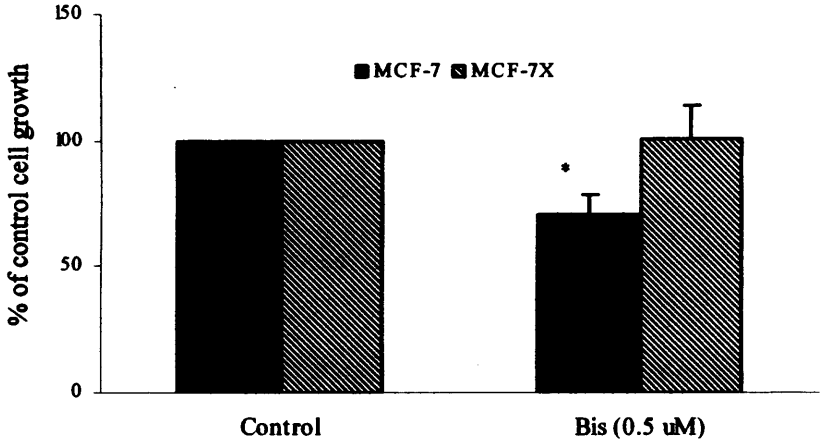

Figure 3.60 Effect of the PKC inhibitor bis-indoylmaleimidine (Bis) on the growth of MCF-7 and MCF-7X cells. MCF-7 and MCF-7X cells were grown on 24-well plates in phenol-red-free RPMI media containing 5% SFCS or XFCS respectively in the absence or presence of Bis (0.5 μM). Conditions were maintained for 7 days prior to trypsin dispersion and Coulter counting (triplicate wells per treatment). Data are displayed as a percentage of control cell growth and include 5 experiments +/- SD. The statistical analysis applied was an ANOVA Test followed by a Tamhane Post-Hoc Test.

* Denotes Bis treatment significantly inhibited MCF-7 ($p=0.001$) cell growth versus control.

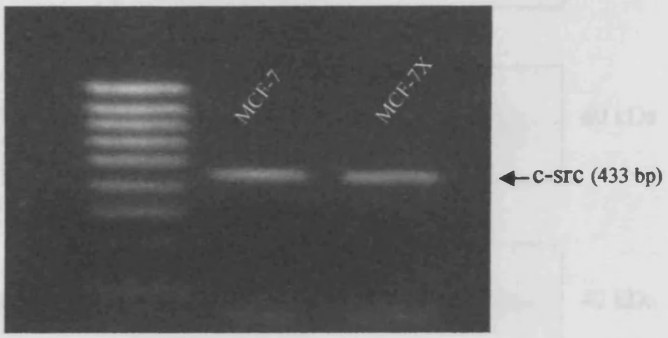

Figure 3.61 Basal MCF-7X versus MCF-7 cell mRNA expression of c-src by RT-PCR.. MCF-7 and MCF-7X cells were grown on 100 mm dishes in phenol-red-free RPMI media containing 5% SFCS or XFCS respectively. Conditions were maintained for 7 days before RNA was isolated and reverse transcribed. RT-PCR of c-src (30 cycles/ 55°C annealing temperature, 433 bp) was performed. RT-PCR product was run on a 2% agarose gel containing ethidium bromide and subsequently photographed. The digital image above is representative of 1 experiment therefore no statistical analysis was applied.

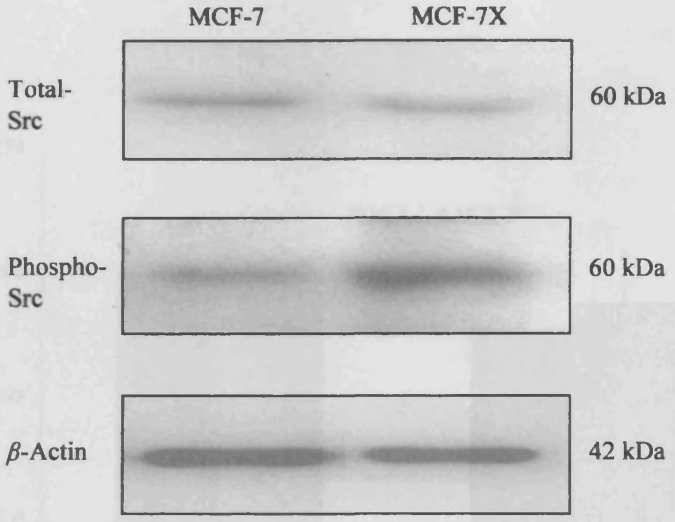

	MCF-7	MCF-7X
Total-Src	1.1 (0.8)	1.0 (0.6)
Phospho-Src	1.3 (0.5)	2.1 (0.8)

Figure 3.62 Basal MCF-7X versus MCF-7 cell levels of total and phosphorylated Src by Western blotting. MCF-7 and MCF-7X cells were grown on 60 mm dishes in phenol-red-free RPMI media containing 5% SFCS or XFCS respectively. Conditions were maintained for 7 days prior to whole cell lysis, SDS-PAGE (40 μg of sample protein/well) and Western blotting. The nitrocellulose membrane (0.45 μm) was probed for total Src (60 kDa), phosphorylated Src (60 kDa) and β-Actin (42 kDa). The developed autoradiography film was scanned using densitometric imaging for each blot probed. Subsequently, both total and phospho- Src blots were normalised to β-Actin. The data is presented as the mean +/- SD and the image above is representative of 3 experiments.

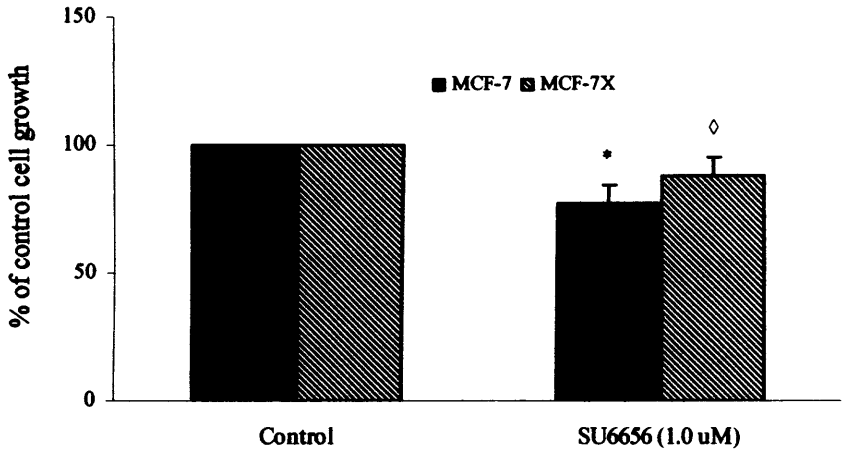

Figure 3.63 Effect of the specific Src inhibitor SU6656 on the growth of MCF-7 and MCF-7X cells. MCF-7 and MCF-7X cells were grown on 24-well plates in phenol-red-free RPMI media containing 5% SFCS or XFCS respectively in the absence or presence of SU6656 (1 μM). Conditions were maintained for 7 days prior to trypsin dispersion and Coulter counting (triplicate wells per treatment). Data are displayed as a percentage of control cell growth and include 3 experiments +/- SD. The statistical analysis applied was an ANOVA Test followed by a Tamhane Post-Hoc Test.

* and ◊ Denotes SU6656 treatment significantly inhibited MCF-7 (p=0.006) and MCF-7X (p=0.011) cell growth versus control.

3.4 GROWTH FACTOR SIGNALLING KINASES AND ERα CROSS-TALK

In addition to their direct promotion of growth, the intracellular kinases MAPK and PI3K/AKT have been shown in anti-oestrogen resistant (Nicholson *et al.*, 2004b) and long-term oestrogen deprived models (Santen *et al.*, 2004a; Martin *et al.*, 2003) to interact with the oestrogen receptor to drive growth. This can occur either via kinase activation of the key AF-1 residues Ser118 or 167 on ER (or alternatively of its co-activators), or through ligand-activated plasma membrane ER triggering downstream kinase activity. In the present study, it was important to investigate whether there was any evidence for kinase/ER cross-talk in MCF-7X cells, focusing on cross-talk at the level of nuclear ERα given the apparent absence of a significant non-genomic contribution either to MCF-7X or their parental cells.

3.4.1 The Influence of MAPK Signalling on ERα Signalling

In both MCF-7 and MCF-7X cells while challenge with the MEK-1 inhibitor PD98059 diminished MAPK activation, modest inhibition of cell growth was only observed in the former cells. There was no significant effect of this agent on total nuclear ERα (Figure 3.64) or on the phosphorylation status of the Ser118ER (Figure 3.65) or Ser167ER residues (Figure 3.66) in the two cells lines as detected using immunocytochemistry. Furthermore, the agent failed to inhibit ERE transcription or endogenous pS2 expression. The ERE reporter assays performed in MCF-7X cells indicated PD98059 inhibition of MAPK did not reduce ERE activity following 18 hour treatment (Figure 3.67). RT-PCR performed on mRNA of MCF-7X cells treated with PD98059 for 7 days revealed no change in pS2 expression (Figure 3.68). There was similarly no significant effect on MCF-7X cell, or indeed MCF-7, pS2 protein expression by immunocytochemistry (Figure 3.69). In total, these data indicate there is no positive MAPK cross-talk with ERα signalling in MCF-7X cells, and similarly that the small growth contribution of MAPK in MCF-7 cells is independent of interplay of this kinase with nuclear ERα.

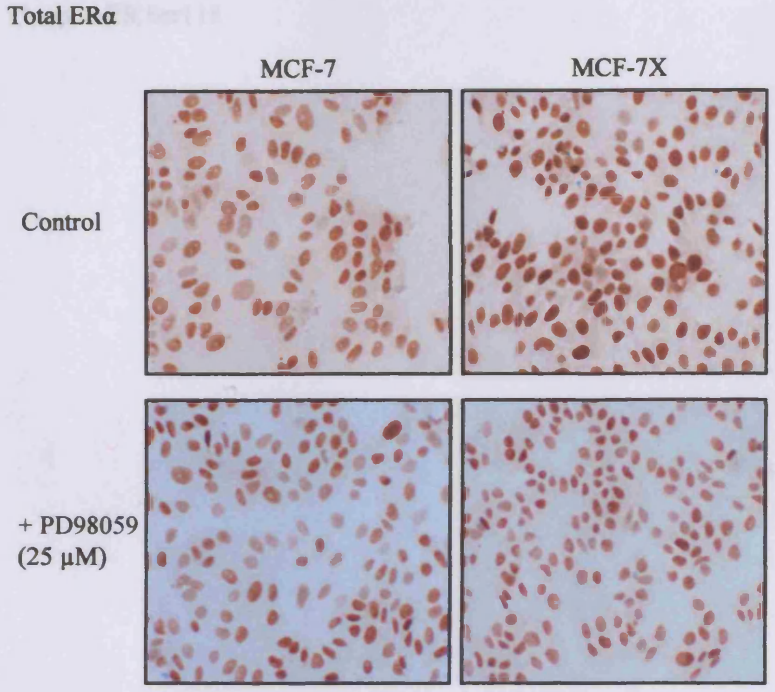

	MCF-7		MCF-7X	
Total ERα (Nuclear)				
Basal Control	147.0 (142.0-155.0)		185.0 (185.0-195.0)	
+ PD98059 (25 μM)	155.0 (147.5-161.3)	p=0.173	180.0 (175.0-186.3)	p=0.204

Figure 3.64 Effect of the MEK-1 inhibitor PD98059 on ERα expression in MCF-7 and MCF-7X cells by immunocytochemistry. MCF-7 and MCF-7X cells were grown on coverslips in phenol-red-free RPMI media containing 5% SFCS or XFCS respectively in the absence or presence of PD98059 (25 μM). Conditions were maintained for 7 days prior to ERCIA fixation. The total ERα (6F11, antibody dilution 1:100) digital images shown above (X20 magnification) are representative of 3 experiments. H-Score data were obtained by dual assessment of 2 representative areas of each coverslip followed by statistical analysis (Mann-Whitney U-Test). The median H-Score and Q1-Q3 values are displayed.

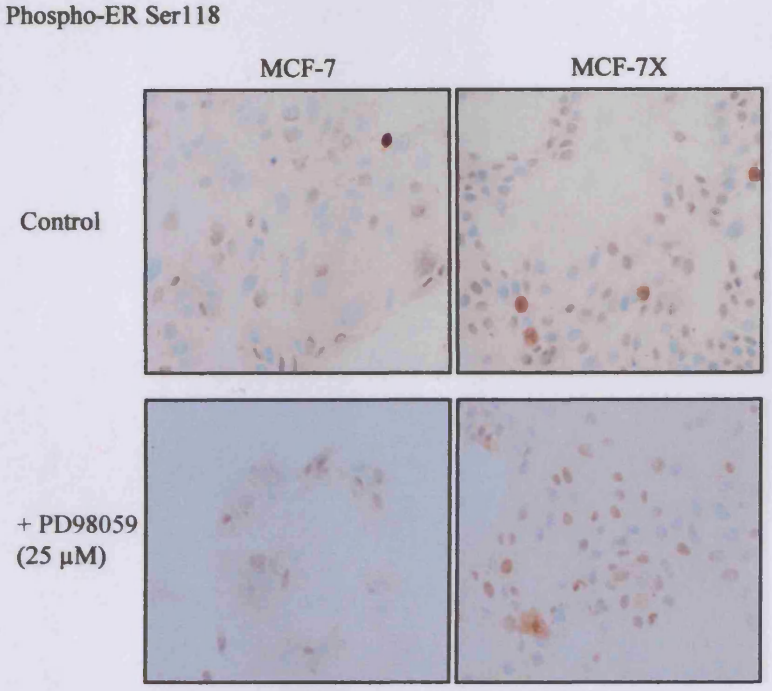

	MCF-7		MCF-7X	
Phospho-ER Ser118 (Nuclear)				
Basal Control	70.0 (63.8-71.3)		90.0 (77.5-110.5)	
+ PD98059 (25 μM)	65.0 (57.5-70.0)	p=0.209	82.5 (78.8-101.3)	p=0.757

Figure 3.65 Effect of the MEK-1 inhibitor PD98059 on phosphorylation of ERα at Ser118 residue in MCF-7 and MCF-7X cells by immunocytochemistry. MCF-7 and MCF-7X cells were grown on coverslips in phenol-red-free RPMI media containing 5% SFCS or XFCS respectively in the absence or presence of PD98059 (25 μM). Conditions were maintained for 7 days prior to paraformaldehyde vanadate fixation. The phospho-ER Ser118 (antibody dilution 1:400) digital images shown above (X20 magnification) are representative of 4 experiments. H-Score data were obtained by dual assessment of 2 representative areas of each coverslip followed by statistical analysis (Mann-Whitney U-Test). The median H-Score and Q1-Q3 values are displayed.

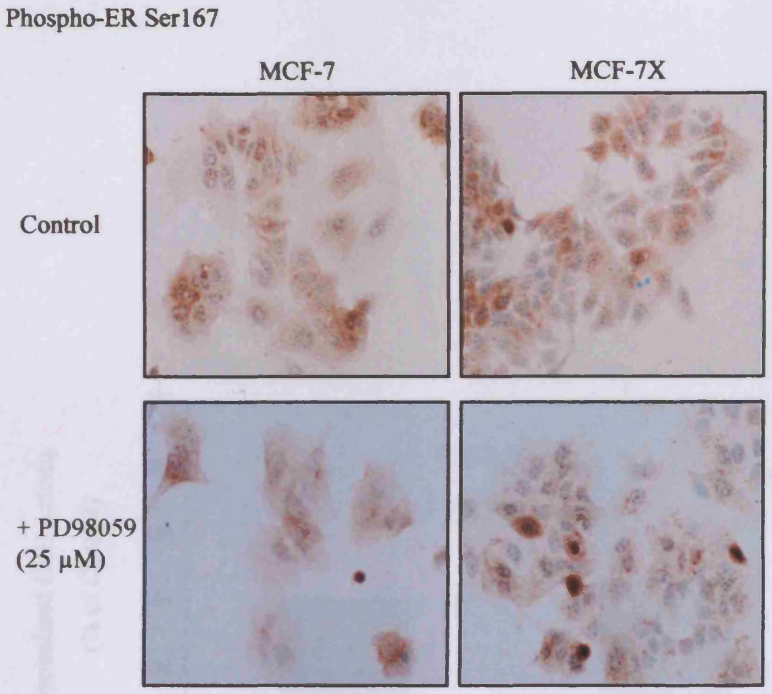

	MCF-7		MCF-7X	
Phospho-ER Ser167 (Nuclear)				
Basal Control	82.5 (71.3-100.0)		50.0 (45.0-70.0)	
+ PD98059 (25 μM)	82.5 (78.8-96.3)	p=0.745	60.0 (55.0-60.0)	p=0.718

Figure 3.66 Effect of the MEK-1 inhibitor PD98059 on phosphorylation of ERα at Ser167 residue in MCF-7 and MCF-7X cells by immunocytochemistry. MCF-7 and MCF-7X cells were grown on coverslips in phenol-red-free RPMI media containing 5% SFCS or XFCS respectively in the absence or presence of PD98059 (25 μM). Conditions were maintained for 7 days prior to ERICA fixation. The phospho-ER Ser167 (antibody dilution 1:25) digital images shown above (X20 magnification) are representative of 4 experiments. H-Score data were obtained by dual assessment of 2 representative areas of each coverslip followed by statistical analysis (Mann-Whitney U-Test). The median H-Score and Q1-Q3 values are displayed.

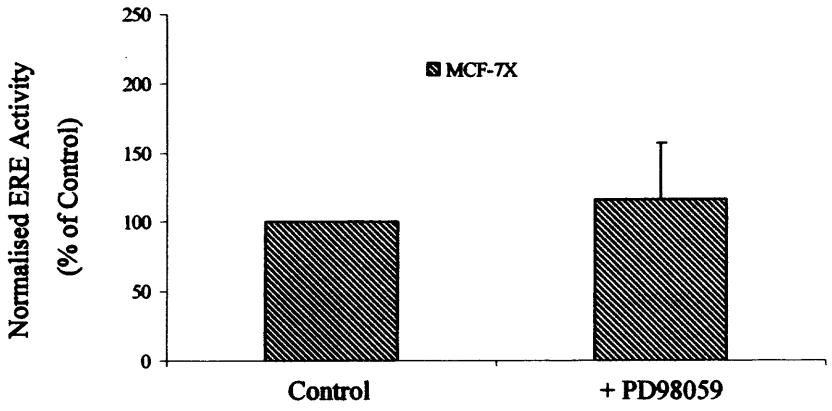

Figure 3.67 Effect on of the MEK-1 inhibitor PD98059 on ER transcriptional activity in MCF-7X cells after 18 hour treatment. MCF-7X cells were grown on 12-well plates in phenol-red-free RPMI media containing 5% XFCS for 24 hours. Cells were transfected in DCCM serum-free media containing transfection lipid (3 µl/well, Lipofectin), ERE reporter construct (400 ng/well), *Renilla* (150 ng/ml), and 'carrier' DNA (550 ng/well, PCRscript) After 6 hours, the transfection medium was replaced with phenol-red-free RPMI media in the absence or presence of PD98059 (25 µM) in triplicate wells. Subsequent to 18 hour treatment incubation, a dual-luciferase reporter assay kit was utilised for cell lysis and luminometer assessment (n=3). Data are displayed as percentage of control ERE activity +/- SD (triplicate wells) and has been β-Galactosidase normalised in the absence and presence of PD98059 (25 µM). The statistical analysis applied was an ANOVA Test followed by a Bonferroni Post-Hoc Test.

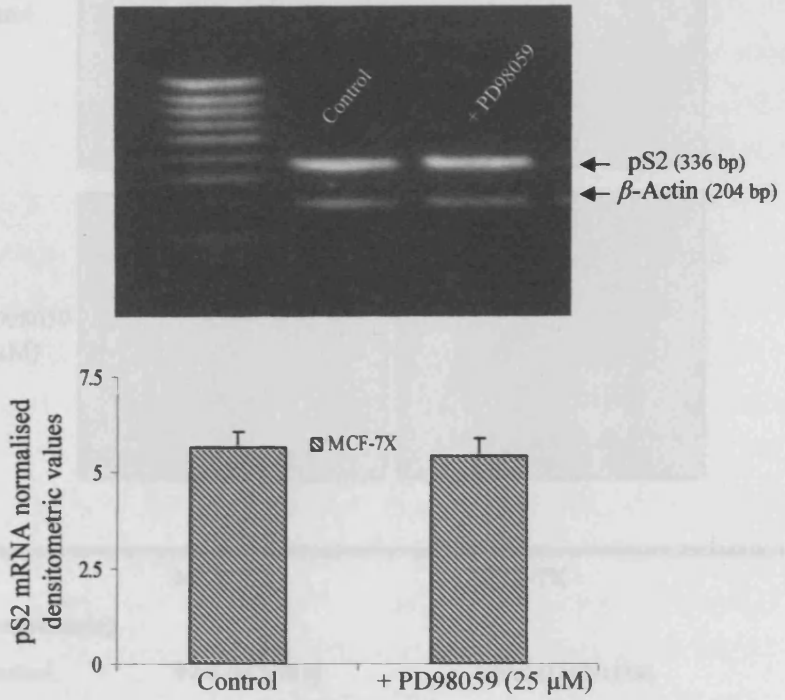

Figure 3.68 Treatment effect of the MEK-1 inhibitor PD98059 on pS2 mRNA in MCF-7X cells by RT-PCR. MCF-7X cells were grown on 100 mm dishes in phenol-red-free RPMI media containing 5% XFCS in the absence or presence of PD98059 (25 μM). Conditions were maintained for 7 days before RNA was isolated and reverse transcribed. Co-amplification RT-PCR of pS2 (25 cycles/ 55°C annealing temperature, 336 bp) and β-Actin (204 bp) was performed. The RT-PCR product was run on a 2% agarose gel containing ethidium bromide, subsequently photographed, scanned and normalised to β-Actin. The digital image above is representative of 3 experiments and the statistical analysis applied was an unpaired-T test (p=1.000) comparing mean pS2 expression in untreated MCF-7X cells (5.7 +/- 0.4) and PD98059 treated MCF-7X cells (5.4 +/- 0.5).

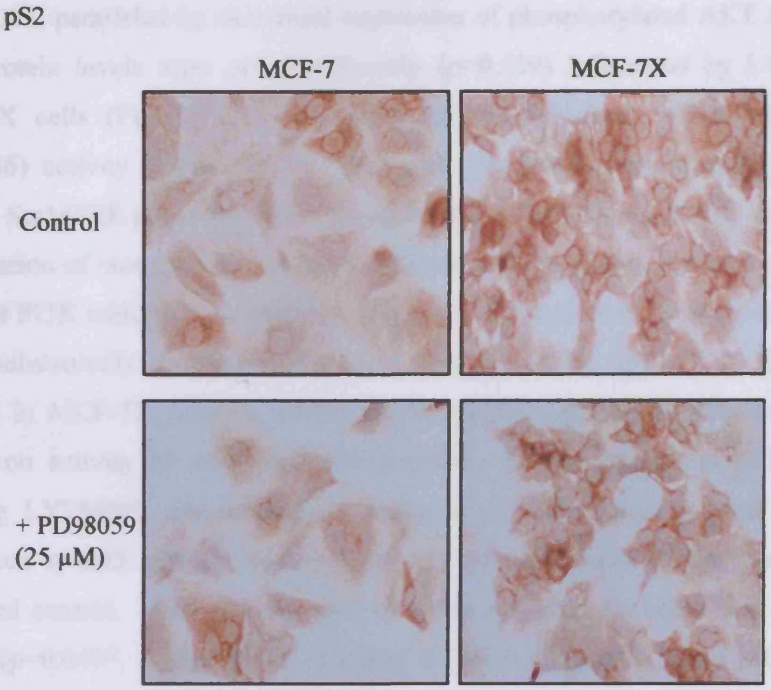

	MCF-7		MCF-7X	
pS2 (Cytoplasmic)				
Basal Control	90.0 (81.3-98.8)		130.0 (121.3-133.8)	
+ PD98059 (25 μM)	92.5 (83.8-101.3)	p=0.740	140.0 (110.0-150.0)	p=0.487

Figure 3.69 Effect of the MEK-1 inhibitor PD98059 on pS2 expression in MCF-7 and MCF-7X cells by immunocytochemistry. MCF-7 and MCF-7X cells were grown on coverslips in phenol-red-free media containing 5% SFCS or XFCS respectively in the absence or presence of PD98059 (25 μM). Conditions were maintained for 7 days prior to ERICA fixation. The pS2 (antibody dilution 1:500) digital images shown above (X20 magnification) are representative of 3 experiments. H-Score data were obtained by dual assessment of 2 representative areas of each coverslip followed by statistical analysis (Mann-Whitney U-Test). The median H-Score and Q1-Q3 values are displayed.

3.4.2 The Influence of PI3K/AKT Signalling on ERα Signalling

MCF-7X cells revealed substantial growth inhibition in response to the PI3K inhibitor LY294002, paralleled by decreased expression of phosphorylated AKT and PDK-1. ERα protein levels were not significantly (p=0.539) influenced by LY294002 in MCF-7X cells (Figure 3.70) and there was no inhibitory effect on Ser118ER (p=0.186) activity (Figure 3.71). However, the inhibitor substantially decreased nuclear Ser167ER phosphorylation by 50.0% (p<0.001*, Figure 3.72). Brief parallel examination of wortmannin treatment in these cells confirmed the lack of inhibitory effect of PI3K inhibition on total ERα (Figure 3.73) or phosphorylated Ser118ER, but again substantially decreased phosphorylated Ser167ER (p=0.001*, Figure 3.74) activity in MCF-7X cells by immunocytochemistry (in parallel with its inhibitory effects on activity of AKT and cell growth). Further studies in MCF-7X cells utilising LY294002 demonstrated a reduction in ERα transcriptional activity as monitored by ERE reporter activity (18 hour) and endogenous pS2 expression versus untreated control. ERE reporter activity measured after 18 hours was reduced by 32.1% (p=0.049*, Figure 3.75). Parallel RT-PCR (Figure 3.76) of MCF-7X cells treated for 7 days with this PI3K inhibitor demonstrated a significant decrease in endogenous oestrogen regulated gene pS2 (p=0.040*). Immunocytochemistry revealed a significant (30.8%, p=0.002*) decrease in pS2 protein expression (Figure 3.77). Cumulatively, these data indicate PI3K signalling contributes to MCF-7X via cross-talk with ERα in a genomic mechanism. This appears to involve AKT promotion of Ser167 phosphorylation, thus influencing ER/ERE transcriptional activity and growth.

In MCF-7 cells, only a small growth inhibition had been achieved with the PI3K inhibitor LY294002, and in parallel there was only a small depletion of downstream AKT and no impact on PDK-1 activity. In these cells ERα levels were very slightly decreased (8.2%, p=0.010*) following 7 day treatment with this inhibitor (Figure 3.70). There was no impact on Ser167ER activity, but a significant decrease in their low levels of Ser118ER was observed (85.7%, p=0.003*, Figures 3.71 & 3.72). While impact on ERE reporter activity and pS2 as detected at the mRNA level was not monitored, immunocytochemical staining for pS2 in MCF-7 was partially decreased by LY294002 (8.3%, p=0.047*, Figure 3.77).

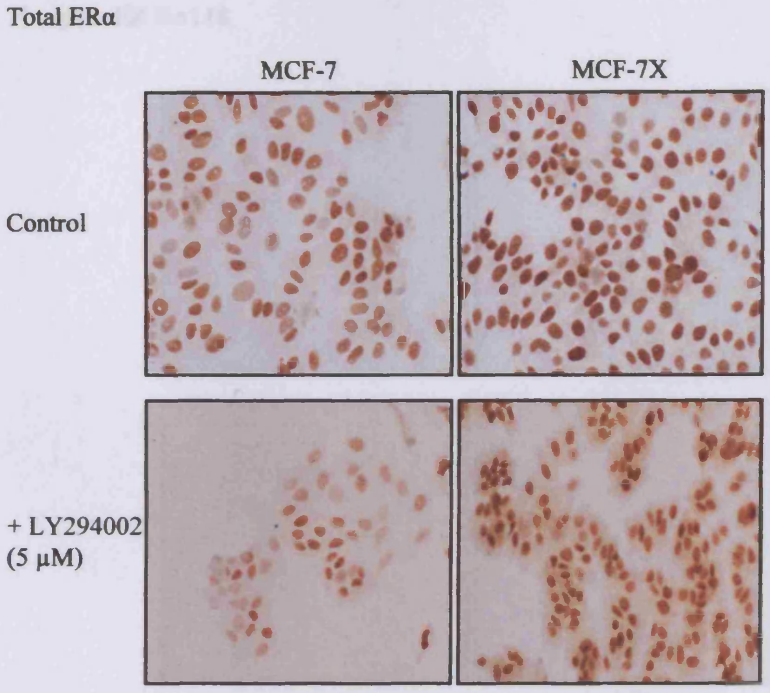

	MCF-7		MCF-7X	
Total ERα (Nuclear)				
Basal Control	147.0 (142.0-155.0)		185.0 (185.0-195.0)	
+ LY294002 (5 μM)	135.0 (126.3-141.3)	p=0.010*	192.5 (183.8-200.0)	p=0.539

Figure 3.70 Effect of the PI3K inhibitor LY294002 on ERα expression in MCF-7 and MCF-7X cells by immunocytochemistry. MCF-7 and MCF-7X cells were grown on coverslips in phenol-red-free RPMI media containing 5% SFCS or XFCS respectively in the absence or presence of LY294002 (5 μM). Conditions were maintained for 7 days prior to ERCIA fixation. The total ERα (6F11, antibody dilution 1:100) digital images shown above (X20 magnification) are representative of 3 experiments. H-Score data were obtained by dual assessment of 2 representative areas of each coverslip followed by statistical analysis (Mann-Whitney U-Test). The median H-Score and Q1-Q3 values are displayed. A p-value <0.05(*) indicates a significant difference in ERα expression following LY294002 treatment.

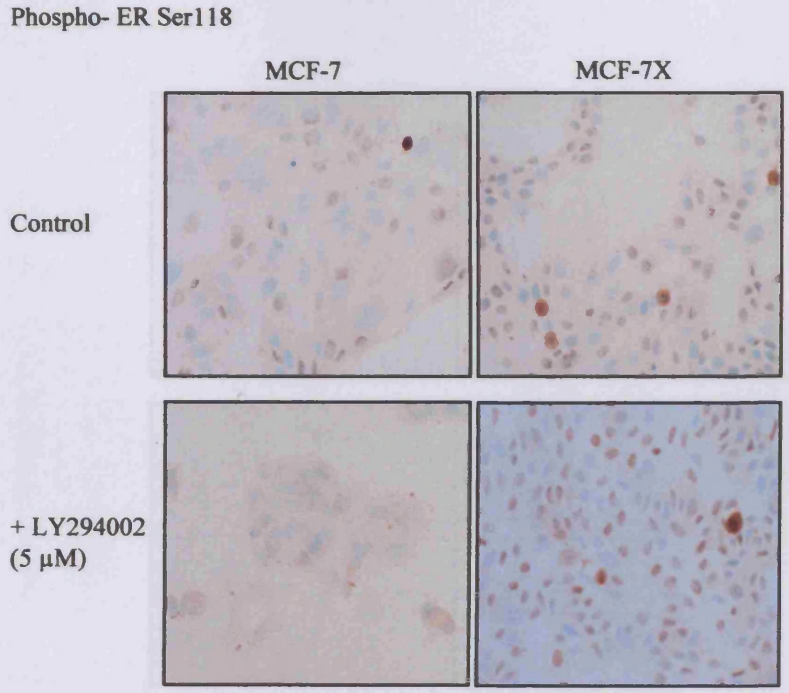

	MCF-7		MCF-7X	
Phospho-ER Ser118 (Nuclear)				
Basal Control	70.0 (63.8-71.3)		90.0 (77.5-110.5)	
+ LY294002 (5 μM)	10.0 (8.8-15.0)	p=0.003*	105.0 (93.8-112.5)	p=0.186

Figure 3.71 Effect of the PI3K inhibitor LY294002 on phosphorylation of ERα at Ser118 residue in MCF-7 and MCF-7X cells by immunocytochemistry. MCF-7 and MCF-7X cells were grown on coverslips in phenol-red-free RPMI media containing 5% SFCS or XFCS respectively in the absence or presence of LY294002 (5 μM). Conditions were maintained for 7 days prior to paraformaldehyde vanadate fixation. The phospho-ER Ser118 (antibody dilution 1:400) digital images shown above (X20 magnification) are representative of 4 experiments. H-Score analysis were obtained by dual assessment of 2 representative areas of each coverslip followed by statistical analysis (Mann-Whitney U-Test). The median H-Score and Q1-Q3 values are displayed. A p-value <0.05(*) indicates a significant difference in phospho-ER Ser118 level following LY294002 treatment.

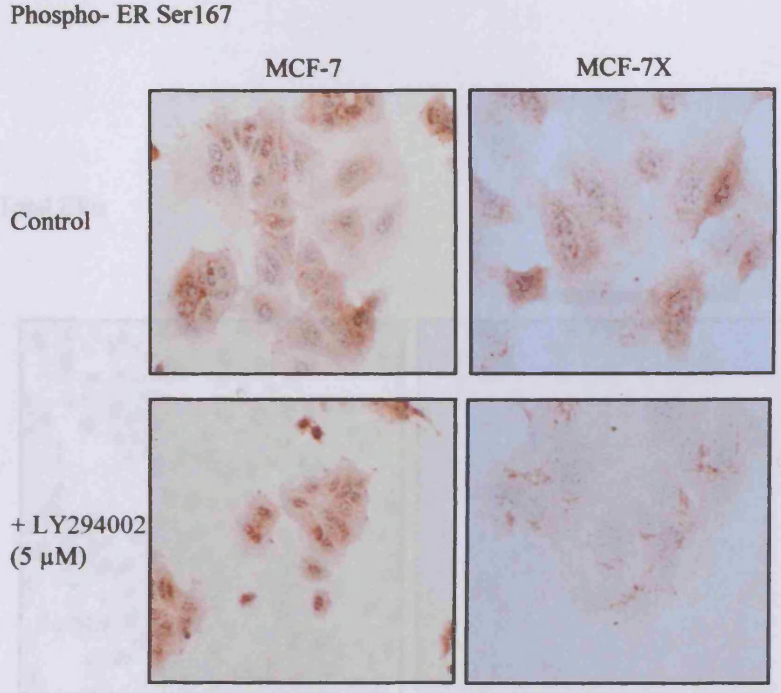

	MCF-7		MCF-7X	
Phospho-ER Ser167 (Nuclear)				
Basal Control	82.5 (71.3-100.0)		50.0 (45.0-70.0)	
+ LY294002 (5 μM)	82.5 (73.8-92.5)	p=0.935	25.0 (20.0-25.0)	p<0.001*

Figure 3.72 Effect of the PI3K inhibitor LY294002 on phosphorylation of ERα at Ser167 residue in MCF-7 and MCF-7X cells by immunocytochemistry. MCF-7 and MCF-7X cells were grown on coverslips in phenol-red-free RPMI media containing 5% SFCS or XFCS respectively in the absence or presence of LY294002 (5 μM). Conditions were maintained for 7 days prior to ERICA fixation. The phospho-ER Ser167 (antibody dilution 1:25) digital images shown above (MCF-7 X20, MCF-7X X40 magnification) are representative of 4 experiments. H-Score data were obtained by dual assessment of 2 representative areas of each coverslip followed by statistical analysis (Mann-Whitney U-Test). The median H-Score and Q1-Q3 values are displayed. A p-value <0.05(*) indicates a significant difference in phospho-ER Ser167 level following LY294002 treatment.

Total ERα

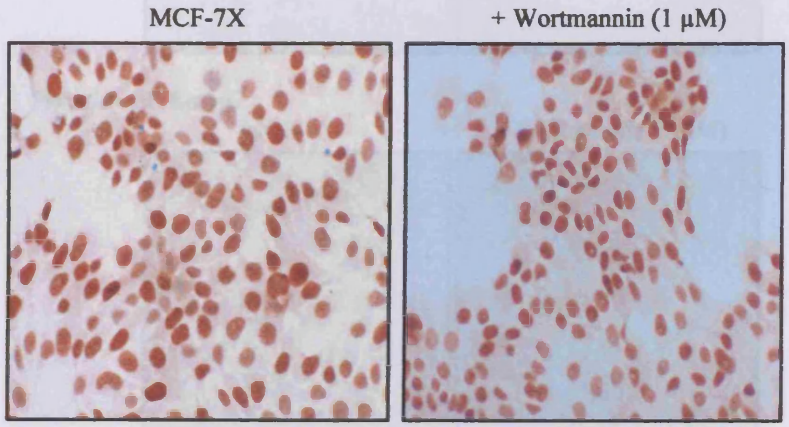

	MCF-7X	+ Wortmannin (1 μM)	
Total ERα			
(Nuclear)	185.0 (185.0-195.0)	180.0 (167.5-190.0)	p=0.491

Figure 3.73 Effect of the PI3K inhibitor wortmannin on ERα expression in MCF-7X cells by immunocytochemistry. MCF-7X cells were grown on coverslips in phenol-red-free RPMI media containing 5% XFCS in the absence or presence of wortmannin (1 μM). Conditions were maintained for 7 days prior to ERCIA fixation. The total ERα (6F11, antibody dilution 1:100) digital images shown above (X20 magnification) are representative of 3 experiments. H-Score data were obtained by dual assessment of 3 representative areas of each coverslip followed by statistical analysis (Mann-Whitney U-Test). The median H-Score and Q1-Q3 values are displayed.

Phospho-ER Ser118

MCF-7X + Wortmannin (1 μM)

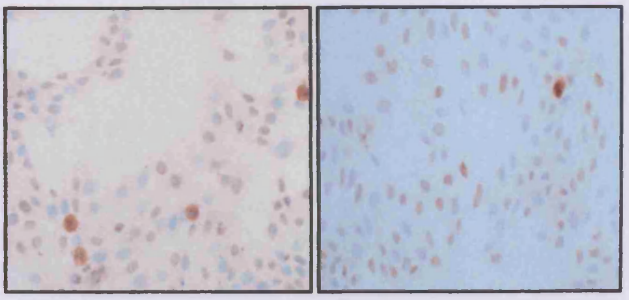

Phospho-ER Ser167

MCF-7X + Wortmannin (1 μM)

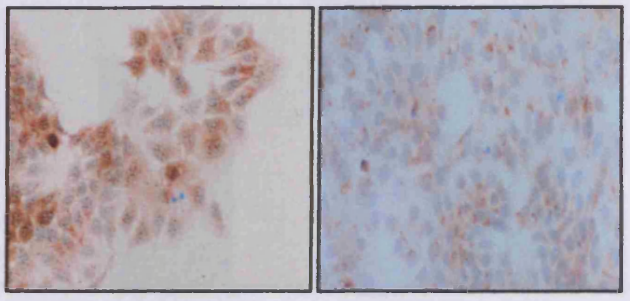

	MCF-7X	+ Wortmannin (1 μM)	
Phospho-ER Ser118			
(Nuclear)	90.0 (77.5-110.5)	117.5 (106.3-122.5)	p=0.012*
Phospho-ER Ser167			
(Nuclear)	50.0 (45.0-70.0)	27.5 (23.8-31.3)	p=0.001*

Figure 3.74 Effect of the PI3K inhibitor wortmannin on phosphorylation of ERα at Ser118 and Ser167 residues in MCF-7X cells by immunocytochemistry. MCF-7X cells were grown on coverslips in phenol-red-free RPMI media containing 5% XFCS in the absence or presence of wortmannin (1 μM). Conditions were maintained for 7 days prior to the appropriate fixation. The phospho-ER Ser118 (antibody dilution 1:400) assay required coverslips paraformaldehyde vanadate fixed and the phospho-ER Ser167 (1:25) assay required coverslips ERICA fixed. The digital images shown above (X20 magnification) are representative of 2 experiments. H-Score data were obtained by dual assessment of 3 representative areas of each coverslip followed by statistical analysis (Mann-Whitney U-Test). The median H-Score and Q1-Q3 values are displayed. A p-value <0.05(*) indicates a significant difference in phospho-ER level following wortmannin treatment.

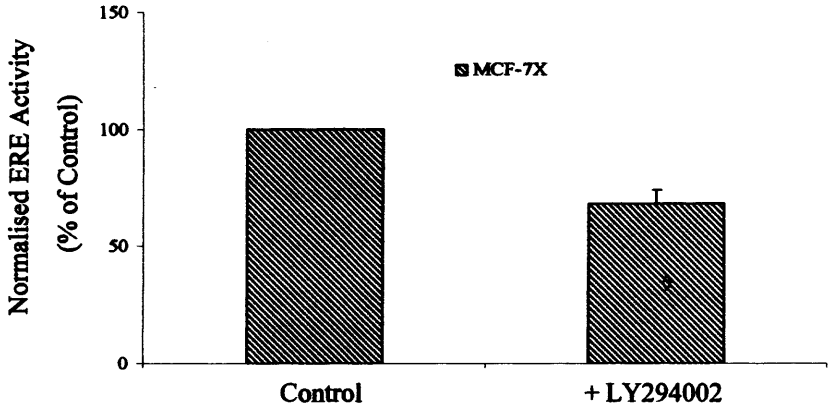

Figure 3.75 Effect on of the PI3K inhibitor LY294002 on ER transcriptional activity in MCF-7X cells after 18 hour treatment. MCF-7X cells were grown on 12-well plates in phenol-red-free RPMI media containing 5% XFCS for 24 hours. Cells were transfected in DCCM serum-free media containing transfection lipid (3 µl/well, Lipofectin), ERE reporter construct (400 ng/well), *Renilla* (150 ng/ml), and 'carrier' DNA (550 ng/well, PCRscript) After 6 hours, the transfection medium was replaced with phenol-red-free RPMI media in the absence or presence of LY294002 (5 µM) in triplicate wells. Subsequent to 18 hour treatment incubation, a dual-luciferase reporter assay kit was utilised for cell lysis and luminometer assessment (n=3). Data are displayed as percentage of control ERE activity +/- SD (triplicate wells) and has been β-Galactosidase normalised in the absence and presence of LY294002 (5 µM). The statistical analysis applied was an ANOVA Test followed by a Bonferroni Post-Hoc Test.

◊ Denotes LY294002 treatment (18 hrs) significantly decreased ERE activity in MCF-7X cells versus untreated control.

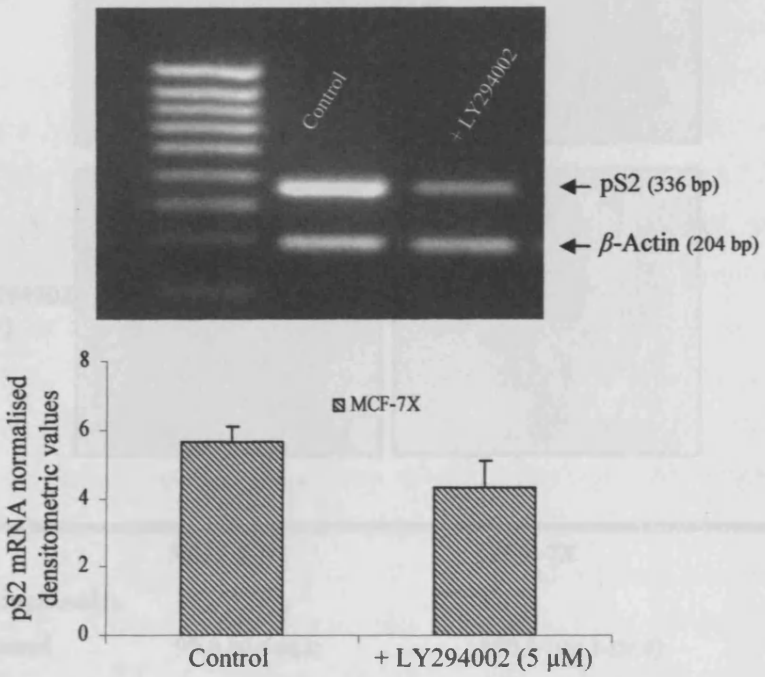

Figure 3.76 Treatment effect of the PI3K inhibitor LY294002 on pS2 mRNA in MCF-7X cells by RT-PCR. MCF-7X cells were grown on 100 mm dishes in phenol-red-free RPMI media containing 5% XFCS in the absence or presence of LY294002 (5 μM). Conditions were maintained for 7 days before RNA was isolated and reverse transcribed. Co-amplification RT-PCR of pS2 (25 cycles/ 55°C annealing temperature, 336 bp) and β-Actin (204 bp) was performed. The RT-PCR product was run on a 2% agarose gel containing ethidium bromide, subsequently photographed, scanned and normalised to β-Actin. The digital image above is representative of 3 experiments and the statistical analysis applied was an unpaired-T test (p=0.040*) comparing mean pS2 expression in untreated MCF-7X cells (5.7 +/- 0.4) and LY294002 treated MCF-7X cells (4.3 +/- 0.8).

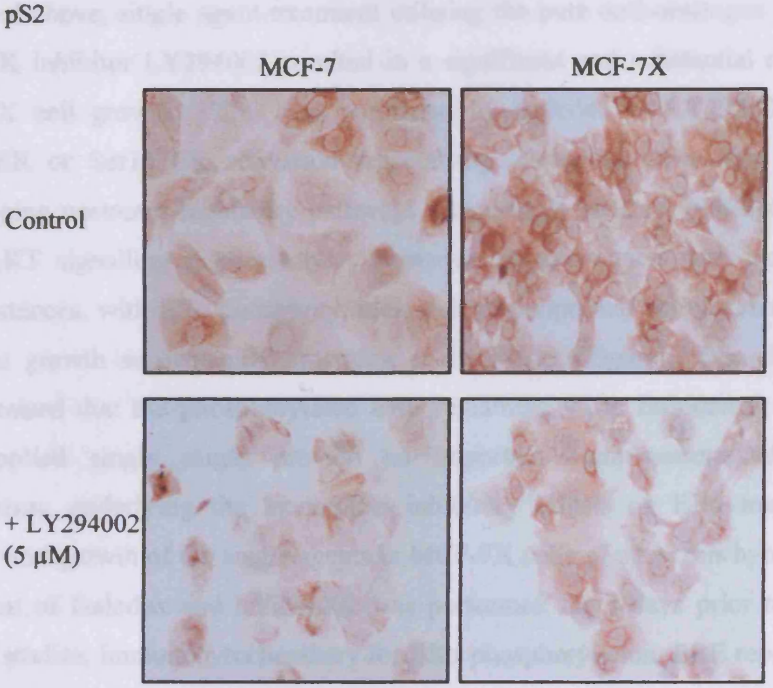

	MCF-7		MCF-7X	
pS2 (Cytoplasmic)				
Basal Control	90.0 (81.3-98.8)		130.0 (121.3-133.8)	
+ LY294002 (5 μM)	82.5 (73.8-86.3)	p=0.047*	90.0 (85.0-112.0)	p=0.002*

Figure 3.77 Effect of the PI3K inhibitor LY294002 on pS2 expression in MCF-7 and MCF-7X cells by immunocytochemistry. MCF-7 and MCF-7X cells were grown on coverslips in phenol-red-free media containing 5% SFCS or XFCS respectively in the absence or presence of LY294002 (5 μM). Conditions were maintained for 7 days prior to ERICA fixation. The pS2 (antibody dilution 1:500) digital images shown above (X20 magnification) are representative of 3 experiments. H-Score data were obtained by dual assessment of 2 representative areas of each coverslip followed by statistical analysis (Mann-Whitney U-Test). The median H-Score and Q1-Q3 values are displayed. A p-value <0.05(*) indicates a significant difference in pS2 expression following LY294002 treatment.

3.4.3 The Influence of Simultaneous Targeting of the PI3K/AKT and ERα Signalling Pathways

As stated above, single agent treatment utilising the pure anti-oestrogen faslodex or the PI3K inhibitor LY294002 resulted in a significant and substantial reduction in MCF-7X cell growth. This was paralleled by faslodex or LY294002 reducing Ser118ER or Ser167ER activation respectively, revealing these sites have non-overlapping upstream regulatory pathways (presumably residual oestrogen/ERα and PI3K/AKT signalling respectively). However, responsiveness was incomplete in both instances, with ERα phosphorylation and transcriptional activity remaining and resistant growth subsequently emerging at 10 weeks (Figure 3.78). It was thus hypothesised that the phosphorylated ERα remaining when faslodex or LY294002 was applied singly might provide an important compensatory cell survival mechanism, underlying the incomplete inhibitory effects on ERα transcriptional activity and growth of the single agents in MCF-7X cells. To test this hypothesis, co-treatment of faslodex and LY294002 was performed for 7 days prior to extensive growth studies, immunocytochemistry for ERα phosphorylation, ERE reporter assays and RT-PCR for the oestrogen regulated gene pS2 being employed. As expected, co-treatment specifically decreased ERα and PI3K/AKT signalling [(with no significant impact on pMAPK) (Figures 3.79, 3.80 & 3.81)] to equivalent levels achieved with each single agent. Total levels of nuclear ERα were decreased 59.5% (p=0.001*) with faslodex/LY294002 co-treatment, consistent with the significant (63.5%, p=0.001*) reduction observed following faslodex single treatment (LY294002 single treatment having no effect). Thus, ER levels were equivalent with faslodex or faslodex/LY294002 co-treatment (p=0.053). Co-treatment decreased membrane plus cytoplasmic and nuclear phosphorylated AKT levels by 74.9% (p=0.004*) and 25.6% (p=0.012*) respectively. Again levels of inhibition were similar to those reached following LY294002 single treatment (66.0% and 32.1% respectively; again faslodex single treatment exerting no significant effect).

However, co-treatment was successful at reducing phosphorylation of ERα at both Ser118 and Ser167 residues (Figures 3.82 & 3.83). At both serine residues, faslodex/LY294002 treatment resulted in a reduced intensity of staining as well as a loss in the percentage of positive stained MCF-7X cells versus basal control. The combination treatment was responsible for a 41.7% (p=0.001*) inhibitory effect at nuclear Ser118ER versus the basal control. This effect was not significantly superior

to single treatment with faslodex (p=0.410), however was superior to LY294002 (p=0.004*) that exerted no inhibitory effect on this parameter as a single agent by immunocytochemistry. Furthermore, the co-treatment was able to deplete Ser167ER activity 60.0% (p<0.001*) versus the basal control. This result was significant versus faslodex treatment (p=0.002*), but was equivalent to LY294002 single treatment (p=0.603).

In parallel with the decreased phosphorylation of both ER AF-1 sites, ERE transcriptional activity measured following 18 hour faslodex/LY294002 treatment was decreased 47.1% (p<0.001*, Figure 3.84). This was a superior depletion compared to LY294002 as a single treatment (32.1% and 46.5% respectively) and 18 hour faslodex treatment (32.5%). Parallel RT-PCR and immunocytochemical analysis of pS2 following co-treatment with faslodex/LY294002 revealed a significant 93.0% (p=0.003*) reduction in mRNA (Figure 3.85) that was again largely equivalent to faslodex alone (92.0%, Figure 3.21). However, the subsequent 61.5% (p=0.001*) loss in cytoplasmic localised pS2 protein (Figure 3.86) proved superior to faslodex or LY294002 alone (44.2%, p=0.044* and 32.7%, p=0.004* respectively). These data were associated with a superior 90.0% (p<0.001*) anti-tumour response in MCF-7X cells by day 15 versus basal control (Figure 3.87), moreover resulting in a superior growth inhibitory effect versus faslodex or LY294002 alone (p<0.001* and p=0.001* respectively). There was also an extended time until resistant growth resumed at 25 weeks for the combination treatment versus 10 weeks with faslodex or LY294002 alone, and furthermore the growth rate achieved remained lower with faslodex/LY294002 co-treatment (Figure 3.88). Again, preliminary growth studies utilising the alternative PI3K blocker wortmannin plus faslodex indicated the combination of a PI3K inhibitor and the pure anti-oestrogen comprises a superior strategy compared to single administration of either agent (Figure 3.89). Clearly, co-treatment resulted in a superior inhibition of ERα signalling and thus a more effective growth inhibition. However, disease progression did eventually resume with co-treatment, and some residual ERα phosphorylation (particularly on Ser118ER) and ERα transcriptional activity (~25%) was left with further profiling of these cells revealing that MAPK activity was not depleted (Figure 3.81). It was thus important to subsequently monitor if a triple inhibitory strategy using faslodex and LY294002 together with the

MEK-1 inhibitor PD98059 was able to maximally block ERα signalling and completely subvert development of resistance.

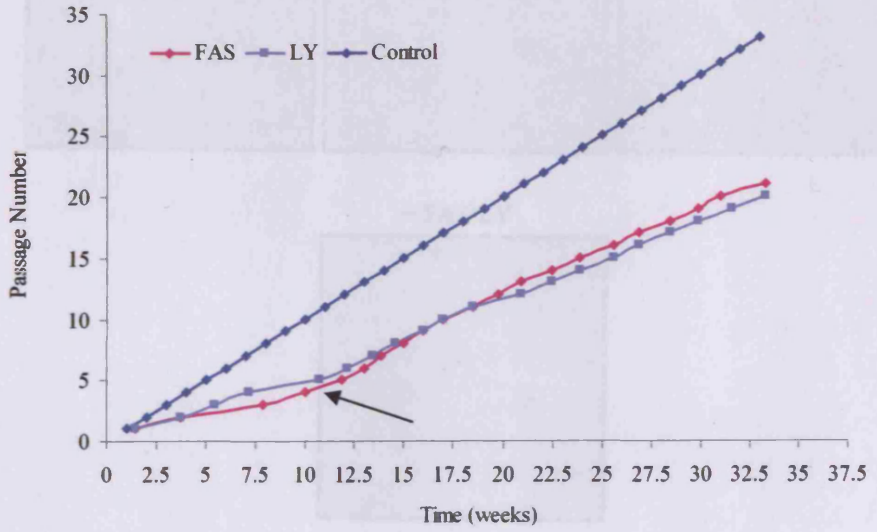

Figure 3.78 Cell culture time-line for long term faslodex and LY294002 treated MCF-7X cells. MCF-7X cells were grown in phenol-red-free RPMI media containing 5% XFCS in the presence of faslodex (10^{-7} M) or LY294002 (5 μM) for long term culture. The arrow signifies the time point at which the rate of cell growth began to increase. Based on the development of rapid log phase growth, there was need to increase the frequency of passaging by week 10. Data are displayed as the number of passages versus time (weeks).

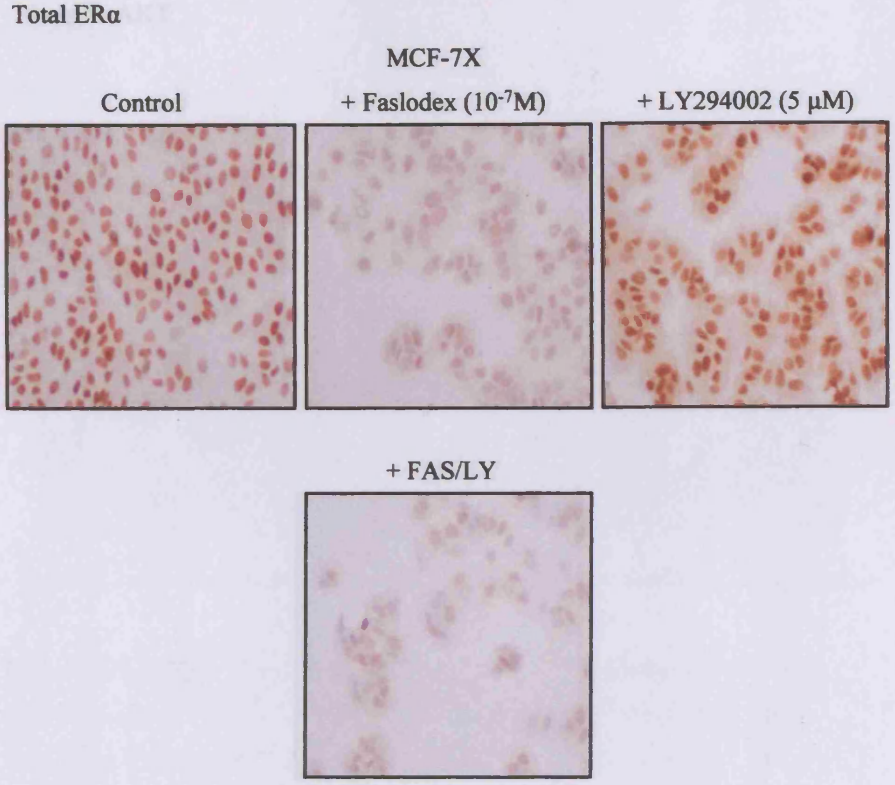

	MCF-7X	
Total ERα (Nuclear)		
Basal Control	185.0 (185.0-195.0)	
+ Faslodex	67.5 (60.0-71.3)	p=0.001*
+ LY294002	192.5 (183.8-200.0)	p=0.539
+ Faslodex/LY294002	75.0 (70.3-87.5)	p=0.001*

Figure 3.79 Effect of faslodex/LY294002 co-treatment on ERα expression in MCF-7X cells by immunocytochemistry. MCF-7X cells were grown on coverslips in phenol-red-free RPMI media containing 5% XFCS in the absence or presence of faslodex/LY294002 (10^{-7} M, 5 μM) co-treatment. Conditions were maintained for 7 days prior to ERCIA fixation. The total ERα (6F11, antibody dilution 1:100) digital images shown above (X20 original magnification) are representative of 3 experiments. H-Score data were obtained by dual assessment of 2 representative areas of each coverslip followed by statistical analysis (Mann-Whitney U-Test). The median H-Score and Q1-Q3 values are displayed. A p-value <0.05(*) indicates a significant treatment effect versus MCF-7X basal control.

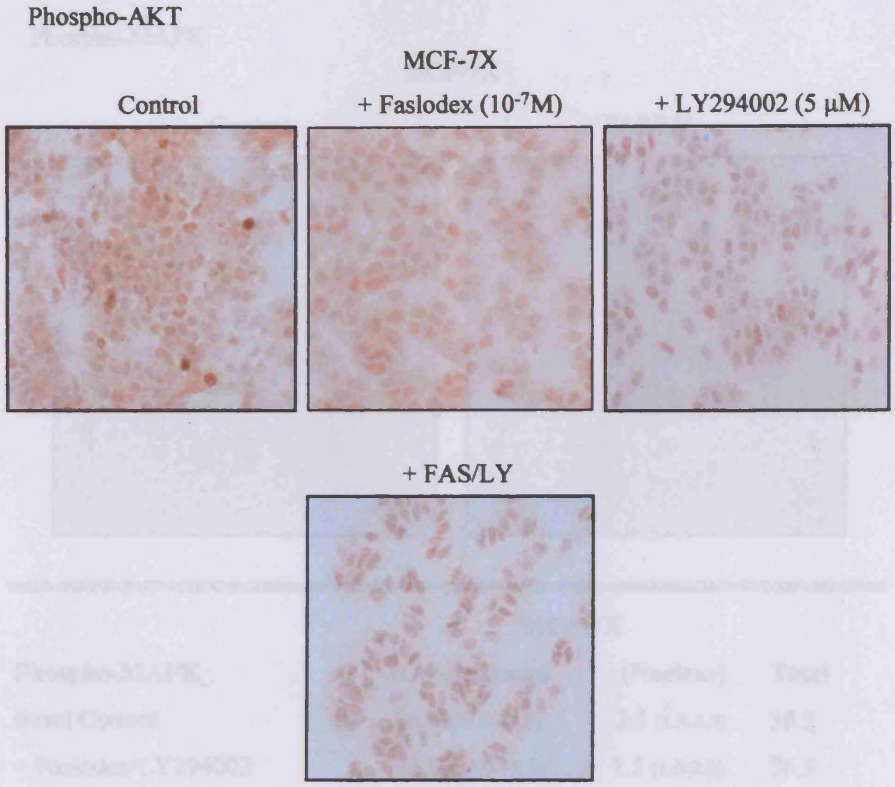

		MCF-7X	
Phospho-AKT	**(Memb. + Cyto.)**	**(Nuclear)**	**Total**
Basal Control	101.5 (76.5-119.3)	107.5 (95.0-112.5)	209.0
+ Faslodex	78.5 (71.0-84.5)	102.5 (98.8-110.0)	181.0
	p=0.127	p=0.680	
+ LY294002	34.5 (32.0-57.0)	73.0 (61.0-81.3)	107.5
	p=0.004*	p=0.004*	
+ Faslodex/LY294002	25.5 (21.8-29.0)	80.0 (73.8-93.8)	105.5
	p=0.004*	p=0.012*	

Figure 3.80 Effect of faslodex/LY294002 on phosphorylated AKT level in MCF-7X cells by immunocytochemistry. MCF-7X cells were grown on coverslips in phenol-red-free RPMI media containing 5% XFCS in the absence or presence of faslodex/LY294002 (10^{-7} M, 5 μM). Conditions were maintained for 7 days prior to ERICA fixation. The phospho-AKT (antibody dilution 1:200) digital images shown above (X20 magnification) are representative of 4 experiments. H-Score data were obtained by dual assessment of 2 representative areas of each coverslip followed by statistical analysis (Mann-Whitney U-Test). The median H-Score and Q1-Q3 values are displayed. A p-value <0.05(*) indicates a significant treatment effect versus MCF-7X basal control.

Phospho-MAPK

MCF-7X

Control + FAS/LY

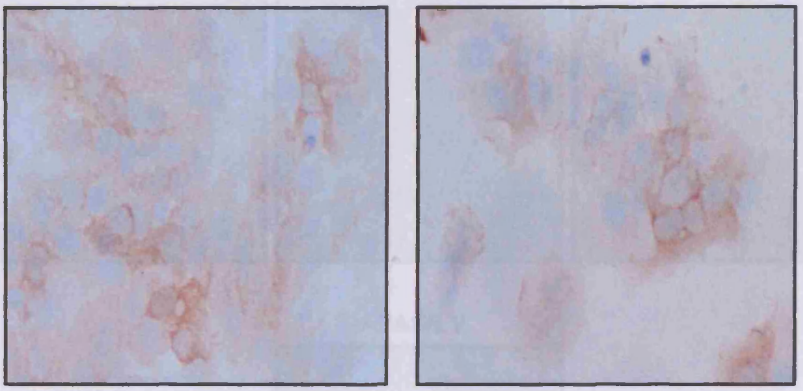

	MCF-7X		
Phospho-MAPK	**(Cytoplasmic)**	**(Nuclear)**	**Total**
Basal Control	35.0 (35.0-48.8)	3.5 (1.3-5.0)	38.5
+ Faslodex/LY294002	35.0 (30.0-35.0)	1.5 (1.0-2.0)	36.5
	p=0.093	p=0.075	

Figure 3.81 Effect of faslodex/LY294002 on phosphorylated MAPK level in MCF-7X cells by immunocytochemistry. MCF-7X cells were grown on coverslips in phenol-red-free RPMI media containing 5% XFCS in the absence or presence of faslodex/LY294002 (10^{-7} M, 5 μM). Conditions were maintained for 7 days prior to formal saline fixation. The phospho-MAPK (antibody dilution 1:20) digital images shown above (X20 magnification) are representative of 4 experiments. H-Score data were obtained by dual assessment of 2 representative areas of each coverslip followed by statistical analysis (Mann-Whitney U-Test). The median H-Score and Q1-Q3 values are displayed.

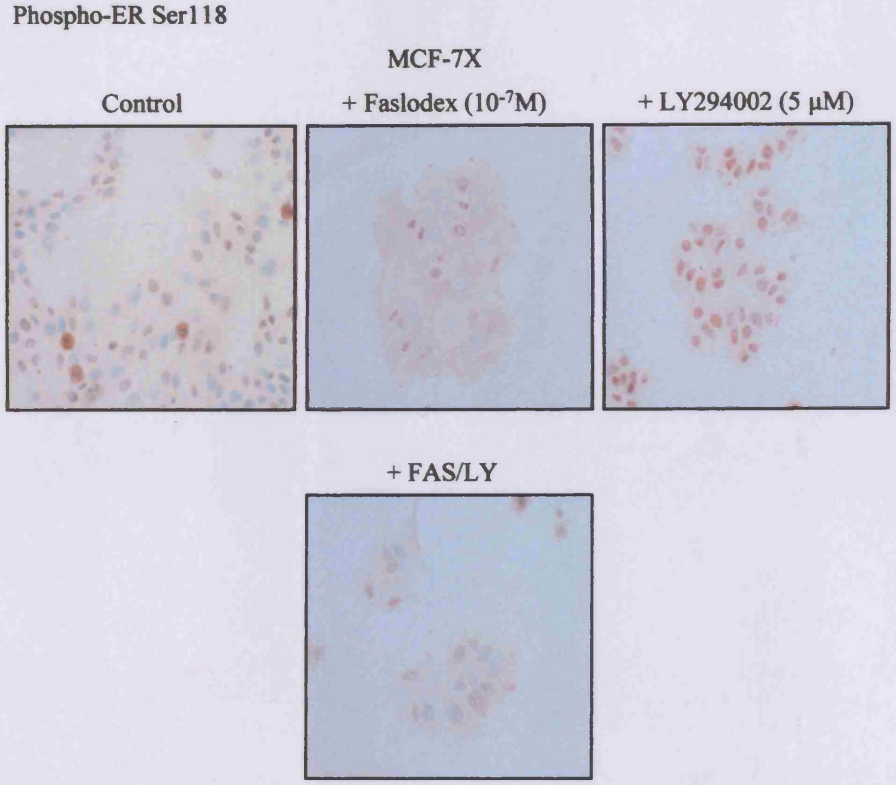

	MCF-7X	
Phospho-ER Ser118 (Nuclear)		
Basal Control	90.0 (77.5-110.5)	
+ Faslodex	77.5 (61.3-80.0)	p=0.030*
+ LY294002	105.0 (93.8-112.5)	p=0.186
+ Faslodex/LY294002	52.5 (43.8-60.0)	p=0.001*

Figure 3.82 Effect of faslodex/LY294002 co-treatment on phosphorylation of ERα at Ser118 residue in MCF-7X cells by immunocytochemistry. MCF-7X cells were grown on coverslips in phenol-red-free RPMI media containing 5% XFCS in the absence or presence of faslodex/LY294002 (10^{-7} M, 5 μM) co-treatment. Conditions were maintained for 7 days prior to paraformaldehyde vanadate fixation. The phospho-ER Ser118 (antibody dilution 1:400) digital images shown above (X20 magnification) are representative of 4 experiments. H-Score data were obtained by dual assessment of 2 representative areas of each coverslip followed by statistical analysis (Mann-Whitney U-Test). The median H-Score and Q1-Q3 values are displayed. A p-value <0.05(*) indicates a significant treatment effect versus MCF-7X basal control.

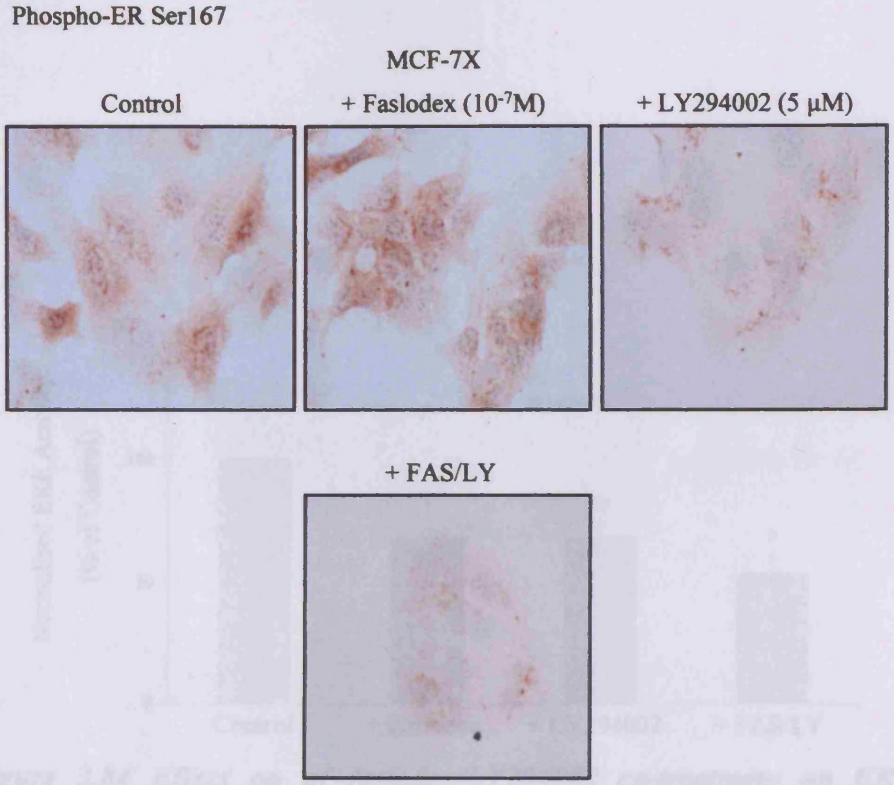

	MCF-7X	
Phospho-ER Ser167 (Nuclear)		
Basal Control	50.0 (45.0-70.0)	
+ Faslodex	55.0 (40.0-70.0)	p=0.841
+ LY294002	25.0 (20.0-25.0)	p<0.001*
+ Faslodex/LY294002	20.0 (12.0-30.0)	p<0.001*

Figure 3.83 Effect of faslodex/LY294002 co-treatment on phosphorylation of ERα at Ser167 residue in MCF-7X cells by immunocytochemistry. MCF-7X cells were grown on coverslips in phenol-red-free RPMI media containing 5% XFCS in the absence or presence of faslodex/LY294002 (10^{-7} M, 5 μM) co-treatment. Conditions were maintained for 7 days prior to ERICA fixation. The phospho-ER Ser167 (antibody dilution 1:25) digital images shown above (X40 magnification) are representative of 4 experiments. H-Score data were obtained by dual assessment of 2 representative areas of each coverslip followed by statistical analysis (Mann-Whitney U-Test). The median H-Sore and Q1-Q3 values are displayed. A p-value <0.05(*) indicates a significant treatment effect versus MCF-7X basal control.

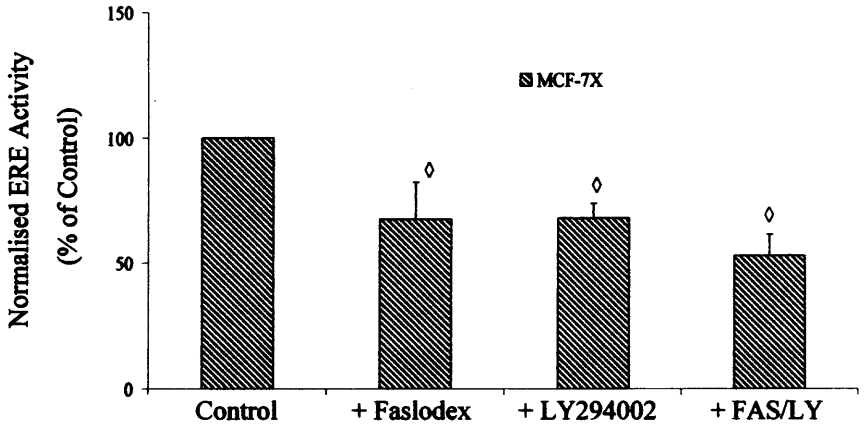

Figure 3.84 Effect on of faslodex/LY294002 co-treatment on ER transcriptional activity in MCF-7X cells after 18 hour treatment. MCF-7X cells were grown on 12-well plates in phenol-red-free RPMI media containing 5% XFCS for 24 hours. Cells were transfected in DCCM serum-free media containing transfection lipid (3 µl/well, Lipofectin), ERE reporter construct (400 ng/well), *Renilla* (150 ng/ml), and 'carrier' DNA (550 ng/well, PCRscript) After 6 hours, the transfection medium was replaced with phenol-red-free RPMI media in the absence or presence of faslodex/LY294002 (10^{-7} M, 5 µM) in triplicate wells. Subsequent to 18 hour treatment incubation, a dual-luciferase reporter assay kit was utilised for cell lysis and luminometer assessment (n=3). Data are displayed as percentage of control ERE activity +/- SD (triplicate wells) and has been β-Galactosidase normalised in the absence and presence of FAS/LY (10^{-7} M, 5 µM). The statistical analysis applied was an ANOVA Test followed by a Bonferroni Post-Hoc Test.

◊ Denotes FAS/LY treatment (18 hrs) significantly decreased ERE activity in MCF-7X cells versus untreated control.

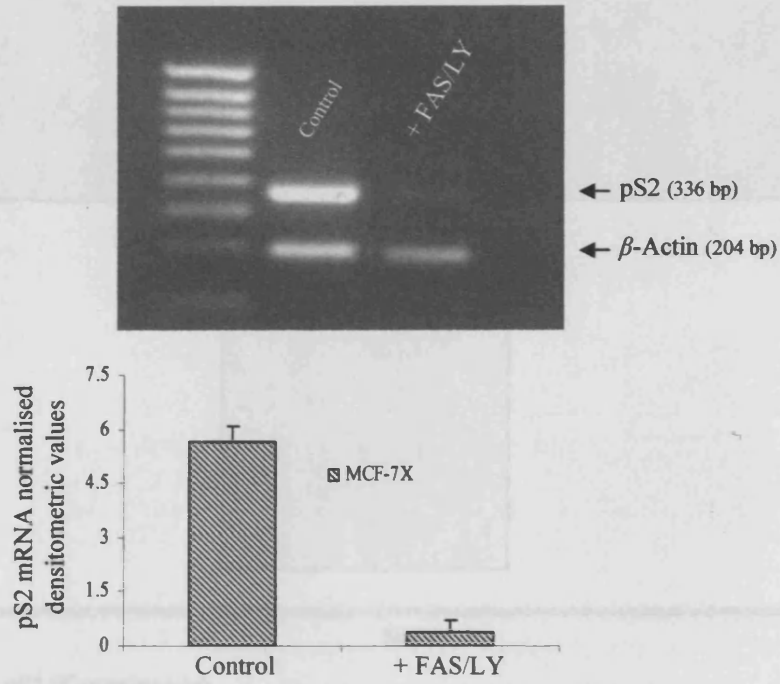

Figure 3.85 Treatment effect of faslodex/LY294002 co-treatment on pS2 mRNA in MCF-7X cells by RT-PCR. MCF-7X cells were grown on 100 mm dishes in phenol-red-free RPMI media containing 5% XFCS in the absence or presence of faslodex/LY294002 (10^{-7} M, 5 μM) co-treatment. Conditions were maintained for 7 days before RNA was isolated and reverse transcribed. Co-amplification RT-PCR of pS2 (25 cycles/ 55°C annealing temperature, 336 bp) and β-Actin (204 bp) was performed. The RT-PCR product was run on a 2% agarose gel containing ethidium bromide, subsequently photographed, scanned and normalised to β-Actin. The digital image above is representative of 3 experiments and the statistical analysis applied was an unpaired-T test (p=0.003*) comparing mean pS2 expression in untreated MCF-7X cells (5.7 +/- 0.4) and faslodex/LY294002 co-treated MCF-7X cells (0.4 +/- 0.3).

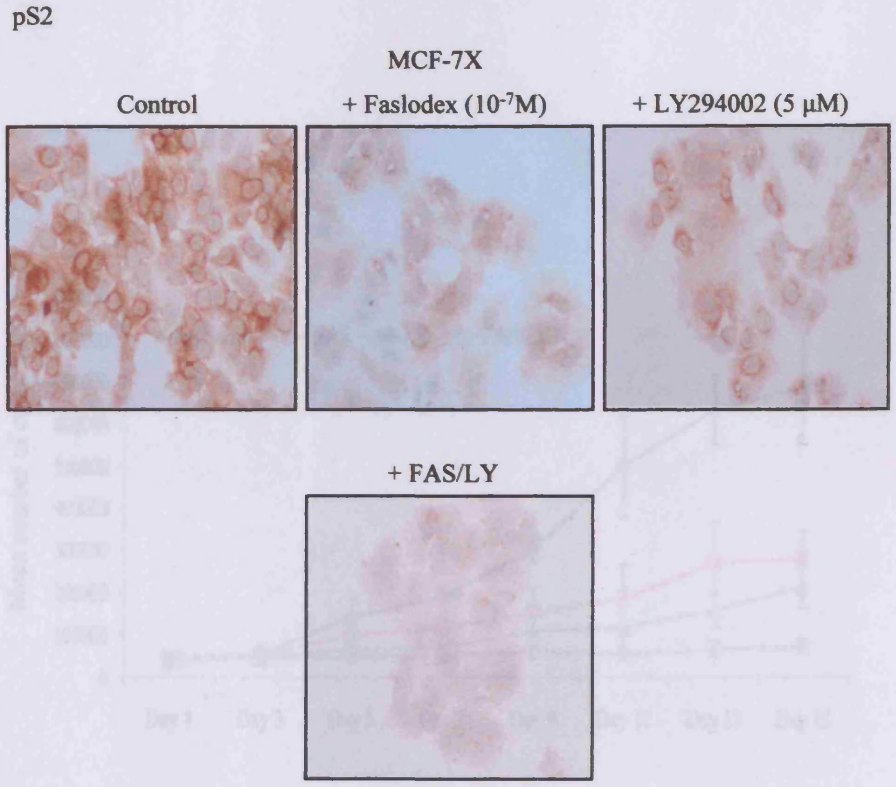

	MCF-7X	
pS2 (Cytoplasmic)		
Basal Control	130.0 (121.3-133.8)	
+ Faslodex	72.5 (58.8-80.0)	p=0.001*
+ LY294002	87.5 (78.8-92.8)	p=0.002*
+ Faslodex/LY294002	50.0 (45.0-70.0)	p=0.001*

Figure 3.86 Effect of faslodex/LY294002 co-treatment on pS2 expression in MCF-7X cells by immunocytochemistry. MCF-7X cells were grown on coverslips in phenol-red-free media containing 5% XFCS in the absence or presence of faslodex/LY294002 (10^{-7} M, 5 μM). Conditions were maintained for 7 days prior to ERICA fixation. The pS2 (antibody dilution 1:500) digital images shown above (X20 magnification) are representative of 3 experiments. H-Score data were obtained by dual assessment of 2 representative areas of each coverslip followed by statistical analysis (Mann-Whitney U-Test). The median H-Score and Q1-Q3 values are displayed. A p-value <0.05(*) indicates a significant treatment effect versus MCF-7X basal control.

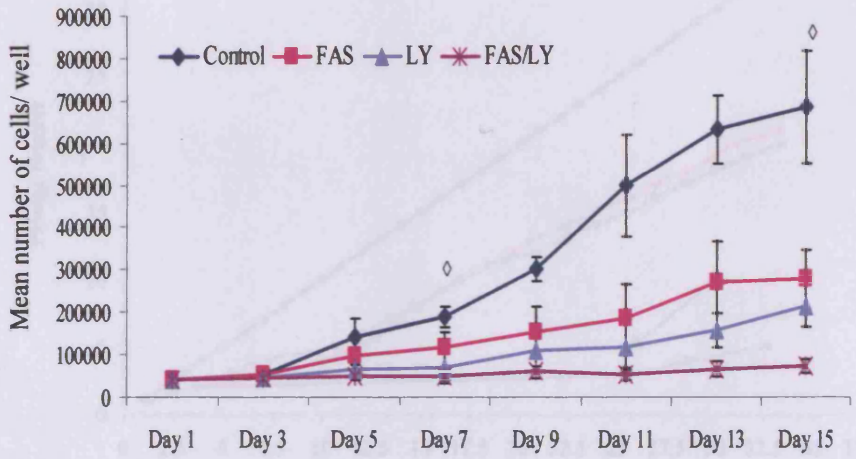

Figure 3.87 Growth challenge with the pure anti-oestrogen faslodex or the PI3K inhibitor LY294002 singly or in combination in MCF-7X cells. MCF-7X cells were grown on 24-well plates in phenol-red-free RPMI media containing 5% XFCS in the absence or presence of faslodex (10^{-7} M), LY294002 (5 μM) singly or in combination for 15 days. At the time points indicated above cells were subject to trypsin dispersion followed by Coulter counting (triplicate wells per time point). These data were log transformed to compare growth rate at day 7 and day 15. The statistical analysis applied was an ANOVA Test followed by a Bonferroni Post-Hoc Test. Data are displayed as the mean number of cells/well +/- SD (n=5).

◊ Denotes faslodex/LY294002 treatment was significant lower at day 7 ($p<0.001$) and day 15 ($p<0.001$) versus untreated MCF-7X cells.

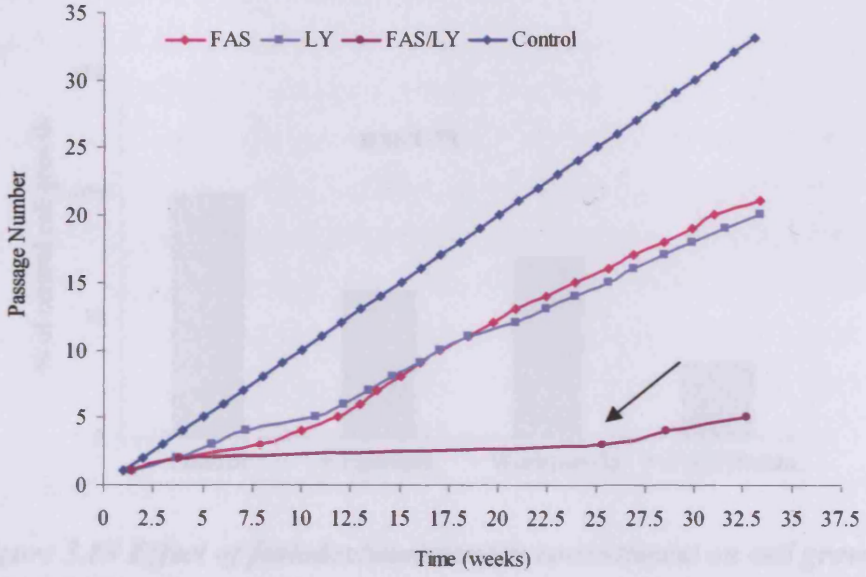

Figure 3.88 Cell culture time-line for long term faslodex/LY294002 treated MCF-7X cells. MCF-7X cells were grown in phenol-red-free RPMI media containing 5% XFCS in the presence of faslodex/LY294002 (10^{-7} M, 5 μM) for long term culture. The arrow signifies the time point at which the rate of cell growth began to increase. Based on the development of rapid log phase growth, there was need to increase the frequency of passaging at approximately week 25. Data are displayed as the number of passages versus time (weeks).

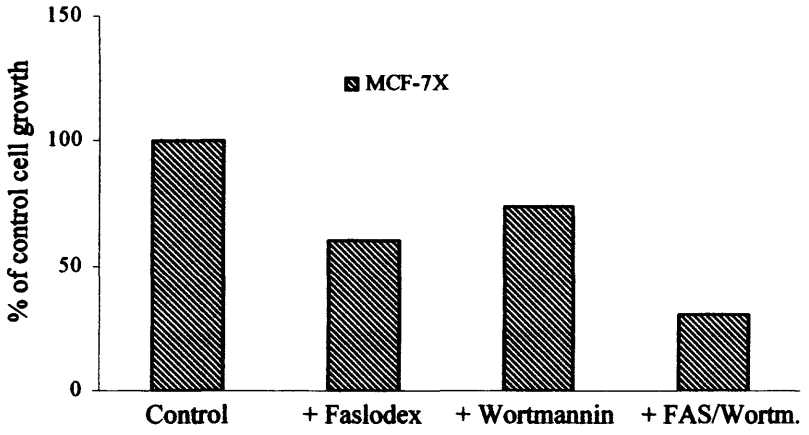

Figure 3.89 Effect of faslodex/wortmannin co-treatment on cell growth in MCF-7X cells. MCF-7X cells were grown on 24-well plates in phenol-red-free RPMI media containing 5% XFCS in the absence or presence of faslodex/wortmannin (10^{-7} M, 1 μM). Conditions were maintained for 7 days prior to trypsin dispersion and Coulter counting (triplicate wells per treatment). Data are displayed as a percentage of control cell growth and include 1 experiment.

3.4.4 The Influence of Simultaneous Targeting of the ERα, PI3K/AKT, and MAPK Signalling Pathways

Considering the maintenance of MAPK activity in MCF-7X cells following faslodex plus LY294002 co-treatment, a triple combination strategy was employed which could identify if such signalling contributed to the incomplete blockade of ERα signalling and residual tumour growth response. After both 7 and 15 day treatment, the triple combination strategy markedly inhibited growth versus control ($p<0.001$* in both instances). While growth at 7 and 15 days was not significantly further inhibited versus faslodex/LY294002 co-treatment, triple challenge with the MEK1 inhibitor PD98059 in combination with faslodex and LY294002 by day 15 was associated with some indication of cell numbers beginning to fall below the initial seeding density [(indicative of cell loss) (Figure 3.90)]. This effect translated out into cultures that could not be maintained further past 16 weeks (Figure 3.91). This blockade of emergence of resistance contrasted the appearance of resistant growth with dual faslodex/LY294002 treatment by week 25. Triple treatment gave an equivalent blockade of total ERα, membrane plus cytoplasmic and nuclear pAKT (Figure 3.92 & 3.93) to faslodex/LY294002 co-treatment ($p=0.225$ and $p=0.162$). Total levels of nuclear ERα were decreased 63.2% ($p=0.001$*) with faslodex/LY294002/PD98059 triple treatment, consistent with the significant (59.5%, $p=0.001$*) reduction observed following faslodex/LY294002 co-treatment. Monitoring of triple treatment on membrane plus cytoplasmic and nuclear phosphorylated AKT levels revealed a 68.5% ($p=0.004$*) and 16.3% ($p=0.008$*) respective fall, where again these levels of inhibition were similar to those reached following faslodex/LY294002 co-treatment (74.9% and 25.6% respectively). While co-treatment with faslodex/LY294002 had no significant impact on the phosphorylation of MAPK, triple treatment importantly reduced cytoplasmic (71.4%, $p=0.001$*) and fully depleted any nuclear ($p=0.039$*) localised activity (Figure 3.94).

Interestingly, the effectiveness of triple treatment in MCF-7X cells also equated with a superior 66.7% ($p<0.001$*) inhibition of Ser118ER phosphorylation (Figure 3.95) versus basal control. However this was not a significant improvement versus the faslodex/LY294002 combination for Ser167ER (Figure 3.96), where triple treatment reduced phosphorylation 70.0% ($p<0.001$*) to a level equivalent to co-treatment with faslodex/LY294002 ($p=0.795$). ERα transcriptional activity was measured again following 18 hour (Figure 3.97) faslodex/LY294002/PD98059 treatment revealing a

increased inhibitory effect versus faslodex/LY294002 co-treatment (66.8% vs. 47.1%). Parallel immunocytochemical staining for endogenous pS2 following triple treatment inhibited cytoplasmic expression 59.6% (p=0.001*) which was a similar fall to dual treatment (61.5%, p=0.001*, Figure 3.98). As MAPK activity and ER have been associated with regulation of AP-1 transcriptional activity, AP-1 reporter assays (Figure 3.99) were also performed. These studies revealed PD98059, either applied singly (where no significant growth inhibitory effect was observed) or as a part of the highly growth-inhibitory triple treatment, was responsible for a ~60% reduction in activity compared to basal MCF-7X cells (p=0.006* and p=0.003* respectively). Finally, preliminary growth studies using wortmannin together with faslodex and PD98059 was able to demonstrate a small superior treatment effect versus wortmannin/faslodex co-treatment (Figure 3.100).

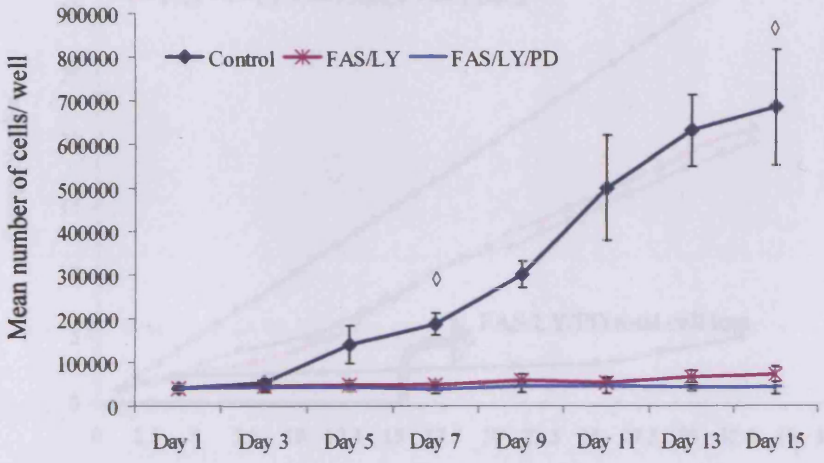

Figure 3.90 Growth challenge with the pure anti-oestrogen faslodex and the PI3K inhibitor LY294002 co-treatment or triple treatment with the addition of the MEK-1 inhibitor PD98059 in MCF-7X cells. MCF-7X cells were grown on 24-well plates in phenol-red-free RPMI media containing 5% XFCS in the absence or presence of faslodex/LY294002 (10^{-7} M, 5 μM) or faslodex/LY294002/PD98059 (10^{-7} M, 5 μM, 25 μM) for 15 days. At the time points indicated above cells were subject to trypsin dispersion followed by Coulter counting (triplicate wells per time point). These data were log transformed to compare growth rate at day 7 and 15. The statistical analysis applied was an ANOVA Test followed by a Bonferroni Pos-Hoc Test. The data are displayed as the mean number of cells/well +/- SD (n=5).

◊ Denotes faslodex/LY294002/PD98059 treatment was significant lower at day 7 ($p<0.001$) and day 15 ($p<0.001$) versus untreated MCF-7X cells.

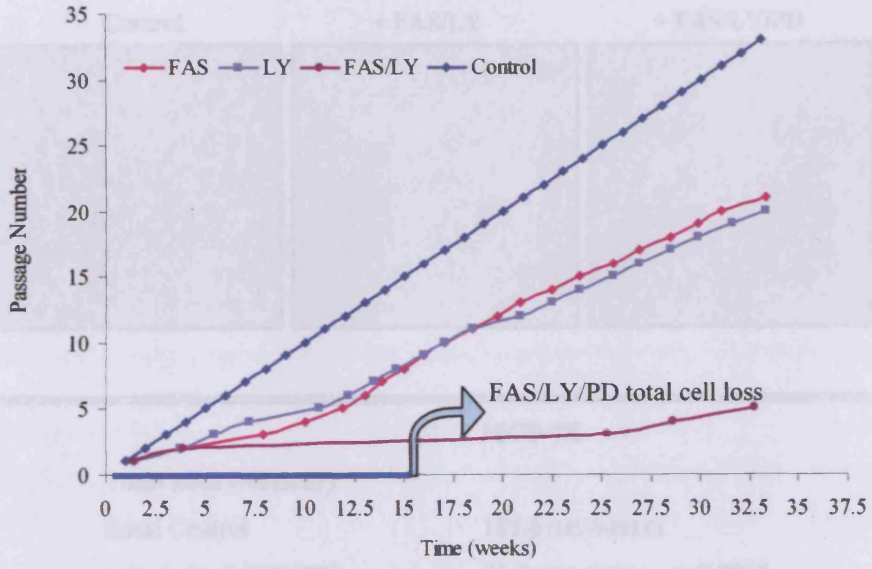

Figure 3.91 Cell culture time-line for long-term faslodex/LY294002/PD98059 treated MCF-7X cells. MCF-7X cells were grown in phenol-red-free RPMI media containing 5% XFCS in the presence of faslodex/LY294002/PD98059 (10^{-7} M, 5 μM, 25 μM) for long term culture. The arrow indicates the time point at which the culture could no longer be maintained due to total cell loss. Data are displayed as the number of passages versus time (weeks).

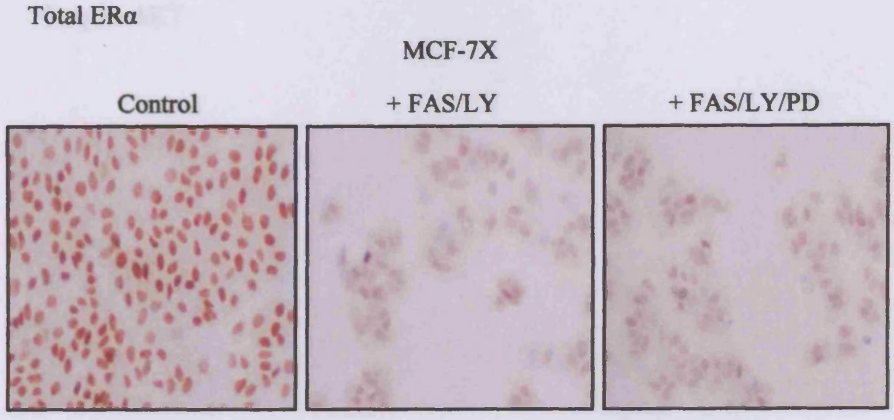

	MCF-7X	
Total ERα (Nuclear)		
Basal Control	185.0 (185.0-195.0)	
+ Faslodex/LY294002	75.0 (70.3-87.5)	p=0.001*
+ Faslodex/LY294002/PD98059	68.0 (63.3-77.5)	p=0.001*

Figure 3.92 Effect of faslodex/LY294002/PD98059 triple treatment on ERα expression in MCF-7X cells by immunocytochemistry. MCF-7X cells were grown on coverslips in phenol-red-free RPMI media containing 5% XFCS in the absence or presence of faslodex/LY294002/PD98059 (10^{-7} M, 5 μM, 25 μM) co-treatment. Conditions were maintained for 7 days prior to ERCIA fixation. The total ERα (6F11, antibody dilution 1:100) digital images shown above (X10 original magnification) are representative of 3 experiments. H-Score data were obtained by dual assessment of 2 representative areas of each coverslip followed by statistical analysis (Mann-Whitney U-Test). The median H-Score and Q1-Q3 values are displayed. A p-value <0.05(*) indicates a significant treatment effect versus MCF-7X basal control.

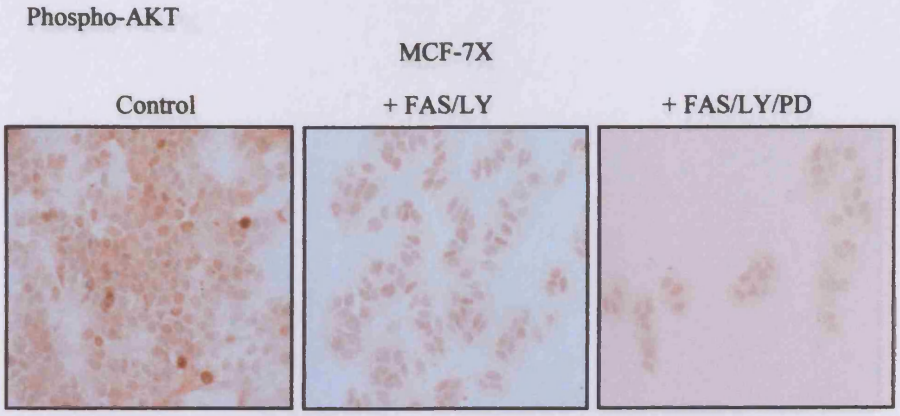

	MCF-7X		
Phospho-AKT	**(Memb. + Cyto.)**	**(Nuclear)**	**Total**
Basal Control	101.5 (76.5-119.3)	107.5 (95.0-112.5)	209.0
+ Faslodex/LY294002	25.5 (21.8-29.0)	80.0 (73.8-93.8)	105.5
	p=0.004*	p=0.012*	
+ Faslodex/LY294002/PD98059	32.0 (29.5-33.8)	90.0 (87.5-95.0)	122.0
	p=0.004*	p=0.008*	

Figure 3.93 Effect of faslodex/LY294002/PD98059 on phosphorylated AKT level in MCF-7X cells by immunocytochemistry. MCF-7X cells were grown on coverslips in phenol-red-free RPMI media containing 5% XFCS in the absence or presence of faslodex/LY294002/PD98059 (10^{-7} M, 5 μM, 25 μM). Conditions were maintained for 7 days prior to ERICA fixation. The phospho-AKT (antibody dilution 1:200) digital images shown above (X20 magnification) are representative of 4 experiments. H-Score data were obtained by dual assessment of 2 representative areas of each coverslip followed by statistical analysis (Mann-Whitney U-Test). The median H-Score and Q1-Q3 values are displayed. A p-value <0.05(*) indicates a significant treatment effect versus MCF-7X basal control.

Phospho-MAPK

MCF-7X

Control + FAS/LY + FAS/LY/PD

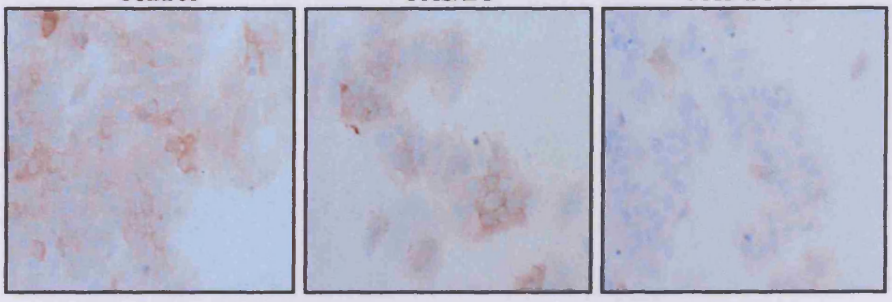

	MCF-7X		
Phospho-MAPK	**(Cytoplasmic)**	**(Nuclear)**	**Total**
Basal Control	35.0 (35.0-48.8)	3.5 (1.3-5.0)	38.5
+ Faslodex/LY294002	35.0 (30.0-35.0)	1.5 (1.0-2.0)	36.5
	p=0.093	p=0.075	
+ Faslodex/LY294002/PD98059	10.0 (10.0-9.0)	1.0 (0.0-1.0)	11.0
	p=0.001*	p=0.007*	

Figure 3.94 Effect of faslodex/LY294002/PD98059 on phosphorylated MAPK level in MCF-7X cells by immunocytochemistry. MCF-7X cells were grown on coverslips in phenol-red-free RPMI media containing 5% XFCS in the absence or presence of faslodex/LY294002/PD98059 (10^{-7} M, 5 μM, 25 μM). Conditions were maintained for 7 days prior to formal saline fixation. The phospho-MAPK (antibody dilution 1:20) digital images shown above (X20 magnification) are representative of 4 experiments. H-Score data were obtained by dual assessment of 2 representative areas of each coverslip followed by statistical analysis (Mann-Whitney U-Test). The median H-Score and Q1-Q3 values are displayed. A p-value <0.05(*) indicates a significant treatment effect versus MCF-7X basal control.

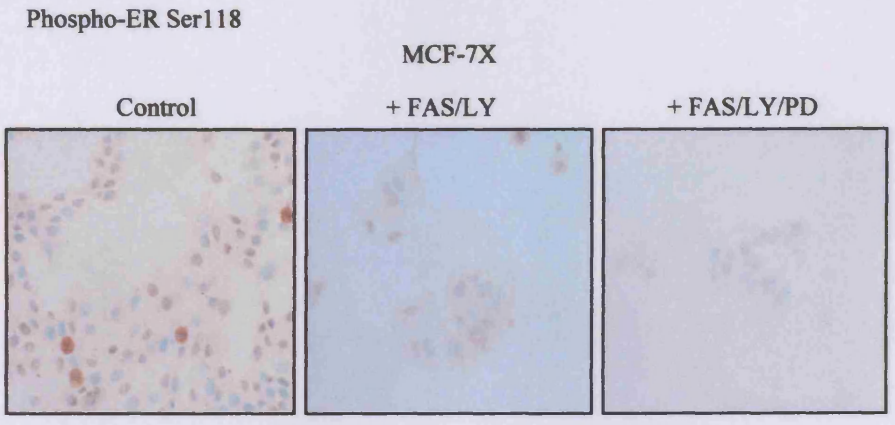

	MCF-7X	
Phospho-ER Ser118 (Nuclear)		
Basal Control	90.0 (77.5-110.5)	
+ Faslodex/LY294002	52.5 (43.8-60.0)	p=0.001*
+ Faslodex/LY294002/PD98059	30.0 (25.0-36.3)	p<0.001*

Figure 3.95 Effect of faslodex/LY294002/PD98059 triple treatment on phosphorylation of ERα at Ser118 residue in MCF-7X cells by immunocytochemistry. MCF-7X cells were grown on coverslips in phenol-red-free RPMI media containing 5% XFCS in the absence or presence of faslodex/LY294002/PD98059 (10^{-7} M, 5 μM, 25 μM). Conditions were maintained for 7 days prior to paraformaldehyde vanadate fixation. The phospho-ER Ser118 (antibody dilution 1:400) digital images shown above (X20 magnification) are representative of 4 experiments. H-Score data were obtained by dual assessment of 2 representative areas of each coverslip followed by statistical analysis (Mann-Whitney U-Test). The median H-Score and Q1-Q3 values are displayed. A p-value <0.05(*) indicates a significant treatment effect versus MCF-7X basal control.

Phospho-ER Ser167

MCF-7X

Control + FAS/LY + FAS/LY/PD

	MCF-7X	
Phospho-ER Ser167 (Nuclear)		
Basal Control	50.0 (45.0-70.0)	
+ Faslodex/LY294002	20.0 (12.0-30.0)	p<0.001*
+ Faslodex/LY294002/PD98059	15.0 (10.0-35.0)	p=0.001*

Figure 3.96 Effect of faslodex/LY294002/PD98059 triple treatment on phosphorylation of ERα at Ser167 residue in MCF-7X cells by immunocytochemistry. MCF-7X cells were grown on coverslips in phenol-red-free RPMI media containing 5% XFCS in the absence or presence of faslodex/LY294002/PD98059 (10^{-7} M, 5 μM, 25 μM). Conditions were maintained for 7 days prior to ERICA fixation. The phospho-ER Ser167 (antibody dilution 1:25) digital images shown above (X20 magnification) are representative of 4 experiments. H-Score data were obtained by dual assessment of 2 representative areas of each coverslip followed by statistical analysis (Mann-Whitney U-Test). The median H-Score and Q1-Q3 values are displayed. A p-value <0.05(*) indicates a significant treatment effect versus MCF-7X basal control.

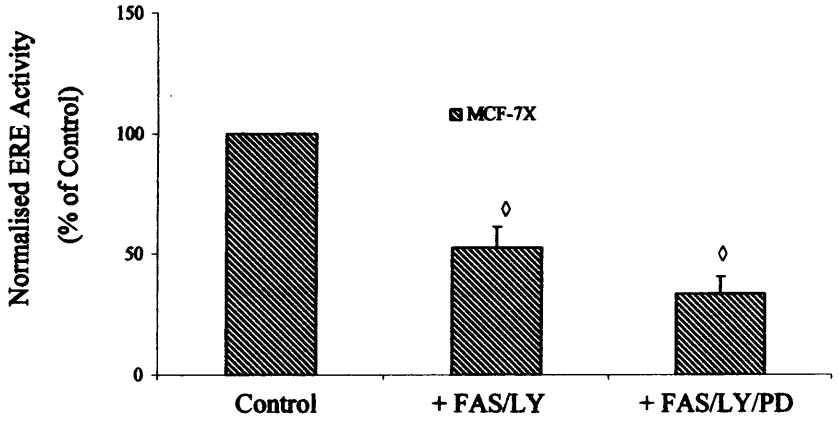

Figure 3.97 Effect on of faslodex/LY294002/PD98059 triple treatment on ER transcriptional activity in MCF-7X cells after 18 hour treatment.
MCF-7X cells were grown on 12-well plates in phenol-red-free RPMI media containing 5% XFCS for 24 hours. Cells were transfected in DCCM serum-free media containing transfection lipid (3 µl/well, Lipofectin), ERE reporter construct (400 ng/well), *Renilla* (150 ng/ml), and 'carrier' DNA (550 ng/well, PCRscript) After 6 hours, the transfection medium was replaced with phenol-red-free RPMI media in the absence or presence of faslodex/LY294002/PD98059 (10^{-7} M, 5 µM, 25 µM) in triplicate wells. Subsequent to 18 hour treatment incubation, a dual-luciferase reporter assay kit was utilised for cell lysis and luminometer assessment (n=3). Data are displayed as percentage of control ERE activity +/- SD (triplicate wells) and has been β-Galactosidase normalized in the absence and presence of FAS/LY/PD (10^{-7} M, 5 µM, 25 µM).

◊ Denotes FAS/LYPD treatment (18 hrs) significantly decreased ERE activity in MCF-7X cells versus untreated control.

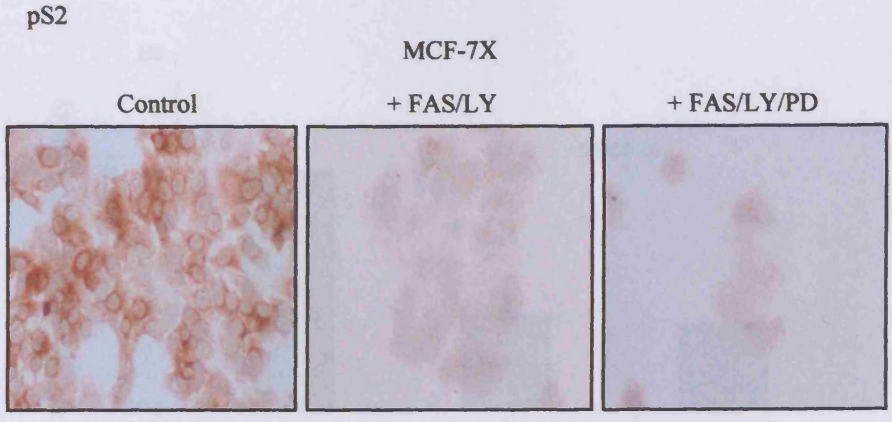

	MCF-7X	
pS2 (Cytoplasmic)		
Basal Control	130.0 (121.3-133.8)	
+ Faslodex/LY294002	50.0 (45.0-70.0)	p=0.001*
+ Faslodex/LY294002/PD98059	52.5 (50.0-58.8)	p=0.001*

Figure 3.98 Effect of faslodex/LY294002/PD98059 triple treatment on pS2 expression in MCF-7X cells by immunocytochemistry. MCF-7X cells were grown on coverslips in phenol-red-free media containing 5% XFCS in the absence or presence of faslodex/LY294002/PD98059 (10^{-7} M, 5 μM, 25 μM). Conditions were maintained for 7 days prior to ERICA fixation. The pS2 (antibody dilution 1:500) digital images shown above (X20 magnification) are representative of 3 experiments. H-Score data were obtained by dual assessment of 2 representative areas of each coverslip followed by statistical analysis (Mann-Whitney U-Test). The median H-Score and Q1-Q3 values are displayed. A p-value <0.05(*) indicates a significant treatment effect versus MCF-7X basal control.

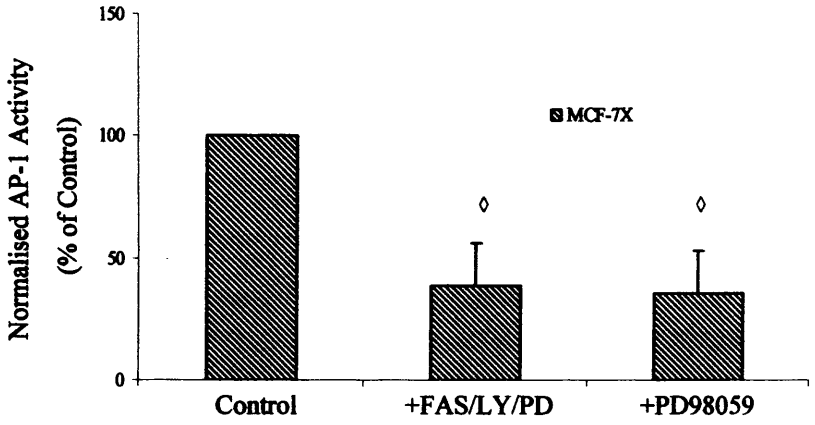

Figure 3.99 Treatment effect of faslodex/LY294002/PD98059 on AP-1 transcriptional activity in MCF-7X cells. MCF-7X cells were grown on 12-well plates in phenol-red-free RPMI media containing 5% XFCS for 24 hours. Cells were transfected in DCCM serum-free media containing lipid (3 µl/well, Lipofectin), AP-1-pTal reporter contruct (400 ng/well) and 'carrier' DNA (700 ng/well PCRscript). Control pTal luciferase reporter constructs were included for each treatment at the same construct and 'carrier' concentrations. After 6 hours, the transfection medium was replaced with phenol-red-free RPMI media in the presence of control (ethanol, 1 µl/ 10 ml), faslodex/LY294002/PD98059 (10^{-7} M, 5 µM, 25 µM) or PD98059 (25 µM) in triplicate wells. Subsequent to 18 hour treatment incubation, a luciferase reporter assay kit was utilised for cell lysis and luminometer assessment (n=3). Data are displayed as a percentage of control AP-1 activity +/- SD and has been β-Galactosidase normalised for transfection efficiency.

◊ Denotes FAS/LY/PD and PD98059 treatment (18 hrs) significantly decreased AP-1 activity in MCF-7X cells versus untreated control.

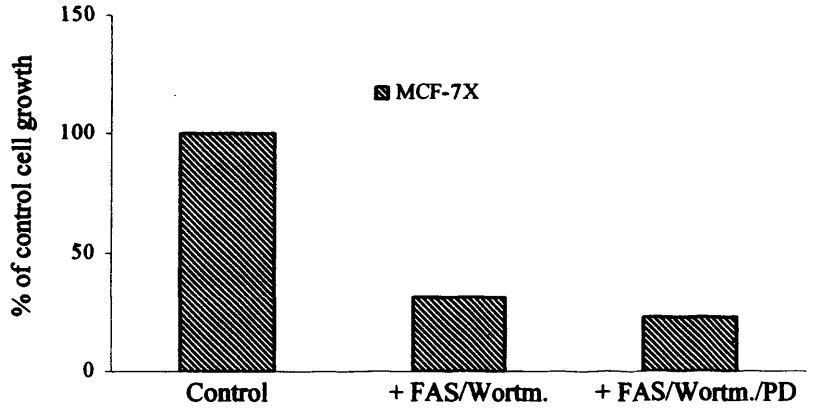

Figure 3.100 Effect of faslodex/wortmannin or faslodex/wortmannin/PD98059 combination treatment on cell growth in MCF-7X cells. MCF-7X cells were grown on 24-well plates in phenol-red-free RPMI media containing 5% XFCS in the absence or presence of faslodex/wortmannin (10^{-7} M, 1 μM) or faslodex/wortmannin/PD98059 (10^{-7} M, 1 μM, 25 μM). Conditions were maintained for 7 days prior to trypsin dispersion and Coulter counting (triplicate well per treatment). Data are displayed as a percentage of control cell growth and includes 1 experiment.

3.4.5 The Influence of Co-targeting of the PI3K/AKT and MAPK Signalling Pathways

Further confirmation that the inhibition of ERα and its phosphorylation was required for the catastrophic effects of triple treatment came from profiling MCF-7X cells co-treated with the PI3K inhibitor LY294002 plus the MEK-1 inhibitor PD98059. This combination treatment was certainly superior in inhibiting growth (75.0%, $p<0.001$*) compared with LY294002 (69.1%, $p<0.001$*) or PD98059 alone (29.0%, $p=1.000$) (Figure 3.101) by day 15. This superior combination effect has also been observed by Martin *et al.* (2003), Yue *et al.* (2003) and Santen *et al.* (2004a) in their long-term oestrogen deprived models. However, in contrast to triple treatment that included faslodex, co-treatment with LY284002/PD98059 in MCF-7X cells did not prevent resistance from emerging, in this instance at 12 weeks (Figure 3.102). Subsequent studies indicated that LY294002/PD98059 co-treatment in the absence of faslodex was capable of maximally decreasing MAPK activity. Immunocytochemistry revealed this co-treatment decreased MAPK cytoplasmic staining by 74.3% ($p=0.001$*), in parallel with a significant 51.7% ($p=0.004$*) depletion of membrane plus cytoplasmic phosphorylated AKT and a 12% ($p=0.016$*) fall in nuclear AKT activity (Figure 3.103). However, LY294002/PD98059 was without significant inhibitory effect on total ERα ($p=0.757$) or Ser118ER phosphorylation ($p=0.197$), versus the basal control level, although Ser167 was significantly depleted as with LY294002 alone (50.0%, $p<0.001$*, Figure 3.104). These data were confirmation that inhibition of ER and its Ser118 phosphorylation was required for the catastrophic effects of triple treatment on MCF-7X cell growth in preventing resistance, rather than any direct effect of MAPK depletion on growth.

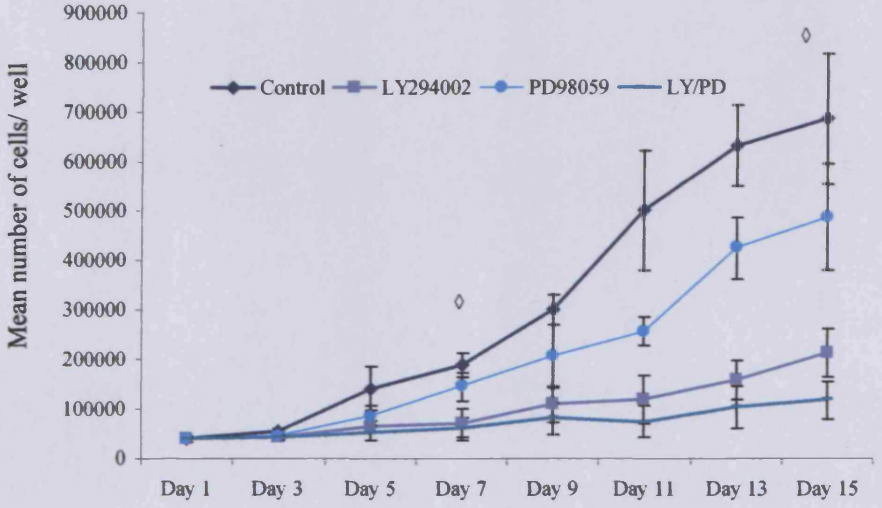

Figure 3.101 Growth challenge with the PI3K inhibitor LY294002 or the MEK-1 inhibitor PD98059 singly or in combination in MCF-7X cells. MCF-7X cells were grown on 24-well plates in phenol-red-free RPMI media containing 5% XFCS in the absence or presence of LY294002 (5 μM), PD98059 (25 μM) singly or in combination for 15 days. Every 48 hours cells were subject to trypsin dispersion followed by Coulter counting (triplicate wells per time point). These data were log transformed to compare growth rate at day 7 and 15. The statistical analysis applied was an ANOVA Test followed by a Bonferroni Pos-Hoc Test. Data are displayed as the mean number of cells/well +/- SD (n=5).

◊ Denotes LY294002/PD98059 treatment was significantly lower at day 7 ($p<0.001$) and day 15 ($p<0.001$) versus untreated MCF-7X cells.

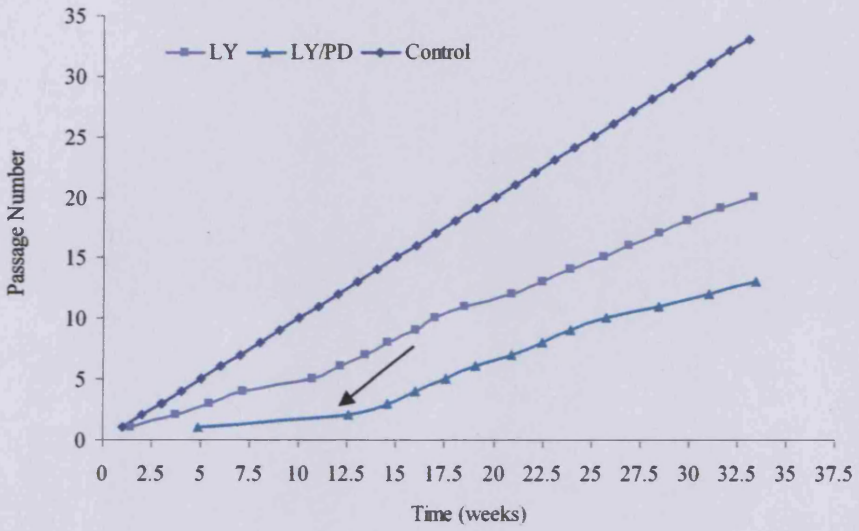

Figure 3.102 Cell culture time-line for long-term LY294002/PD98059 treated MCF-7X cells. MCF-7X cells were grown in phenol-red-free RPMI media containing 5% XFCS in the presence of LY294002/PD98059 (5 μM, 25 μM) for long term culture. The arrow signifies the time point at which the rate of cell growth began to increase. Based on the development of rapid log phase growth, there was need to increase the frequency of passaging at approximately week 12. Data are displayed as the number of passages versus time (weeks).

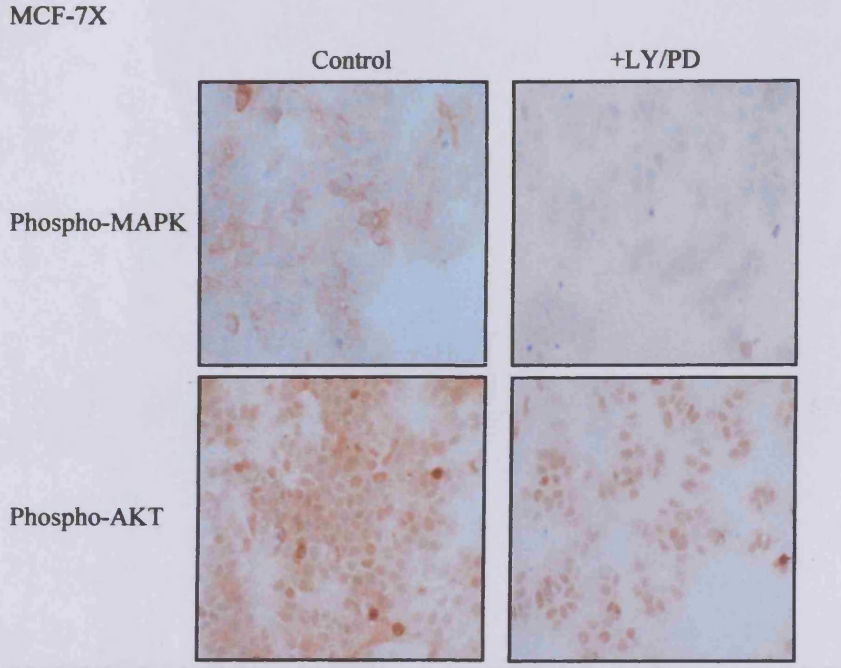

	MCF-7X		
Phospho-MAPK	**(Cytoplasmic)**	**(Nuclear)**	**Total**
Basal Control	35.0 (35.0-48.8)	3.5 (1.3-5.0)	38.5
+ LY294002/PD98059	9.0 (6.0-10.0)	1.0 (0.3-1.8)	10.0
	p=0.001*	p=0.016*	
Phospho-AKT	**(Memb. + Cyto.)**	**(Nuclear)**	**Total**
Basal Control	101.5 (76.5-119.3)	107.5 (95.0-112.5)	209.0
+ LY294002/PD98059	49.0 (46.0-55.3)	95.0 (88.8-95.0)	144.0
	p=0.004*	p=0.016*	

Figure 3.103 Effect of LY294002/PD98059 on phosphorylated MAPK and AKT levels in MCF-7X cells by immunocytochemistry. MCF-7X cells were grown on coverslips in phenol-red-free RPMI media containing 5% XFCS in the absence or presence of LY294002/PD98059 (5 μM, 25 μM). Conditions were maintained for 7 days prior to the appropriate fixation. The phospho-MAPK (antibody dilution 1:20) assay required coverslips formal saline fixed and the phospho-AKT (1:200) assay required coverslips ERICA fixed. The digital images shown above (X20 magnification) are representative of 4 experiments. H-Score data were obtained by dual assessment of 2 representative areas of each coverslip followed by statistical analysis (Mann-Whitney U-Test). The median H-Score and Q1-Q3 values are displayed. A p-value <0.05(*) indicates a significant treatment effect versus MCF-7X basal control.

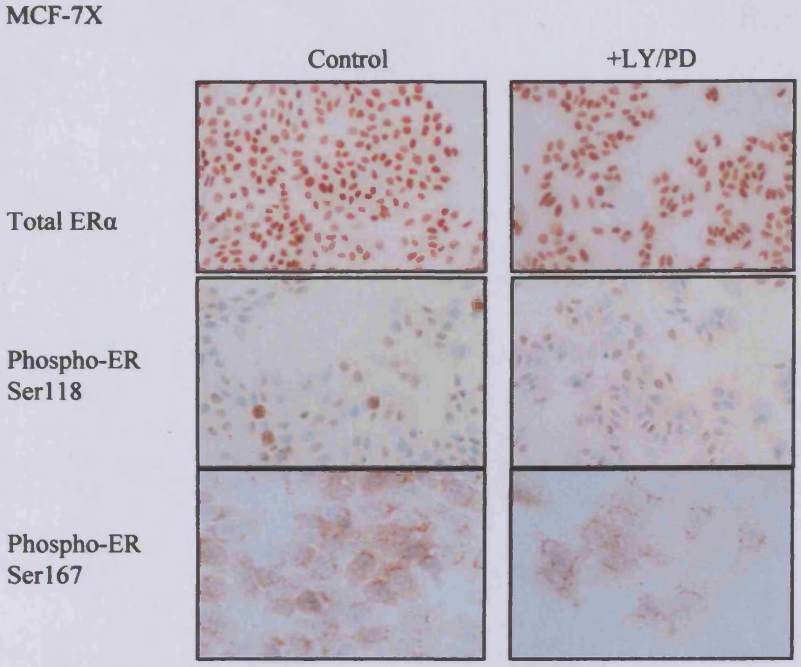

	MCF-7X	
Total ERα (Nuclear)		
Basal Control	185.0 (185.0-195.0)	
+ LY294002/PD98059	187.5 (183.8-205.0)	p=0.797
Phospho-ER Ser118 (Nuclear)		
Basal Control	90.0 (77.5-110.5)	
+ LY294002/PD98059	92.5 (78.8-112.5)	p=0.197
Phospho-ER Ser167 (Nuclear)		
Basal Control	50.0 (45.0-70.0)	
+ LY294002/PD98059	25.0 (10.0-35.0)	p=0.001*

Figure 3.104 Effect of LY294002/PD98059 co-treatment on total ERα and the phosphorylation of ERα at Ser118 and Ser167 residues in MCF-7X cells by immunocytochemistry. MCF-7X cells were grown on coverslips in phenol-red-free RPMI media containing 5% XFCS in the absence or presence of LY294002/PD98059 (5 μM, 25 μM). Conditions were maintained for 7 days prior to the appropriate fixation. The total nuclear ERα (antibody dilution 1:100) and the phospho-ER Ser167 (1:25) assays required coverslips ERICA fixed. The phospho-ER Ser118 (antibody dilution 1:400) assay required coverslips paraformaldehyde vanadate fixed. The digital images shown above (X20 magnification) are representative of 3 experiments. H-Score data were obtained by dual assessment of 2 representative areas of each coverslip followed by statistical analysis (Mann-Whitney U-Test). The median H-Score and Q1-Q3 values are displayed. A p-value <0.05(*) indicates a significant treatment effect versus MCF-7X basal control.

3.5 DEVELOPMENT OF RESISTANCE TO SINGLE AND CO-TREATMENT STRATEGIES

3.5.1 Faslodex Resistance in the MCF-7X Model

Faslodex sensitivity is a feature retained by many of the acquired resistance models, including the MCF-7X model where this project has shown the agent partially down-regulated ERα, lowered Ser118ER activity, diminished ERE reporter activity and reduced endogenous pS2 expression. The pure anti-oestrogen inhibited growth by nearly 60% and this response was maintained for approximately 10 weeks (Figure 3.78). However, faslodex failed to block Ser167ER activity and residual ERα transcriptional activity remained, culminating in emergence of resistance to the agent with the resultant proliferative activity of these cells restored to that of the untreated MCF-7X cells.

Visual characterisation of the subsequent faslodex resistant MCF-7X phenotype [X(FAS)] by phase contrast imaging (Figure 3.105A) and Haematoxylin & Eosin staining (Figure 3.105B) revealed small irregular colonies, where cells were heterogeneous with more elongated pseudopodia and a 'kite-like' cellular shape. The nuclear to cytoplasmic ratio was equal and the nuclei were heterogeneous ovoid or round with prominent nucleoli. These morphological features of the culture became evident during initial faslodex treatment of MCF-7X cells and were retained throughout the development of X(FAS) cell resistance. Studies in the Tenovus Centre for Cancer Research (Nicholson *et al.*, 2005) suggest an increase in aggressive behaviour on acquisition of faslodex resistance by breast cancer cells, and in accordance with this an increase in motility and, to a lesser extent, invasiveness was detected in the X(FAS) sub-line compared to the MCF-7X parental cells (Figure 3.106A/B).

This resistance to faslodex was associated with diminished ERα expression (45.9%, p=0.001*, Figure 3.107) and Ser118ER activity (44.4%, p=0.001*, Figure 3.108) versus the basal control. While ERα expression was slightly recovered in X(FAS) cells versus the responsive phase (48.0%, p=0.004*, X(FAS) vs. faslodex treated), this Ser118ER phosphorylation observed in X(FAS) cells was further significantly lowered (p=0.017*) versus treatment of MCF-7X cells with faslodex for 7 days primarily due to an increased percentage of cells negative for Ser118ER phosphorylation. In contrast, however, a significant 95.0% (p=0.003*) increase in

Ser167ER activity on the residual ER was observed in the resistant cells versus the basal control as well as versus faslodex treatment (p=0.003*, Figure 3.108). In parallel, while ER transcriptional activity was not measured in these studies, evaluation of pS2 protein by immunocytochemistry revealed considerable recovery in expression in the resistant cells by 62.1% versus faslodex treatment (p=0.001*) nearing basal levels in the parental MCF-7X cells (Figure 3.109).

7 day faslodex treatment failed to alter MAPK cytoplasmic or nuclear activity (p=0.418 and p=0.708 respectively) in MCF-7X cells by immunocytochemistry, and there was also no significant influence on AKT activity (membrane plus cytoplasmic p=0.127, or nuclear p=0.680) suggesting the inhibitory effect of this agent on ERα activity and growth was independent of these kinases. However, the resistant phenotype exhibited a substantial 207.1% (p=0.001*) increase in cytoplasmic-localised MAPK phosphorylation versus basal MCF-7X cells and a 152.9% rise versus faslodex treatment (p=0.003*) while nuclear levels were maintained (Figure 3.110). Some increases were also achieved for AKT activity (Figure 3.111), although increases were more modest in the X(FAS) resistant cells. Thus while there was no significant effect on membrane plus cytoplasmic activity (p=0.109), there was a 20.9% (p=0.004*) increase in nuclear AKT activity versus MCF-7X cell control equating to a 26.8% (p=0.003*) increase versus faslodex treatment. These kinases could thus be contributory towards ERα activity (alongside the modest increases in ERα expression level) and growth in the X(FAS) cells.

Our established *in vitro* breast cancer cell lines that have acquired anti-oestrogen resistance have clearly demonstrated a pivotal role for autocrine EGFR/HER2/IGF1R signalling in promoting increased activation of downstream elements MAPK and PI3K/AKT that drive ERα phosphorylation and transcriptional activity, resistant cell growth and also increased invasiveness (McClelland *et al.*, 2001; Knowlden *et al.*, 2003b). It is thus feasible that the residual Ser118ER, increased Ser167ER activity, and ERα transcriptional activity driven by increases in MAPK and AKT phosphorylation (alongside some increases in ERα expression level) may also lie downstream of such receptor signalling in the X(FAS) cells and be of potential importance in promoting their increased aggressive behaviour and growth. While investigation of the parental MCF-7X cell line had revealed only low expression levels of IGF-1R, EGFR and HER2, observations made on acquisition of faslodex

resistance indicated such signalling was significantly altered. Thus, increases in EGFR expression were observed in X(FAS) cells versus the parental line. The X(FAS) cells exhibited a substantial 235.7% (p=0.004*) increase in membrane localised EGFR paralleled by a 125.0% (p=0.004*) increase in cytoplasmic expression compared to the low levels in MCF-7X cells (Figure 3.112). HER2 expression levels were also increased significantly in the X(FAS) resistant phenotype by 63.0% (p=0.001*) for membrane localised HER2, coupled with a 120.0% (p=0.003*) rise in cytoplasmic expression versus the parental line (Figure 3.113). In addition, IGF-1R membrane and cytoplasmic expression was increased by 155.0% (p=0.003*) and 77.3% (p=0.004*) respectively once resistance occurred (Figure 3.114).

Interestingly, while HER2 and IGF-1R expression was unchanged, EGFR levels began to increase during early faslodex treatment of MCF-7X cells, with membrane and cytoplasmic expression increasing by 50.0% (p=0.004*) and 100% (p=0.004*) respectively versus basal control (Figure 3.112). More modest increases were also observed in HER2 membrane (22.2%, p=0.056) and cytoplasmic staining (20.0%, p=0.016*). Following the faslodex responsive phase in MCF-7X cells, the membrane EGFR level increased 123.8% (p=0.004*) further once the resistance phenotype developed. While EGFR/HER2 does not appear to contribute substantially to MCF-7X cells under basal conditions, such signalling may contribute to the MAPK, AKT, substantial levels of Ser167ER and the residual Ser118ER activity detectable during faslodex response, as we have observed previously in association with cell survival during anti-oestrogen treatment of MCF-7 cells (Gee *et al.*, 2003).

A.

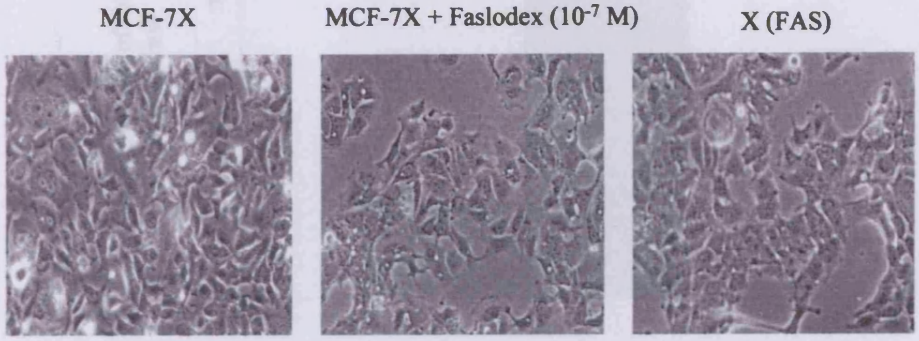

B.

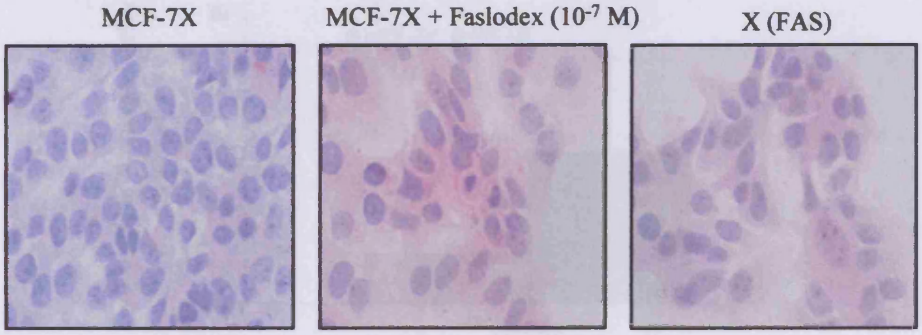

Figure 3.105 The visual morphology of MCF-7X versus X(FAS) phenotype by phase contrast (A) and H&E staining (B). MCF-7X and the X(FAS) resistant cells were grown in phenol-red-free RPMI media containing 5% XFCS in the appropriate absence or presence of faslodex (10^{-7} M). (A) Cell phase contrast digital images were obtained during log phase growth (X20 magnification). (B) MCF-7X and X(FAS) cells were grown under the same conditions as previously described for 7 days on coverslips prior to ERICA fixation. The cells were H&E stained with 10% Ehrlich Haematoxylin (10 min) followed by 1% Eosin (2½ hrs). The H&E digital images shown above are X40 magnification.

A.

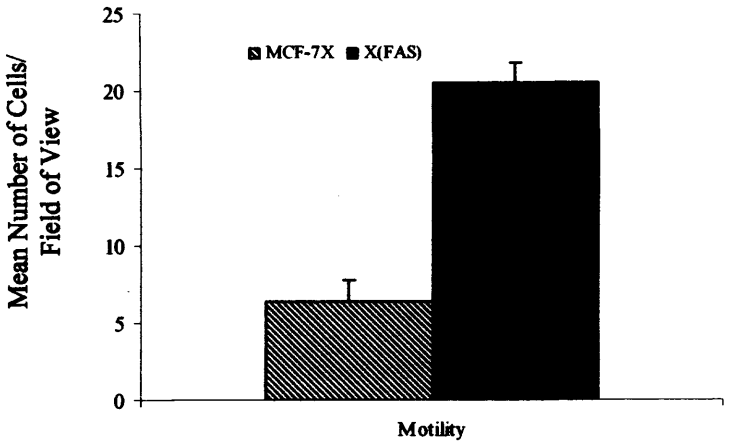

B.

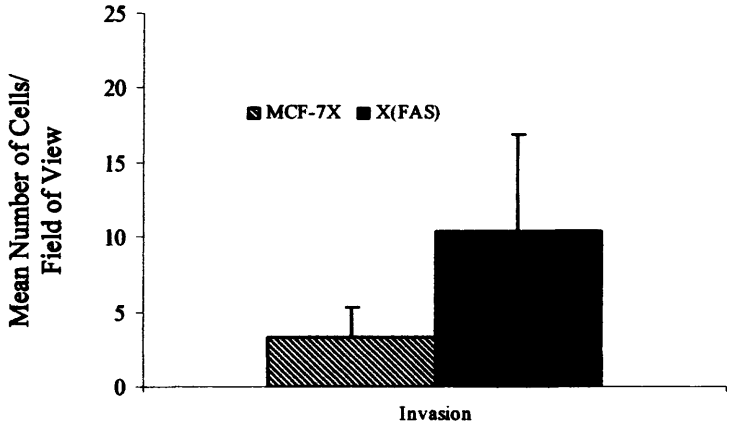

Figure 3.106 MCF-7X and X(FAS) cell motility (A) and invasive capacity (B). (A) MCF-7X and X(FAS) cells were seeded onto fibronectin coated Transwell® permeable supports for 24 hours prior to formaldehyde fixation and crystal violet staining. (B) MCF-7X and X(FAS) cells were seeded onto matrigel coated Transwell® permeable supports for 72 hours prior to formaldehyde fixation and mounting to glass slides with mounting medium containing DAPI. These data above represent the mean number if cells/field of view +/- SD of triplicate inserts.

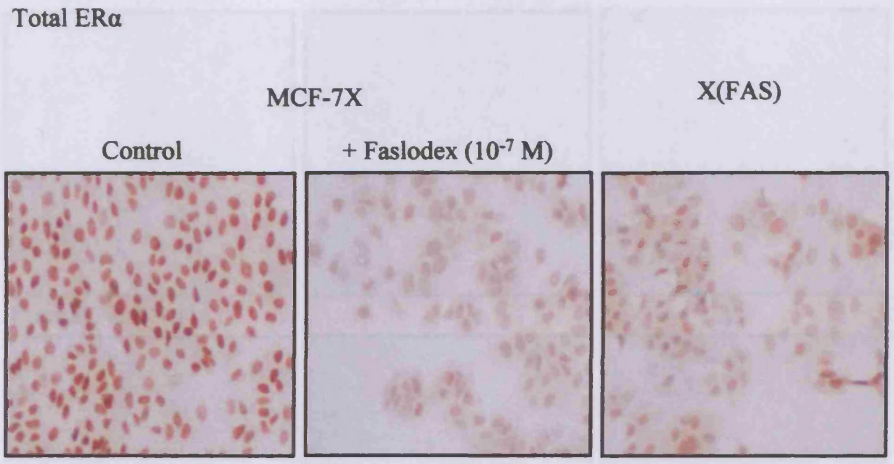

	MCF-7X	+ Faslodex	X(FAS)
Total ERα			
(Nuclear)	185.0 (185.0-195.0)	67.5 (60.0-71.3)	100.0 (93.8-106.3)
		p=0.001*	p=0.001*

Figure 3.107 MCF-7X versus X(FAS) cell ERα expression by immunocytochemistry. MCF-7X and X(FAS) cells were grown on coverslips in phenol-red-free RPMI media containing 5% XFCS with the appropriate absence or presence of faslodex (10^{-7} M). Conditions were maintained for 7 days prior to ERICA fixation. The total nuclear ERα (6F11, antibody dilution 1:100) digital images shown above (X10 original magnification) are representative of 3 experiments. H-Score data were obtained by dual assessment of 2 representative areas of each coverslip followed by statistical analysis (Mann-Whitney U-Test). The median H-Score and Q1-Q3 values are displayed. A p-value <0.05(*) indicates a significant difference in ERα expression versus MCF-7X basal control.

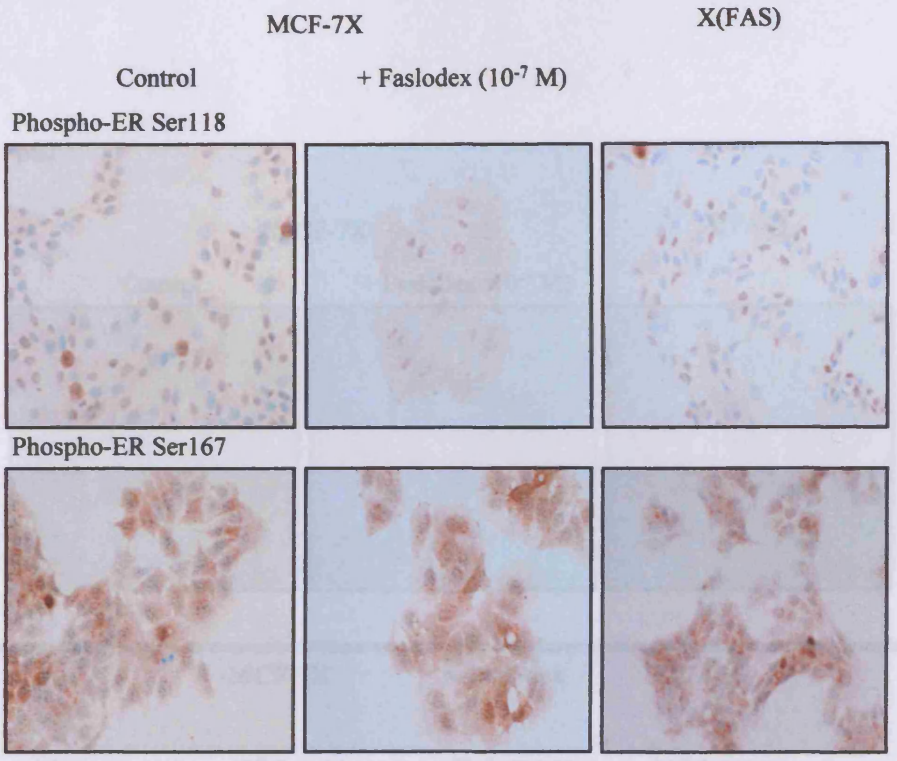

	MCF-7X	+ Faslodex	X(FAS)
Phospho-ER Ser118			
(Nuclear)	90.0 (77.5-110.5)	77.5 (61.3-80.0)	50.0 (47.5-55.0)
		p=0.030*	p=0.001*
Phospho-ER Ser167			
(Nuclear)	50.0 (45.0-70.0)	50.0 (40.0-60.0)	97.5 (81.3-102.5)
		p=0.841	p=0.003*

Figure 3.108 MCF-7X versus X(FAS) cell phosphorylation of ERα at Ser118 and Ser167 residues by immunocytochemistry. MCF-7X and X(FAS) cells were grown on coverslips in phenol-red-free RPMI media containing 5% XFCS with the appropriate absence or presence of faslodex (10^{-7} M). Conditions were maintained for 7 days prior to the appropriate fixation. The phospho-ER Ser118 (antibody dilution 1:400) assay required coverslips paraformaldehyde vanadate fixed. The phospho-ER Ser167 (antibody dilution 1:25) assay required coverslips ERICA fixed. The digital images shown above (X20 magnification) are representative of 4 experiments. H-Score data were obtained by dual assessment of 2 representative areas of each coverslip followed by statistical analysis (Mann-Whitney U-Test). The median H-Score and Q1-Q3 values are displayed. A p-value <0.05(*) indicates a significant difference in phospho-ER Ser118 or Ser167 level versus MCF-7X basal control.

pS2

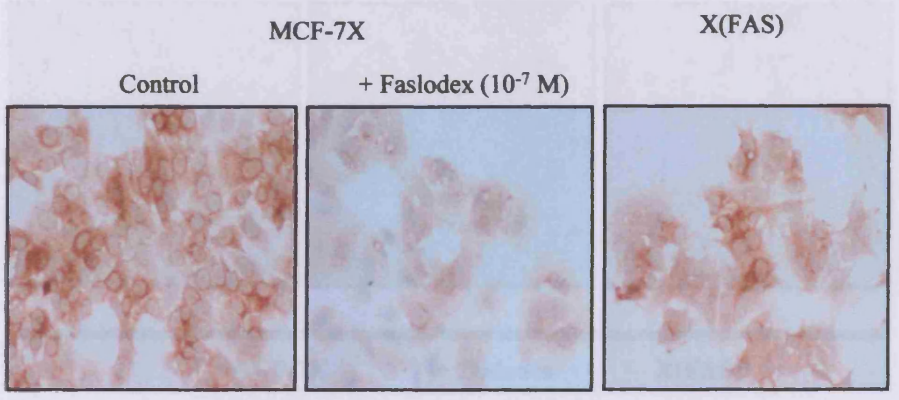

	MCF-7X	+ Faslodex	X(FAS)
pS2			
(Cytoplasmic)	130.0 (121.3-133.8)	72.5 (58.8-80.0)	117.5 (105.0-125.0)
		p=0.001*	p=0.034*

Figure 3.109 MCF-7X versus X(FAS) cell pS2 expression by immunocytochemistry. MCF-7X and X(FAS) cells were grown on coverslips in phenol-red-free RPMI media containing 5% XFCS with the appropriate absence of presence of faslodex (10^{-7} M). Conditions were maintained for 7 days prior to ERICA fixation. The pS2 (antibody dilution 1:500) digital images shown above (X20 magnification) are representative of 3 experiments. H-Score data were obtained by dual assessment of 2 representative areas of each coverslip followed by statistical analysis (Mann-Whitney U-Test). The median H-Score and Q1-Q3 values are displayed. A p-value <0.05(*) indicates a significant difference in pS2 expression versus MCF-7X basal control.

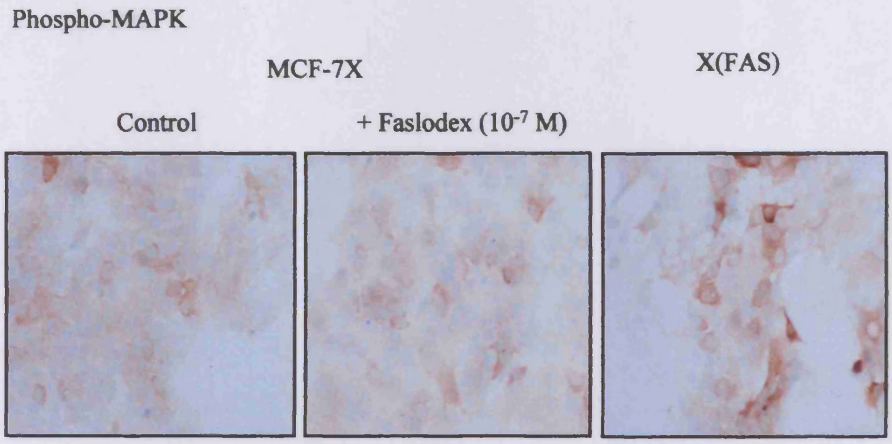

	MCF-7X	+ Faslodex	X(FAS)
Phospho-MAPK			
(Cytoplasmic)	35.0 (35.0-48.8)	42.5 (35.0-64.5)	107.5 (73.8-110.0)
		p=0.418	p=0.001*
(Nuclear)	3.5 (1.3-5.0)	3.0 (2.0-6.5)	2.0 (2.0-4.3)
		p=0.708	p=0.576
Total	38.5	45.5	109.5

Figure 3.110 MCF-7X versus X(FAS) cell phosphorylated MAPK level by immunocytochemistry. MCF-7X and X(FAS) cells were grown on coverslips in phenol-red-free RPMI media containing 5% XFCS with the appropriate absence or presence of faslodex (10^{-7} M). Conditions were maintained for 7 days prior to formal saline fixation. The phospho-MAPK (antibody dilution 1:20) digital images shown above (X20 magnification) are representative of 4 experiments. H-Score data were obtained by dual assessment of 2 representative areas of each coverslip followed by statistical analysis (Mann-Whitney U-Test). The median H-Score and Q1-Q3 values are displayed. A p-value <0.05(*) indicates a significant difference in phospho-MAPK level versus MCF-7X basal control.

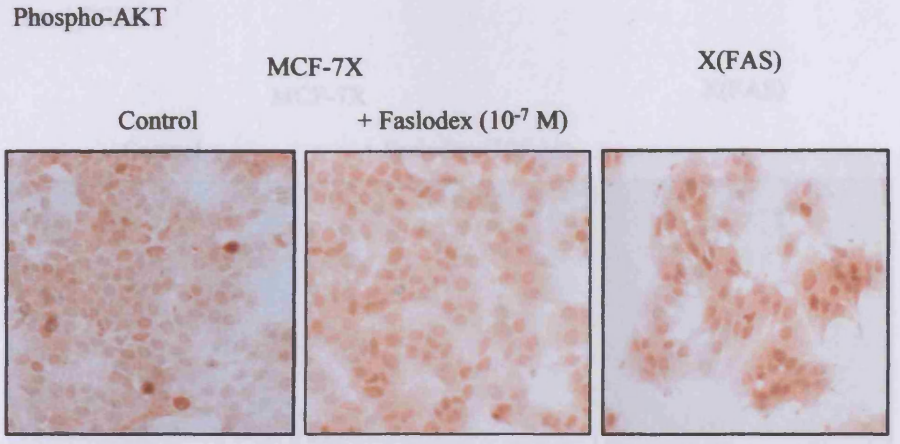

	MCF-7X	+ Faslodex	X(FAS)
Phospho-AKT			
(Memb. + Cyto.)	101.5 (76.5-119.3)	78.5 (71.0-84.5)	115.0 (111.0-125.8)
		p=0.127	p=0.109
(Nuclear)	107.5 (95.0-112.5)	102.5 (98.8-110.0)	130.0 (128.8-135.0)
		p=0.680	p=0.004*
Total	209.0	181.0	245.0

Figure 3.111 MCF-7X versus X(FAS) cell phosphorylated AKT level by immunocytochemistry. MCF-7X and X(FAS) cells were grown on coverslips in phenol-red-free RPMI media containing 5% XFCS with the appropriate absence or presence of faslodex (10^{-7} M). Conditions were maintained for 7 days prior to ERICA fixation. The phospho-AKT (antibody dilution 1:200) digital images shown above assay photographed (X20 original magnification) are representative of 3 experiments. H-Score data were obtained by dual assessment of 2 representative areas of each coverslip followed by statistical analysis (Mann-Whitney U-Test). The median H-Score and Q1-Q3 values are displayed. A p-value <0.05(*) indicates a significant difference in phospho-AKT level versus MCF-7X basal control.

Total EGFR

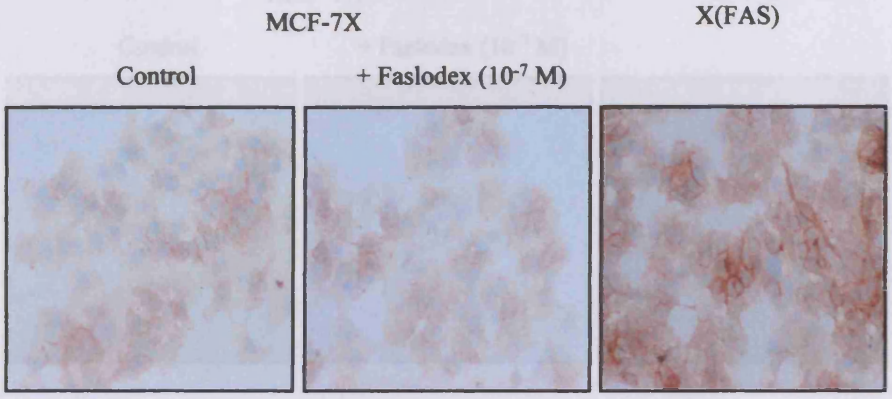

	MCF-7X	+ Faslodex	X(FAS)
Total EGFR			
(Membrane)	35.0 (30.0-40.0)	52.5 (45.0-56.3)	117.5 (97.5-120.0)
		p=0.004*	p=0.004*
(Cytoplasmic)	30.0 (28.0-35.0)	60.0 (53.8-61.3)	67.5 (60.0-71.3)
		p=0.004*	p=0.004*
Total	65.0	112.5	185.0

Figure 3.112 MCF-7X versus X(FAS) cell total EGFR expression by immunocytochemistry. MCF-7X and X(FAS) cells were grown on coverslips in phenol-red-free RPMI media containing 5% XFCS with the appropriate absence or presence of faslodex (10^{-7} M). Conditions were maintained for 7 days prior to phenol formal saline fixation. The total EGFR (antibody dilution 1:100) digital images shown above (X20 magnification) are representative of 2 experiments. H-Score data were obtained by dual assessment of 3 representative areas of each coverslip followed by statistical analysis (Mann-Whitney U-Test). The median H-Score and Q1-Q3 values are displayed. A p-value <0.05(*) indicates a significant difference in total EGFR expression versus MCF-7X basal control.

Total HER2

MCF-7X X(FAS)

Control + Faslodex (10^{-7} M)

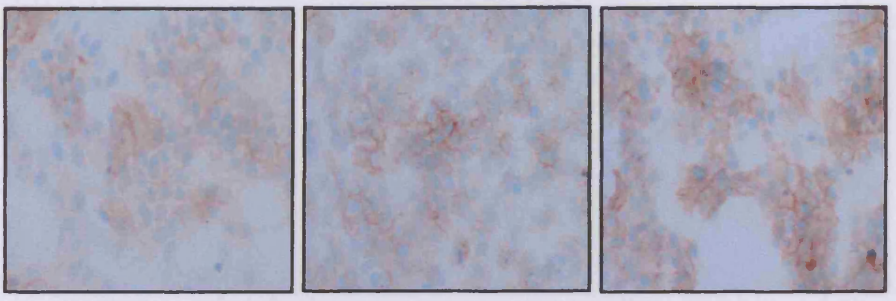

	MCF-7X	+ Faslodex	X(FAS)
Total HER2			
(Membrane)	67.5 (51.3-78.8)	82.5 (78.8-86.3)	110.0 (107.5-120.0)
		p=0.056	p=0.001*
(Cytoplasmic)	25.0 (20.0-30.0)	30.0 (28.8-31.3)	55.0 (50.0-61.3)
		p=0.016*	p=0.001*
Total	92.5	112.5	165.0

Figure 3.113 MCF-7X versus X(FAS) cell total HER2 expression by immunocytochemistry. MCF-7X and X(FAS) cells were grown on coverslips in phenol-red-free RPMI media containing 5% XFCS with the appropriate absence or presence of faslodex (10^{-7} M). Conditions were maintained for 7 days prior to ERICA fixation. The total HER2 (antibody dilution 1:100) digital images shown above (X20 magnification) are representative of 2 experiments. H-Score data were obtained by dual assessment of 3 representative areas of each coverslip followed by statistical analysis (Mann-Whitney U-Test). The median H-Score and Q1-Q3 values are displayed. A p-value <0.05(*) indicates a significant difference in total HER2 expression versus MCF-7X basal control.

Total IGF-1R

MCF-7X X(FAS)

Control + Faslodex (10^{-7} M)

	MCF-7X	+ Faslodex	X(FAS)
Total IGF-1R			
(Membrane)	10.0 (10.0-12.8)	10.0 (10.0-12.8)	25.5 (20.0-30.0)
		p=1.000	p=0.003*
(Cytoplasmic)	55.0 (50.0-61.3)	60.0 (59.0-65.0)	97.5 (77.5-101.3)
		p=0.177	p=0.004*
Total	65.0	70.0	123.0

Figure 3.114 MCF-7X versus X(FAS) cell total IGF-1R expression by immunocytochemistry. MCF-7X and X(FAS) cells were grown on coverslips in phenol-red-free RPMI media containing 5% XFCS with the appropriate absence or presence of faslodex (10^{-7} M). Conditions were maintained for 7 days prior to phenol formal saline fixation. The total IGF-1R (antibody dilution 1:125) digital images shown above (X20 magnification) are representative of 2 experiments. H-Score data were obtained by dual assessment of 3 representative areas of each coverslip followed by statistical analysis (Mann-Whitney U-Test). The median H-Score and Q1-Q3 values are displayed. A p-value <0.05(*) indicates a significant difference in total IGF-1R expression versus MCF-7X basal control

3.5.2 LY294002 Resistance in the MCF-7X Model

This project has shown that PI3K inhibitor LY294002 decreased AKT and PDK-1 activity, and by day 15 inhibited MCF-7X growth by nearly 70%. In contrast to the pure anti-oestrogen faslodex, the agent substantially decreased Ser167ER phosphorylation leaving Ser118ER activity unchanged. LY294002 subsequently partially reduced ERα transcriptional activity both with regards to ERE reporter activity and endogenous pS2 expression. However like faslodex the treatment only delayed (10 weeks, Figure 3.78) the progression of cell growth, in parallel with the incomplete blockade of ERα phosphorylation and transcriptional activity. There was subsequent emergence of an LY294002 resistant MCF-7X sub-line [X(LY)] and preliminary investigation (passages 13-15) was performed to better understand the mechanism underlying the development of resistance.

The visual morphology of the X(LY) cells by phase contrast imaging and Haematoxylin & Eosin staining revealed these cells were a homogeneous population mostly round in shape (Figure 3.115A/B). Similar to X(FAS) cells the nuclear to cytoplasmic ratio was equal; there were prominent nucleoli in the nuclei however in this case the nuclei were large and ovoid. Again these morphological features became evident during the initial treatment of MCF-7X cells with the agent and were retained as the X(LY) resistant phenotype emerged. Motility and invasion studies showed that these LY294002 resistant cells did not show increased aggressive behaviour versus the parental MCF-7X cell line, and indeed motility was somewhat reduced (Figure 3.116A/B).

Resistance to LY294002 was not associated with any change in total ERα ($p=0.279$, Figure 3.117) or phosphorylated Ser118ER ($p=0.596$, Figure 3.118) versus basal control consistent with the high levels maintained during the responsive phase. Phosphorylation at Ser167ER, however was recovered to a level comparable to MCF-7X cell control ($p=0.790$) and significantly elevated (150%, $p=0.021$*) versus the decreased levels observed in the LY294002 responsive phase (Figure 3.118). Parallel evaluation of the oestrogen regulated gene pS2 revealed that levels were also increased significantly versus the LY294002 responsive phase of MCF-7X cells (80.0%, $p<0.001$*), resulting in a 21.2% ($p=0.001$*) increase versus basal control (Figure 3.119).

During LY294002 treatment phosphorylated MAPK was unchanged versus the basal control; however, once resistance was established cytoplasmic MAPK activity was significantly increased 107.0% (p=0.016*, Figure 3.120) versus basal MCF-7X cells and (p=0.002*) versus the LY294002 responsive phase. Phosphorylated AKT was also investigated and while LY294002 treatment could inhibit a significant portion of AKT activity in MCF-7X cells, immunocytochemistry revealed X(LY) cell membrane plus cytoplasmic localised AKT activity was significantly recovered (p=0.004*) to a level equal to that of the untreated MCF-7X parental line (Figure 3.121), as was nuclear staining (37.0%, p=0.003*). Thus, increases in these kinases are also apparent where there are obvious increases in Ser167ER phosphorylation and ERα transcriptional activity recovery in the X(LY) resistant cells (alongside the maintained levels of Ser118ER activity).

Parallel studies monitoring growth factor receptors in the X(LY) resistant model revealed no change in EGFR cytoplasmic expression. However, there was a modest 35.7% (p=0.006*) increase in membrane EGFR versus MCF-7X cells by immunocytochemistry (Figure 3.122). Furthermore, X(LY) cell EGFR membrane expression was increased 137.5% (p=0.004*) versus MCF-7X cells treated with LY294002. Total HER2 expression followed a similar pattern of modest increases on development of LY294002 resistance (Figure 3.123). Thus, the X(LY) sub-line revealed a 26.7% (p=0.004*) increase in membrane staining with a more substantial 70.0% (p=0.001*) increase in cytoplasmic HER2 expression versus the basal MCF-7X control. Membrane and cytoplasmic HER2 expression again increased significantly 56.1% (p=0.004*) and 29.4% (p=0.003*) from LY294002 treated cells to the resistant phenotype. Immunocytochemistry revealed membrane IGF-1R expression in the LY294002 resistant cells was equivalent to the low level of basal MCF-7X cell expression (Figure 3.124), although there were modest increases in cytoplasmic staining (22.0%, p=0.013*). It is thus feasible that the Ser167ER activity and recovered ERα transcriptional activity may be driven by phosphorylated MAPK and AKT downstream of modestly increased growth factor receptor signalling. Together with the maintained Ser118ER activity, this may promote growth of X(LY) cells (but appears insufficient to promote invasive behaviour).

In this instance, however, neither EGFR nor HER2 were increased substantially during early LY294002 treatment of MCF-7X cells (Figures 3.122 & 3.123; only

20.0% increase for cytoplasmic HER2, p=0.003*), and indeed EGFR and HER2 membrane localisation were reduced by such treatment (42.9%, p=0.003* and 44.4%, p=0.001* respectively). As such, these particular receptors may not be major contributors to the remaining ERα activity (predominately pSer118ER) and associated cell survival during the phase of partial LY294002 response. Early LY294002 treatment also did not effect membrane localisation of IGF-1R although cytoplasmic expression was increased 45.5% (p=0.009*) versus untreated MCF-7X cells (Figure 3.124).

A.

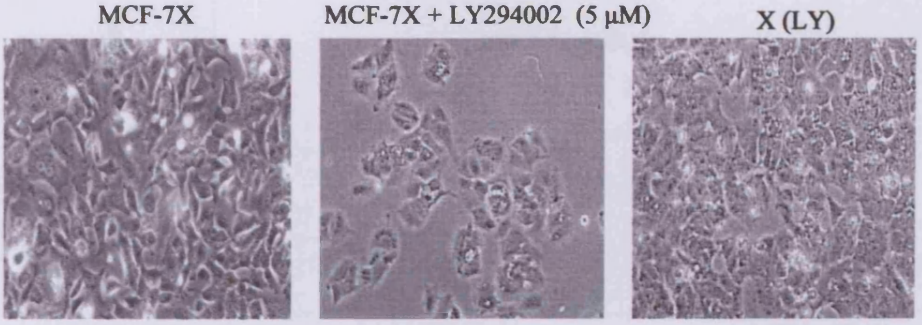

B.

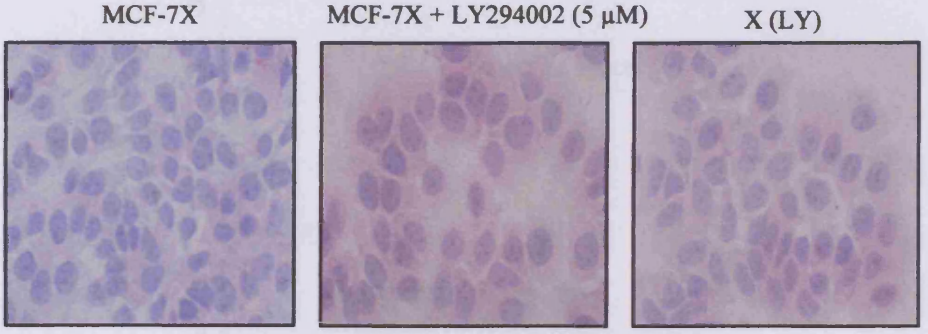

Figure 3.115 The visual morphology of MCF-7X versus X(LY) phenotype by phase contrast (A) and H&E staining (B). MCF-7X and X(LY) resistant cells were grown in phenol-red-free RPMI media containing 5% XFCS in the appropriate absence or presence of LY294002 (5 µM). (A) Cell phase contrast digital images were obtained during log phase growth (X20 magnification). (B) MCF-7X and X(LY) cells were grown under the same conditions as previously described for 7 days on coverslips prior to ERICA fixation. The cells were H&E stained with 10% Ehrlich Haematoxylin (10 min) followed by 1% Eosin (2½ hrs). The H&E digital images shown above are X40 magnification.

A.

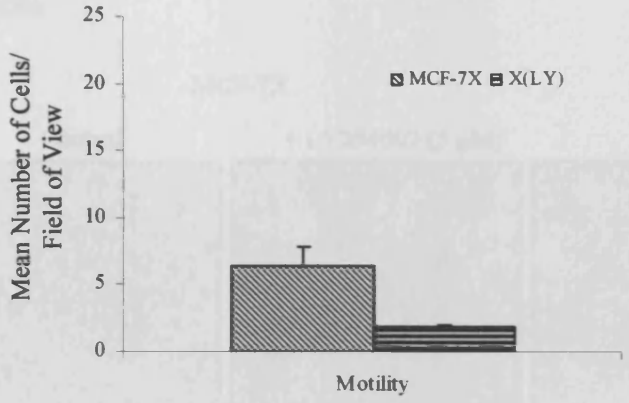

B.

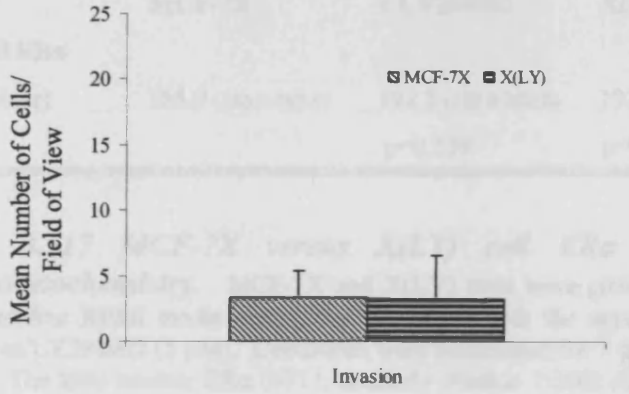

Figure 3.116 MCF-7X and X(LY) cell motility (A) and invasive capacity (B). (A) MCF-7X and X(LY) cells were seeded onto fibronectin coated Transwell® permeable supports for 24 hours prior to formaldehyde fixation and crystal violet staining. (B) MCF-7X and X(LY) cells were seeded onto matrigel coated Transwell® permeable supports for 72 hours prior to formaldehyde fixation and mounting to glass slides with mounting medium containing DAPI. These data above represent the mean number if cells/field of view +/- SD of triplicate inserts.

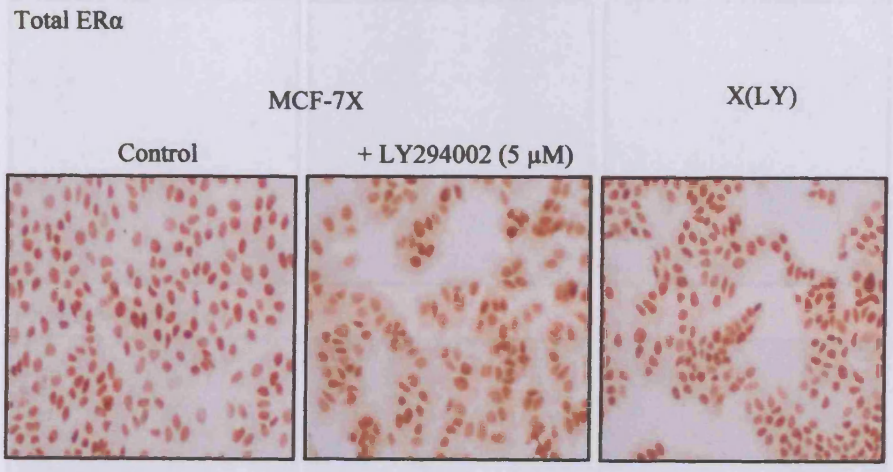

	MCF-7X	+ LY294002	X(LY)
Total ERα			
(Nuclear)	185.0 (185.0-195.0)	192.5 (183.8-200.0)	192.5 (185.0-202.5)
		p=0.539	p=0.279

Figure 3.117 MCF-7X versus X(LY) cell ERα expression by immunocytochemistry. MCF-7X and X(LY) cells were grown on coverslips in phenol-red-free RPMI media containing 5% XFCS with the appropriate absence or presence of LY294002 (5 μM). Conditions were maintained for 7 days prior to ERICA fixation. The total nuclear ERα (6F11, antibody dilution 1:100) digital images shown above (X10 original magnification) are representative of 3 experiments. H-Score data were obtained by dual assessment of 2 representative areas of each coverslip followed by statistical analysis (Mann-Whitney U-Test). The median H-Score and Q1-Q3 values are displayed.

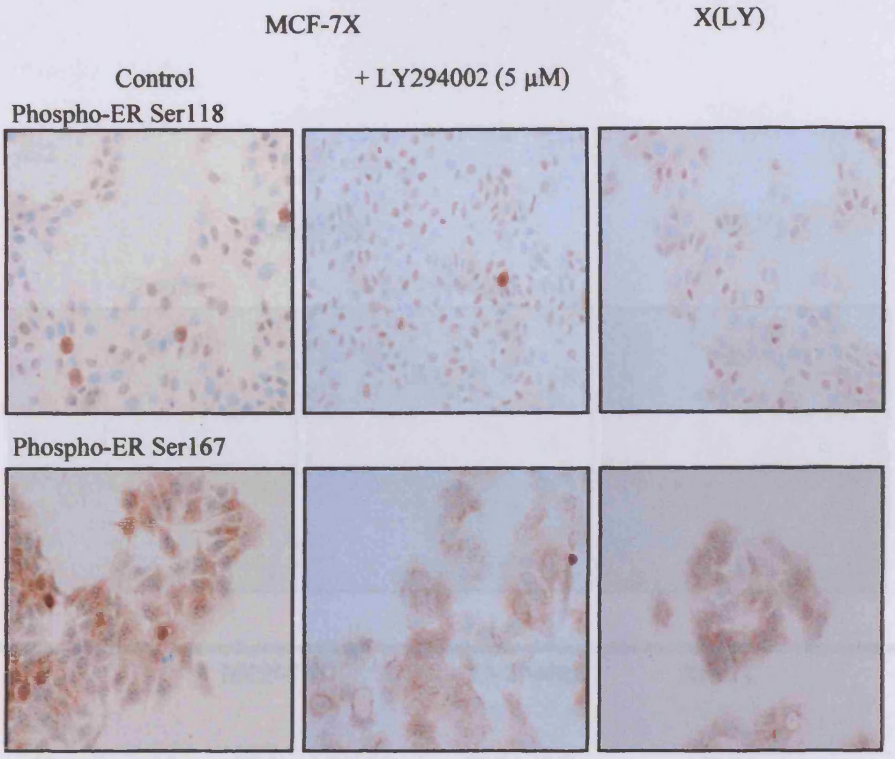

	MCF-7X	+ LY294002	X(LY)
Phospho-ER Ser118			
(Nuclear)	90.0 (77.5-110.5)	105.0 (93.8-112.5)	95.0 (90.0-106.3)
		p=0.186	p=0.596
Phospho-ER Ser167			
(Nuclear)	50.0 (45.0-70.0)	25.0 (20.0-25.0)	62.5 (42.5-71.3)
		p<0.001*	p=0.790

Figure 3.118 MCF-7X versus X(LY) cell phosphorylation of ERα on Ser118 and Ser167 residues by immunocytochemistry. MCF-7X and X(LY) cells were grown on coverslips in phenol-red-free RPMI media containing 5% XFCS with the appropriate absence or presence of LY294002 (5 μM). Conditions were maintained for 7 days prior to the appropriate fixation. The phospho-ER Ser118 (antibody dilution 1:400) assay required coverslips paraformaldehyde fixed. The phospho-ER Ser167 (antibody dilution 1:25) assay required coverslips ERICA fixed. The digital images shown above (X20 magnification) are representative of 4 experiments. H-Score data were obtained by dual assessment of 2 representative areas of each coverslip followed by statistical analysis (Mann-Whitney U-Test). The median H-Score and Q1-Q3 values are displayed. A p-value <0.05(*) indicates a significant difference in phospho-ER Ser167 versus MCF-7X basal control.

pS2

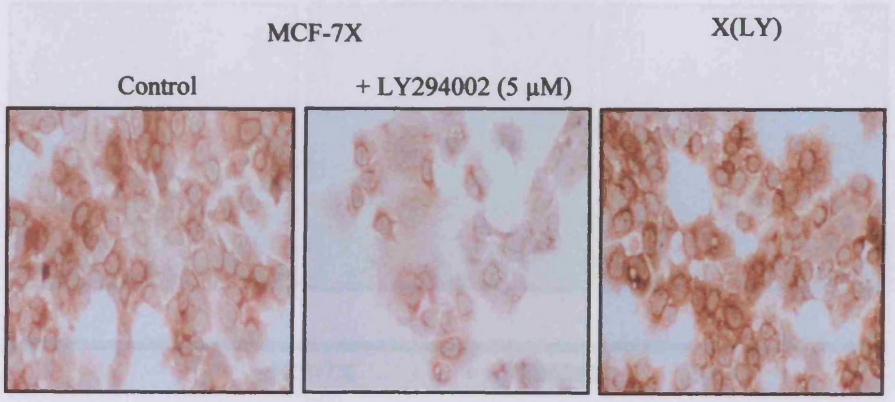

	MCF-7X	+ LY294002	X(LY)
pS2			
(Cytoplasmic)	130.0 (121.3-133.8)	87.5 (78.8-92.8)	157.5 (146.3-160.0)
		p=0.002*	p=0.002*

Figure 3.119 MCF-7X versus X(LY) cell pS2 expression by immunocytochemistry. MCF-7X and X(LY) cells were grown on coverslips in phenol-red-free RPMI media containing 5% XFCS with the appropriate absence of presence of LY294002 (5 μM). Conditions were maintained for 7 days prior to ERICA fixation. The pS2 (antibody dilution 1:500) digital images shown above (X20 magnification) are representative of 3 experiments. H-Score data were obtained by dual assessment of 2 representative areas of each coverslip followed by statistical analysis (Mann-Whitney U-Test). The median H-Score and Q1-Q3 values are displayed. A p-value <0.05(*) indicates a significant difference in pS2 expression versus MCF-7X basal control.

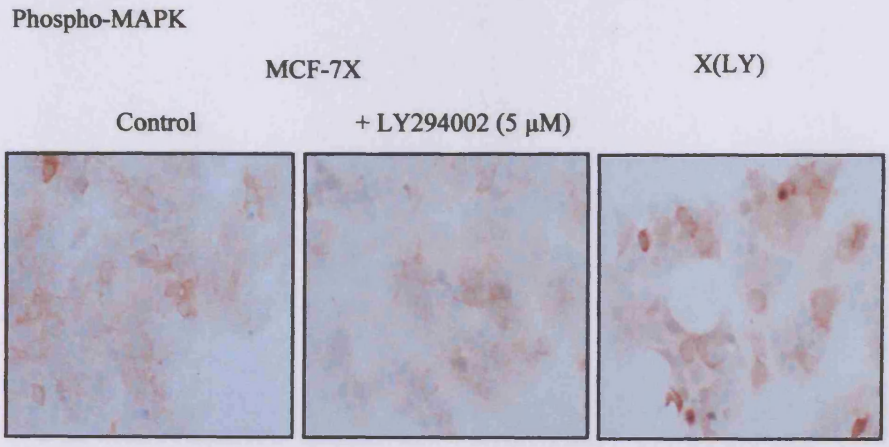

	MCF-7X	+ LY294002	X(LY)
Phospho-MAPK			
(Cytoplasmic)	35.0 (35.0-48.8)	35.0 (21.3-38.8)	72.5 (50.0-107.5)
		p=0.187	p=0.016*
(Nuclear)	3.5 (1.3-5.0)	2.0 (1.3-2.8)	5.0 (2.0-5.0)
		p=0.275	p=0.777
Total	38.5	37.0	77.5

Figure 3.120 MCF-7X versus X(LY) cell phosphorylated MAPK level by immunocytochemistry. MCF-7X and X(LY) cells were grown on coverslips in phenol-red-free RPMI media containing 5% XFCS with the appropriate absence or presence of LY294002 (5 μM). Conditions were maintained for 7 days prior to formal saline fixation. The phospho-MAPK (antibody dilution 1:20) digital images shown above (X20 magnification) are representative of 4 experiments. H-Score data were obtained by dual assessment of 2 representative areas of each coverslip followed by statistical analysis (Mann-Whitney U-Test). The median H-Score and Q1-Q3 values are displayed. A p-value <0.05(*) indicates a significant difference in phospho-MAPK level versus MCF-7X basal control.

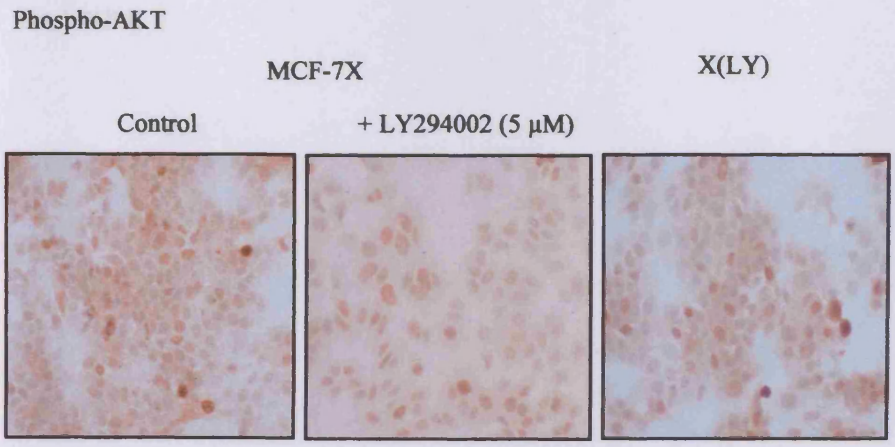

	MCF-7X	+ LY294002	X(LY)
Phospho-AKT			
(Memb. + Cyto.)	101.5 (76.5-119.3)	34.5 (32.0-57.0)	107.0 (99.0-113.0)
		p=0.004*	p=0.520
(Nuclear)	107.5 (95.0-112.5)	73.0 (61.0-81.3)	100.0 (98.8-101.3)
		p=0.004*	p=0.284
Total	209.0	107.5	207.0

Figure 3.121 MCF-7X versus X(LY) cell phosphorylated AKT level by immunocytochemistry. MCF-7X and X(LY) cells were grown on coverslips in phenol-red-free RPMI media containing 5% XFCS with the appropriate absence or presence of LY294002 (5 µM). Conditions were maintained for 7 days prior to ERICA fixation. The phospho-AKT (antibody dilution 1:200) digital images shown above (X20 magnification) are representative of 3 experiments. H-Score data were obtained by dual assessment of 2 representative areas of each coverslip followed by statistical analysis (Mann-Whitney U-Test). The median H-Score and Q1-Q3 values are displayed. A p-value <0.05(*) indicates a significant difference in phospho-AKT level versus MCF-7X basal control.

Total EGFR

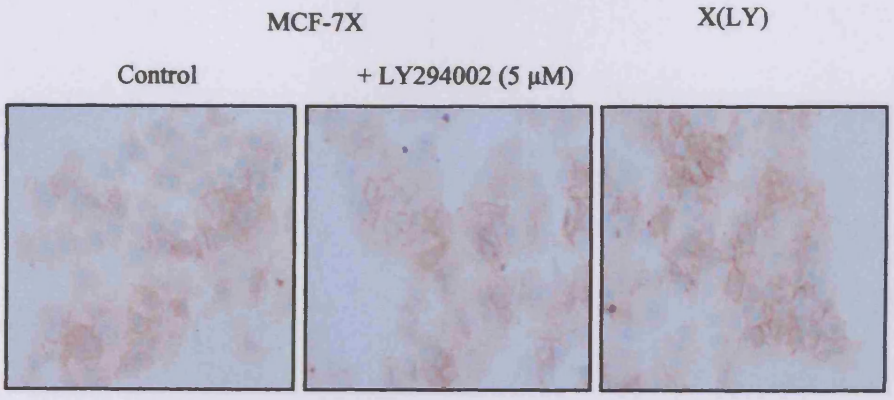

	MCF-7X	+ LY294002	X(LY)
Total EGFR			
(Membrane)	35.0 (30.0-40.0)	20.0 (18.8-25.0)	47.5 (43.8-55.0)
		p=0.003*	p=0.006*
(Cytoplasmic)	30.0 (28.0-35.0)	30.0 (28.8-34.3)	32.5 (28.8-40.0)
		p=0.933	p=0.365
Total	65.0	50.0	80.0

Figure 3.122 MCF-7X versus X(LY) cell total EGFR expression by immunocytochemistry. MCF-7X and X(LY) cells were grown on coverslips in phenol-red-free RPMI media containing 5% XFCS with the appropriate absence or presence of LY29002 (5 μM). Conditions were maintained for 7 days prior to phenol formal saline fixation. The total EGFR (antibody dilution 1:100) digital images shown above (X20 magnification) are representative of 2 experiments. H-Score data were obtained by dual assessment of 3 representative areas of each coverslip followed by statistical analysis (Mann-Whitney U-Test). The median H-Score and Q1-Q3 values are displayed. A p-value <0.05(*) indicates a significant difference in total EGFR expression versus MCF-7X basal control.

Total HER2

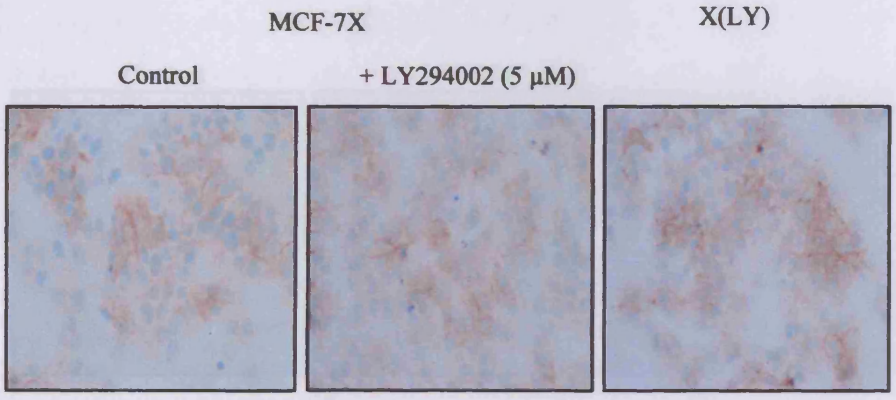

	MCF-7X	+ LY294002	X(LY)
Total HER2			
(Membrane)	67.5 (51.3-78.8)	37.5 (35.0-41.3)	85.5 (82.5-91.3)
		p=0.001*	p=0.004*
(Cytoplasmic)	25.0 (20.0-30.0)	30.0 (28.8-36.0)	42.5 (40.0-51.3)
		p=0.033*	p=0.001*
Total	92.5.0	67.5	128.0

Figure 3.123 MCF-7X versus X(LY) cell total HER2 expression by immunocytochemistry. MCF-7X and X(LY) cells were grown on coverslips in phenol-red-free RPMI media containing 5% XFCS with the appropriate absence or presence of LY29002 (5 μM). Conditions were maintained for 7 days prior to ERICA fixation. The total HER2 (antibody dilution 1:100) digital images shown above (X20 magnification) are representative of 2 experiments. H-Score data were obtained by dual assessment of 3 representative areas of each coverslip followed by statistical analysis (Mann-Whitney U-Test). The median H-Score and Q1-Q3 values are displayed. A p-value <0.05(*) indicates a significant difference in total HER2 expression versus MCF-7X basal control.

Total IGF-1R

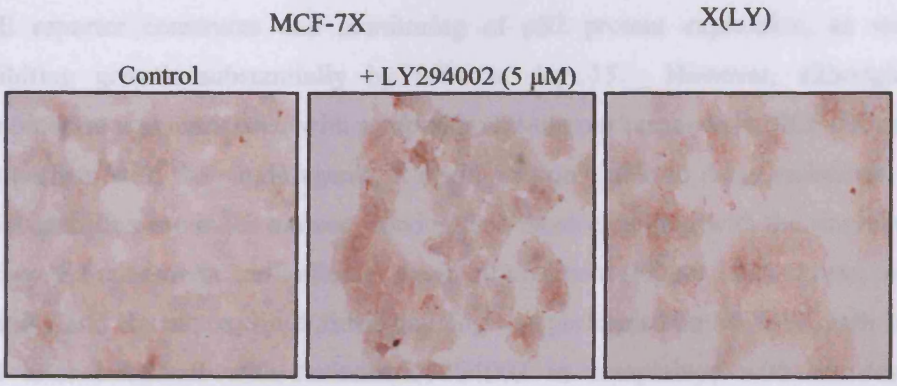

	MCF-7X	+ LY294002	X(LY)
Total IGF-1R			
(Membrane)	10.0 (10.0-12..8)	12.5 (10.0-15.0)	10.0 (10.0-14.3)
		p=0.411	p=0.924
(Cytoplasmic)	55.0 (50.0-61.3)	80.0 (71.3-86.3)	67.5 (63.8-70.0)
		p=0.009*	p=0.013*
Total	65.0	92.5	77.5

Figure 3.124 MCF-7X versus X(LY) cell total IGF-1R expression by immunocytochemistry. MCF-7X and X(LY) cells were grown on coverslips in phenol-red-free RPMI media containing 5% XFCS with the appropriate absence or presence of LY29002 (5 μM). Conditions were maintained for 7 days prior to phenol formal saline fixation. The total IGF-1R (antibody dilution 1:125) digital images shown above (X20 magnification) are representative of 2 experiments. H-Score data were obtained by dual assessment of 3 representative areas of each coverslip followed by statistical analysis (Mann-Whitney U-Test). The median H-Score and Q1-Q3 values are displayed. A p-value <0.05(*) indicates a significant difference in total IGFR expression versus MCF-7X basal control.

3.5.3 Faslodex/LY294002 Resistance in the MCF-7X Model

Co-treatment of MCF-7X cells with faslodex plus LY294002 was able to significantly decrease ERα expression, ERα phosphorylation at both Ser118 and Ser167 residues, promote some further decrease ERα transcriptional activity using ERE reporter constructs and monitoring of pS2 protein expression, as well as inhibiting growth substantially by 90% at day 15. However, although this combination was associated with a superior anti-tumour response in MCF-7X cells in comparison with the single agents, it again was only able to delay resistance. The resistant cells were much slower growing than those emerging with the single agents as they did not emerge until after 25 weeks of treatment (Figure 3.88). Phase contrast imaging and Haematoxylin & Eosin staining was performed on MCF-7X cells before and after treatment with faslodex/LY294002 in comparison with the resistant X(FAS/LY) sub-line to investigate the alteration in morphological features (Figure 3.125A/B). The X(FAS/LY) cells were a heterogeneous cell population with more frequent apoptotic bodies, and nuclear appearance and nuclear/cytoplasmic ratio was approximately 1 : 1. The colony appearance of the faslodex/LY294002 resistant cells, X(FAS/LY), was very irregular and these cells appeared to be more loosely-adherent to each other than the X(FAS) or X(LY) cells. The cells resembled the X(FAS) cells to some degree in that they were elongated in shape with some pseudopodia, characteristics that developed during the treatment phase and persisted in resistance. Despite these morphological changes however, there was little change in motility versus MCF-7X cells, and invasion was only slightly increased (Figure 3.126A/B).

Faslodex/LY294002 co-treatment significantly reduced ERα expression and ERα phosphorylation versus the MCF-7X cell basal control. The resistant X(FAS/LY) cells also had a reduction in ERα expression (47.3%, p=0.001*) compared to the MCF-7X cells, although this level was slightly elevated versus the responsive phase (30.0%, p=0.013*, Figure 3.127). In parallel, there was a significant recovery of activity at both Ser118 and Ser167 ER sites (Figure 3.128). Thus, X(FAS/LY) Ser118ER activity was increased 147.6% (p=0.004*) and Ser167ER activity increased 325.0% (p=0.003*) compared to the short-term combination treatment, furthermore equating to a significant 44.4% (p=0.004*) and 70.0% (p=0.013*) increase respectively versus MCF-7X cell control. Moreover, while co-treatment resulted in a marked inhibitory effect on ERα transcriptional activity as measured by

monitoring the oestrogen regulated protein pS2, the X(FAS/LY) cells recovered this expression by 120.0% (p=0.001*) versus short-term treatment to a level only 15.4% lower (p=0.017*) than in the MCF-7X cells pre-treatment (Figure 3.129).

In parallel with these gains in ERα phosphorylation and transcriptional activity, MAPK cytoplasmic activity was significantly increased by 100.0% (p=0.002*) in the X(FAS/LY) cells versus the untreated MCF-7X cells and versus response to FAS/LY co-treatment (p=0.001*, Figure 3.130). For MAPK activity, changes observed on resistance to FAS/LY co-treatment thus equated with the patterns noted on development of resistance to each single agent. With regards to AKT activity that was inhibited during the responsive phase with faslodex/LY294002, membrane plus cytoplasmic levels were significantly increased versus response (278.4%, p=0.004*) and restored to the MCF-7X pre-treatment level, while nuclear activity was increased by 68.8% versus treatment (p=0.004*) and further increased by 25.6% (p=0.005*,) once the resistant phenotype emerged (Figure 3.131). This pattern mirrored the increases in kinase activity observed on development of resistance versus the responsive phase with faslodex or LY294022 as single agents. Such increases in kinase activity may promote the recovery of ERα phosphorylation and ERα transcriptional activity in X(FAS/LY) cells.

Investigation of growth factor receptor expression in the X(FAS/LY) cells revealed (as in resistance to faslodex as a single agent) significant increases in EGFR (Figure 3.132), with membrane expression increased by 242.9% (p=0.003*) and cytoplasmic localised expression increased by 125.0% (p=0.004*) versus the parental MCF-7X cells. Total IGF-1R membrane and cytoplasmic levels were also increased substantially by 250.0% (p=0.003*) and 81.8% (p=0.003*) respectively in the X(FAS/LY) cells versus MCF-7X cells (Figure 3.133) where increases had also been noted in faslodex resistance. In the case of membrane staining, there was also a significant increase in the X(FAS/LY) resistant cells versus the FAS/LY responsive phase (p=0.003*). These substantial increases in EGFR and IGF-1R may lie upstream of kinase and ERα activity on both Ser118 and Ser167 in the X(FAS/LY) cells, and may contribute to resistant growth. However in contrast to resistance to faslodex alone (and as noted in resistance to LY294002), there were only small increases in HER2 expression (18.0%, p=0.015*, membrane and 20.0%, p=0.042*, cytoplasmic; Figure 3.134). This lack of substantial increase HER2, together with the

recovery of both serine 118 and 167 activity, may in some way preclude substantially increased aggressive invasive behaviour in the X(FAS/LY) cells.

In contrast to treatment with faslodex as a single agent, there was no change in membrane EGFR staining during faslodex/LY294002 treatment of MCF-7X cells, although a 66.7% ($p=0.003^*$) increase in cytoplasmic expression was noted versus basal MCF-7X control (Figure 3.132). There was some increase in HER2 membrane and particularly cytoplasmic staining during the responsive phase with this co-treatment (25.9%, $p=0.034^*$ and 60.0%, $p=0.002^*$; Figure 3.134), with increases in cytoplasmic staining only for IGF-1R observed (118.2%, $p=0.003^*$; Figure 3.133). While the relevance of cytoplasmic staining for such receptors remains unknown, they may in some way contribute to residual kinase/ERα activity and cell survival during the responsive phase with co-treatment.

A.

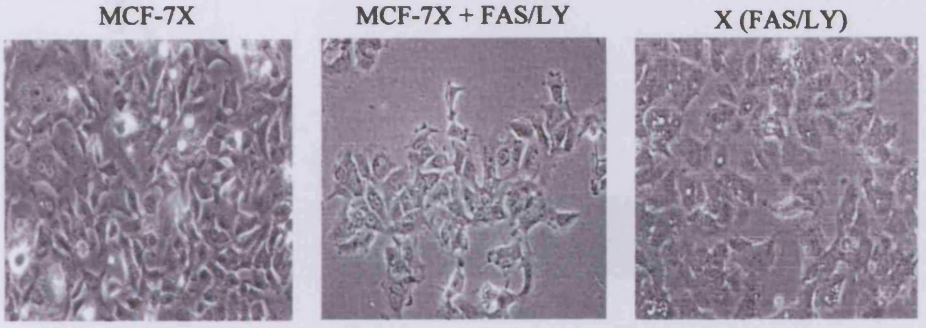

B.

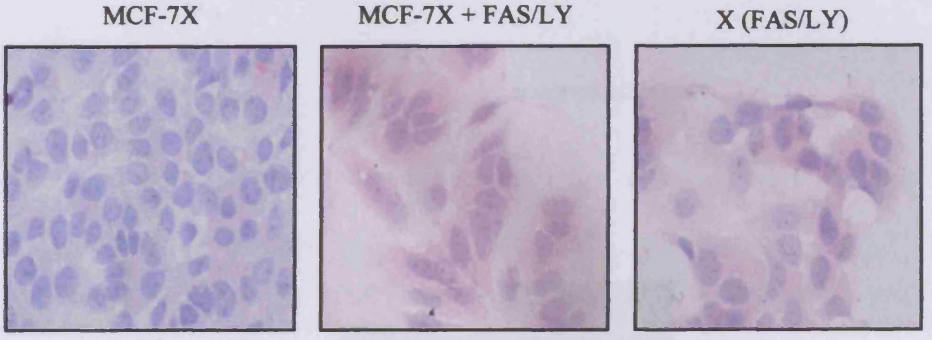

Figure 3.125 The visual morphology of MCF-7X versus X(FAS/LY) phenotype by phase contrast (A) and H&E staining (B). MCF-7X and the X(FAS/LY) resistant cells were grown in phenol-red-free RPMI media containing 5% XFCS in the appropriate absence or presence of faslodex/LY294002 (10^{-7} M, 5 μM). (A) Cell phase contrast digital images were obtained during log phase growth (X20 original magnification). (B) MCF-7X and X(FAS/LY) cells were grown under the same conditions as previously described for 7 days on coverslips prior to ERICA fixation. The cells were H&E stained with 10% Ehrlich Haematoxylin (10 min) followed by 1% Eosin (2½ hrs). The digital images shown above are X40 magnification.

A.

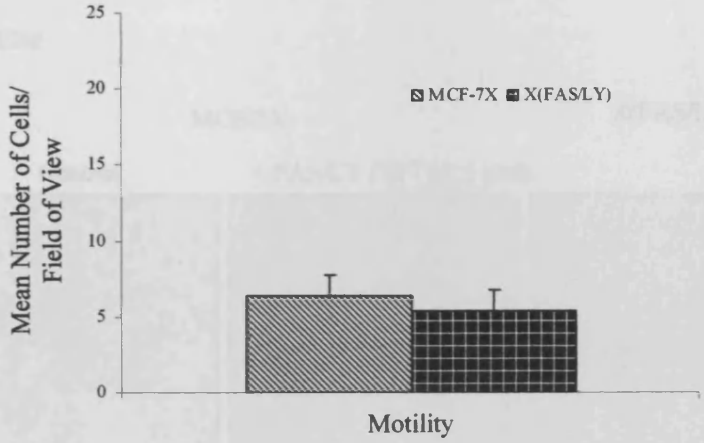

B.

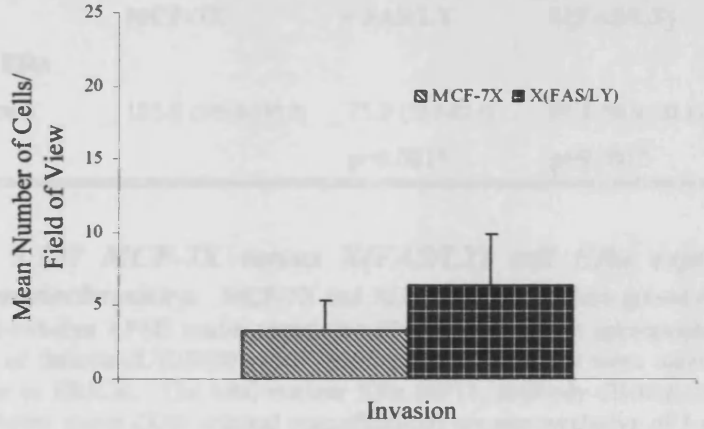

Figure 3.126 MCF-7X and X(FAS/LY) cell motility (A) and invasive capacity (B). (A) MCF-7X and X(FAS/LY) cells were seeded onto fibronectin coated Transwell® permeable supports for 24 hours prior to formaldehyde fixation and crystal violet staining. (B) MCF-7X and X(FAS/LY) cells were seeded onto matrigel coated Transwell® permeable supports for 72 hours prior to formaldehyde fixation and mounting to glass slides with mounting medium containing DAPI. These data above represent the mean number if cells/field of view +/- SD of triplicate inserts.

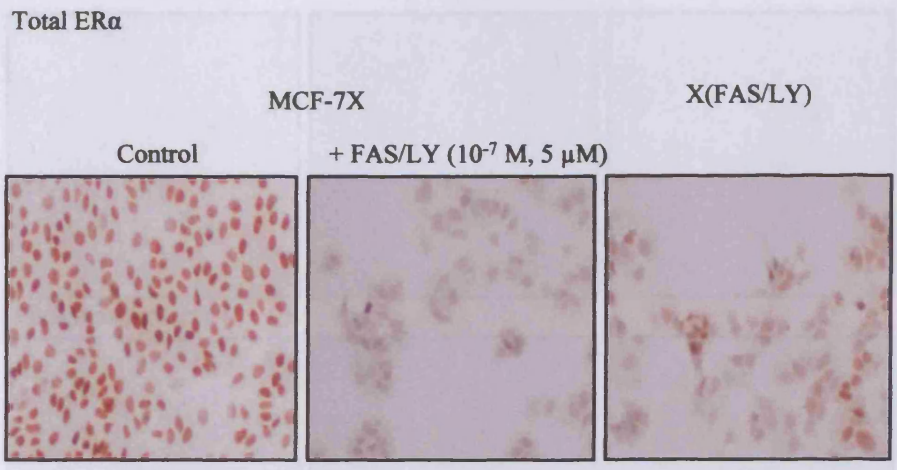

	MCF-7X	+ FAS/LY	X(FAS/LY)
Total ERα			
(Nuclear)	185.0 (185.0-195.0)	75.0 (70.3-87.5)	97.5 (90.0-112.5)
		p=0.001*	p=0.001*

Figure 3.127 MCF-7X versus X(FAS/LY) cell ERα expression by immunocytochemistry. MCF-7X and X(FAS/LY) cells were grown on coverslips in phenol-red-free RPMI media containing 5% XFCS with the appropriate absence or presence of faslodex/LY294002 (10^{-7} M, 5 μM). Conditions were maintained for 7 days prior to ERICA. The total nuclear ERα (6F11, antibody dilution 1:100) digital images shown above (X10 original magnification) are representative of 3 experiments. H-Score data were obtained by dual assessment of 2 representative areas of each coverslip followed by statistical analysis (Mann-Whitney U-Test). The median H-Score and Q1-Q3 values are displayed. A p-value <0.05(*) indicates a significant difference in ERα expression versus MCF-7X basal control.

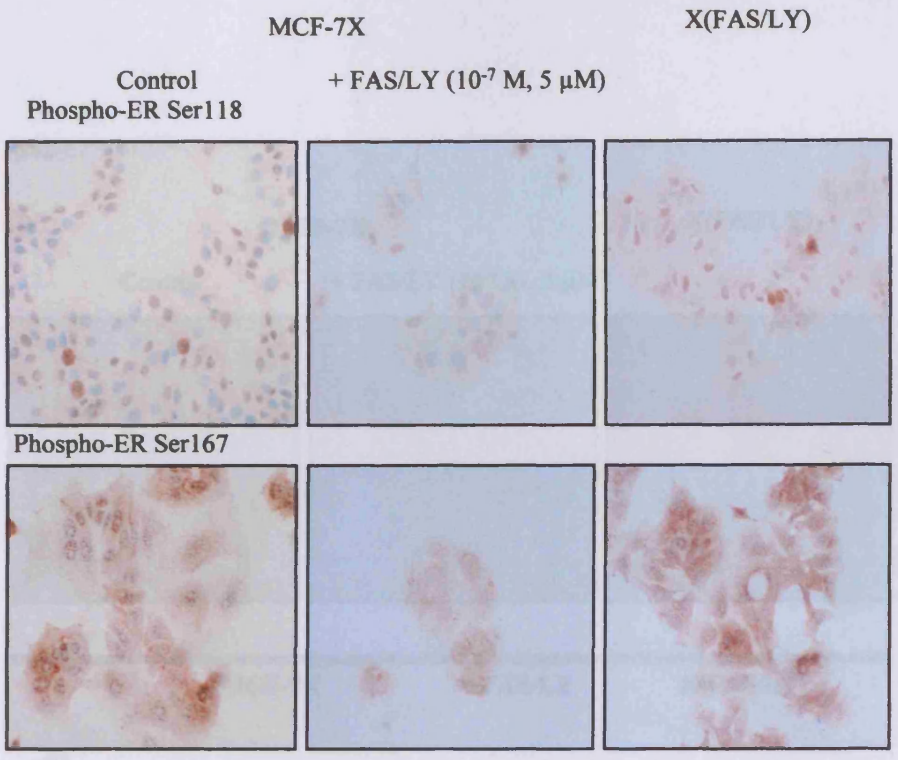

	MCF-7X	+ FAS/LY	X(FAS/LY)
Phospho-ER Ser118			
(Nuclear)	90.0 (77.5-110.5)	52.5 (43.8-60.0)	130.0 (111.3-150.0)
		p=0.001*	p=0.004*
Phospho-ER Ser167			
(Nuclear)	50.0 (45.0-70.0)	20.0 (12.0-30.0)	85.0 (77.5-92.5)
		p<0.001*	p=0.013*

Figure 3.128 MCF-7X versus X(FAS/LY) cell phosphorylation of ERα on Ser118 and Ser167 residues by immunocytochemistry. MCF-7X and X(FAS/LY) cells were grown on coverslips in phenol-red-free RPMI media containing 5% XFCS with the appropriate absence or presence of faslodex/LY294002 (10^{-7} M, 5 μM). Conditions were maintained for 7 days prior to the appropriate fixation. The phospho-ER Ser118 (antibody dilution 1:400) assay required coverslips paraformaldehyde fixed. The phospho-ER Ser167 (antibody dilution 1:25) assay required ERICA fixed coverslips. The digital images shown above (X20 magnification) are representative of 4 experiments. H-Score data were obtained by dual assessment of 2 representative areas of each coverslip followed by statistical analysis (Mann-Whitney U-Test). The median H-Score and Q1-Q3 values are displayed. A p-value <0.05(*) indicates a significant difference in phospho-ER Ser118 or Ser167 level versus MCF-7X basal control.

pS2

MCF-7X X(FAS/LY)

Control + FAS/LY (10^{-7} M, 5 μM)

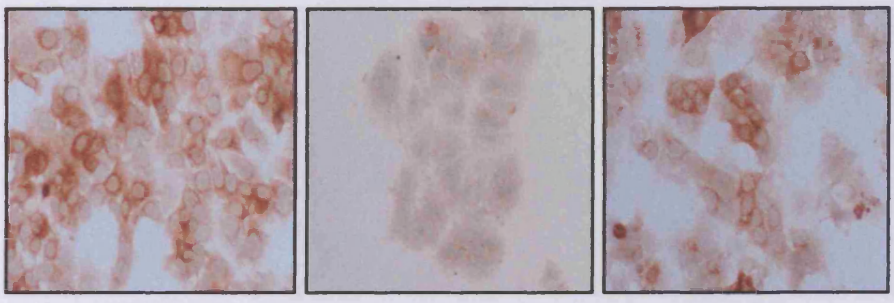

	MCF-7X	+ FAS/LY	X(FAS/LY)
pS2			
(Cytoplasmic)	130.0 (121.3-133.8)	50.0 (45.0-70.0)	110.0 (101.3-123.8)
		p=0.001*	p=0.017*

Figure 3.129 MCF-7X versus X(FAS/LY) cell pS2 expression by immunocytochemistry. MCF-7X and X(FAS/LY) cells were grown on coverslips in phenol-red-free RPMI media containing 5% XFCS with the appropriate absence of presence of faslodex/LY294002 (10^{-7} M, 5 μM). Conditions were maintained for 7 days prior to ERICA fixation. The pS2 (antibody dilution 1:500) digital images shown above (X20 magnification) are representative of 3 experiments. H-Score data were obtained by dual assessment of 2 representative areas of each coverslip followed by statistical analysis (Mann-Whitney U-Test). The median H-Score and Q1-Q3 values are displayed. A p-value <0.05(*) indicates a significant difference in pS2 expression versus MCF-7X basal control.

Phospho-MAPK

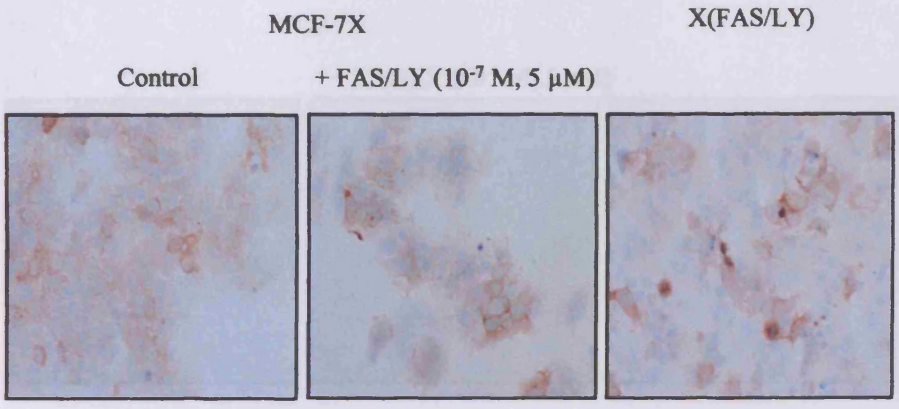

	MCF-7X	+ FAS/LY	X(FAS/LY)
Phospho-MAPK			
(Cytoplasmic)	35.0 (35.0-48.8)	35.0 (30.0-35.0)	70.0 (55.0-100.0)
		p=0.093	p=0.002*
(Nuclear)	3.5 (1.3-5.0)	1.5 (1.0-2.0)	3.5 (1.3-5.0)
		p=0.075	p=0.824
Total	38.5	36.5	73.5

Figure 3.130 MCF-7X versus X(FAS/LY) cell phosphorylated MAPK level by immunocytochemistry. MCF-7X and X(FAS/LY) cells were grown on coverslips in phenol-red-free RPMI media containing 5% XFCS with the appropriate absence or presence of faslodex/LY294002 (10^{-7} M, 5 μM). Conditions were maintained for 7 days prior to formal saline fixation. The phospho-MAPK (antibody dilution 1:20) digital images shown above (X20 magnification) are representative of 4 experiments. H-Score data were obtained by dual assessment of 2 representative areas of each coverslip followed by statistical analysis (Mann-Whitney U-Test). The median H-Score and Q1-Q3 values are displayed. A p-value <0.05(*) indicates a significant difference in phospho-MAPK level versus MCF-7X basal control.

Phospho-AKT

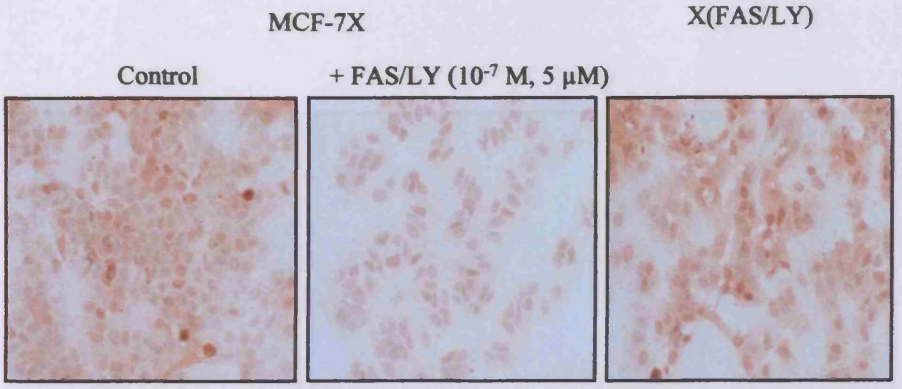

	MCF-7X	+ FAS/LY	X(FAS/LY)
Phospho-AKT			
(Memb. + Cyto.)	101.5 (76.5-119.3)	25.5 (21.8-29.0)	96.5 (93.8-101.0)
		p=0.004*	p=0.575
(Nuclear)	107.5 (95.0-112.5)	80.0 (73.8-93.8)	135.0 (123.8-141.3)
		p=0.012*	p=0.005*
Total	209.0	105.5	231.5

Figure 3.131 MCF-7X versus X(FAS/LY) cell phosphorylated AKT level by immunocytochemistry. MCF-7X and X(FAS/LY) cells were grown on coverslips in phenol-red-free RPMI media containing 5% XFCS with the appropriate absence or presence of faslodex/LY294002 (10^{-7} M, 5 μM). Conditions were maintained for 7 days prior to ERICA fixation. The phospho-AKT (antibody dilution 1:200) digital images shown above (X20 magnification) are representative of 3 experiments. H-Score data were obtained by dual assessment of 2 representative areas of each coverslip followed by statistical analysis (Mann-Whitney U-Test). The median H-Score and Q1-Q3 values are displayed. A p-value <0.05(*) indicates a significant difference in phospho-AKT level versus MCF-7X basal control.

Total EGFR

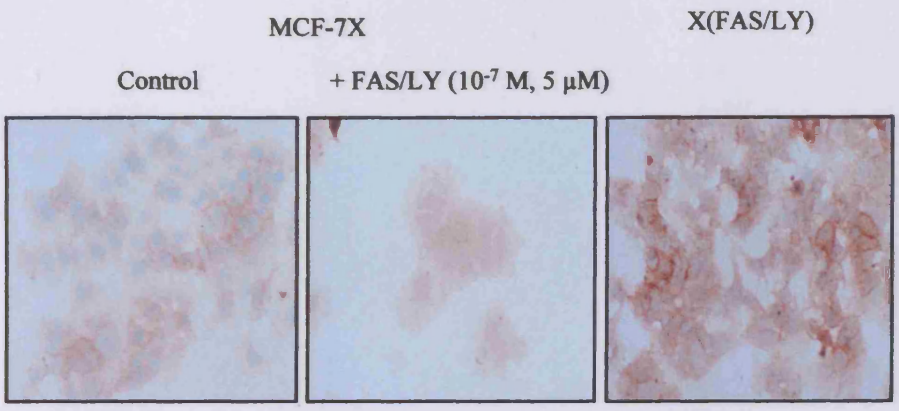

	MCF-7X	+ FAS/LY	X(FAS/LY)
Total EGFR			
(Membrane)	35.0 (30.0-40.0)	35.0 (33.8-37.0)	120.0 (108.8-120.0)
		p=0.866	p=0.003*
(Cytoplasmic)	30.0 (28.0-35.0)	50.0 (48.8-51.3)	67.5 (60.0-71.3)
		p=0.003*	p=0.004*
Total	65.0	85.0	187.5

Figure 3.132 MCF-7X versus X(FAS/LY) cell total EGFR expression by immunocytochemistry. MCF-7X and X(FAS/LY) cells were grown on coverslips in phenol-red-free RPMI media containing 5% XFCS with the appropriate absence or presence of faslodex/LY29002 (10^{-7} M, 5 μM). Conditions were maintained for 7 days prior to phenol formal saline fixation. The total EGFR (antibody dilution 1:100) digital images shown above (X20 magnification) are representative of 2 experiments. H-Score data were obtained by dual assessment of 3 representative areas of each coverslip followed by statistical analysis (Mann-Whitney U-Test). The median H-Score and Q1-Q3 values are displayed. A p-value <0.05(*) indicates a significant difference in total EGFR expression versus MCF-7X basal control.

Total IGF-1R

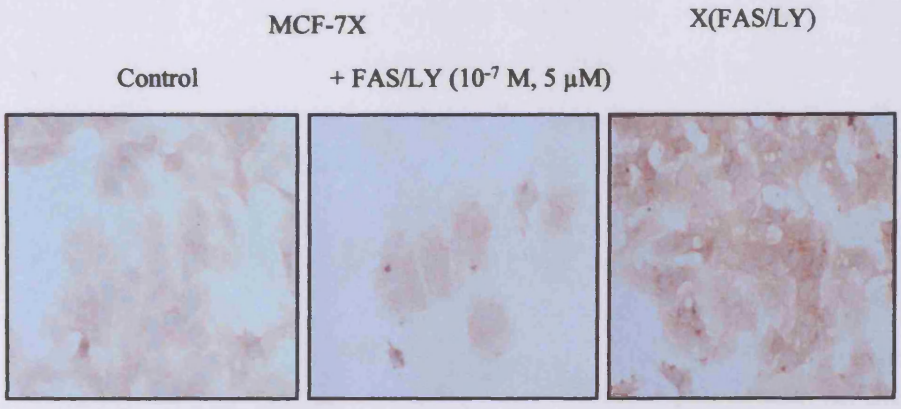

	MCF-7X	+ FAS/LY	X(FAS/LY)
Total IGF-1R			
(Membrane)	10.0 (10.0-12.8)	5.0 (5.0-6.3)	35.0 (30.0-45.0)
		p=0.006*	p=0.003*
(Cytoplasmic)	55.0 (50.0-61.3)	120.0 (112.5-121.3)	100.0 (90.0-110.0)
		p=0.003*	p=0.003*
Total	65.0	125.0	135.0

Figure 3.133 MCF-7X versus X(FAS/LY) cell total IGF-1R expression by immunocytochemistry. MCF-7X and X(FAS/LY) cells were grown on coverslips in phenol-red-free RPMI media containing 5% XFCS with the appropriate absence or presence of faslodex/LY294002 (10^{-7} M, 5 μM). Conditions were maintained for 7 days prior to phenol formal saline fixation. The total IGF-1R (antibody dilution 1:125) digital images shown above (X20 magnification) are representative of 2 experiments. H-Score data were obtained by dual assessment of 3 representative areas of each coverslip followed by statistical analysis (Mann-Whitney U-Test). The median H-Score and Q1-Q3 values are displayed. A p-value <0.05(*) indicates a significant difference in total IGF-1R expression versus MCF-7X basal control.

Total HER2

MCF-7X X(FAS/LY)

Control + FAS/LY (10^{-7} M, 5 μM)

	MCF-7X	+ FAS/LY	X(FAS/LY)
Total HER2			
(Membrane)	67.5 (51.3-78.8)	85.0 (68.8-96.3)	79.5 (75.0-85.0)
		p=0.034*	p=0.015*
(Cytoplasmic)	25.0 (20.0-30.0)	40.0 (33.8-41.3)	30.0 (30.0-35.0)
		p=0.002*	p=0.042*
Total	92.5	125.0	109.5

Figure 3.134 MCF-7X versus X(FAS/LY) cell total HER2 expression by immunocytochemistry. MCF-7X and X(FAS/LY) cells were grown on coverslips in phenol-red-free RPMI media containing 5% XFCS with the appropriate absence or presence of faslodex/LY29002 (10^{-7} M, 5 μM). Conditions were maintained for 7 days prior to ERICA fixation. The total HER2 (antibody dilution 1:100) digital images shown above (X20 magnification) are representative of 2 experiments. H-Score data were obtained by dual assessment of 3 representative areas of each coverslip followed by statistical analysis (Mann-Whitney U-Test). The median H-Score and Q1-Q3 values are displayed. A p-value <0.05(*) indicates a significant difference in total HER2 expression versus MCF-7X basal control.

3.5.4 LY294002/PD98059 Resistance in the Oestrogen Deprived Model

The LY294002 plus PD98059 combination was superior in inhibiting growth (75% at day 15) versus these agents applied singly. However long-term exposure still produced a resistant sub-line [X(LY/PD)] following 12 weeks of co-treatment (Figure 3.102), in parallel with retention of significant ERα activity, primarily serine 118 phosphorylation. As stated previously, this contrasted the catastrophic effects of a triple treatment of LY294002 and PD98059 together with faslodex that was able to promote superior depletion of ERα activation on both serine 118 and serine 167.

Phase contrast imaging and Haematoxylin & Eosin staining revealed these cells were mostly round in shape, contained very large nuclei with prominent nucleoli and the majority of cells were multi-nuclear (Figure 3.135A/B). As observed during the LY294002/PD98059 response, there was no impact on ERα expression (Figure 3.136) or Ser118ER phosphorylation in the X(LY/PD) resistant phenotype versus the parental MCF-7X cells (Figure 3.137). Ser167 activity which was reduced 50.0% during LY294002/PD98059 treatment recovered to basal MCF-7X level (Figure 3.137). While the co-treatment did not affect endogenous pS2 expression, once resistance occurred pS2 cytoplasmic localised staining increase 23.1% (p=0.001*) versus basal control by immunocytochemistry (Figure 3.138).

While LY294002/PD98059 co-treatment significantly reduced MAPK cytoplasmic and nuclear activity, the X(LY/PD) resistant cells demonstrated some recovery (127.8%, p=0.001*) in the low level of cytoplasmic activity and a detectable increase (p=0.001*) in nuclear staining. X(LY/PD) cytoplasmic staining remained 41.4% (p=0.001*) less than basal control, but there was a rise (p=0.015*) in nuclear MAPK activity (Figure 3.139) in the resistant phenotype. The combination treatment was also successful at reducing membrane plus cytoplasmic (51.7%, p=0.004*) and nuclear (11.6%, p=0.016*) AKT activity in MCF-7X cells (Figure 3.140). Once again, characterisation of the resistance phenotype revealed substantial recovery of both membrane plus cytoplasmic (206.1%, p=0.004*) and nuclear (31.6%, p=0.003*) compared to the responsive phase. This measured recovery was in fact a significant increase from the basal control levels of membrane plus cytoplasmic and nuclear staining (47.8%, p=0.004* and 16.3%, p=0.019* respectively).

These recovery observations of MAPK, AKT and ERα activity were paralleled by modest immunocytochemical increases in EGFR expression following emergence of LY294002/PD98059 resistance (Figure 3.141). While co-treatment for 7 days reduced both membrane as well as cytoplasmic EGFR 42.9% (p=0.003*) and 33.3% (p=0.006*) respectively in MCF-7X cells, the resistant phenotype modestly recovered total EGFR expression reaching increased expression levels of 57.1% (p=0.003*, membrane) and 33.3% (p=0.003*, cytoplasmic) versus basal control. This result equates to a 175.0% (p=0.003*) and 100.0% (p=0.003*) increase in membrane and cytoplasmic X(LY/PD) expression respectively, versus the MCF-7X cell responsive phase. MCF-7X cell HER2 membrane and cytoplasmic localised expression was unaffected by LY294002/PD98059 combination treatment, and while once resistance developed there was a 23.8% increase in membrane staining significant versus the responsive phase (p=0.019*, Figure 3.142), there was little change versus the basal control.

Once the X(LY/PD) resistant phenotype emerged immunocytochemistry revealed a significant increase in membrane and cytoplasmic localised IGF-1R expression (100.0%, p=0.004* and 68.2%, p=0.004* respectively) versus basal control (Figure 3.143). The data suggest the increase in IGF-1R began during the responsive phase as membrane and cytoplasmic staining did rise during 7 day treatment significantly (50.0%, p=0.016* and 145.5%, p=0.003* respectively) versus basal control and so may contribute to cell survival at this time.

A.

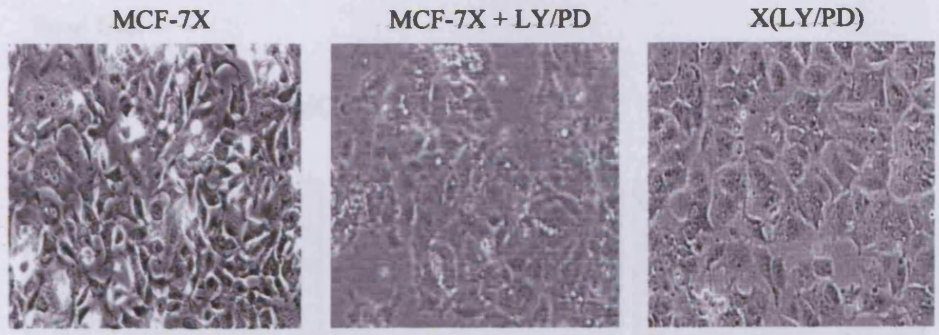

B.

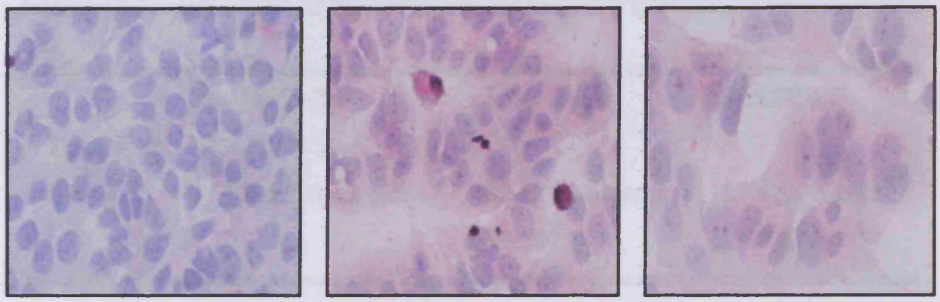

Figure 3.135 The visual morphology of MCF-7X versus X(LY/PD) phenotype by phase contrast (A) and H&E staining (B). MCF-7X and the X(LY/PD) resistant cells were grown in phenol-red-free RPMI media containing 5% XFCS in the appropriate absence or presence of LY294002/PD98059 (5 μM, 25 μM). (A) Cell phase contrast digital images were obtained during log phase growth (X20 original magnification). (B) MCF-7X and X(LY/PD) cells were grown under the same conditions as previously described for 7 days on coverslips prior to ERICA fixation. The cells were H&E stained with 10% Ehrlich Haematoxylin (10 min) followed by 1% Eosin (2½ hrs). The digital images shown above are X40 magnification.

Total ERα

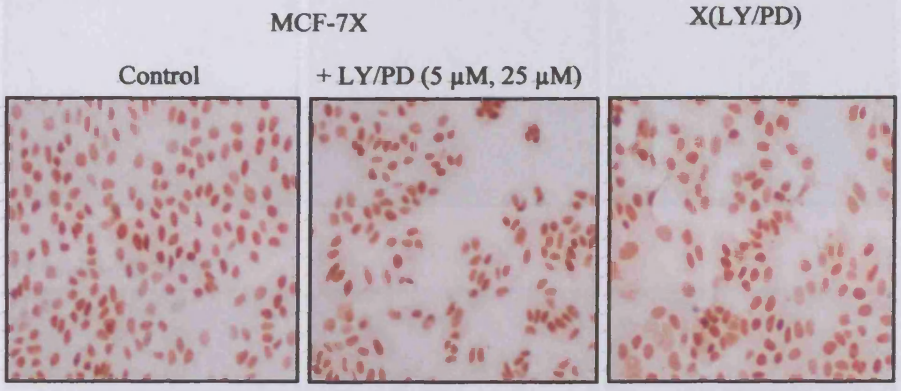

	MCF-7X	+ LY/PD	X(LY/PD)
Total ERα			
(Nuclear)	185.0 (185.0-195.0)	187.5 (183.8-205.0)	187.5 (183.8-206.3)
		p=0.797	p=0.757

Figure 3.136 MCF-7X versus X(LY/PD) cell ERα expression by immunocytochemistry. MCF-7X and X(LY/PD) cells were grown on coverslips in phenol-red-free RPMI media containing 5% XFCS with the appropriate absence or presence of LY294002/PD98059 (5 μM, 25 μM). Conditions were maintained for 7 days prior to ERICA fixation. The total nuclear ERα (6F11, antibody dilution 1:100) digital images shown above (X10 original magnification) are representative of 3 experiments. H-Score data were obtained by dual assessment of 2 representative areas of each coverslip followed by statistical analysis (Mann-Whitney U-Test). The median H-Score and Q1-Q3 values are displayed.

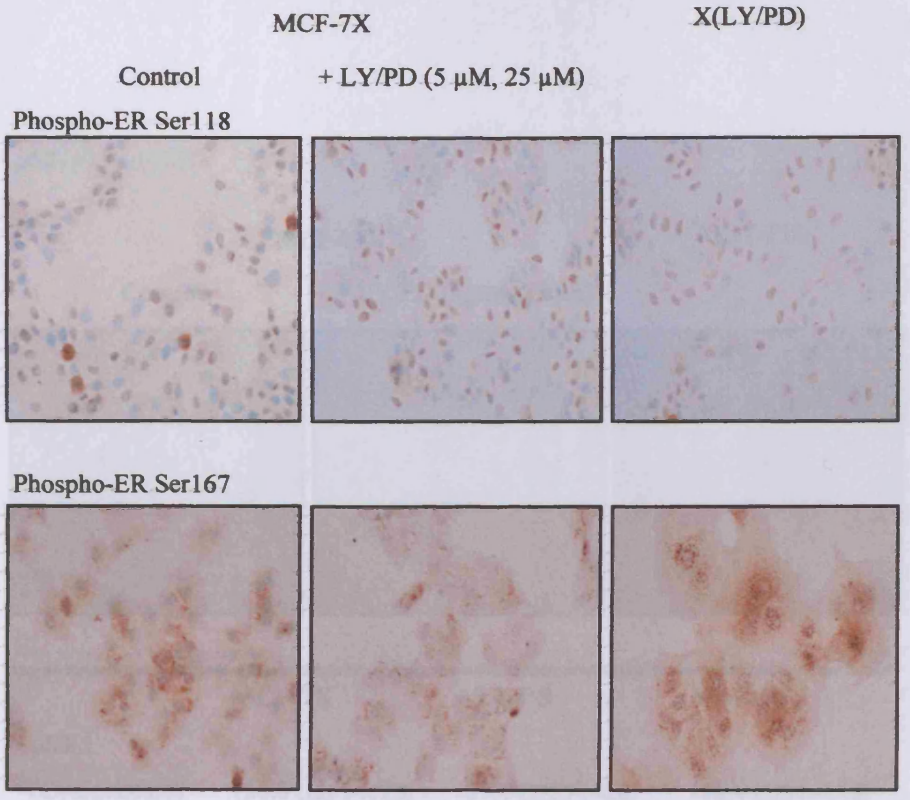

	MCF-7X	+ LY/PD	X(LY/PD)
Phospho-ER Ser118			
(Nuclear)	90.0 (77.5-110.5)	92.5 (78.8-112.5)	80.0 (68.8-92.5)
		p=0.197	p=0.807
Phospho-ER Ser167			
(Nuclear)	50.0 (45.0-70.0)	25.0 (10.0-35.0)	75.0 (62.5-82.5)
		p=0.001*	p=0.122

Figure 3.137 MCF-7X versus X(LY/PD) cell phosphorylation of ERα on Ser118 and Ser167 residues by immunocytochemistry. MCF-7X and X(LY/PD) cells were grown on coverslips in phenol-red-free RPMI media containing 5% XFCS with the appropriate absence or presence of LY294002/PD98059 (5 μM, 25 μM). Conditions were maintained for 7 days prior to the appropriate fixation. The phospho-ER Ser118 (antibody dilution 1:400) assay required coverslips paraformaldehyde fixed and the phospho-ER Ser167 (1:25) assay required coverslips ERICA fixed. The digital images shown above (X20 magnification) are representative of 4 experiments. H-Score data were obtained by dual assessment of 2 representative areas of each coverslip followed by statistical analysis (Mann-Whitney U-Test). The median H-Score and Q1-Q3 values are displayed. A p-value <0.05(*) indicates a significant difference in phospho-ER level versus MCF-7X basal control.

pS2

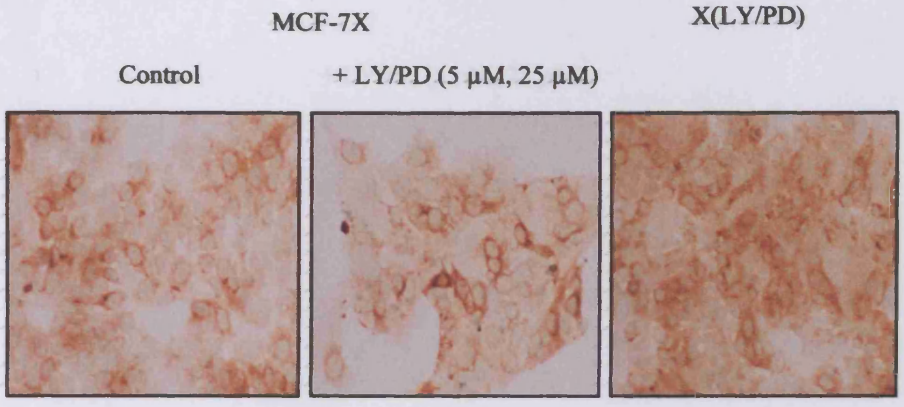

	MCF-7X	+ LY/PD	X(LY/PD)
pS2			
(Cytoplasmic)	130.0 (121.3-133.8)	135.0 (106.3-148.8)	160.0 (152.5-168.8)
		p=0.671	p=0.001*

Figure 3.138 MCF-7X versus X(LY/PD) cell pS2 expression by immunocytochemistry. MCF-7X and X(LY/PD) cells were grown on coverslips in phenol-red-free RPMI media containing 5% XFCS with the appropriate absence of presence of LY294002/PD98059 (5 μM, 25 μM). Conditions were maintained for 7 days prior to ERICA fixation. The pS2 (antibody dilution 1:500) digital images shown above (X20 magnification) are representative of 3 experiments. H-Score data were obtained by dual assessment of 2 representative areas of each coverslip followed by statistical analysis (Mann-Whitney U-Test). The median H-Score and Q1-Q3 values are diaplayed. A p-value <0.05(*) indicates a significant difference in pS2 expression versus MCF-7X basal control.

Phospho-MAPK

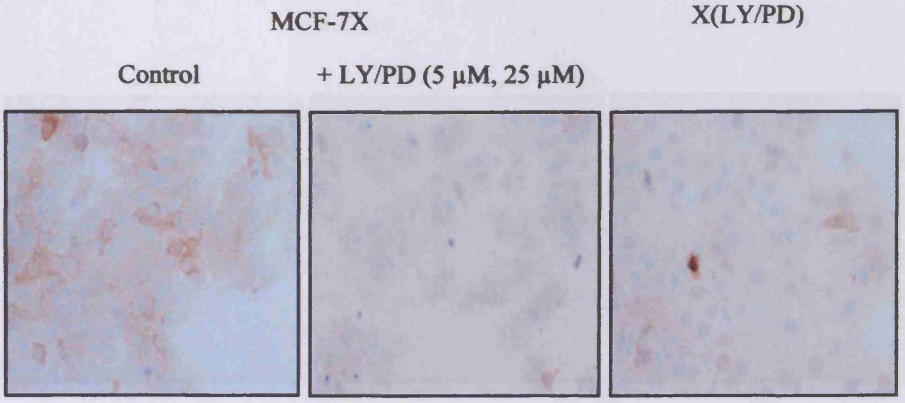

	MCF-7X	+ LY/PD	X(LY/PD)
Phospho-MAPK			
(Cytoplasmic)	35.0 (35.0-48.8)	9.0 (6.0-10.0)	20.5 (20.0-25.0)
		p=0.001*	p=0.001*
(Nuclear)	3.5 (1.3-5.0)	1.0 (0.3-1.8)	9.5 (4.0-13.8)
		p=0.016*	p=0.015*
Total	38.5	10.0	30.0

Figure 3.139 MCF-7X versus X(LY/PD) cell phosphorylated MAPK level by immunocytochemistry. MCF-7X and X(LY/PD) cells were grown on coverslips in phenol-red-free RPMI media containing 5% XFCS with the appropriate absence or presence of LY294002/PD98059 (5 μM, 25 μM). Conditions were maintained for 7 days prior to formal saline fixation. The phospho-MAPK (antibody dilution 1:20) digital images shown above (X20 magnification) are representative of 4 experiments. H-Score data were obtained by dual assessment of 2 representative areas of each coverslip followed by statistical analysis (Mann-Whitney U-Test). The median H-Score and Q1-Q3 values are displayed. A p-value <0.05(*) indicates a significant difference in phospho-MAPK level versus MCF-7X basal control.

Phospho-AKT

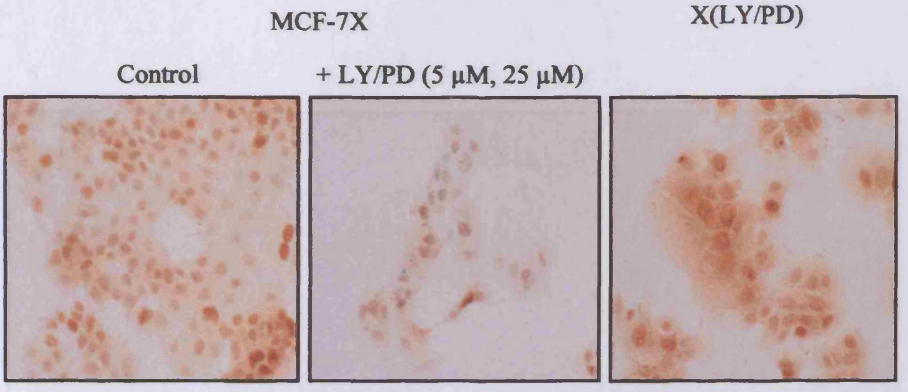

	MCF-7X	+ LY/PD	X(LY/PD)
Phospho-AKT			
(Memb. + Cyto.)	101.5 (76.5-119.3)	49.0 (46.0-55.3)	150.0 (145.0-160.0)
		p=0.004*	p=0.004*
(Nuclear)	107.5 (95.0-112.5)	95.0 (88.8-95.0)	125.0 (120.0-130.0)
		p=0.016*	p=0.019*
Total	209.0	144.0	275.0

Figure 3.140 MCF-7X versus X(LY/PD) cell phosphorylated AKT level by immunocytochemistry. MCF-7X and X(LY/PD) cells were grown on coverslips in phenol-red-free RPMI media containing 5% XFCS with the appropriate absence or presence of LY294002/PD98059 (5 μM, 25 μM). Conditions were maintained for 7 days prior to ERICA fixation. The phospho-AKT (antibody dilution 1:200) digital images shown above (X20 magnification) are representative of 3 experiments. H-Score data were obtained by dual assessment of 2 representative areas of each coverslip followed by statistical analysis (Mann-Whitney U-Test). The median H-Score and Q1-Q3 values are displayed. A p-value <0.05(*) indicates a significant difference in phospho-AKT level versus MCF-7X basal control.

Total EGFR

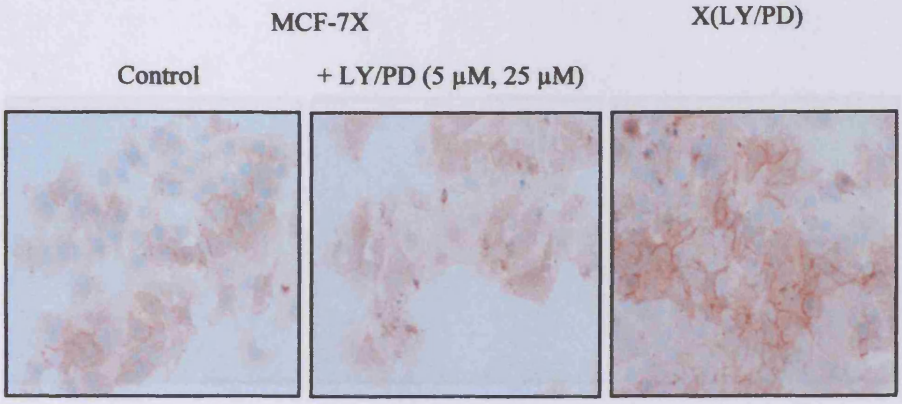

	MCF-7X	+ LY/PD	X(LY/PD)
Total EGFR			
(Membrane)	35.0 (30.0-40.0)	20.0 (15.0-21.3)	55.0 (53.8-56.3)
		p=0.003*	p=0.003*
(Cytoplasmic)	30.0 (28.0-35.0)	20.0 (15.0-25.0)	40.0 (40.0-46.3)
		p=0.006*	p=0.003*
Total	65.0	40.0	95.0

Figure 3.141 MCF-7X versus X(LY/PD) cell total EGFR expression by immunocytochemistry. MCF-7X and X(LY/PD) cells were grown on coverslips in phenol-red-free RPMI media containing 5% XFCS with the appropriate absence or presence of LY29002/PD98059 (5 μM, 25 μM). Conditions were maintained for 7 days prior to phenol formal saline fixation. The total EGFR (antibody dilution 1:100) digital images shown above (X20 magnification) are representative of 2 experiments. H-Score data were obtained by dual assessment of 3 representative areas of each coverslip followed by statistical analysis (Mann-Whitney U-Test). The median H-Score and Q1-Q3 values are displayed. A p-value <0.05(*) indicates a significant difference in total EGFR expression versus MCF-7X basal control.

Total HER2

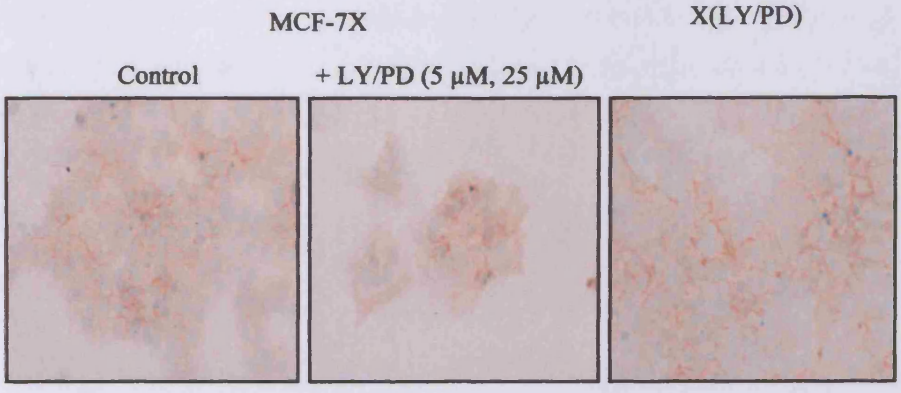

	MCF-7X	+ LY/PD	X(LY/PD)
Total HER2			
(Membrane)	67.5 (51.3-78.8)	52.5 (48.8-60.0)	65.0 (58.8-72.5)
		p=0.099	p=0.964
(Cytoplasmic)	25.0 (20.0-30.0)	25.0 (18.8-30.0)	20.0 (18.8-25.0)
		p=0.770	p=0.076
Total	92.5	77.5	85.0

Figure 3.142 MCF-7X versus X(LY/PD) cell total HER2 expression by immunocytochemistry. MCF-7X and X(LY/PD) cells were grown on coverslips in phenol-red-free RPMI media containing 5% XFCS with the appropriate absence or presence of LY29002/PD98059 (5 μM, 25 μM). Conditions were maintained for 7 days prior to ERICA fixation. The total HER2 (antibody dilution 1:100) digital images shown above (X20 magnification) are representative of 2 experiments. H-Score data were obtained by dual assessment of 3 representative areas of each coverslip followed by statistical analysis (Mann-Whitney U-Test). The median H-Score and Q1-Q3 values are displayed.

Total IGF-1R

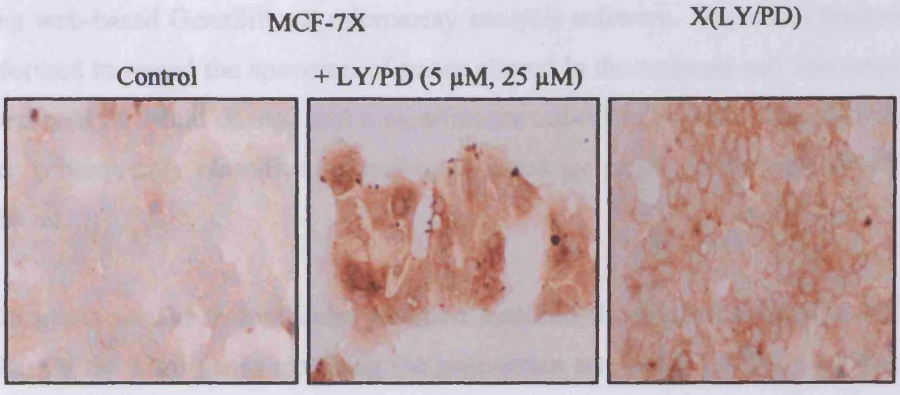

	MCF-7X	+ LY/PD	X(LY/PD)
Total IGF-1R			
(Membrane)	10.0 (10.0-12.8)	15.0 (14.0-17.5)	20.0 (18.8-21.3)
		p=0.016*	p=0.004*
(Cytoplasmic)	55.0 (50.0-61.3)	135.0 (134.8-140.0)	92.5 (87.5-96.3)
		p=0.003*	p=0.004*
Total	65.0	150.0	112.5

Figure 3.143 MCF-7X versus X(LY/PD) cell total IGF-1R expression by immunocytochemistry. MCF-7X and X(LY/PD) cells were grown on coverslips in phenol-red-free RPMI media containing 5% XFCS with the appropriate absence or presence of LY29002/PD98059 (5 μM, 25 μM). Conditions were maintained for 7 days prior to phenol formal saline fixation. The total IGF-1R (antibody dilution 1:125) digital images shown above (X20 magnification) are representative of 2 experiments. H-Score data were obtained by dual assessment of 3 representative areas of each coverslip followed by statistical analysis (Mann-Whitney U-Test). The median H-Score and Q1-Q3 values are displayed. A p-value <0.05(*) indicates a significant difference in total IGF-1R expression versus MCF-7X basal control.

3.6 AFFYMETRIX HUMAN GENOME U133A GENECHIP® ARRAYS

3.6.1 Microarray Analysis of MCF-7X versus MCF-7 cells

In an attempt to decipher any alternative receptor input that may be contributing to MCF-7X cell growth signalling (notably promoting the PI3K/AKT pathway and ER signalling), Affymetrix microarray technology was utilised (UWCM). MCF-7 versus MCF-7X cell expression profiles were investigated from triplicate cell preparations using web-based GeneSifter® microarray analysis software. Statistical analysis was performed to reveal the spectrum of genes altered in the resistant cell line employing a threshold of 2-fold change and a significance cut-off of $p<0.05$. The altered genes were subsequently classified according to ontology provided through GeneSifter® software.

3126 genes related to molecular function matched the applied criteria in MCF-7X cells. Of the 3126 genes matching the parameters set, 349 (11.16%) were described as being related to signal transducer activity (Figure 3.144). As there were 1852 genes in total on the Affymetrix arrays associated with such an ontology, approximately 20% (349/1852) of genes in this signalling category were altered in MCF-7X cells. Further ontological sub-grouping revealed the majority (207/349 genes; 60%) of the signal transducer activity genes altered in MCF-7X were implicated specifically in receptor activity (Figure 3.145). Of these 207 genes, approximately 63% were induced in MCF-7X versus MCF-7. Of particular interest among these induced receptor activity genes were FGFR4, EphA3 receptor, and transferrin receptor.

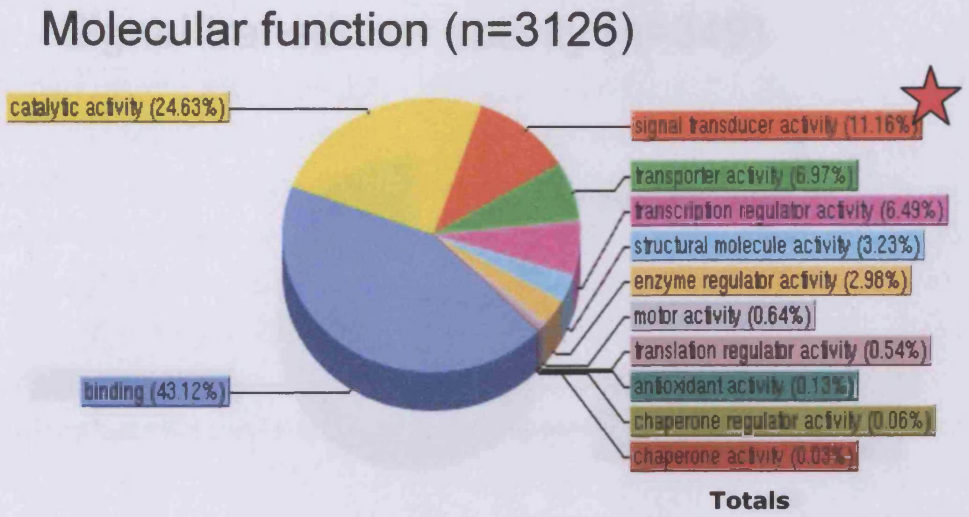

Ontology	List	Array
binding	1348	6782
catalytic activity	770	3695
signal transducer activity	349	1852
transporter activity	218	1158
transcription regulator activity	203	1022
structural molecule activity	101	572
enzyme regulator activity	93	460
motor activity	20	118
translation regulator activity	17	84
antioxidant activity	4	26
chaperone regulator activity	2	5
chaperone activity	1	1
nutrient reservoir activity	0	1

Figure 3.144 Affymetrix Human Genome U133A Genechip® Array molecular function ontology clustering. The web-based Genesifter® microarray software was utilised for the data analysis of the Affymetrix microarray results. Ontology clustering was employed to identify genes involved in molecular function revealing out of 15,776 genes on the array, 3,126 were altered in MCF-7X cells versus MCF-7 cells. Parameter settings included a 2-fold threshold change and significance cut-off of $p<0.05$ for statistical analysis. This ontology profile revealed 349 signal transducer activity genes significantly altered in MCF-7X cells.

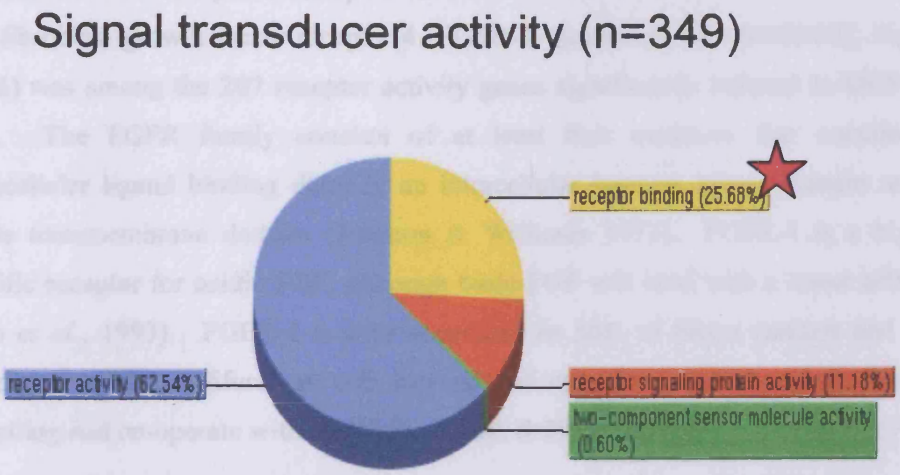

Ontology	Totals List	Totals Array
receptor activity	207	1114
receptor binding	85	507
receptor signalling protein activity	37	132
two-component sensor molecule activity	2	11
activin inhibitor activity	0	3

Figure 3.145 Affymetrix Human Genome U133A Genechip® Array signal transducer activity ontology clustering. The web-based Genesifter® microarray software was utilised for the data analysis of the Affymetrix microarray results. Ontology clustering was employed to identify genes involved in signal transducer activity revealing out of 1,767 genes on the array, 349 were altered in MCF-7X cells versus MCF-7 cells. Parameter settings included a 2-fold threshold change and significance cut-off of $p<0.05$ for statistical analysis. This ontology profile revealed 207 receptor activity genes significantly altered in MCF-7X cells.

3.6.2 Receptor Input Potentially Contributory to MCF-7X Cell Signalling and Growth Revealed by Affymetrix Analysis

3.6.2.1 FGFR-4 and EphA3 Receptor

The fibroblast growth factor receptor-4 (FGFR-4, Accession No. AF202063, Figure 3.146) was among the 207 receptor activity genes significantly induced in MCF-7X cells. The FGFR family consists of at least four members that contain an extracellular ligand binding domain, an intracellular tyrosine kinase domain and a single transmembrane domain (Johnson & Williams 1993). FGFR-4 is a highly specific receptor for acidic FGF, although basic FGF will bind with a lower affinity (Ron *et al.*, 1993). FGFR-4 is over expressed in 30% of breast cancers and can contribute to cell proliferation, cell survival and migration, and can trigger kinase signalling and co-operate with HER2 (Koziczak & Hynes 2004).

According to the parameter settings used in the Affymetrix analysis (threshold of 2 fold change, significance cut-off of $p<0.05$), FGFR-4 expression was markedly increased in MCF-7X cells versus an absent call in the parental MCF-7 cells (~3-fold). While the project has previously observed a lack of stimulatory effect of exogenous FGFs on MCF-7X cell growth (Figure 3.42), a role for such signalling is still feasible in the absence of challenging MCF-7X cells with a selective FGFR-4 inhibitor (unavailable for this project). However, since the Affymetrix data also revealed the natural ligands for the FGFR-4, FGF1 (acidic FGF, Accession No. NM_013394) and FGF2 (basic FGF, Accession No. NM_002006) were absent in both the oestrogen deprived and parental cell lines (Figure 3.147), the data imply that FGFR4 signalling is unlikely to provide a major receptor input in these cells.

A further gene identified by Affymetrix as significantly increased (4.5-fold) in MCF-7X cells compared to the parental cell line was the EphA3 receptor (HEK, Accession No. AF213459, Figure 3.148). Ephrin receptors comprise the largest family of receptor tyrosine kinases and are divided into two sub-categories based on ligand and binding differences (Heroult *et al.*, 2006). There are at least five ephrin A ligands with eight corresponding EphA receptors, where ephrin A3 receptor binds to ephrin-A2, -A3, -A4 and -A5 (Accession No's. NM_001405, AW189015, NM_005227 and NM_001962 respectively). Interestingly, the profiles for each of these ligands indicate that MCF-7X cells do not over express an endogenous ligand stimulus for the EphA3 receptor (Figure 3.149). Ephrin A2 and A5 called as absent in MCF-7X cells.

However, MCF-7X cells do produce ephrin A3 and A4, albeit at a much lower level compared to MCF-7 cells (~1-fold and 2-fold less respectively). It is feasible that these ephrins may exert a more prominent effect in MCF-7X cells via the increased EphA3 receptor. EphA3 receptor has previously been linked with tumour progression and so may positively contribute to growth; however since it has also been described as a tumour suppressor in some cell contexts, its role remains unclear in MCF-7X cells (Brantley *et al.*, 2002).

3.6.2.2 Transferrin Receptor

A further receptor whose expression was significantly increased (~2-fold) in MCF-7X cells compared to the parental MCF-7 cells within the list of genes involved in receptor activity from Affymetrix analysis was the transferrin receptor (CD71, TFR1, Accession No. NM_003234, Figure 3.150). The transferrin receptor (TfR) is a transmembrane homodimer consisting of two identical monomers with a molecular weight of 90 kDa located in the plasma membrane that bind iron-loaded transferrin with a very high affinity. Maintained iron uptake is pivotal for energy metabolism, DNA synthesis, cell survival and proliferation [where CD71 immunostaining invariably equates with proliferative capacity in clinical disease (Wrba *et al.*, 1989)]. Indeed transferrin supplementation is an essential component of defined media for *in vitro* studies, and TfR increases in breast cancer cells (e.g. T47D) occur in response to reduced concentrations of fetal calf serum in media. Breast cancer cell models have previously been shown to produce transferrin and express transferrin receptor to maximise their iron delivery and enable proliferative activity (Vandewalle *et al.*, 1989). Moreover, transferrin/TfR over expression has also been equated with metastastic growth in rat breast cancer model systems (Cavanaugh *et al.*, 1999) and progression in the clinic (Agarwal *et al.*, 2001). It was therefore hypothesised that increases in TfR may also play a vital contributory role in MCF-7X cell growth by maintaining iron delivery under the severe oestrogen and growth factor depleted conditions, thereby aiding mitogenic signalling pathways (e.g. AKT/ER) and conferring a selective growth advantage.

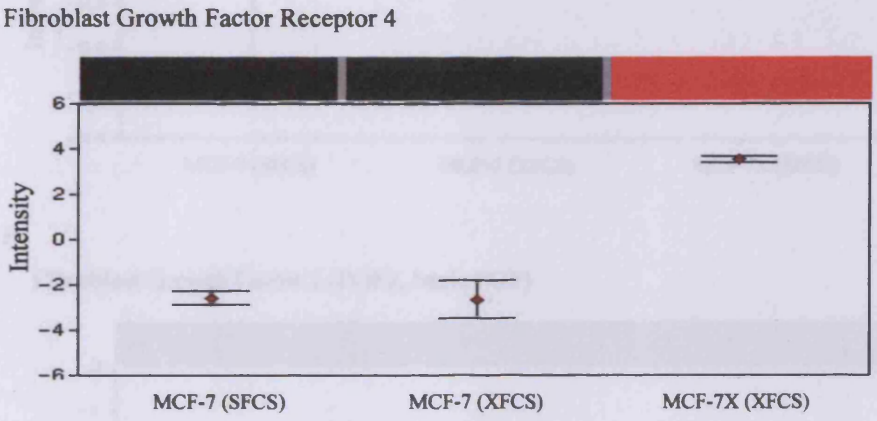

Figure 3.146 Affymetrix fibroblast growth factor receptor 4 (FGFR4) log intensity profile and heat map for MCF-7 and MCF-7X cells. MCF-7 and MCF-7X cells were grown in phenol-red-free RPMI media containing 5% SFCS or XFCS respectively. Conditions were maintained for 7 days before RNA was isolated for Affymetrix microarray analysis (U133A Genechip® arrays). The web-based Genesifter® microarray software was utilised to generate the intensity profile and heat map for FGFR4 (Accession No. AF202063) shown above. A negative intensity value denotes an affymetrix call of absent.

A.

Fibroblast Growth Factor 1 (FGF1, acidic FGF)

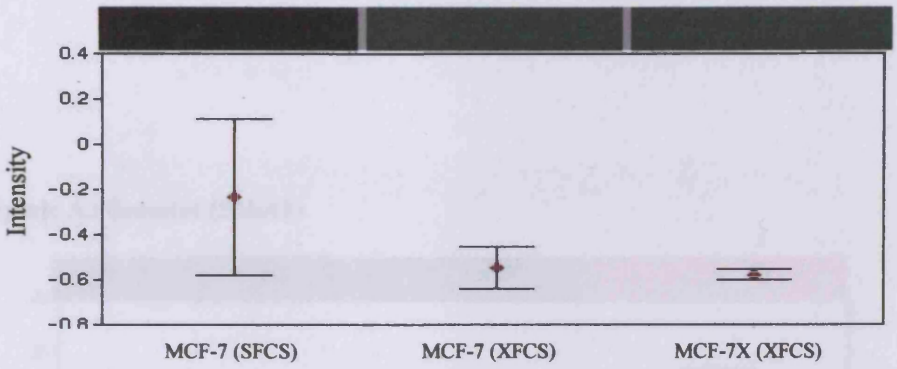

B.

Fibroblast Growth Factor 2 (FGF2, basic FGF)

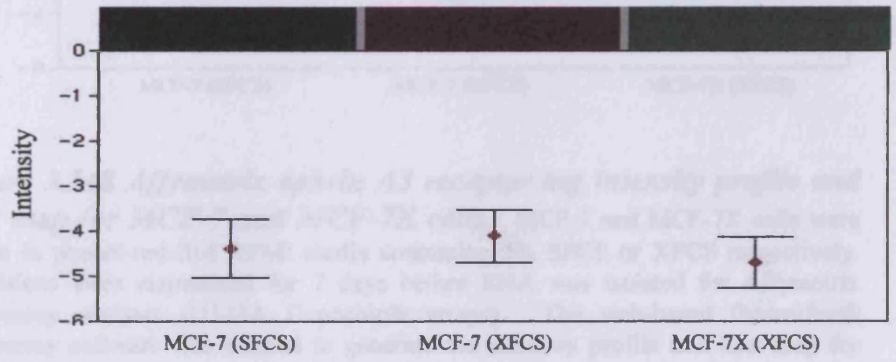

Figure 3.147 Affymetrix fibroblast growth factor -1 (A) and -2 (B) log intensity profiles and heat maps for MCF-7 and MCF-7X cells. MCF-7 and MCF-7X cells were grown in phenol-red-free RPMI media containing 5% SFCS or XFCS respectively. Conditions were maintained for 7 days before RNA was isolated for Affymetrix microarray analysis (U133A Genechip® arrays). The web-based Genesifter® microarray software was utilised to generate the intensity profile and heat map for FGF-1 and -2 (Accession No. NM_013394 and NM_002006) shown above. A negative intensity value denotes an affymetrix call of absent.

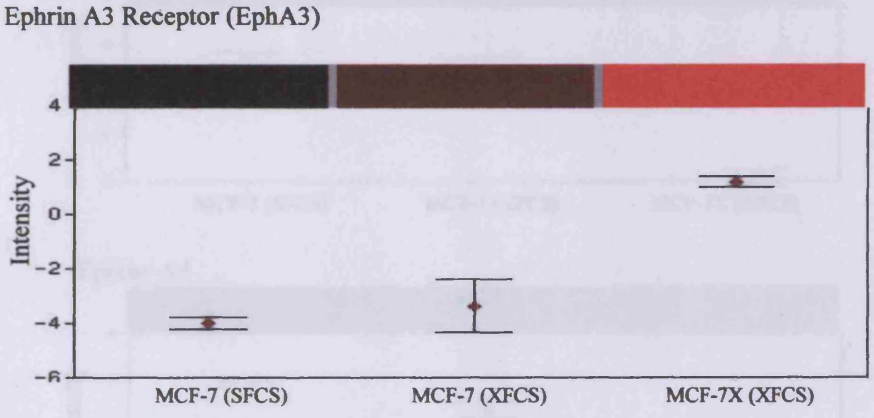

Figure 3.148 Affymetrix ephrin A3 receptor log intensity profile and heat map for MCF-7 and MCF-7X cells. MCF-7 and MCF-7X cells were grown in phenol-red-free RPMI media containing 5% SFCS or XFCS respectively. Conditions were maintained for 7 days before RNA was isolated for Affymetrix microarray analysis (U133A Genechip® arrays). The web-based Genesifter® microarray software was utilised to generate the intensity profile and heat map for EphA3 receptor (Accession No. AF213459) shown above. A negative intensity value denotes an affymetrix call of absent.

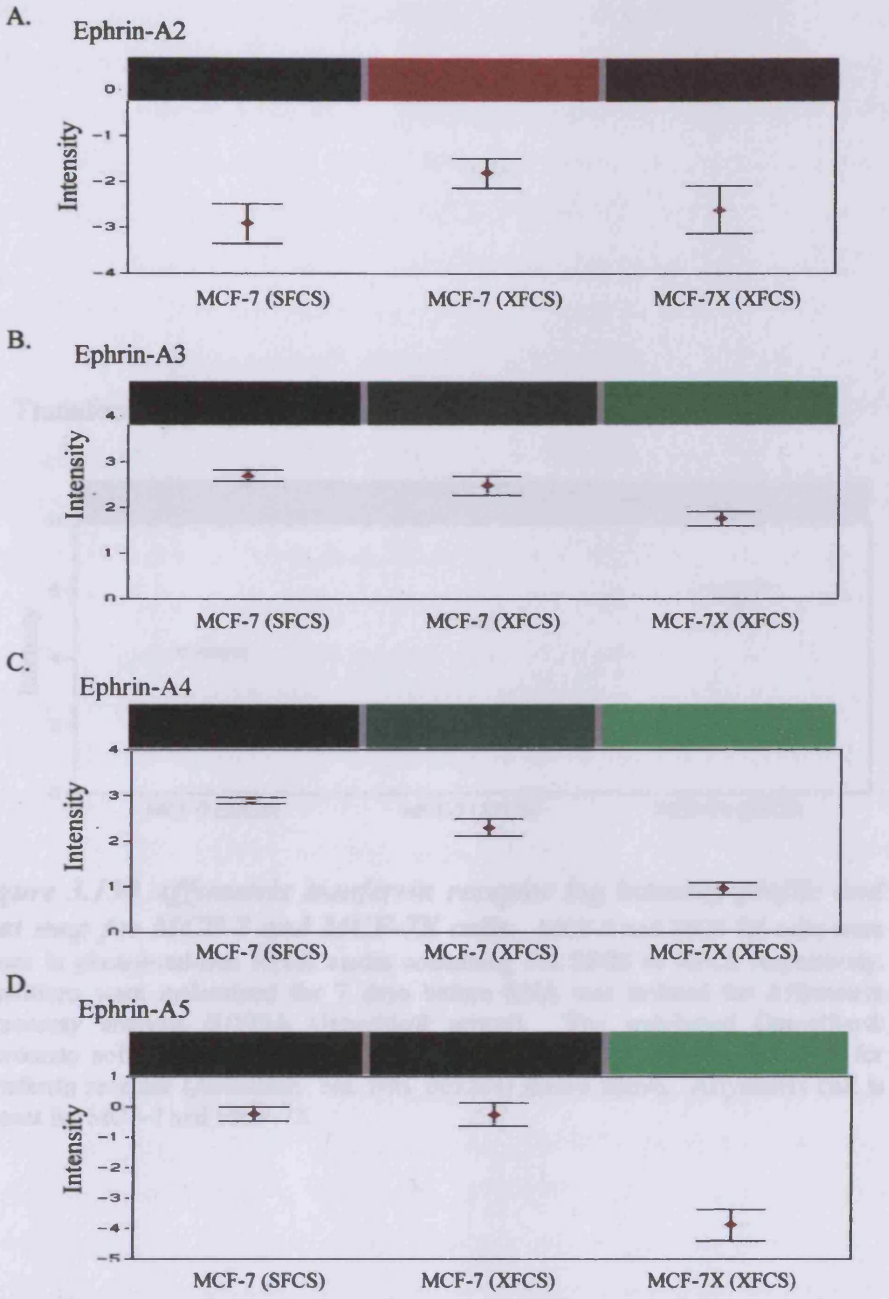

Figure 3.149 Affymetrix ephrin -A2 (A), -A3(B), -A4(C) and -A5(D) log intensity profiles and heat maps for MCF-7 and MCF-7X cells.
MCF-7 and MCF-7X cells were grown in phenol-red-free RPMI media containing 5% SFCS or XFCS respectively. Conditions were maintained for 7 days before RNA was isolated for Affymetrix microarray analysis (U133A Genechip® arrays). The web-based Genesifter® microarray software was utilised to generate the intensity profile and heat map for the ephrin ligands -A2, -A3, -A4 and -A5 (Accession No. NM_001405, AW189015, NM_005227 and NM_001962 respectively) shown above. A negative intensity value denotes an affymetrix call of absent.

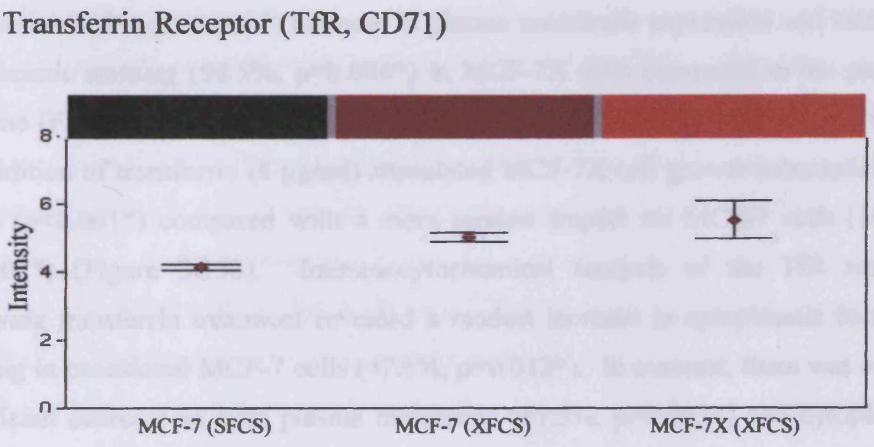

Figure 3.150 Affymetrix tranferrin receptor log intensity profile and heat map for MCF-7 and MCF-7X cells. MCF-7 and MCF-7X cells were grown in phenol-red-free RPMI media containing 5% SFCS or XFCS respectively. Conditions were maintained for 7 days before RNA was isolated for Affymetrix microarray analysis (U133A Genechip® arrays). The web-based Genesifter® microarray software was utilised to generate the intensity profile and heat map for transferrin receptor (Accession No. NM_003234) shown above. Affymetrix call is present for MCF-7 and MCF-7X.

3.7 IMPACT OF TRANSFERRIN/TRANSFERRIN RECEPTOR SIGNALLING IN MCF-7X CELLS

Based on the promising transferrin receptor Affymetrix profile, several experiments including growth studies, RT-PCR and immunocytochemistry were employed to investigate transferrin/transferrin receptor signalling in further detail in MCF-7X cells. RT-PCR confirmed the above described Affymetrix data, demonstrating a marked 241.2% ($p<0.001$*) increase in MCF-7X cell TfR mRNA expression versus MCF-7 cells (Figure 3.151). RT-PCR also revealed equivalent MCF-7 and MCF-7X cell production of low, but detectable, levels of transferrin (Figure 3.151). Protein level assessed by immunocytochemistry revealed prominent TfR staining with a substantial 77.8% ($p=0.003$*) increase in plasma membrane expression and increased cytoplasmic staining (90.5%, $p=0.004$*) in MCF-7X cells compared to the parental cell line (Figure 3.152). These data were paralleled by 7 day growth studies, where the addition of transferrin (4 μg/ml) stimulated MCF-7X cell growth substantially by 100% ($p<0.001$*) compared with a more modest impact on MCF-7 cells (50.0%, $p<0.001$*) (Figure 3.153). Immunocytochemical analysis of the TfR receptor following transferrin treatment revealed a modest increase in cytoplasmic localised staining in occasional MCF-7 cells (47.6%, $p=0.012$*). In contrast, there was a large significant decrease in both plasma membrane (87.5%, $p=0.003$*) and cytoplasmic (65.0%, $p=0.003$*) immunostaining (Figure 3.154) in MCF-7X cells following transferrin treatment.

3.7.1 Effect of Transferrin/Transferrin Receptor Input on Kinase Activity in MCF-7X Cells

Growth studies performed over 15 days supported the concept of significant positive TfR/PI3K interplay in MCF-7X cells, since LY294002 was able to fully abrogate transferrin-induced growth in these cells ($p=0.002$*, Figure 3.155). Surprisingly, however, further investigation of the interplay between transferrin and the PI3K pathway revealed some negative impact of transferrin treatment on AKT activity observed by immunocytochemistry (Figure 3.156). Thus, transferrin treatment significantly reduced nuclear phosphorylated AKT by 46.5% in MCF-7X cells ($p=0.004$*), also with some decline in cytoplasmic activity. Further growth studies indicated that the MEK1 inhibitor PD98059 was substantially less effective in abrogating transferrin-induced growth of MCF-7X cells ($p=1.000$, Figure 3.157) at day 15, in contrast to the PI3K inhibitor. Again, immunocytochemistry revealed that

transferrin exerted some negative impact on MAPK phosphorylation in MCF-7X cells (Figure 3.158). Transferrin treatment reduced MCF-7X cell cytoplasmic MAPK activity by 28.6% (p=0.026*), and the low levels of nuclear localised activity in these cells were abrogated.

In total, these data do not appear to advocate the concept that increased transferrin receptor is an upstream positive regulator of kinase signalling activity in MCF-7X cells. Indeed, there appears to be significant negative cross-talk following transferrin challenge that may in some way serve to limit excessive growth responses in the presence of transferrin. However, since LY294002 clearly abrogates transferrin-induced growth, it does seem that transferrin/transferrin receptor signalling effects in MCF-7X cells are in some way positively regulated by PI3K. Interestingly, PI3K signalling has been shown to be able to regulate trafficking of transferrin/transferrin receptor, where PI3K inhibitors deplete cell surface TfR levels (Jess *et al.*, 1996). It is thus possible that LY294002 may interfere with transferrin-induced growth via such a mechanism. As such, expression of transferrin receptor was examined following treatment with LY294002 in MCF-7X cells. This showed LY294002 treatment had no effect on membrane expression, but the compound was responsible for a small significant 10% (p=0.011*, Figure 3.159) reduction in cytoplasmic localised staining.

3.7.2 The Effect of Transferrin/Transferrin Receptor Input on ERα Signalling in MCF-7X Cells

Growth studies over 15 days with faslodex revealed that transferrin-stimulated growth could be significantly inhibited by this pure anti-oestrogen (Figure 3.160). These data suggest interplay between ERα and transferrin/TfR signalling in MCF-7X cells. In order to further decipher this potential positive cross-talk, immunocytochemistry was utilised to investigate the effect of transferrin treatment on nuclear ERα, phosphorylation of Ser118ER and Ser167ER and expression of the oestrogen regulated gene pS2. Again, surprisingly total nuclear ERα was slightly reduced by 13.9% (p=0.002*) in MCF-7X cells (Figure 3.161). Moreover, while there was no significant change in Ser118ER phosphorylation (Figure 3.162), Ser167ER activity was reduced significantly by 50.0% (p<0.001*) following transferrin treatment (Figure 3.162). In parallel there was a significant 34.6% (p=0.002*) loss of pS2 cytoplasmic localised expression in MCF-7X cells (Figure 3.163).

These data do not appear to advocate the increased transferrin receptor as an upstream positive regulator of ERα signalling activity in MCF-7X cells, and indeed again there appears to be significant negative cross-talk following transferrin challenge, where potentially its depletion of kinase activity (alongside a modest decline in ERα level) contributes to decreases in Ser167ER phosphorylation and ER-regulated gene expression. Such inhibitory effects may again serve to limit excessive growth responses in the presence of transferrin. However, since faslodex can abrogate transferrin-induced growth, it does seem that transferrin/TfR signalling is in some way positively regulated by ERα (and indeed oestrogens have previously been shown to positively regulate transferrin/transferrin receptor expression [Vandewalle & Lefebvre, 1989]). As such, immunocytochemistry was used to examine if there was any influence of faslodex on TfR expression in MCF-7X cells. However, in this case the anti-oestrogen had no significant effect on membrane or cytoplasmic localised TfR ($p=1.000$ and $p=0.150$ respectively, Figure 3.164).

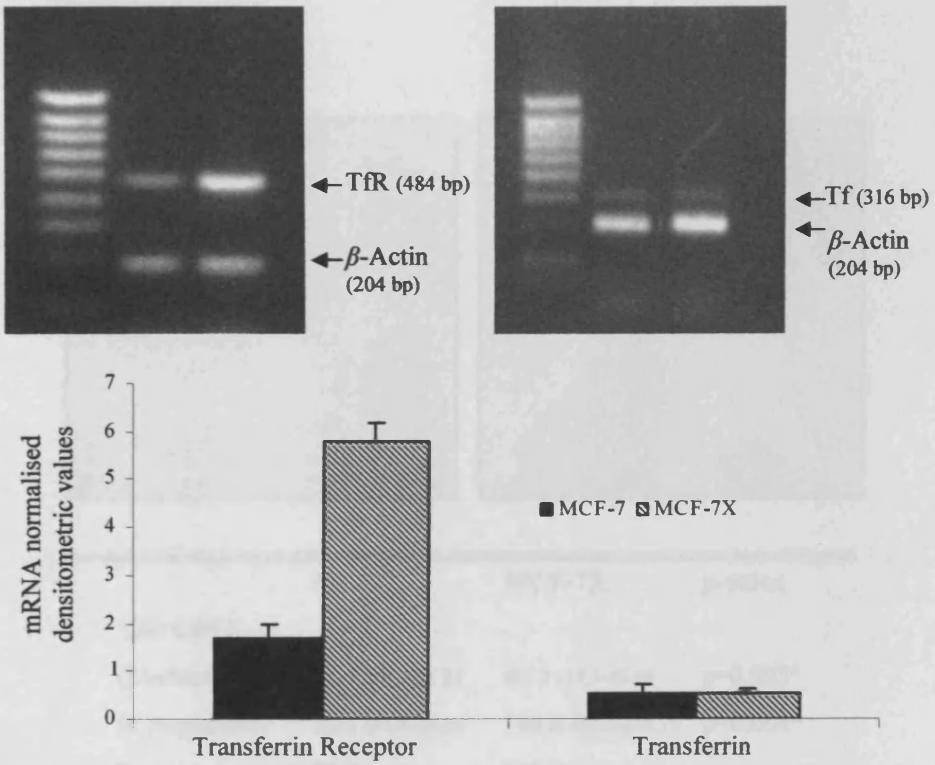

Figure 3.151 Basal MCF-7X versus MCF-7 mRNA expression of transferrin receptor and transferrin by RT-PCR. MCF-7 and MCF-7X cells were grown on 100 mm dishes in phenol-red-free RPMI media containing 5% SFCS or XFCS respectively. Conditions were maintained for 7 days before RNA was isolated and reverse transcribed. Co-amplification RT-PCR of transferrin receptor (25 cycles/ 55°C annealing temperature, 484 bp) and β-Actin (204 bp) was performed. Individual RT-PCR of transferrin (32 cycles/ 55°C annealing temperature, 316 bp) and β-Actin (25 cycles/ 55°C annealing temperature, 204 bp) was performed. Product from each reaction was run a 2% agarose gel containing ethidium bromide, subsequently photographed, scanned and normalised to β-Actin. The digital images above are representative 3 experiments (for each target sequence) and the statistical analysis applied was an unpaired-T test (transferrin receptor $p<0.001$*, transferrin $p=0.932$) comparing mean MCF-7 cell expression to mean MCF-7X cell expression.

Transferrin Receptor

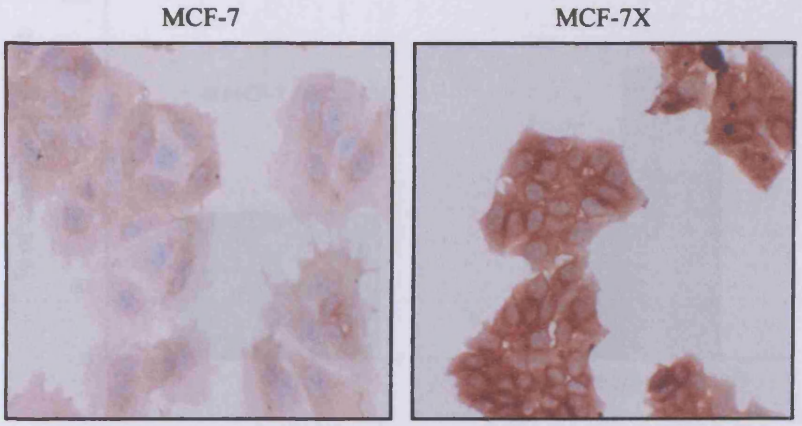

	MCF-7	MCF-7X	p-value
TfR CD71			
(Membrane)	22.5 (18.8-26.3)	40.0 (37.5-45.0)	p=0.003*
(Cytoplasmic)	52.5 (48.8-60.0)	100.0 (98.8-101.3)	p=0.004*
Total	75.0	140.0	

Figure 3.152 Basal MCF-7X versus MCF-7 cell transferrin receptor (TfR, CD71) expression by immunocytochemistry. MCF-7 and MCF-7X cells were grown on coverslips in phenol-red-free RPMI media containing 5% SFCS or XFCS respectively. Conditions were maintained for 7 days prior to phenol formal saline fixation. The CD71 (antibody dilution 1:100) digital images shown above (X20 magnification) are representative of 4 experiments. H-Score data were obtained by dual assessment of 2 representative areas of each coverslip followed by statistical analysis (Mann-Whitney U-Test). The median H-Score and Q1-Q3 values are displayed. A p-value <0.05(*) indicates a significant difference in transferrin receptor expression between MCF-7 and MCF-7X cells.

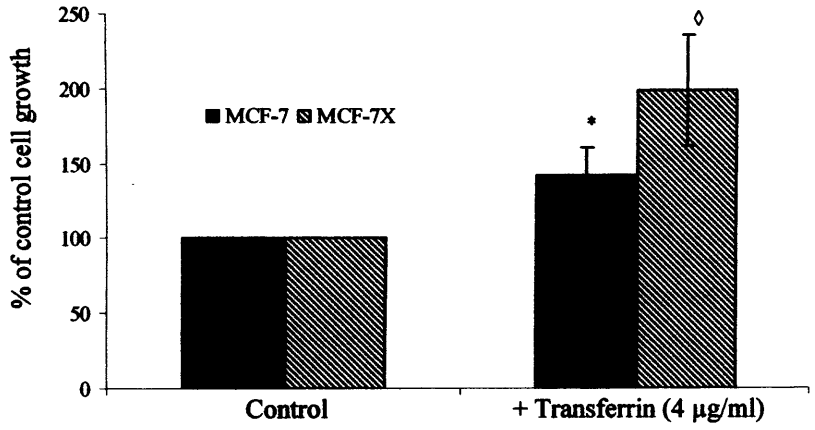

Figure 3.153 Effect of transferrin on growth of MCF-7 versus MCF-7X cells. MCF-7 and MCF-7X cells were grown on 24-well plates in phenol-red-free RPMI media containing 5% SFCS or XFCS respectively in the absence or presence of transferrin (4 µg/ml). Conditions were maintained for 7 days prior to trypsin dispersion followed by Coulter counting (triplicate wells per treatment). Data are displayed as a percentage of control cell growth and include 3 separate experiments +/- SD.

* and ◊ Denotes transferrin significantly stimulated MCF-7 ($p<0.001$) and MCF-7X ($p<0.001$) cell growth versus their respective controls.

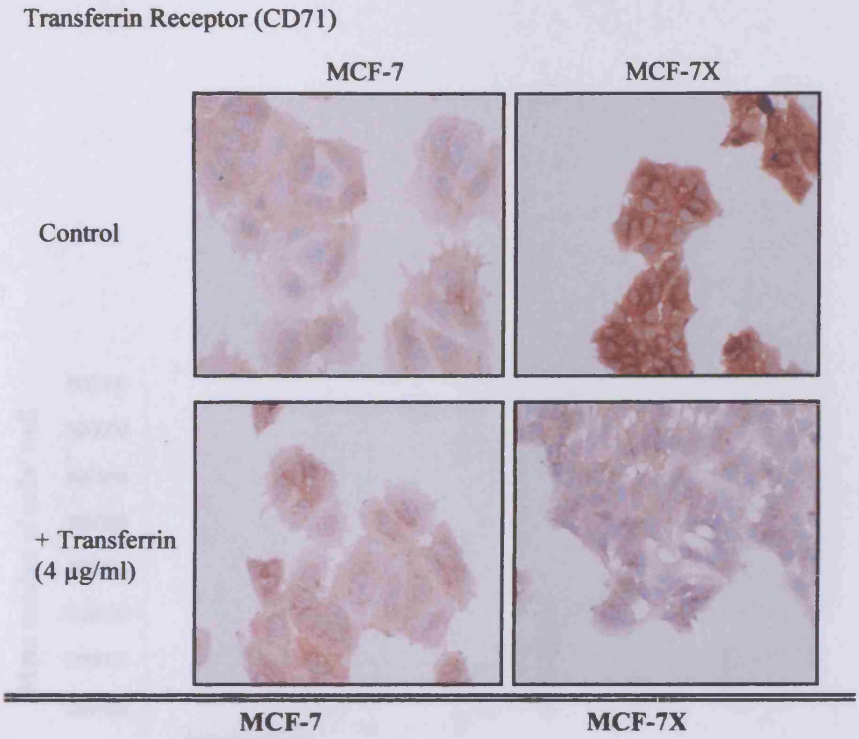

	MCF-7		MCF-7X	
TfR CD71				
Basal Control				
(Membrane)	22.5 (18.8-26.3)		40.0 (37.5-45.0)	
(Cytoplasmic)	52.5 (48.8-60.0)		100.0 (98.8-101.3)	
Total	75.0		140.0	
+ Transferrin (4 µg/ml)				
(Membrane)	22.5 (17.5-25.0)	p=0.735	5.0 (5.0-10.0)	p=0.003*
(Cytoplasmic)	77.5 (66.3-86.3)	p=0.012*	35.0 (28.8-40.0)	p=0.003*
Total	100.0		40.0	

Figure 3.154 Effect of transferrin on transferrin receptor (CD71) expression in MCF-7 and MCF-7X cells by immunocytochemistry. MCF-7 and MCF-7X cells were grown on coverslips in phenol-red-free RPMI media containing 5% SFCS or XFCS respectively in the absence or presence of transferrin (4 µg/ml). Conditions were maintained for 7 days prior to phenol formal saline fixation. The CD71 (antibody dilution 1:100) digital images shown above (X20 magnification) are representative of 3 experiments. H-Score data were obtained by dual assessment of 2 representative areas of each coverslip followed by statistical analysis (Mann-Whitney U-Test). The median H-Score and Q1-Q3 values are displayed. A p-value of <0.05(*) indicates a significant difference in transferrin receptor expression following transferrin treatment.

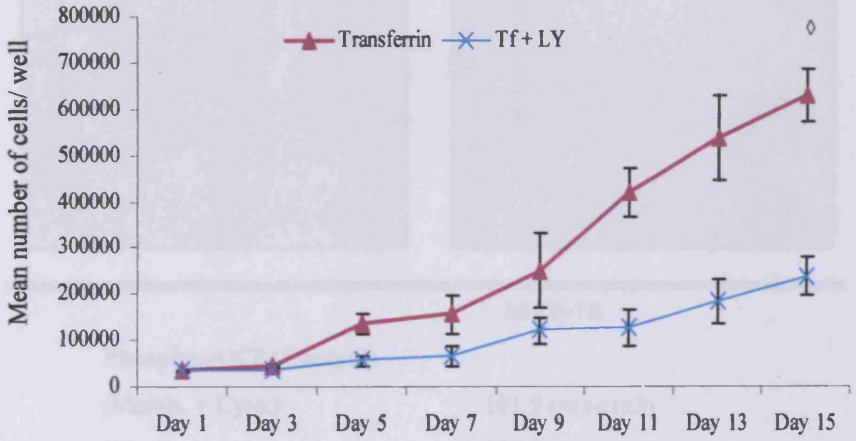

Figure 3.155 Growth challenge with transferrin singly or in combination with the PI3K inhibitor LY294002 in MCF-7X cells. MCF-7X cells were grown on 24-well plates in phenol-red-free RPMI media containing 5% XFCS in the presence of transferrin (4 µg/ml) or transferrin/LY294002 (4 µg/ml, 5 µM) for 15 days. Every 48 hours cells were subject to trypsin dispersion followed by Coulter counting (triplicate wells per time point). These data were log transformed to compare growth rate at day 15. The statistical analysis applied was an ANOVA Test followed by a Bonferroni Post-Hoc Test. The data are displayed as the mean number of cells/well +/- SD (n=3).

◊ Denotes transferrin/LY294002 treatment was significantly lower at day 15 ($p=0.002$) versus transferrin treatment control.

Phospho-AKT

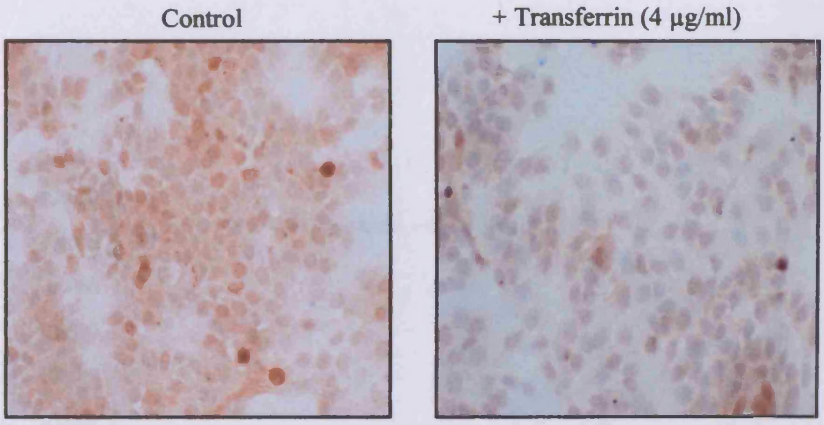

	MCF-7X	
Phospho-AKT (Control)		
(Memb. + Cyto.)	101.5 (76.5-119.3)	
(Nuclear)	107.5 (95.0-112.5)	
Total	209.0	
+ Transferrin (4 µg/ml)		
(Memb. + Cyto.)	77.0 (70.5-80.3)	p=0.077
(Nuclear)	57.5 (55.0-61.3)	p=0.004*
Total	134.5	

Figure 3.156 Effect of transferrin on phosphorylated AKT level in MCF-7X cells by immunocytochemistry. MCF-7 and MCF-7X cells were grown on coverslips in phenol-red-free RPMI media containing 5% SFCS or XFCS respectively in the absence or presence of transferrin (4 µg/ml). Conditions were maintained for 7 days prior to ERICA fixation. The phospho-AKT (antibody dilution 1:200) digital images shown above (X20 magnification) are representative of 3 experiments. H-Score data were obtained by dual assessment of 2 representative areas of each coverslip followed by statistical analysis (Mann-Whitney U-Test). The median H-Score and Q1-Q3 values are displayed. A p-value <0.05(*) indicate a significant difference in phospho-AKT level following transferrin treatment.

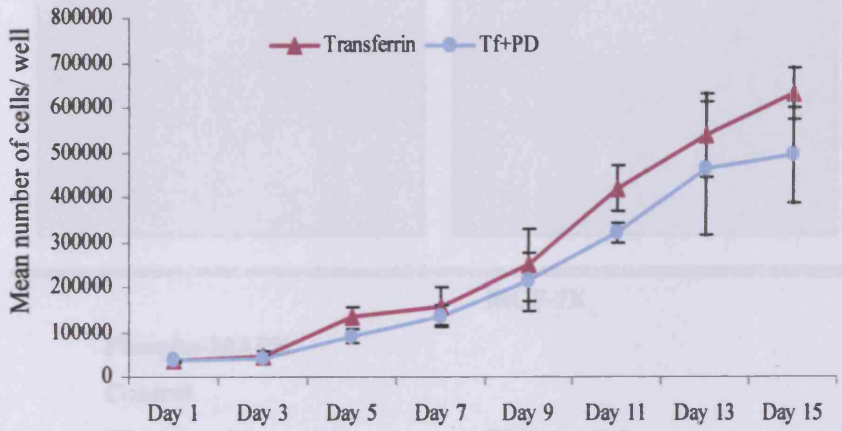

Figure 3.157 Growth challenge with transferrin singly or in combination with the MEK-1 inhibitor PD98059 in MCF-7X cells. MCF-7X cells were grown on 24-well plates in phenol-red-free RPMI media containing 5% XFCS in the presence of transferrin (4 µg/ml) or transferrin/PD98059 (4 µg/ml, 25 µM) for 15 days. Every 48 hours cells were subject to trypsin dispersion followed by Coulter counting (triplicate wells per time point). These data were log transformed to compare growth rate at day 15. The statistical analysis applied was an ANOVA Test followed by a Bonferroni Post-Hoc Test. The data are displayed as the mean number of cells/well +/- SD (n=3).

Phospho-MAPK

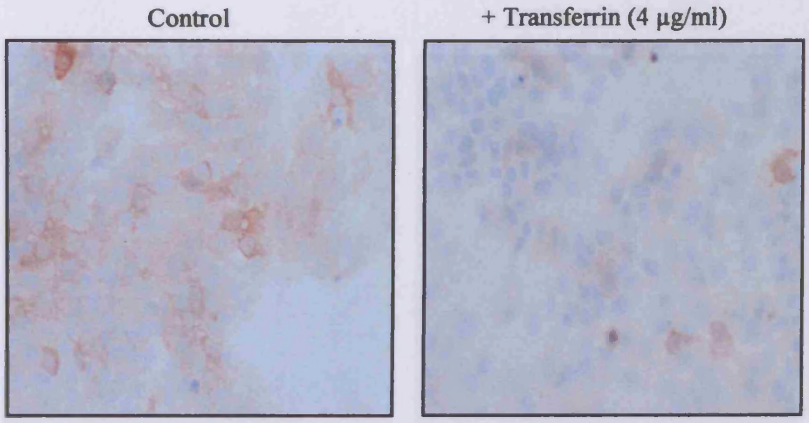

	MCF-7X	
Phospho-MAPK		
Control		
(Cytoplasmic)	35.0 (35.0-48.8)	
(Nuclear)	3.5 (1.3-5.0)	
Total	38.5	
+ Transferrin (4 µg/ml)		
(Cytoplasmic)	25.0 (20.0-32.5)	p=0.026*
(Nuclear)	0.5 (0.0-2.0)	p=0.024*
Total	25.5	

Figure 3.158 Effect of transferrin on phosphorylated MAPK level in MCF-7X cells by immunocytochemistry. MCF-7 and MCF-7X cells were grown on coverslips in phenol-red-free RPMI media containing 5% SFCS or XFCS respectively in the absence or presence of transferrin (4 µg/ml). Conditions were maintained for 7 days prior to formal saline fixation. The phospho-MAPK (antibody dilution 1:20) digital images shown above (X20 magnification) are representative of 3 experiments. H-Score data were obtained by dual assessment of 2 representative areas of each coverslip followed by statistical analysis (Mann-Whitney U-Test). The median H-Score and Q1-Q3 values are displayed. A p-value <0.05(*) indicates a significant difference in phospho-MAPK level following transferrin treatment.

Transferrin Receptor (CD71)

Control + LY294002 (5 μM)

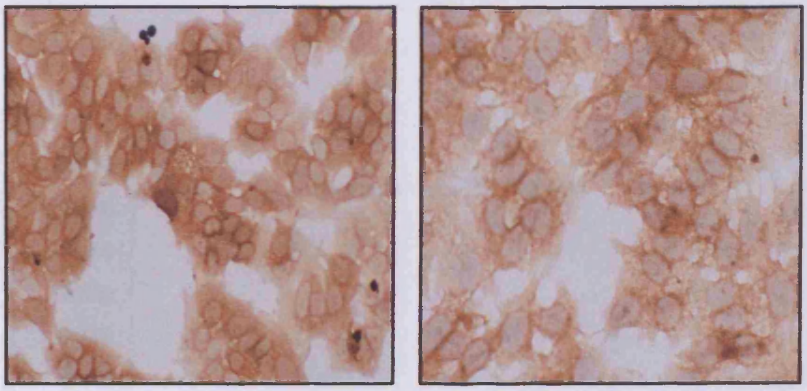

	MCF-7X	
TfR CD71		
Basal Control		
(Membrane)	40.0 (37.5-45.0)	
(Cytoplasmic)	100.0 (98.8-101.3)	
Total	140.0	
+ LY294002 (5 μM)		
(Membrane)	40.0 (35.0-41.3)	p=0.589
(Cytoplasmic)	90.0 (86.3-92.5)	p=0.011*
Total	130.0	

Figure 3.159 Effect of LY294002 on transferrin receptor (CD71) expression in MCF-7X cells by immunocytochemistry. MCF-7X cells were grown on coverslips in phenol-red-free RPMI media containing 5% XFCS in the absence or presence of LY294002 (5 μM). Conditions were maintained for 7 days prior to phenol formal saline fixation. The CD71 (antibody dilution 1:100) digital images shown above (X20 original magnification) are representative of 3 experiments. H-Score data were obtained by dual assessment of 2 representative areas of each coverslip followed by statistical analysis (Mann-Whitney U-Test). The median H-Score and Q1-Q3 values are displayed. A p-value of <0.05(*) indicates a significant difference in transferrin receptor expression following LY294002 treatment.

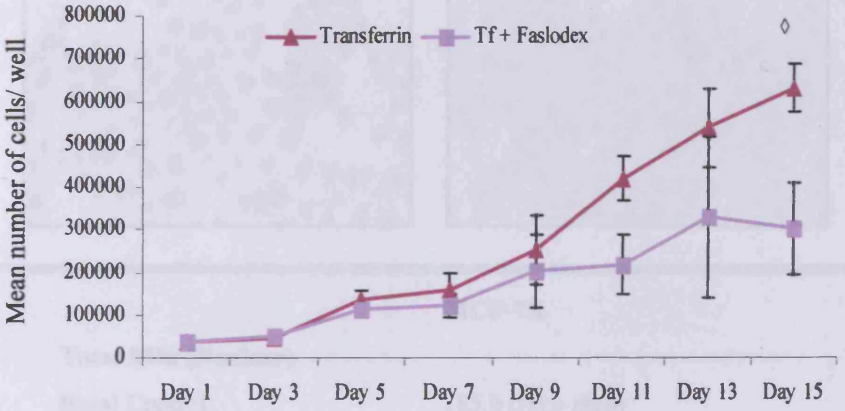

Figure 3.160 Growth challenge with transferrin singly or in combination with the pure anti-oestrogen faslodex in MCF-7X cells. MCF-7X cells were grown on 24-well plates in phenol-red-free RPMI media containing 5% XFCS in the presence of transferrin (4 µg/ml) or transferrin/faslodex (4 µg/ml, 10^{-7} M) for 15 days. Every 48 hours cells were subject to trypsin dispersion followed by Coulter counting (triplicate wells per time point). These data were log transformed to compare growth rate at day 15. The statistical analysis applied was an ANOVA Test followed by a Bonferroni Post-Hoc Test. The data are displayed as the mean number of cells/well +/- SD (n=3).

◊ Denotes transferrin/faslodex treatment was significantly lower at day 15 (p=0.012) versus transferrin treatment control.

Total ERα

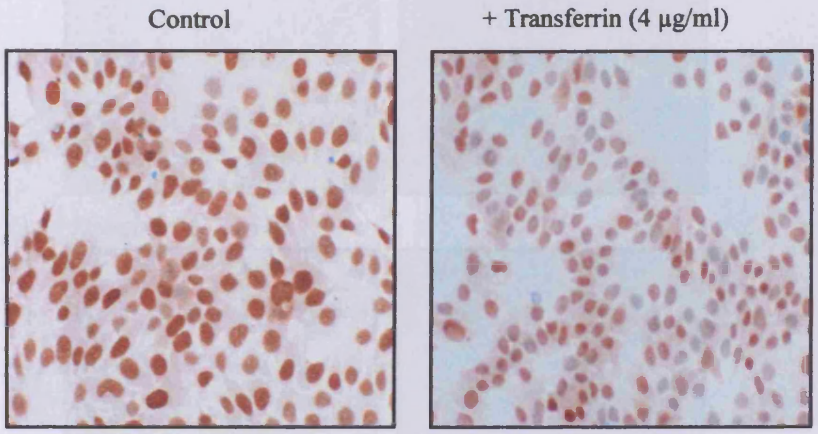

	MCF-7X	
Total ERα (Nuclear)		
Basal Control	185.0 (185.0-195.0)	
+ Transferrin (4 µg/ml)	152.5 (141.3-161.3)	p=0.002*

Figure 3.161 Effect of transferrin on ERα protein expression in MCF-7X cells by immunocytochemistry. MCF-7 and MCF-7X cells were grown on coverslips in phenol-red-free RPMI media containing 5% SFCS or XFCS respectively in the absence or presence of transferrin (4 µg/ml). Conditions were maintained for 7 days prior to ERICA fixation. The total nuclear ERα (6F11, antibody dilution 1:100) digital images shown above (X20 magnification) are representative of 3 experiments. H-Score data were obtained by dual assessment of 2 representative areas of each coverslip followed by statistical analysis (Mann-Whitney U-Test). The median H-Score and Q1-Q3 values are displayed. A p-value <0.05(*) indicates a significant difference in ERα expression following transferrin treatment.

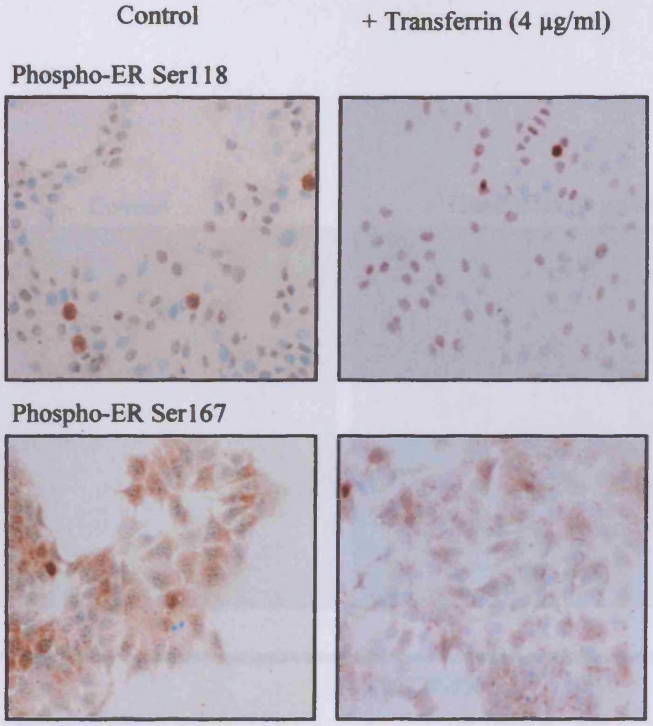

	MCF-7X	
Phospho-ER Ser118 (Nuclear)		
Basal Control	90.0 (77.5-110.5)	
+ Transferrin (4 µg/ml)	77.5 (68.8-91.3)	p=0.102
Phospho-ER Ser167 (Nuclear)		
Basal Control	50.0 (45.0-70.0)	
+ Transferrin (4 µg/ml)	25.0 (20.0-30.0)	p<0.001*

Figure 3.162 Effect of transferrin on phosphorylation of ERα on Ser118 and Ser167 residues in MCF-7X cells by immunocytochemistry. MCF-7 and MCF-7X cells were grown on coverslips in phenol-red-free RPMI media containing 5% SFCS or XFCS respectively in the absence or presence of transferrin (4 µg/ml). Conditions were maintained for 7 days prior to the appropreiate fixation. The phospho-ER Ser118 (antibody dilution 1:400) assay required coverslips paraformaldehyde fixed. The phospho-ER Ser167 (antibody dilution 1:25) assay required coverslips ERICA fixed. The digital images shown above (X20 magnification) are representative of 3 experiments. H-Score data were obtained by dual assessment of 2 representative areas of each coverslip followed by statistical analysis (Mann-Whitney U-Test). The median H-Score and Q1-Q3 values are displayed. A p-value <0.05(*) indicates a significant difference in phospho-ER Ser118 or Ser167 level following transferrin treatment.

pS2

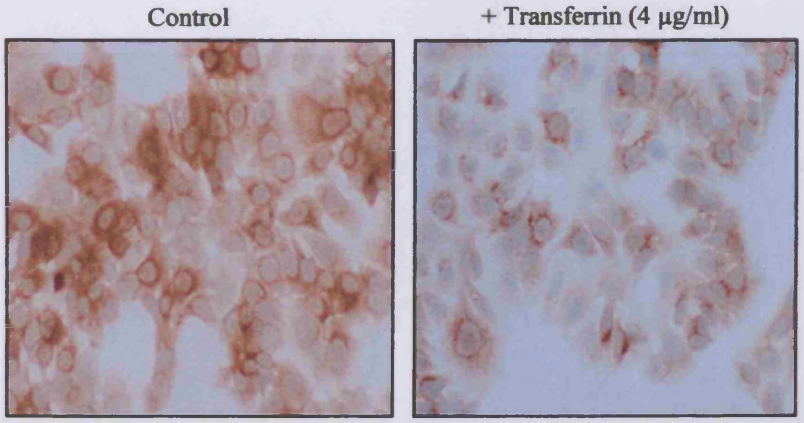

	MCF-7X	
pS2 (Cytoplasmic)		
Basal Control	130.0 (121.3-133.8)	
+ Transferrin (4 µg/ml)	85.0 (81.3-91.3)	p=0.002*

Figure 3.163 Effect of transferrin on pS2 expression in MCF-7X cells by immunocytochemistry. MCF-7 and MCF-7X cells were grown on coverslips in phenol-red-free media containing 5% SFCS or XFCS respectively in the absence or presence of transferrin (4 µg/ml). Conditions were maintained for 7 days prior to ERICA fixation. The pS2 (antibody dilution 1:500) digital images shown above (X20 magnification) are representative of 3 experiments. H-Score data were obtained by dual assessment of 2 representative areas of each coverslip followed by statistical analysis (Mann-Whitney U-Test). The median H-Score and Q1-Q3 values are displayed. A p-value <0.05(*) indicates a significant difference in pS2 expression following transferrin treatment.

Transferrin Receptor (CD71)

Control + Faslodex (10^{-7} M)

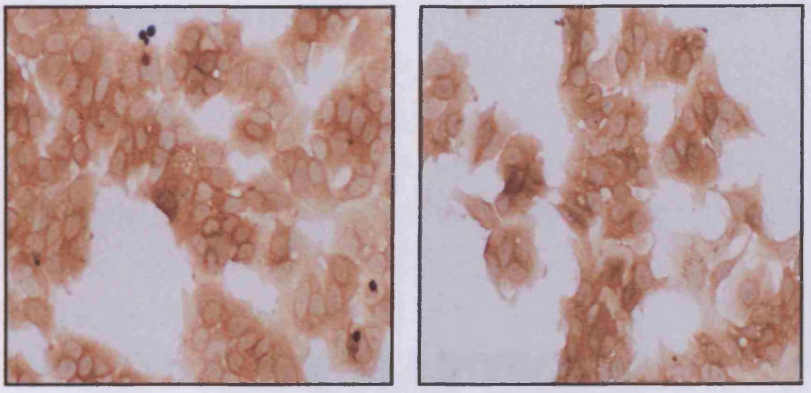

	MCF-7X	
TfR CD71		
Basal Control		
(Membrane)	40.0 (37.5-45.0)	
(Cytoplasmic)	100.0 (98.8-101.3)	
Total	140.0	
+ Faslodex (10^{-7} M)		
(Membrane)	40.0 (37.5-45.0)	p=1.000
(Cytoplasmic)	102.5 (100.0-106.3)	p=0.150
Total	142.5	

Figure 3.164 Effect of faslodex on transferrin receptor (CD71) expression in MCF-7X cells by immunocytochemistry. MCF-7X cells were grown on coverslips in phenol-red-free RPMI media containing 5% XFCS in the absence or presence of faslodex (10^{-7} M). Conditions were maintained for 7 days prior to phenol formal saline fixation. The CD71 (antibody dilution 1:100) digital images shown above (X20 magnification) are representative of 3 experiments. H-Score data were obtained by dual assessment of 2 representative areas of each coverslip followed by statistical analysis (Mann-Whitney U-Test). The median H-Score and Q1-Q3 values are displayed. A p-value of <0.05(*) indicates a significant difference in transferrin receptor expression following faslodex treatment.

CHAPTER 4

∞ *DISCUSSION* ∞

4.1 RESISTANCE TO OESTROGEN DEPRIVATION

Oestrogen deprivation as a therapeutic strategy is not a new concept in the experimental or clinical setting. However, with good cause this type of therapy has gained significant clinical momentum within the last few years. Due to the development of potent third generation aromatase inhibitors and LHRH agonists which block oestrogen production, pivotal changes in endocrine treatment strategies for breast cancer have taken shape. An increasing body of clinical data indicate oestrogen deprivation strategies are superior to the gold standard tamoxifen in postmenopausal advanced and early disease (Mouridsen *et al.*, 2003; Paridaens *et al.*, 2004; ATAC Trialists' Group, 2005). In clinical studies concerning premenopausal disease, the combination of an LHRH agonist and tamoxifen is also favoured over CMF chemotherapy in ER^+ advanced breast cancer (Jakesz *et al.*, 2002). Furthermore it was found that the addition of an LHRH agonist to standard tamoxifen therapy was more effective than tamoxifen alone in early premenopausal disease (Baum *et al.*, 2006). While such clinical studies have been underway, parallel experimental studies have been initiated to better understand mechanisms of action. Unfortunately, however, the development of resistance yet again remains a disruptive obstacle with respect to the treatment of hormone sensitive breast cancer. There has been an encouraging surge of research focused on the resistance mechanisms involved in oestrogen deprivation strategies from the various *in vivo* and *in vitro* cell model systems, notably the Brodie/Sabnis (UMB-1Ca), Martin/Dowsett (LTED), Stephen, Jensen (MCF-7/S9), Santen (LTED) and our own MCF-7X models. Among these models, there are obvious complementary results, but also contradictory data, where basic explanation to these issues may lie in the conditions employed for model development notably encompassing the presence of growth factors in the charcoal-stripped serum used in the media to maintain the cells, and in some instances addition of further exogenous growth factors such as insulin.

4.1.1 Severe Oestrogen and Growth Factor Deprived MCF-7X Model

The *in vitro* MCF-7X model developed during long-term culture in phenol red-free medium with 5% stripped, heat-inactivated medium clearly demonstrates a sobering example of the adaptability ER^+ breast cancer cells are capable of achieving (Figure 4.1A/B, the elements of this figure will be discussed in further detail as this chapter proceeds). This model was created to evaluate the absolute capability that breast cancer cells severely deprived of oestrogen and exogenous growth factors may

possess to ultimately enable resistant growth (while ensuring the culture conditions still maintain the necessary attachment factors and viability; van der Burg *et al.*, 1988). Remaining inputs for MCF-7X cells would presumably be predominantly autocrine growth factors, and exquisitely low levels of any residual steroid hormone (where the exogenous oestradiol concentration is depleted to 10^{-13}M in stripped serum). Importantly, without an exogenous growth factor-rich environment, these cells were not potentially forced to utilise one particular mitogenic signalling pathway to initiate resistant growth, and in this regard MCF-7X cells contrast many previous models of resistance to oestrogen withdrawal. Furthermore, this model revealed just how complex cell survival and adaptive mitogenic signalling is once an oestrogen/growth factor resistant phenotype develops. The MCF-7X cell data also demonstrate that a resilient cell line does not necessarily have to involve the development of a more aggressive motile/invasive phenotype. The MCF-7X sub-line appeared to have a non-invasive profile compared to the parental MCF-7 cell line. This contrasts the Sabnis *et al.* (2005) model. The UMB-1Ca cells demonstrate a significant increase in their ability to migrate when compared to the MCF-7_{CA} parental cell line. The UMB-1Ca cells are routinely grown in steroid depleted 5% dextran-coated charcoal-treated serum, which may contain residual exogenous growth factors perhaps causing the altered phenotype compared to MCF-7X cell. In particular, UMB-1Ca cells are reported to employ significant HER2 signalling, a feature absent in MCF-7X cells, and previously linked with aggressive cellular behaviour in models of anti-oestrogen resistance (Nicholson *et al.*, 2005; Hiscox *et al.*, 2005) as well as with poor prognosis in the clinic (Gee *et al.*, 2005). While MCF-7X cells showed some increase in c-Myc expression and significantly decreased $p21^{cip1/waf1}$, features that may promote increased cell proliferation, MCF-7X have merely recovered their growth to that of the parental cells, again contrasting the more highly proliferative phenotypes that can be associated with anti-oestrogen resistant models where there can be marked increases in EGFR/HER2 receptors.

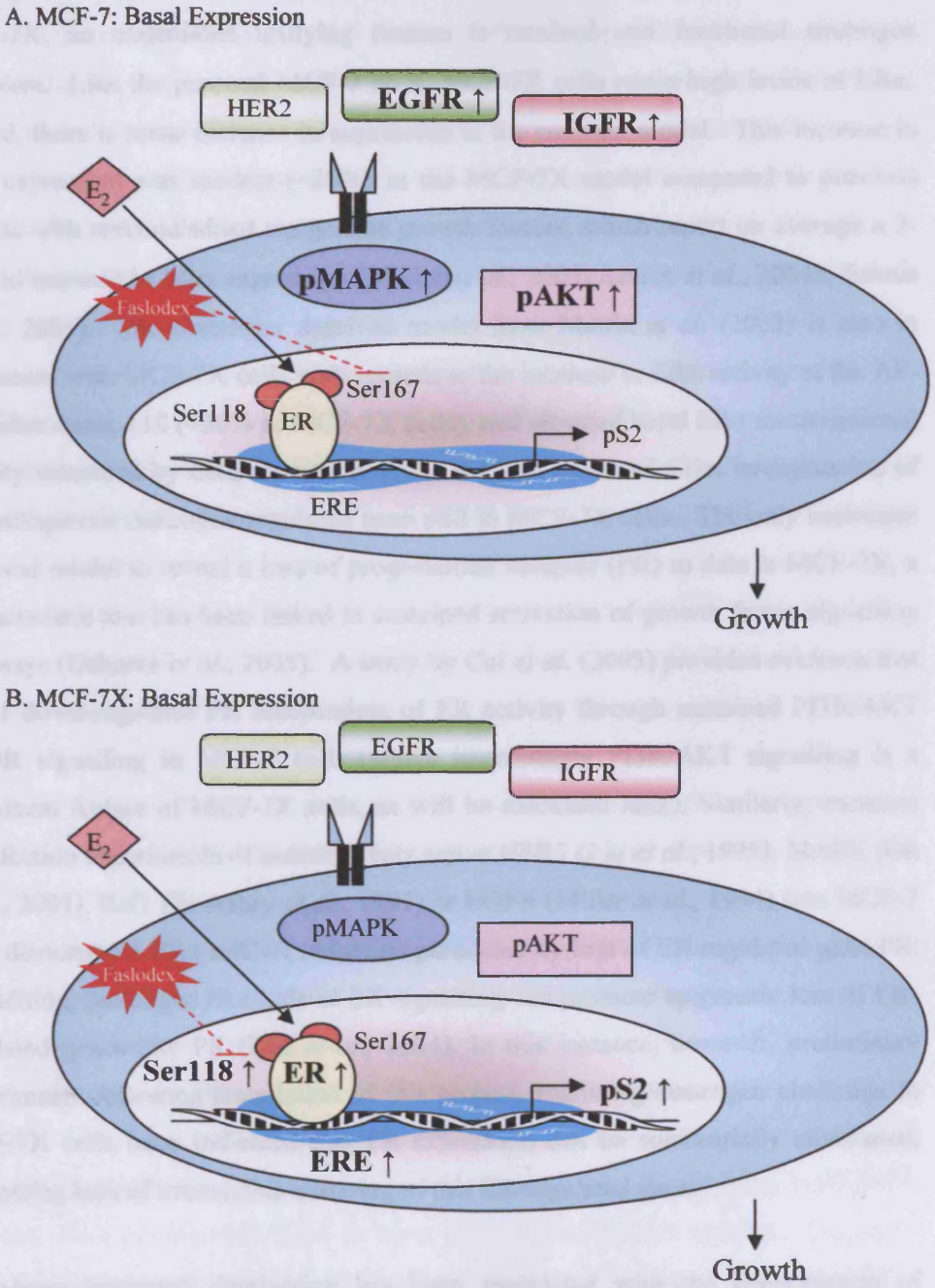

Figure 4.1 Schematic illustration of basal characterisation for MCF-7 (A) versus MCF-7X (B) cells. Above illustrates the basal characterisation of the parental MCF-7 cell line (A) versus the oestrogen growth factor deprived MCF-7X (B) cell line.

4.1.2 Retained Importance of the Oestrogen Receptor

Among the long-term oestrogen deprived (*in vivo/in vitro*) models including the MCF-7X, an undeniable unifying feature is retained and functional oestrogen receptors. Like the parental MCF-7 cells, MCF-7X cells retain high levels of ERα. Indeed, there is some increase in expression in the resistant model. This increase in ERα expression was modest (~20%) in the MCF-7X model compared to previous models with residual/added exogenous growth factors, which report on average a 3-10 fold increase in ERα expression (Martin *et al.*, 2003; Santen *et al.*, 2004a; Sabnis *et al.*, 2005). The oestrogen deprived model from Martin *et al.* (2003) is also in agreement with MCF-7X cells with regards to the increase in ERα activity at the AF-1 residue serine 118 (~30% in MCF-7X cells), and elevated basal ERα transcriptional activity measured by ERE reporter assays. We also observed a rise in expression of the endogenous oestrogen-regulated gene pS2 in MCF-7X cells. The only oestrogen deprived model to reveal a loss of progesterone receptor (PR) to date is MCF-7X, a characteristic that has been linked to sustained activation of growth factor signalling pathways (Osborne *et al.*, 2005). A study by Cui *et al.* (2003) provides evidence that IGF-1 down-regulates PR independent of ER activity through sustained PI3K/AKT mTOR signalling in MCF-7 cells (where interestingly PI3K/AKT signalling is a prominent feature of MCF-7X cells, as will be discussed later). Similarly, transient transfection experiments of constitutively active HER2 (Liu *et al.*, 1995), MAPK (Oh *et al.*, 2001), Raf1 (El-Ashry *et al.*, 1997) or EGFR (Miller *et al.*, 1994) into MCF-7 cells demonstrate ERα mRNA reduction paralleled by loss of ER-regulated gene PR. In addition, prolonged blockade of ER signalling can promote epigenetic loss of ER-regulated genes like PR (Leu *et al.*, 2004). In this instance, however, preliminary experiments following completion of this project examining oestrogen challenge in MCF-7X cells have indicated that PR expression can be substantially stimulated, suggesting lack of irreversible silencing of this ER-regulated gene.

Long-term oestrogen deprivation has been associated with the phenomenon of adaptive oestrogen hypersensitivity. Two models that give a detailed illustration of oestrogen action from a genomic and non-genomic point of view are the LTED models of Martin/Dowsett and Santen respectively. The Martin/Dowsett model suggests the adaptation in ERα function and the hypersensitive state are primarily a result of increased genomic ERα/growth factor signalling cross-talk (Johnston & Dowsett, 2003), although more recently some non-genomic contribution has been

suggested. The characterisation of this model includes elevated ERα expression, increased phosphorylation of serine 118 level, increased expression of the ER-regulated gene c-Myc and parallel increased ERE transcriptional activity. These LTED cells reportedly are oestrogen hypersensitive and maximally growth stimulated at doses of oestradiol as low as 10^{-13} M versus 10^{-9} M for the parental MCF-7 cells. In contrast, Santen (2004a) explains the LTED model oestrogen hypersensitivity by a non-genomic mechanism involving increased cell membrane-localised ERα. In this instance, the binding of oestrogen to this membrane ERα was observed to rapidly recruit a network of classical growth factors signalling elements. Similar to the LTED model of Martin/Dowsett, these cells have adapted to low levels of residual oestrogens again as low as 10^{-13} M. However, while significant growth stimulation by exogenous oestradiol was achieved, MCF-7X cells were not growth hypersensitive to sub-physiological oestradiol levels. Similar results were revealed by measuring ERE transcriptional activity, data collectively inferring that exogenous growth factors (signalling through increased growth factor receptors such as EGFR and IGF-1R that are notably depleted in MCF-7X cells) are critical in the development of oestrogen hypersensitivity.

While not fully addressed (still requires detailing of any rapid signalling activity initiated by E_2), the data in the present project do suggest that a genomic ERα mechanism is dominant in MCF-7X cells (i.e. nuclear ERα event resulting in increased ERE transcriptional activity). Thus, immunofluorescence studies revealed MCF-7X cells lack membrane ERα basally and subsequent to 10 minute E_2 challenge, and also the membrane growth factor receptors required for such a mechanism. Such events hallmark non-genomic signalling in LTED cells (Santen *et al.*, 2003; 2004a) and some tamoxifen resistant cells (Schiff & Osborne, 2005). There also seemed to be an apparent lack of importance for non-classical nuclear ER signalling in MCF-7X cells i.e. ER interplay with AP-1 priming AP-1 transcriptional activity. This is an unlikely growth mechanism in MCF-7X cells since AP-1 basal activity and Fos expression was depleted versus the parental MCF-7 line, while ERα manipulation (using oestradiol or faslodex) that promoted obvious changes in MCF-7X growth were not associated with any rational changes in AP-1 transcriptional activity.

Finally, despite the mechanistic ERα signalling differences, a feature shared by all the models of resistance to oestrogen deprivation, including MCF-7X cells, is

substantial growth sensitivity to the ER down regulator faslodex (60% inhibition in MCF-7X cells). Maximal faslodex inhibitory responses were achieved at an equivalent dosage (10^{-7} M) to MCF-7 cells. The growth inhibitory response to faslodex in MCF-7X cells was long-lived, lasting 10 weeks in culture before resistance emerged. These data provide powerful evidence that there remains a substantial contribution for ERα signalling following acquisition of this resistant state. In keeping with its mechanism of action (Wakeling, 1991), faslodex depleted ERα by 80%, promoted some depletion in Ser118ER activity on the residual ERα and substantially depleted ERE transcriptional activity and hence pS2 expression in MCF-7X cells. Data from the MCF-7X cell and other oestrogen deprived resistance models (including the MCF-7/S9 cell line recently developed by Jensen *et al.* (2003) under serum-free culture conditions) cumulatively support the use of faslodex in targeting the prominent ERα signalling. Recent *in vitro* studies from Martin *et al.* (2005) demonstrating LTED sensitivity to faslodex have resulted in a phase III randomised trial (SOFEA) among postmenopausal women with ER^+ and/or PR^+ locally advanced/metastatic breast cancer following progression on non-steroidal aromatase inhibitors (Johnston *et al.*, 2005). Comparing progression-free survival of patients treated with faslodex plus anastrozole versus faslodex alone, as well as the progression-free survival of patients treated with faslodex alone versus those treated with the steroidal aromatase inactivator exemestane are the primary aims of the trial. Brodie *et al.* (2005) has recently investigated in their MCF-7_{CA} model the use of letrozole and faslodex combined, which revealed the combination was more effective than either treatment alone. These experimental and clinical data collectively suggest ERα remains an important growth contributor and therefore an appropriate target during or following an oestrogen deprivation strategy to prolong a treatment response.

4.1.3 Classical Growth Factor Receptor Signalling in the MCF-7X Model

Aberrant growth factor signalling has been implicated in both *de novo* and acquired resistance of breast cancer cells subject to endocrine manipulation. Experimental and clinical *de novo* endocrine resistance, whether ER^- or ER^+, is invariably associated with increased levels of EGFR, HER2 and in some instances transforming growth factor-α (TGF-α) (Normanno *et al.*, 1994; Tusda 2001; Gee *et al.*, 2005). Inappropriate activation of these growth factor pathways either through an increase in natural ligand supply and/or up-regulation of their respective growth factor receptors can alternatively promote failure during anti-oestrogen treatment, yielding acquired

resistance (Nicholson *et al.*, 2004a). Our *in vitro* acquired anti-oestrogen (both tamoxifen and faslodex) resistant models demonstrate as much as a 40-fold increase in EGFR immunostaining paralleled by significant increased HER2 immunostaining (Knowlden *et al.*, 2003b; Nicholson *et al.*, 2001; McClelland *et al.*, 2001). Accepting this concept of receptor over expression having such profound influence on both *de novo* endocrine resistance and acquired anti-oestrogen resistance, these growth factor receptors were explored in our oestrogen deprived resistant model. However, extensive profiling of the MCF-7X *in vitro* cell model for receptor expression and phosphorylation status revealed no dominant role for several classical plasma membrane receptors, notably including EGFR, HER2 or IGF-1R in promoting growth. These studies included challenge with an extensive range of peptide growth factors paralleled by specific receptor inhibitors (i.e. gefitinib, herceptin and ADW742 for EGFR, HER2 and IGF-1R respectively). All failed to achieve any obvious impact on growth. These data contrast observations in many anti-oestrogen resistant models, including our own TAMR cells that demonstrate effective inhibition utilising the EGFR tyrosine kinase inhibitor gefitinib (1 μM) or the humanised HER2 monoclonal antibody herceptin [(100 nM) (Knowlden *et al.*, 2003b; Hutcheson *et al.*, 2003; Nicholson *et al.*, 2004a)] and thus a substantial dependency on mitogenic growth factor receptor signalling. Furthermore, Massarweh *et al.* (2003) illustrate *in vivo* studies where challenged of HER2 transfected MCF-7 cells with gefitinib was able to delay resistance to tamoxifen resistance therefore confirming a growth contribution for such signalling. The lack of effect of such agents in the MCF-7X model is also in contrast to the oestrogen hypersensitive models, of particular note the Martin *et al.* (2003) model, where growth contributory HER2 activity is significantly reduced with high dose gefitinib (5 μM). UMB-1Ca cells are also reported to be responsive to gefitinib at doses targeting HER2 signalling (Sabnis *et al.*, 2005). The unifying feature shared by these resistant models whether *de novo*/acquired tamoxifen resistant, LTED resistant or *in vivo* manipulated (transfection studies) is a marked increase in EGFR and/or HER2 receptor expression, an increase that clearly was not observed in the MCF-7X model. Indeed, receptor activity was further depleted versus the parental MCF-7 cells whose growth is already established as largely independent of such signalling. These MCF-7X data suggest that targeting of EGFR/HER2 signalling could prove to have limited success in effectively treating resistance to oestrogen deprivation. Questionable EGFR/HER2 relevance is not the only data revealed in the MCF-7X model. In addition there was little indication that IGF-1R

signalling participates in a dominant growth promoting role for these cells. Again multiple studies suggest a prominent function of this receptor independent and in cooperation with EGFR/HER2, ultimately contributing to anti-oestrogen resistance (Coppola *et al.*, 1994; Balana *et al.*, 2001; Knowlden *et al.*, 2003a). Again, models of LTED resistance developed in the presence of serum growth factors or exogenous insulin indicate prominent significance of IGF-1R mediated signalling (Stephen *et al.* 2001; Martin *et al.*, 2003; Santen *et al.*, 2004a) paralleled by gene transfer studies over expressing IGF-II, IGF-1R or insulin substrate-1 also suggesting a causative relationship with oestrogen independence (Guvakova & Surmacz 1997). Martin *et al.* (2005) report a 2-3-fold increase in IGF-1R, suggesting the significant increase is a result of the marked elevation in ERα signalling. The LTED model of Santen *et al.* (2004a; Song *et al.*, 2004) has shown that Shc and non-genomic membrane ERα co-immunoprecipitate using an anti-IGF-1R antibody, and the binding of ERα to the IGF-1R occurs in minutes of the addition of oestradiol orchestrating a downstream kinase cascade. Stephen *et al.* (2001) have revealed in their long-term oestrogen deprived model increased IGF-1R correlating with cell density, and also suggest that this increase may enable the cells to respond to the reduced IGF levels present in the culture medium and/or endogenously produced. Meanwhile, the MCF-7X model (stripped of exogenous growth factor input) displayed decreased expression/activation of IGF-1R in accordance with no response to IGFs and an inferior response to ADW742 IGF-1R selective inhibitor challenge compared to the MCF-7 parental cell line, where IGF-1R comprises a dominant pathway that interplays with and enhances the E_2/ER pathway. Thus, there seems to be a markedly diminished role for the IGF-1R in MCF-7X cells versus MCF-7 cells, and could indicate that IGF-1R blockade may not prove fully effective in resistance to oestrogen deprivation.

In summary, the collective MCF-7X data indicate that neither exogenous growth factor ligands nor any autocrine signalling through their classical receptors are essential to maintain growth in an oestrogen deprived environment. However, this growth factor ligand/receptor relationship appears to be of some importance in facilitating the growth and oestrogen hypersensitivity *in vitro* models derived in the presence of serum growth factors, as evidenced by the emerging relevance of HER2 and IGF-1R described for such cells. These data cumulatively indicate that while future use of inhibitors targeting such pathways may have some value, they are

unlikely to provide completely effective treatments in acquired resistant to oestrogen deprivation.

4.1.4 Kinase Promotion of Growth in the MCF-7X Model

Within previous models of acquired resistance to oestrogen deprivation there are clear implications of roles for EGFR/HER2 and IGF-1R receptor signalling which in turn influence the activation of downstream signalling pathways. It is widely accepted that these growth factor receptors can initiate activity of such intracellular elements like ERK1/2 MAP kinase (MAPK), phosphatidylinositol-3-OH kinase (PI3K)/AKT and protein kinase C isoforms (PKC). Activation of these kinases simplistically can lead to a number of key cellular functions, notably cell proliferation and cell survival (and in some instances gain of aggressive invasive behaviour) eventually contributing to the resistant phenotype.

4.1.4.1 MAPK

Of particular interest is MAPK, as increased activity of this kinase is an established component of anti-oestrogen resistant intracellular signalling (Knowlden *et al.*, 2003b) and recent findings suggest this kinase also contributes to adaptive growth changes observed in oestrogen deprived breast cancer cells and their oestrogen hypersensitivity. Increased MAPK activity is a common feature of many models that have adapted to long-term oestrogen deprivation both *in vitro* and *in vivo* (Jeng *et al.*, 2000; Martin *et al.*, 2003; Santen *et al.*, 2004a). Invariably this has been associated with increased upstream input from elevated growth factor receptors (i.e. EGFR/HER2; IGF-1R). There appears to date to be only one exception to this rule, where UMB-1Ca cells which show a 4.1-fold increase in HER2 expression do not show increased phosphorylation of MAPK and are unaffected by the MEK-1 inhibitor PD98059 (Sabnis *et al.*, 2005).

The long-term oestrogen deprived *in vitro* model from Martin/Dowsett showed significantly elevated HER2 activity and they concluded this alteration could explain the rise (8-fold) in MAPK activity within their cells (Martin *et al.*, 2003) that subsequently facilitates genomic ERα signalling. However, in an updated study, they have also shown a 2-3-fold increase in IGF-1R (with elevated IRS-2) and suggest this scenario as a possible non-genomic adaptation, augmenting any membrane ERα/IGF-1R interaction resulting in enhanced MAPK activity that contributes to oestrogen

hypersensitivity in their LTED cells (Martin *et al.*, 2005). This possible interaction is strikingly similar to the Santen/Song explanation for increased MAPK activity in conjunction with plasma membrane ERα associated oestrogen hypersensitivity. Song *et al.* (2004) suggest the intimate relationship of Shc and IGF-1R in their LTED cells serves two functions; the first is to lead to ERα membrane translocation, and the second is to markedly activate downstream MAPK in an IGF-1R-dependent manner. Previous studies including those by Lee *et al.* (1999) have shown that oestrogen/ER signalling can promote a rise in IGF-1R, IRS-1 and IRS-2 expression and expression of IGF-1R can be regulated by faslodex in the LTED cells from Martin *et al.* (2005). However, E_2/ER signalling can also directly enhance IGF-1R activity and subsequently IRS phosphorylation, which can lead to increased MAPK activity via the non-genomic mechanism. Cumulatively, these data suggest a positive feed back loop, where membrane ERα binds to the IGF-1R and activates the IGF-1R signalling cascade including MAPK which in turn stimulates the genomic activity of nuclear ERα to promote expression of components of the IGF-1R cascade. Based on this information any available growth factor ligands in exogenous serum would feasibly enhance this signalling loop therefore providing a reasonable mechanism underlying increases in MAPK activity and its contribution to long-term oestrogen deprived cell growth. Furthermore, in the LTED resistant model of Martin/Dowsett, insulin supplementation during the development and maintenance of this cell line could have substantially primed the IGF-1R pathway leading to a prominent MAPK signalling mechanism that provides a potential contribution to the observed oestrogen hypersensitivity. However, in the MCF-7X model endogenous growth factors are depleted, and increases in the classical growth factor receptor/activity are not apparent (coupled with an apparent absence of non-genomic ER contribution). Not surprisingly, therefore, the MCF-7X model fails to demonstrate increased MAPK activity versus the parental MCF-7 ER^+ cell line and the resistant cells are not oestrogen hypersensitive. Indeed some MAPK activity decreases were observed compared to MCF-7 cells, in parallel with a decline in expression and/or activity of the classical growth factor receptors. These data were paralleled by the MEK-1 inhibitor PD98059 having a markedly reduced inhibitory effect in the oestrogen/growth factor deprived cells versus the parental MCF-7 line (despite being able to further deplete the low levels of MAPK activity in such cells), and no significant duration of response with this agent. Clearly, although there is some contribution for MAPK signalling in MCF-7 cells, this kinase does not provide a

dominant mechanism in MCF-7X cells, markedly contrasting the contribution for the substantial MAPK increases in previous models generated in the presence of exogenous growth factors and a key factor contributory towards their oestrogen hypersensitivity. Of note, however, such signalling was reported to not be the only growth contribution in LTED cells. Cumulatively, the MCF-7X cell data suggest that resistance to oestrogen deprivation is unlikely to be fully-treated using a MAPK inhibitory approach.

4.1.4.2 PI3K/AKT

Activation of IGF-1R is known to recruit the p85 regulatory domain of phosphatidyl-inositol-3-OH kinase (PI3K) initiating a cascade of signalling events in MCF-7 cells (Castoria *et al.*, 2001). The serine/threonine protein kinase AKT is one of the downstream targets of PI3K and its activation generally promotes cell growth and proliferation, as well as cell survival. Interestingly, AKT activity is significantly enhanced in several anti-oestrogen resistance models, notably including our own TAMR cells (Jordan *et al.*, 2004), where in this instance activity is also regulated by enhanced EGFR/HER2 signalling. Enhanced AKT activity similarly equates with tamoxifen resistance and poorer outlook in clinical disease (Perez-Tenorio *et al.*, 2002). It has also been reported that, like MAPK, PI3K/AKT activity can be triggered by a non-genomic ERα mechanism (Song *et al.*, 2002; 2004; Wessler *et al.*, 2006).

With regards to oestrogen deprivation, there is evidence from some previous models of enhanced PI3K/AKT signalling. Brodie/Sabnis have reported that UMB-1Ca cells showed increased levels of phosphorylated AKT at serine 473 (3.3-fold) and threonine 308 (2.7-fold) versus the MCF-7_{CA} parental cells (Sabnis *et al.*, 2005). There is similarly elevated AKT activity in the Santen LTED model. Once activated, AKT can phosphorylate a number of proteins leading to regulation of metabolism (glycogen synthase kinase 3) and translational control, for example, via p70 S6 kinase (Kandel and Hay, 1999; Fry, 2001). Amplification of the p70 S6 kinase gene is associated with a poor prognosis in breast cancer (van der Hage *et al.*, 2004). AKT can influence cell survival through the forkhead family of transcription factors, including inactivation of BAD, a bcl-2 family member and inhibition of cell death pathway enzyme caspase-9 (Cardone *et al.*, 1998; Fry, 2001). Furthermore, AKT can influence mTOR (mammalian target of rapamycin), facilitating the regulation of the

cell cycle through cyclin D, E2F and c-Myc (Kandel and Hay, 1999; Johnston *et al.*, 2003). Santen/Yue recently confirmed alongside significantly enhanced AKT activation, elevated mTOR, p70 S6 kinase and eukaryotic translation initiation factor-4E binding protein in their LTED cell line (Yue *et al.*, 2003) resulting in increased cell cycle progression and proliferation. While Martin *et al.* (2003) observed levels of AKT equivalent to MCF-7 cells this was paralleled by significant altered p90 ribosomal S6 kinase (RSK) in their model.

In the present study, characterisation of the MCF-7X cell line revealed that while AKT activity was equivalent overall to MCF-7 cells, there was enhanced cytoplasmic/membrane activation in the resistant model. Interestingly in parallel, the PI3K inhibitor LY294002 caused a marked reduction in AKT activity and displayed a substantial growth inhibitory effect (70% by day 15) on the oestrogen/growth factor deprived cells. This anti-tumour response was prolonged, lasting 10 weeks before resistance emerged. Some significant inhibitory effects on growth and AKT activity were also apparent with a further PI3K inhibitor wortmannin. PI3K can also activate phosphoinositide-dependent protein kinase-1 (PDK-1) whereby, upon activation it can influence both AKT and RSK (Williams *et al.*, 2000). Like AKT, cytoplasmic PDK-1 activity was increased in the MCF-7X model (versus MCF-7 cells), which was also shown to be sensitive to LY294002 treatment. Growth, AKT and PDK signalling inhibition with LY294002 proved superior in MCF-7X versus MCF-7 cells. Clearly, PI3K/AKT is a likely contributor to resistant MCF-7X cell growth and of increased importance versus the parental cell line. Since it was observed that PDK-1 activity was refractory to wortmannin, the MCF-7X data suggest that it is AKT, rather than PDK, that is the major downstream PI3K signalling element promoting growth of the MCF-7X cells. Challenge with PI3K inhibitors in the LTED models from the Santen and Martin laboratories has also revealed PI3K signalling is (in addition to MAPK) contributory to their oestrogen hypersensitivity, thus it appears that PI3K signalling comprises a universal growth signalling input, independent of any requirement for exogenous growth factor/classical receptor input, in oestrogen deprivation resistance, contrasting the more limited impact of MAPK inhibition implied from these MCF-7X studies.

4.1.4.3 PKC Isoforms and Src

Protein kinases are an integral part of the network of intracellular signalling, critical to growth, differentiation, motility and survival. PKCs have been implicated as regulatory steps of the PI3K pathway and in enhancement of AP-1 promoter activity (Moscat *et al.*, 2001). PKCs have again been associated with anti-oestrogen failure (Chisamore *et al.*, 2001) and more aggressive forms of breast cancer (Patrick & Heimbrook, 1996). Among these PKCδ and PKCα have been shown to be elevated in tamoxifen resistance (Kruger & Reddy, 2003; Fournier *et al.*, 2001)) and are both increased in our TAMR model, while PKCα has also been linked with ER negativity (Chisamore *et al.*, 2001). Interestingly, PKCδ has also been shown to promote phosphorylation of serine 122 of the mouse (Lahooti *et al.*, 1998) (equivalent to serine 118 in human). However, despite a small increase in PKCδ activity in the MCF-7X cells (versus MCF-7 cells) predominantly within the nuclei [a localisation increasingly linked to promoting therapeutic resistance (Jones *et al.* 2004)], the PKC inhibitor bis-indolylmaleimide (Bis) was without impact on resistant cell growth, in contrast to an inhibitory effect in MCF-7 cells. Furthermore, PKCα was at a lower level in MCF-7X cells versus the parental line. In total, these data suggest that there is no obvious growth regulatory role of PKCs in MCF-7X cells growth, although continued exploration in the future could encompass further PKC isoforms not influenced by this inhibitor.

Downstream kinase recruited in growth factor pathways and contributes to the non-genomic mechanism from Santen *et al.* (2003; 2004a). Also contributes to anti-oestrogen resistant growth signalling and invasive behaviour (part of EGFR/IGF-1R cross talk mechanism in TAMR cells Knowlden *et al.*, 2003a; Hiscox *et al.*, 2005), and can also cross-talk with ERα activity at serine 118. However, despite increased Src activity in MCF-7X, a diminished growth contribution was evidenced by the lack of effect of SU6656, and there was moreover no increase in invasiveness versus the parental line. Collectively, suggesting that Src did not provide a dominant signalling mechanism for MCF-7X cells.

4.2 KINASE DEPENDENT REGULATION OF ERα PHOSPHORYLATION

The human ERα is a phosphoprotein that is hyperphosphorylated in response to steroid binding and associated receptor conformational changes. Phosphorylation residues including the AF-1 residues serine 167 (Ser167ER) and 118 (Ser118ER) have been implicated, but these appear to vary according to cell context (Lannigan 2003). ERα phosphorylation acts to regulate aspects of steroid receptor function, notably transcriptional activation of ER-regulated genes. A number of studies following anti-oestrogen failure have demonstrated growth factor induced kinase ability to target and activate the key regulatory sites on the ERα protein, notably Ser 118 and 167. Previously shown within our own acquired tamoxifen resistant cells is a correlation between substantially increased AF-1 ERα phosphorylation (Ser118ER and Ser167ER) and elevated MAPK and AKT phosphorylation regulated by increased upstream EGFR/HER2/IGF-1R activity (Nicholson *et al.*, 2004a). The growth factor receptor signalling acts via this ligand independent activation of the ERα to enhance coactivator recruitment and subsequently the transcriptional activity of the tamoxifen/ER complex to promote growth. It is conceivable that such kinases might also induce nuclear ERα phosphorylation and thereby transcriptional activity in a ligand-independent manner, facilitating the action of ER as a transcription factor in the steroid-depleted environment. Indeed, transcriptional activity induced by substantial kinase activation of nuclear ERα on Ser118ER (3-fold increase) has been implicated by the Martin/Dowsett model as a mechanism in promoting oestrogen hypersensitivity (Martin *et al.*, 2003). A study by Font de Mora and Brown (2000) revealed MAPK was not only a prime kinase candidate for Ser118ER phosphorylation, but the kinase was involved in transcriptional activity mediated by the coactivator AIB1. In addition they found the AIB1/MAPK relationship increased the recruitment of p300/CBP and its associated histone acetyl transferase (HAT) activity. Reported potential kinase mediators of Ser167ER phosphorylation are AKT, casein kinase II and also MAPK-activated RSK (Arnold *et al.*, 1994; Lannigan, 2003). Again kinase/ER cross-talk reaches another level of complexity. MAPK phosphorylates RSK where in the nucleus it forms a stable complex with p300/CBP which has been shown to regulate transcription (Nakajima *et al.*, 1996). However, Joel *et al.* (1998) have provided data that suggest RSK can also directly phosphorylate Ser167ER thereby mediating transcription. Although coactivator involvement was not measured in the MCF-7X model, this project was able to decipher the impact kinase activity had on the phosphorylation at Ser118ER and

Ser167ER. Using immunocytochemistry, MCF-7X cells were shown to have detectable levels of nuclear ERα AF-1 phosphorylation on Ser167ER and Ser118ER and in parallel with the adaptive increase in ERα expression, there was a ~30% increase in Ser118ER phosphorylation versus the parental MCF-7 cells, although Ser167ER activity was unchanged. The lack of substantial increases in such ERα AF-1 phosphorylation noted in MCF-7X may be a consequence of relatively modest ERα expression and growth factor kinase activity in these cells, as well as the apparent absence of any classical growth factor ligand/receptor input under conditions of oestrogen and serum growth factor depletion.

4.2.1 Absence of MAPK Regulation of ERα Phosphorylation in MCF-7X Model

Challenge with MEK-1 inhibitor PD98059 blocked the phosphorylation of MAPK but barely inhibited MCF-7X cell growth. It was also without inhibitory effect on Ser118ER or Ser167ER activity. There was further indication that any very small contribution for MAPK to growth in MCF-7X cells was direct rather than via nuclear ERα signalling, as PD98059 failed to inhibit ERE transcriptional and endogenous pS2 expression. Moreover, ERα phosphorylation was also not MAPK regulated in MCF-7 cells, alongside lack of impact on ER transcriptional activity and pS2 expression, indicating that the growth contribution of MAPK in MCF-7 cells is again independent of interplay of this kinase with nuclear ERα. In this regard, Ser118ER is reported to be a dominant ligand phosphorylated site in MCF-7 that may occur independently of MAPK (Martin *et al.* 2003) and can perhaps be promoted by CDK7/TFIIH (Joel *et al.*, 1998; Chen *et al.*, 2002; Lannigan, 2003), and so it is feasible that activity of this site may also be promoted by residual steroid hormone in the MCF-7X cells. The Martin/Dowsett oestrogen hypersensitive model has also failed to show any involvement of MAPK activity of Ser118ER phosphorylation. However, contrary to the MCF-7X model the LTED resistant cells did demonstrate a partial contribution from increased MAPK activity to ER transcriptional and growth, an event that they suggest may occur via MAPK regulating ER coactivator activity or additional AF-1 phosphorylation sites (Martin *et al.*, 2003). On a final note, a long-term oestrogen deprived model by Santen describes the basal growth regulation of their cells by MAPK occurs independently of any impact on ER transcriptional activity, although growth stimulation of their cells by exogenous oestrogen appears in part to involve such interplay (Jeng *et al.*, 2000).

4.2.2 PI3K/AKT Dependent Regulation of ERα Phosphorylation at Ser167

Collectively the data revealed in this study demonstrate a prominent contribution for PI3K/AKT signalling in MCF-7X cells. The PI3K inhibitors LY294002 and wortmannin were clearly effective at reducing growth as well as decreasing AKT activity and, in the case of the former inhibitor PDK-1 activity. In parallel they demonstrated a significant inhibitory effect on ERα activity. MCF-7X cells subject to PI3K inhibition showed decreased phosphorylation of ERα by 50% at serine 167 (where total ERα expression and Ser118ER were unaffected). It also partially reduced ERα transcriptional activity with respect to ERE reporter activity and endogenous pS2 expression. It is acknowledged and important to note that studies have previously suggested LY294002 (1-25 μM) may, in equivalence to the anti-oestrogen faslodex, be able to act as a competitive inhibitor of oestrogen binding to the ERα and thereby subvert ERα transcriptional activity. This is in addition to its ability to decrease PI3K/AKT signalling that can influence ERα phosphorylation status and transcriptional activity (Pasapera Limon *et al.*, 2003). However, studies in the present project utilising wortmannin support the latter PI3K/AKT cross-talk with ERα as significant inhibition was again achieved at Ser167ER. Interestingly, an AKT/Ser167ER mechanism has also been reported to contribute to tamoxifen resistance (Campbell *et al.* 2001; Nicholson *et al.* 2004a). Moreover, Martin/Dowsett report LY294002 impacts adversely on ERα transcriptional activity in their LTED model (Martin *et al.*, 2003). Brodie/Sabnis also report their increase in AKT activity shown in UMB-1Ca cells was sensitive to wortmannin treatment and that concomitant immunoprecipitation studies (immunoprecipitation with anti-AKT followed by immunoblot for total ERα) revealed an increased association of AKT/ER (Sabnis *et al.*, 2005) that could also be decreased somewhat by wortmannin, although Ser167ER activity was not measured in this study. In total, these data demonstrate that there is a prominent cross-talk between PI3K/AKT and genomic ERα in MCF-7X cells, where PI3K/AKT regulation of Ser167ER activity appears to play a leading role in undermining the inhibitory effects of oestrogen deprivation on ERα transcriptional activity and growth.

4.3 MAPK AND AKT INDEPENDENT REGULATION OF ERα PHOSPHORYLATION

As noted with the PI3K inhibitor LY294002, Faslodex was substantially growth inhibitory in MCF-7X cells, an event paralleled by significant inhibition of ERE activity as measured using reporter gene construct studies, and of endogenous ER-regulated gene expression (pS2). However, in contrast to LY294002, faslodex treatment was associated with reduced nuclear ERα, and a decrease in Ser118ER phosphorylation. This effect was observed while the anti-oestrogen caused no alteration in Ser167ER activity on the remaining ERα in the cells.

The lack of impact of faslodex on Ser167ER is paradoxical given the partial decrease in ERα protein level achieved with this agent. Thus, faslodex may even be enabling Ser167 activity on the residual ERα in MCF-7X cells. In this regard, Faslodex, and a further pure anti-oestrogen, ICI 164,384, have been previously reported to be able to promote ERα serine phosphorylation, although it is uncertain which AF-1 sites are targets for its action and this may also be cell context specific (Le Goff *et al.*, 1994; Joel *et al.*, 1998; Chen *et al.*, 2002). Potential kinase mediators of Ser167ER phosphorylation in MCF-7X cells are AKT, MAPK-promoted p90 ribosomal S6 kinase (RSK), and casein kinase II (Lannigan 2003). As stated above, the lack of effect of PD98059 and inhibitory impact of LY294002 on Ser167ER phosphorylation (paralleled by inhibitory effects with wortmannin) indicate AKT is the kinase driving Ser167ER activity in MCF-7X cells in the presence of faslodex. How this is achieved remains unknown, since faslodex treatment does not obviously increase AKT activity: perhaps there is in some way improved accessibility of this kinase to the Ser167 residue in the presence of faslodex. Importantly, the observations with faslodex challenge suggest an additional growth importance for phosphorylation of Ser118ER in MCF-7X cells. In the MCF-7X model Ser118ER phosphorylation appears to be independent of MAPK and AKT since faslodex treatment did not alter activity of these kinases. It is possible that activity if this site may be promoted by residual steroid hormone in this model. Ser118ER can comprise a ligand phosphorylated site, and we have previously observed in MCF-7X cells substantial further Ser118ER (but not Ser167ER) activation following oestrogen challenge (data not shown). Martin *et al.* (2003) have also shown ligand stimulated Ser118ER phosphorylation to occur independently of MAPK and PI3K/AKT and others suggest activation of the serine residue may be mediated via CDK7/TFIIH (Joel *et al.*, 1998;

Chen *et al.*, 2002; Lannigan, 2003). Interestingly, the Affymetrix list of induced genes in MCF-7X revealed some increase in TFIIH and CDK7 expression which may facilitate such activity. Since MCF-7X cells nuclear ERα and Ser118ER phosphorylation increased by approximately 20%, it is also feasible that faslodex-driven decreases in ERα protein may be a contributory factor to the reduced Ser118ER phosphorylation observed with this agent.

4.4 TARGETING RESIDUAL ERα PHOSPHORYLATION

The MCF-7X model data indicate that activation of both Ser118ER and Ser167ER contributes to ERα transcriptional activity and growth. Furthermore, non-overlapping regulatory pathways for these ER activity sites have been revealed through treatment challenge with of the pure anti-oestrogen faslodex and the PI3K inhibitors LY294002 and wortmannin. It was thus hypothesised that any phosphorylated ERα remaining when faslodex or LY294002 are applied singly might provide an important compensatory cell survival mechanism, underlying incomplete inhibitory effects on ERα transcriptional activity and growth in MCF-7X cells and ultimately enabling emergence of resistance to each agent after 10 weeks.

In parallel with its depletion of both ERα level and PI3K/AKT signalling, the co-treatment data of faslodex plus LY294002 clearly displayed a decrease in both Ser118ER and Ser167ER phosphorylation. In parallel, there was a superior depletion of ERα transcriptional activity measured by ERE reporter assays after 18hr treatment (although by 7 days this appeared to be equivalent to faslodex), and a superior depletion of pS2 protein. Moreover the combination was associated with a superior (90%) anti-tumour response versus the single agents and an extended duration of growth inhibitory response (25 weeks), where resistant cells were subsequently slower growing than those emerging with the single agents. Again the preliminary growth studies with wortmannin substituted for LY294002 complemented these data. In agreement, studies from Brodie/Sabnis have also shown this latter combination to be an effective growth inhibitory strategy. Their UMB-1Ca cells demonstrated a 40% reduction in proliferation to both wortmannin and faslodex as single agents, however when combined these two compounds imposed an 80% growth inhibitory effect (Sabnis *et al.*, 2005). Clearly, this strategy may have considerable potential for therapeutic exploration in patients who have become resistant to oestrogen deprivation. However, while co-treatment with faslodex plus LY294002 proved a

superior approach compared to the single agents in MCF-7X cells, this strategy was unable to prevent the development of therapeutic resistance (cell growth resumed following 25 weeks continuous culture), heralding that such strategies may not prove maximally effective in the clinic.

Extensive profiling of MCF-7X cells treated with the above combination revealed the cells retained MAPK activity, alongside residual ERα phosphorylation (particularly on Ser118) and ERα transcriptional activity. It was therefore possible that the low levels of MAPK activity unchanged by faslodex or LY294002 treatment were now able to trigger Ser118ER phosphorylation (or coactivator activation initiating transcriptional activity). To assess if it was possible to improve upon the faslodex/LY294002 combination, therefore, the MEK-1 inhibitor PD98059 was added to this strategy which resulted in an improved anti-tumour effect for the triple treatment (again also shown with wortmannin substitution for LY294002). There was marked growth inhibition, and interestingly following approximately 2 weeks of treatment, cell numbers fell below the initial seeding density and by week 16 the culture could no longer be maintained. Thus, this triple treatment had efficiently abrogated emergence of therapeutic resistance. The triple treatment was associated with decreases in ERα expression and AKT activity, as observed with faslodex and LY294002 alone. However, the addition of PD98059 as predicted also targeted MAPK activity. While the decrease in Ser167ER activity was as observed with dual faslodex/LY294002 treatment, importantly there was a superior depletion of Ser118ER. This effect was again associated with marked depletion of ERE activity and endogenous pS2 expression.

Thus, while MAPK activity does not contribute to basal ERα phosphorylation in MCF-7X, it does appear that this kinase interplays with ERα via Ser118ER phosphorylation under conditions of faslodex plus LY294002 co-treatment, an event that contributes to cell survival. The mechanism underlying this new coupling remains unknown. However, it is feasible that the low levels of MAPK activity are now sufficient to trigger Ser118ER phosphorylation because there is effective blockade of the basal ER phosphorylation regulators by faslodex plus LY294002 co-treatment, or alternatively that MAPK access to this site is now enabled because of ERα conformational changes occurring with co-treatment (Lannigan 2003). However, the present study does not appear to advocate a link between growth of

MCF-7X cells and activity of the AP-1 response element in MCF-7X cells. Indeed, both PD98059 alone and triple treatment were equally effective in reducing AP-1 activity in reporter assays, despite a lack of growth inhibitory effect of the former agent. Nevertheless, it remains possible that there is interplay with further response elements though interplay between ER and other transcription factors, perhaps including SP-1 which is a key regulatory element in the cell survival gene bcl-2 (DeNardo *et al.*, 2005).

The project was subsequently able to confirm that inhibition of Ser118ER phosphorylation was required for the catastrophic effects of triple treatment on MCF-7X. Dual treatment with LY294002 plus PD98059 again reduced MAPK and AKT activity and significantly inhibited MCF-7X cell growth. This combination treatment was certainly superior in inhibiting growth versus LY294002 or PD98059 alone. This combination strategy has also been investigated in the LTED models from Santen/Yue and Martin/Dowsett. The Santen/Yue studies revealed in their LTED cells that adaptive hypersensitivity involved the dual activation of PI3K and MAPK signalling pathways, and showed the combination of LY294002/PD98059 shifted the level of oestradiol sensitivity dramatically more than 2 logs to the right (Yue *et al.*, 2003; Santen *et al.*, 2004a). The LTED model of Martin/Dowsett also revealed PI3K/MAPK dual inhibition results in a 70% reduction in basal transcription which was susceptible to partial rescue by high doses of oestradiol (Martin *et al.* 2003). Importantly, this combination applied to the MCF-7X non-oestrogen hypersensitive model confirmed that inhibition of Ser118ER phosphorylation is required for the catastrophic effects of the triple treatment. However, in MCF-7X cells, Ser118ER phosphorylation was unaffected and the cells survived LY294002 plus PD98059 co-treatment, resulting in resistance emerging following 12 weeks of continuous treatment in marked contrast to the triple treatment where faslodex that targets ER. These studies in MCF-7X demonstrate that combination therapy to target all regulators of ER AF-1 phosphorylation (i.e. PI3K/AKT inhibitor plus MAPK inhibitor plus faslodex in MCF-7X) may be required to eradicate the cell survival mechanism in cells refractory to oestrogen deprivation, and prevent subsequent emergence of therapeutic resistance.

4.5 MCF-7X RESISTANT SUB-LINES: RATIONAL FOR COMBINATION THERAPY

4.5.1 Faslodex Response and Development of Resistance

The pure anti-oestrogen faslodex is involved in several clinical trials as a single strategy following tamoxifen or aromatase inhibitors (NCCTG and SAKK) or in combination with aromatase inhibitors (FACT, SOFEA, and SWOG 226) (Johnston *et al.*, 2005)]. There is an abundance of experimental data that suggest the substantial retained ERα following oestrogen deprivation is faslodex sensitive, and therefore this agent is a logical choice of treatment following or concurrent with an aromatase inhibitor/inactivator. Investigation of the MCF-7X cells similarly revealed significant faslodex growth sensitivity. This was paralleled by the drug decreasing nuclear ERα and its phosphorylation at Ser118 (via influencing a kinase other than MAPK or AKT), coupled with a reduction in ERα transcriptional activity and endogenous pS2 expression. These are all reasonable alterations considering the compound binds ERα to adversely impact on its activity as a nuclear transcription factor and leads to receptor degradation (Figure 4.2A). Other *in vitro* models of long-term oestrogen deprivation have also been used to investigate short-term faslodex treatment and again suggest it as a viable therapeutic intervention. However, based on the MCF-7X cell data reported here, there is strong indication that such a strategy will not be fully-effective in tumours resistant to oestrogen deprivation. Indeed, breast cancer cells resistant to oestrogen deprivation seem able to ultimately evade the substantial ERα inhibitory effects of faslodex and furthermore promote an adverse phenotype in the presence of this agent. Thus, while the faslodex responsive phase in MCF-7X cells lasted 10 weeks, a cohort of tumour cells survived this strategy and subsequently became faslodex resistant. The incomplete inhibition was associated with a failure to deplete AKT-driven Ser167ER phosphorylation and thus incomplete block of ERα transcriptional activity. Characterisation of the faslodex resistant oestrogen deprived X(FAS) phenotype showed a disconcerting increase in aggressive behaviour [(increased cellular motility and to a lesser extent invasive capacity) (Figure 4.2B)]. It seems likely that the emergence of faslodex resistance and the associated disease progression was driven by the substantial gains in expression of the classical growth factor receptors EGFR, HER2 and IGF-1R observed in the X(FAS) cells and subsequent increased downstream kinase activity, in particular MAPK that is known to promote growth and motility of cells (Kruger & Reddy, 2003).

The increases in EGFR (coupled with more modest HER2 increases) began early during targeting of ERα in MCF-7X cells with faslodex during response. These increases had become very substantial by the time of emergence of X(FAS) resistant cells. Such increases have also been previously reported (Gee *et al.*, 2003) to arise during treatment with anti-oestrogens such as tamoxifen and faslodex in ER+ endocrine responsive cells such as MCF-7 that express only low levels of EGFR/HER2 prior to treatment. The event has been linked with anti-oestrogen-mediated de-repression of an oestrogen/ER inhibitory effect at the first intron in the promoters of these genes (Chrysogelos *et al.*, 1994), where the EGFR/HER2 expression gain is maximised and growth contributory by the time of emergence of anti-oestrogen resistance (Knowlden *et al.*, 2003b). The observation that EGFR/HER2 expression are not elevated in MCF-7X cells basally indicates that the ER blockade in MCF-7 cells as a consequence of steroid hormone depletion in the X medium, in contrast to the effect of the pure anti-oestrogen faslodex, is insufficient for this de-repressive event. The mechanism of anti-oestrogen induction of genes normally repressed by oestrogen/ER signalling remains poorly-characterised, but may not involve influences at ERE-like sites in the EGFR or HER2 genes. One proposed explanation is that anti-oestrogen treatment prevents non-classical ER protein/transcription factor interactions that normally transrepress gene expression from response elements such as NFkB (Zhou *et al.*, 2005). A second is that anti-oestrogen treatment may free-up coactivators normally promoted to the ERE in the presence of oestrogen, so these are now available to activate alternative response elements (Oesterreich *et al.*, 2001). Whatever the underlying molecular mechanism, the EGFR/HER2 gains during anti-oestrogen treatment, including faslodex, can provide a cell survival mechanism that limits maximal anti-tumour response and maintains the cohort of cells from which resistance (TAMR or FASR cells) subsequently emerge (Gee *et al.*, 2003; Yarden *et al.*, 2001). These events appear likely to be equally contributory to acquisition of resistance by the MCF-7X line and subsequent maintenance of X(FAS) cells.

As we have observed in the acquired TAMR and FASR cells developed from MCF-7 (Knowlden *et al.*, 2003b; McClelland *et al.*, 2001), the substantial gain in EGFR/HER2 signalling in X(FAS) was also paralleled by a very marked rise in phosphorylated MAPK and some increase in AKT activity, presumably downstream of the elevated growth factor receptors. Interestingly, these alterations were

associated with a substantial increase in Ser167ER activity in X(FAS) cells versus untreated MCF-7X cells, and while Ser118ER activity remained lower it was nevertheless also detectable. In parallel with this re-activation of ER, there was substantial recovery in ER-regulated gene (pS2) expression. It seems likely that the recovery in ER signalling seen in X(FAS) cells is driven by the increased growth factor receptor-promoted kinases triggering ER phosphorylation. In support of this concept, we have previously noted that in acquired TAMR cells, increased EGFR/HER2 drives phosphorylation of MAPK and AKT that in turn re-activate ER on both Ser118 and Ser167 to promote ER-regulated EGF-like ligand expression (Britton *et al.*, 2006). This supports an autocrine mitogenic EGFR signalling loop in such cells that may also prove relevant in X(FAS) cells (Britton *et al.*, 2006). In addition, re-activation of ER results in expression of IGF-1R signalling components that in turn further enhance the EGFR pathway (Knowlden *et al.*, 2003a). Similarly, in our acquired FASR model developed from MCF-7 cells, we have seen increases in EGFR/HER2 signalling (McClelland *et al.*, 2001) that again promote downstream kinase activity to maintain phosphorylation on residual ERα in such cells, and IGF-1R signalling is also detectable in such cells. It is again possible that the reactivation of ERα in X(FAS) cells underlies their substantial gain in IGF-1R. The observation that EGFR/HER2 is not subsequently repressed on re-instigation of substantial ERα activity in the X(FAS) cells suggests the mechanism of expression of these receptors is indeed independent of an ERE mechanism.

Encouragingly, in both our acquired TAMR and FASR models, growth can be substantially inhibited by targeting the increased growth factor receptor signalling loop, for example using gefitinib (Knowlden *et al.*, 2003b, McClelland *et al.*, 2001) that is currently being explored in endocrine resistance through several clinical trials (Johnston *et al.*, 2003; 2005). While not examined in the present study, one might similarly envisage that targeting of the increased EGFR/HER2/IGF-1R (and MAPK/AKT kinase signalling) could provide an inhibitory strategy for X(FAS) cells, where this project suggests this should be of superior benefit compared with the oestrogen deprived-resistant (MCF-7X) phase. Excitingly, our studies in TAMR cells indicate that such depletion of the elevated growth factor receptor signalling also has potential to decrease aggressive cellular behaviour. Targeted growth factor receptor or MAPK/AKT inhibition could similarly prove useful in limiting this adverse feature in oestrogen deprived cells that have acquired resistance to faslodex. Interestingly, a

further key element to growth and invasive behaviour in TAMR (and possibly FASR) cells that can be targeted is Src (Hiscox *et al.*, 2005), and it thus it would be interesting to examine in the future if the contribution of this non-receptor tyrosine kinase is also enhanced on acquisition of faslodex resistance by MCF-7X cells. Finally, since EGFR/HER2 increases begin early during faslodex treatment and may, via MAPK and AKT, sustain the residual Ser118ER and also the substantial levels of Ser167 in the presence of this agent, it is possible that combined treatment of faslodex plus agents such as gefitinib (or relevant kinase inhibitors as shown in this project) will provide a superior strategy to faslodex alone in oestrogen deprivation resistance and could subvert emergence of the more aggressive X(FAS) phenotype. Certainly, we have observed that in MCF-7 such co-treatment can block the increased EGFR and residual kinase activity during anti-oestrogen treatment, more effectively deplete ERα activity and subsequent ER-regulated cell survival gene expression (i.e. bcl-2), and improve anti-proliferative and pro-apoptotic effects versus tamoxifen or faslodex alone. There is consequently an enhanced anti-tumour response and a delay in/prevention of emergence of resistance (Gee *et al.*, 2003). Similarly, in our TAMR cells we have shown that a combined treatment of faslodex with gefitinib is again more effective than either single agent in depleting ER phosphorylation, exerting an improved anti-tumour response and preventing subsequent acquisition of resistance (Nicholson *et al.*, 2005).

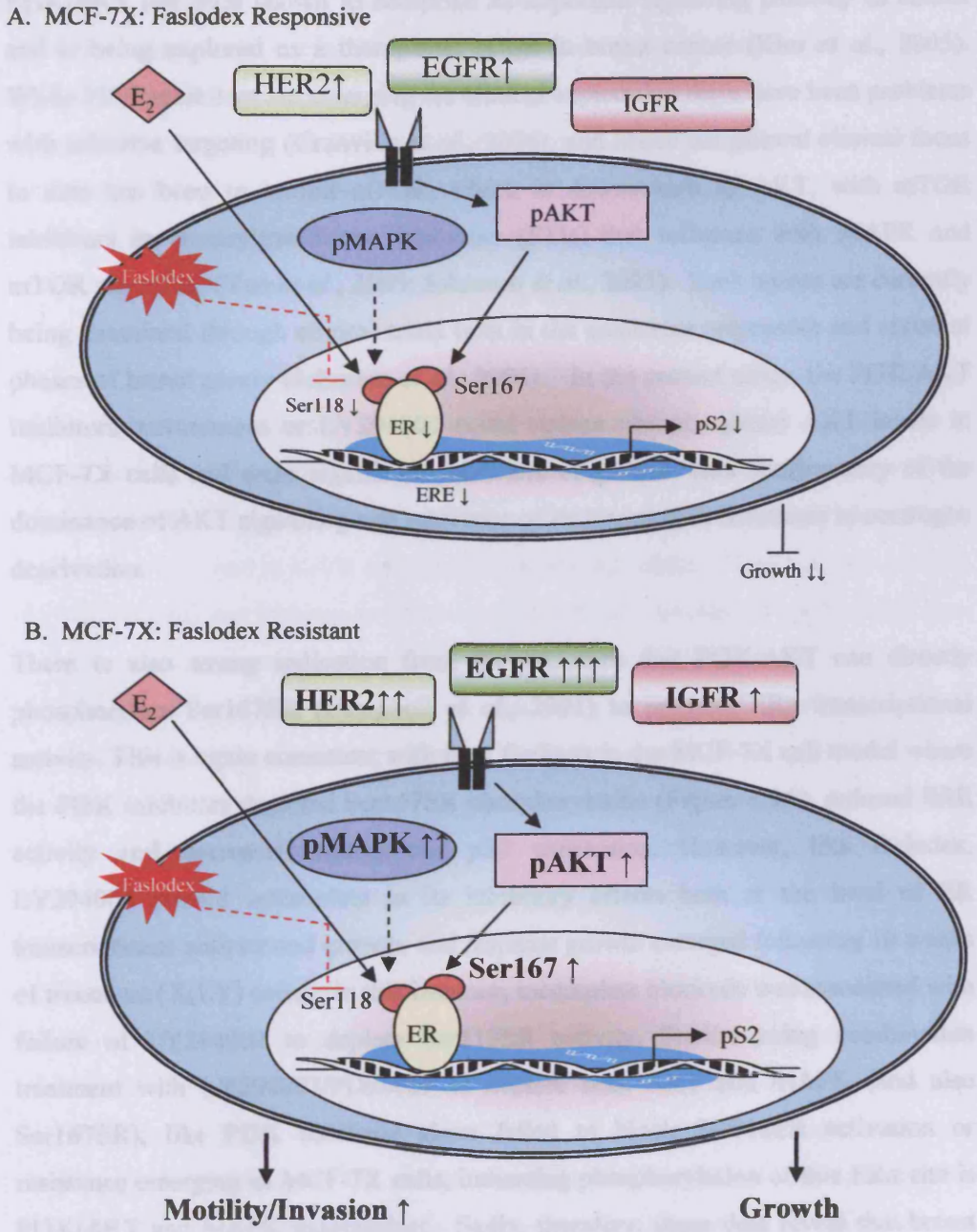

Figure 4.2 Schematic illustration of faslodex responsive (A) and faslodex resistant (B) MCF-7X cells. Above illustrates the changes MCF-7X cells undergo during short term faslodex treatment (A) and when MCF-7X cells become resistant to faslodex (B).

4.5.2 LY294002 Response and Development of Resistance

PI3K/AKT has been shown to comprise an important signalling pathway in cancer and is being explored as a therapeutic target in breast cancer (Kim *et al.*, 2005). While PI3K inhibitors are emerging for clinical exploration there have been problems with selective targeting (Granville *et al.*, 2006), and hence the general clinical focus to date has been to inhibit mTOR, which is downstream of AKT, with mTOR inhibitors or farnesyltransferase inhibitors (FTIs) that influence both MAPK and mTOR signalling (Yue *et al.*, 2005; Johnston *et al.*, 2005). Such agents are currently being examined through clinical trials both in the endocrine responsive and resistant phases of breast cancer (Johnston *et al.*, 2005). In the present study, the PI3K/AKT inhibitors wortmannin or LY294002 could reduce phosphorylated AKT levels in MCF-7X cells and were significant inhibitors of growth, data confirmatory of the dominance of AKT signalling and relevance of its targeting in resistance to oestrogen deprivation.

There is also strong indication from the literature that PI3K/AKT can directly phosphorylate Ser167ER (Campbell *et al.*, 2001) to promote ERα transcriptional activity. This is again consistent with the t findings in the MCF-7X cell model where the PI3K inhibitors depleted Ser167ER phosphorylation (Figure 4.3A), reduced ERE activity and decreased endogenous pS2 expression. However, like faslodex, LY294002 proved incomplete in its inhibitory effects both at the level of ER transcriptional activity and growth, and resistant growth emerged following 10 weeks of treatment [X(LY) cells]. In this instance, incomplete blockade was associated with failure of LY294002 to deplete Ser118ER activity. Studies using combination treatment with LY294002/PD98059 to deplete both AKT and MAPK (and also Ser167ER), like PI3K blockade alone failed to block Ser118ER activation or resistance emerging in MCF-7X cells, indicating phosphorylation of this ERα site is PI3K/AKT and MAPK independent. Sadly, therefore, these data reveal that breast cancers resistant to oestrogen deprivation may again ultimately be able to bypass therapeutic inhibition of the key mitogenic pathway PI3K/AKT, as well as any agent that blocks both PI3K/AKT signalling and MAPK, to reinstate resistant growth. The survival mechanism in both instances appears to involve residual oestrogen/Ser118ER signalling and the data thus support combination strategies that include faslodex for maximal depletion of ERα activity.

Interestingly, during the LY294002 responsive phase in MCF-7X cells there was no increase in HER2 or EGFR expression. Thus, despite decreased Ser167ER and ER transcriptional activity during PI3K inhibition, this appears insufficient to de-repress expression of the growth factor receptor genes, in contrast to faslodex treatment. This may indicate that depletion of ligand-promoted Ser118ER activity, or alternatively functional PI3K signalling, is essential for increases in EGFR/HER2 to arise during treatment, and also suggests only limited value of inclusion of anti-growth factor receptor agents in this phase in the absence of faslodex.

While apparently of limited relevance to cell survival during the LY294002 responsive phase, it seems likely that maintenance of X(LY) resistant growth was at least in part due to increased EGFR and HER2, and their promotion of kinase activity. Although the increase in EGFR and HER2 expression were modest in X(LY) cells no comparative increase in IGFR membrane staining was noted. However, X(LY) cells showed a significant increase in phosphorylated MAPK versus the parental cell line. However, there were much larger changes observed for all three receptors and MAPK in X(FAS) cells, possibly explaining why the X(LY) cells failed to exhibit increased aggressive behaviour. Interestingly, X(LY) cells also recovered their AKT activity, a somewhat surprising observation given that LY294002 should deplete such signalling. Hence increased MAPK activity in X(LY) cells, perhaps EGFR/HER2-driven, may underlie their apparently PI3K inhibitor-refractory phosphorylation of AKT and growth. (Figure 4.3B). This appears to contrast the basal input for AKT activity in MCF-7X cells, which is not driven by classical growth factor receptor or MAPK since such receptors are only at very low levels in untreated MCF-7X cells while PD98059 exerts no impact on this kinase or growth under basal conditions. In parallel with the gains in MAPK and recovery of AKT in X(LY) cells, there was recovery in Ser167ER activity, alongside retained levels of Ser118ER presumably driven by ligand–promoted ERα. This reinstating of ERα activity in resistance was associated with recovery (and marginal increase) in pS2 expression. It thus seems that oestrogen deprivation resistant cells can ultimately fully re-activate their ERα signalling and growth following treatment with a PI3K inhibitor, although it remains unclear why this does not in turn promote substantial expression of the ER-regulated IGF-1R (other than small cytoplasmic increases).

The data suggest that treatment with agents targeting EGFR/HER2 may be of some value in established oestrogen deprived, PI3K resistant cells if such signalling does indeed lie upstream of the recovered MAPK/AKT and Ser167ER activity in X(LY) cells. Addition of MAPK inhibition may also be valuable. However, LY294002 in combination with PD98059 again failed to block Ser118ER activation in MCF-7X cells and could not prevent resistance from ultimately emerging. Moreover, the resultant phenotype, X(LY/PD), was in many ways comparable with that of cells resistant to PI3K inhibitor alone (i.e. modestly increased EGFR, little effect on HER2, some recovery in MAPK and increased AKT activity, retained Ser118ER phosphorylation, recovered Ser167ER activity and a marginal increase in pS2 expression versus untreated MCF-7X cells). These data reiterate the necessity to include faslodex in any combination treatment strategy for resistance to oestrogen deprivation in order to eliminate ligand-promoted Ser118ER phosphorylation for more effective growth inhibition.

A. MCF-7X: LY294002 Responsive

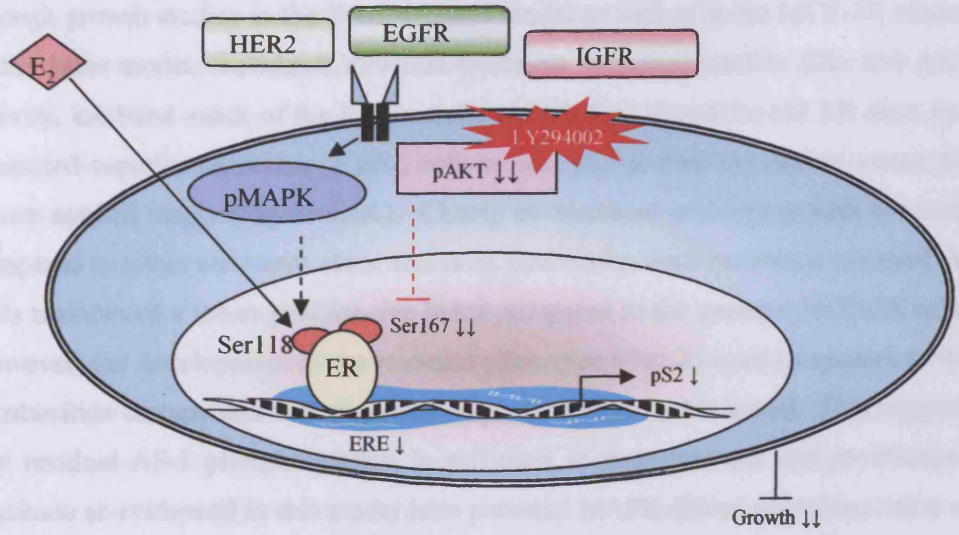

B. MCF-7X: LY294002 Resistant

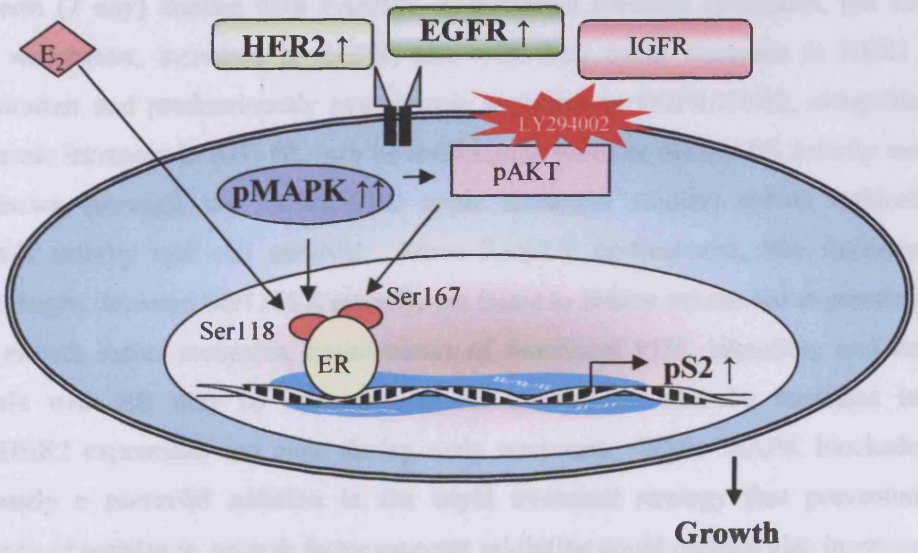

Figure 4.3 Schematic illustration of LY294002 responsive (A) and LY294002 resistant (B) MCF-7X cells. Above illustrates the changes MCF-7X cells undergo during short term LY294002 treatment (A) and when MCF-7X cells become resistant to LY294002 (B).

4.5.3 Faslodex/LY294002 Co-treatment Response and Development of Resistance

The combination of a PI3K inhibitor with pure anti-oestrogen has proven a superior treatment strategy for several models resistant to oestrogen deprivation, as observed through growth studies in the Brodie/Sabnis model as well as in the MCF-7X model. In the latter model, faslodex/LY294002 treatment decreased nuclear ERα and AKT activity, inhibited much of the ERα activity at both Ser118 and Ser167 ER sites, and promoted superior reduction in ERE activity and pS2 protein expression versus the agents applied singly (Figure 4.4A). Clearly co-treatment prolongs growth blockade compared to either treatment alone and most noteworthy once resistance emerged the cells maintained a lower proliferative index compared to the parental MCF-7X cells. However, the development of the resistant phenotype after 25 weeks exposure to the combination therapy demonstrated marked plasticity within this model. This suggests any residual AF-1 phosphorylation is sufficient to overcome the anti-proliferative blockade as evidenced in this model here potential MAPK-driven phosphorylation of Ser118 ER when inhibited by the triple treatment with FAS/LY/PD negates growth.

Short term (7 day) studies with FAS/LY co-treatment revealed cytoplasm, but no plasma membrane, increases in EGFR, also with only small increases in HER2. These modest and predominantly cytoplasmic increases in EGFR/HER2, alongside cytoplasmic increases in IGF-1R, may be sufficient to promote the MAPK activity we have shown (through the FAS/LY/PD triple treatment studies) drives residual Ser118ER activity and cell survival. Since FAS/LY co-treatment, like faslodex applied singly, depleted Ser118ER activity, yet failed to induce substantial expression of the growth factor receptors, maintenance of functional PI3K signalling and its cross-talk with ER may be important to the mechanism whereby increases in EGFR/HER2 expression can arise during early treatment. While MAPK blockade was clearly a powerful addition in the triple treatment strategy that prevented emergence of resistance, growth factor receptor inhibition could perhaps also improve FAS/LY response. However, the rational for this latter strategy is perhaps not as obvious as in improving response to faslodex alone, where more significant increases in growth factor receptor expression arise during treatment with this anti-oestrogen. Subsequent profiling of the faslodex/LY294002 MCF-7X resistant cells [X(FAS/LY)] revealed some similarity to the X(FAS) cells in that there were large increases in the classical growth factor receptors EGFR and IGF-1R. However, HER2 increases were minor and the X(FAS/LY) cells did not exhibit aggressive behaviour,

in obvious contrast to the X(FAS) cells, an observation implying that it is increased HER2 that is particularly required for disease progression during treatment of oestrogen deprivation resistant cells. Thus concept is in keeping with observations made by Sabnis *et al.* in UMB1-Ca cells (2005) and clinical links between increased HER2 and poor prognosis (De Lorenzo *et al.*, 2002; Gee *et al.*, 2005). In parallel with the marked increases in EGFR and IGF1R, both phosphorylated MAPK and AKT (presumably again MAPK/RSK-driven) were increased in X(FAS/LY) cells versus MCF-7X, and there was similarly recovery of both Ser118ER and Ser167ER phosphorylation so that their levels exceeded MCF-7X cells. There was clearly also a gain in ERα transcriptional activity as measured by substantial recovery of pS2 expression. Thus, ERα signalling has again been fully reactivated on emergence of resistance to co-treatment, perhaps underlying the substantial increases in IGF-1R expression also noted in such cells (Figure 4.4B). Cumulatively, the data suggest that treatment with a MAPK inhibitor, or perhaps blockade of upstream EGFR or IGF-1R, would be valuable after long-term FAS/LY treatment.

A. MCF-7X: Faslodex/LY294002 Responsive

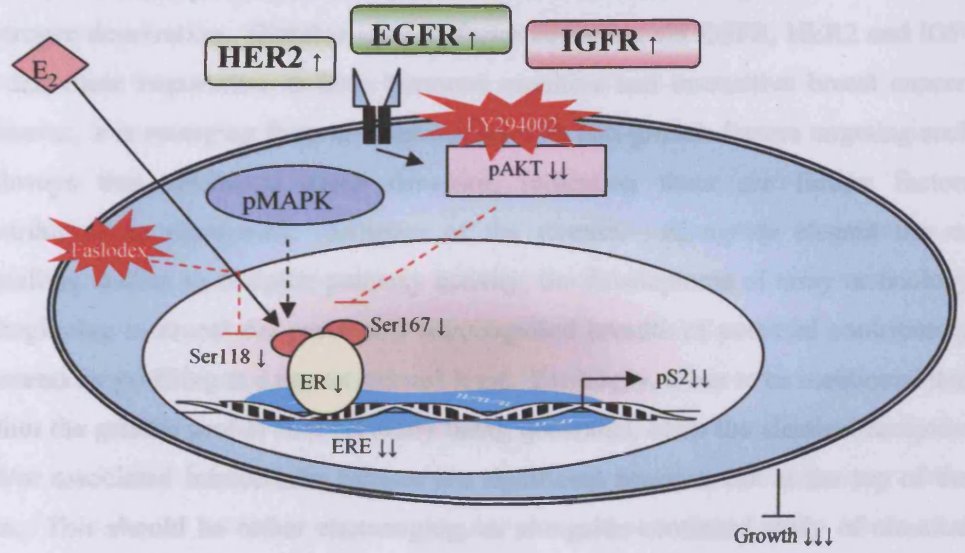

B. MCF-7X: Faslodex/LY294002 Resistant

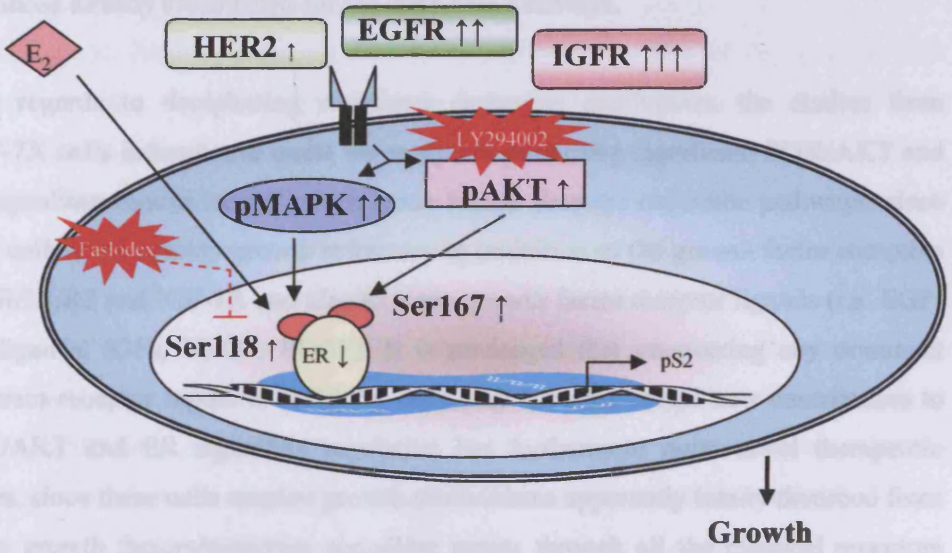

Figure 4.4 Schematic illustration of faslodex/LY294002 responsive (A) and faslodex/LY294002 resistant (B) MCF-7X cells. Above illustrates the changes MCF-7X cells undergo during short term faslodex/LY294002 treatment (A) and when MCF-7X cells become resistant to faslodex/LY294002 (B).

4.6 POTENTIAL RECEPTOR CONTRIBUTION TO MCF-7X CELL GROWTH

Ultimately, by further understanding inherent resistance mechanisms, we can determine effective treatment strategies for cells that have acquired resistance to oestrogen deprivation. Classical growth factor signalling via EGFR, HER2 and IGF-1R has clear importance in both hormone sensitive and insensitive breast cancer. However, it is emerging from clinical studies with anti-growth factors targeting such pathways that resistance again develops, indicating there are further factors contributory to therapeutic resilience of the disease. Alongside elegant use of signalling studies to decipher pathway activity, the development of array technology is beginning to reveal the previously unrecognised breadth of potential contributory elements by profiling at a transcriptional level. Excitingly, it has to be mentioned that within the genetic profile lists currently being generated, often the classical receptors and/or associated intracellular kinases are significant however not at the top of the lists. This should be rather encouraging, as alongside continued study of classical signalling pathways, future research can now also begin to piece in the new elements ultimately optimising and integrating any emerging novel targeting strategies together with those already established for the candidate pathways.

With regards to deciphering resistance oestrogen deprivation, the studies from MCF-7X cells indicate our quest for receptors promoting significant PI3K/AKT and ER signalling should indeed sweep much further than the candidate pathways, since these cells were notably growth refractory to inhibition of the growth factor receptors EGFR/HER2 and IGF-1R and also to many growth factor receptor ligands (i.e. EGF-like ligands, IGFs, VEGF, PDGF). It is envisaged that uncovering any dominant upstream receptor inputs in MCF-7X cells may not only reveal new contributors to PI3K/AKT and ER signalling regulation but furthermore quite novel therapeutic angles, since these cells employ growth mechanisms apparently totally divorced from serum growth factors/autocrine signalling inputs through all the classical receptors examined in this project. As such, the observation that 207 of the gene probes representing aspects of receptor activity were induced in MCF-7X using Affymetrix with GeneSifter® analysis clearly should provide a valuable future resource to uncover such novel mechanisms and to evaluate their targeting potential. In this regard, the present project has initially focussed around examining 3 interesting induced receptors, FGFR-4, EphA3 receptor and transferrin receptor.

4.6.1 Contribution of FGFR-4 Signalling to MCF-7X Cell Growth

The Affymetrix data revealed a marked, significant increase in fibroblast growth factor receptor-4 (FGFR-4) expression in MCF-7X cells. This is interesting since over expression of FGFR-4 has been detected in approximately 30% of breast cancers, correlates to a poor patient prognosis and can contribute to cell proliferation, cell survival and migration (Penault-Llorca *et al.*, 1995). Studies have shown activation of FGFR-4, like EGFR, HER2 and IGF-1R, initiates MAPK and PI3K/AKT downstream signalling (Klint & Claesson-Welsh, 1999). A current study by Koziczak and Hynes (2004) suggests increased FGFR-4 and HER2 control both MAPK and PI3K signalling which enhance S6K1 and 4E-BP1 phosphorylation, thereby cooperatively regulating the activity of the mTOR pathway. In this study, it was shown that either targeting FGFR-4/HER2 (PD173074 and PKI166 respectively) or MAPK/PI3K/AKT (UO126 and wortmannin respectively) simultaneously caused a complete block of S6K1 activity. These data are complementary of the Santen/Yue data which indicate mTOR as the nodal point of MAPK and PI3K/AKT signalling and therefore a strategic therapeutic target (Yue *et al.*, 2005).

Unfortunately, however, the MCF-7X cell Affymetrix data revealed very little expression of the natural ligands FGF1 or -2, and moreover growth of MCF-7X cells could not be stimulated by exogenous addition of these growth factors. In the absence of a selective inhibitor for FGFR-4 in this study, it is hard to definitively rule out a growth contribution for such signalling and this is clearly required in the future. Nevertheless, if MAPK and PI3K/AKT are the predominant signalling kinases involved following activation of FGFR-4, the MCF-7X oestrogen deprived model already suggests residual ERα activity at Ser118 would remain a critical concern if treating cells with an FGFR-4-selective agent, and thus again that combination treatment with faslodex to maximally deplete ERα activity would be required.

4.6.2 Contribution of EphA3 Receptor Signalling to MCF-7X Cell Growth

It was not completely naïve to consider at least one member of the ephrin receptor family would be singled out as induced by the MCF-7X cell Affymetrix analysis as this does comprise the largest receptor tyrosine kinase group. The group are transmembrane receptors, activated by clustered, membrane-bound ligands, where activation relies on cell-cell interactions. Their signalling is complex, but many of the downstream signalling pathways from such receptors converge on the

cytoskeleton (Kullander & Klein, 2002). Interestingly, the Affymetrix array data revealed ephrin A3 receptor (EphA3) was markedly and significantly increase in MCF-7X cells (versus MCF-7 cells). Ephrin A3 receptor has been linked with tumour progression and so has potential to positively contribute in MCF-7X cells, although it has also been described as a tumour/invasion suppressor (Fox & Kandpal, 2004). Unfortunately, the observation of increases in this receptor were paralleled by virtually no expression of ephrin A5 and A2, and while detectable, in MCF-7X cells there were lower levels versus the parental MCF-7 cells for the further natural ligands of this receptor, ephrin-A3 and ephrin-A4. Nevertheless, since these data are the first demonstrating increased EphA3 receptor in oestrogen deprived resistant breast cancer, and since the various ephrin receptors themselves can also act as ligands and their signalling is likely to depend on the tumour cellular microenvironment (Kullander & Klein, 2002), more detailed deciphering, including selective inhibition, remains important for the future to investigate if there is indeed any contribution to this resistant state. There has certainly been some interest in further members of this receptor family in breast cancer, where emerging data indicates some associations with aggressive cellular behaviour and poor outlook. For example, there are a number of *in vitro* studies implicating over expression of EphA2 in non-neoplastic epithelia (Paine *et al.*, 1992; Pauley *et al.*, 1993) and metastatic breast cancer cells (Price 1996). Furthermore a more recent *in vivo* study from Zelinski *et al.* (2001) revealed over expression of the EphA2 receptor in approximately 40% of their breast cancer clinical specimens. EphA2 has been shown to interact and/or enhance cell signalling via FAK, SHP-2 and PI3K (Miao *et al.*, 2000; Pandey *et al.*, 1994). Suggested factors that can contribute to increases of EphA2 include Ras oncogene, E-cadherin (Zantek *et al.*, 1999), members of the p53 family of transcriptional regulators, DNA damage, and interestingly loss of oestrogen receptors and c-Myc (Zelinski *et al.*, 2002). The latter association might explain why EphA2 also did not appear in our Affymetrix profiling as oestrogen receptor and c-Myc were both increased somewhat in MCF-7X cells.

4.6.3 Contribution of Transferrin Receptor Signalling to MCF-7X Cell Growth

Characterised fifty years ago, transferrin (Tf) is an important iron-transport protein and therefore an essential component for iron metabolism. Iron is essential for cell growth and metabolic processes including enzyme function, oxygen transport, DNA synthesis and electron transport and in turn proliferation and also cell survival. Iron

is taken into cells by high-affinity binding of iron-loaded transferrin to its receptor (TfR) with receptor-mediated endocytosis of monoferric and diferric transferrin. Thus, after binding to its receptor on the cell surface, transferrin is rapidly internalised by invagination of clathrin- coated pits with formation of endocytic vesicles (Elliott *et al.*, 1993). TfR expression is controlled by the amount of iron required by the cell to maintain its metabolism. This receptor is expressed on rapidly dividing cells, with 10,000 to 100,000 molecules per cell, commonly found on highly proliferative tumour cells or cells in culture (Inoue *et al.*, 1993). Interestingly, breast cancer cells have previously been shown to produce Tf and express TfR an event that in improving iron delivery may facilitate proliferative events (Vandewalle *et al.*, 1989), and again TfR correlates with proliferative capacity in clinical breast cancer (Wrba *et al.*, 1989). Antisense inhibition of TfR or selective antibodies to this receptor inhibit cell survival and proliferation in breast cancer models showing its fundamental growth importance to such cells (Yang *et al.*, 2001) and there has been some interest in this avenue for cancer therapeutics.

Interestingly, the MCF-7X model revealed significantly increased transferrin receptor levels by Affymetrix analysis, verified at the PCR level and subsequently at the protein level, coupled with detectable autocrine production of transferrin (also observed in MCF-7 cells; Vandewalle *et al.*, 1989). There was a markedly superior mitogenic response to exogenous transferrin challenge (associated with down regulation of transferrin receptor) in the MCF-7X cells. We surmised, therefore, that it is feasible that increased TfR may facilitate MCF-7X resistant cell growth under oestrogen and growth factor depleted conditions by improving iron delivery and thereby aiding mitogenic signalling pathways in such cells (i.e. AKT/ER), ultimately conferring a selective growth advantage. While not examined at the protein level, the increase in TfR mRNA expression appeared to begin during exposure of the parental MCF-7 cells with oestrogen/growth factor depleted medium, an observation that has been previously reported in other cell models in response to very low concentrations of fetal calf serum in media. The finding of increased TfR in MCF-7X cells may have clinical relevance, since TfR has been shown to alter during disease progression (Elliott *et al.*, 1993; Inoue *et al.*, 1993), and the Tenovus laboratories have obtained preliminary data showing increase TfR mRNA associates with elevated proliferative activity and poorer patient survival in clinical disease.

Growth studies supported the concept of significant positive TfR/PI3K interplay in MCF-7X cells (a feature clearly not apparent for MAPK since there was no significant impact of the MEK-1 inhibitor PD98059). The MCF-7X model revealed that PI3K inhibition by LY294002 could fully interfere with transferrin-induced growth, so growth was depleted to a level equivalent to that following LY294002 treatment of MCF-7X cells under control conditions. However, transferrin treatment imposed a negative effect on AKT as well as MAPK activity in MCF-7X cells as measured by immunocytochemistry. The pure anti-oestrogen faslodex was also able to fully abrogate transferrin stimulated growth, again suggesting positive cross talk between TfR and ERα. However, transferrin treatment imposed a negative effect on nuclear ERα, causing slightly reduced ERα levels, diminished Ser167ER activity (with no impact on Ser118ER) and reduced pS2 expression.

In total, these data suggest that transferrin receptor is not the positive upstream regulator of kinase or ERα signalling in MCF-7X cells. Indeed, some negative cross talk is suggested, where depletion of AKT activity (alongside a modest decline in ERα level) is likely to result in the depleted Ser167ER activity and reduce ER-regulated gene expression, effects that in total may serve to limit excessive growth responses in the presence of transferrin. Transferrin/transferrin receptor trafficking has been closely associated with the intracellular kinase PI3K (Jess *et al.*, 1996), where inhibitors of the kinase can deplete cell surface TfR level, and this observation may explain the apparent interplay with PI3K/AKT revealed using LY294002. Similarly, oestrogen signalling has been shown to regulate transferrin/TfR (Vyhlidal & Safe, 2002; Vandewalle *et al.*, 1989), although this was not apparent at the level of TfR expression using faslodex in the present study.

4.7 CONCLUSIONS, THERAPEUTIC IMPLICATIONS AND OPTIONS FOR INTELLIGENT THERAPY

These studies in MCF-7X cells reveal the high level of flexibility of the breast cancer cell when key growth-promoting pathways are blocked. Thus, breast cancer cells can clearly survive the rigors of oestrogen deprivation and of a severely reduced growth factor environment. However, while resistance to oestrogen deprivation can evolve in the absence of exogenous growth factors in MCF-7X cells, their primarily

autocrine input appears insufficient to support development of oestrogen hypersensitivity. This feature may relate to the lack of input from classical growth factor receptors and only modestly altered kinase signalling versus the parental cells. There does not seem to be a significant dominant contribution of EGFR, HER2 or IGF-1R to the basal growth of MCF-7X cells, and so these findings would suggest that agents targeting these pathways would not be fully effective as treatments when used singly in tumours resistant to oestrogen deprivation, or indeed when used in combination with oestrogen deprivation strategies. Moreover, while there may be some role for the significantly increased FGFR-4, EphA3 and transferrin receptors, further investigation (i.e. ligand profiling/challenge studies) has suggested these inputs are unlikely to be the key upstream positive growth regulators under basal conditions. Thus, future detailed investigation of any further receptors identified by Affymetrix microarray analysis remains important to fully decipher this resistant state and design improved tyrosine kinase inhibitory approaches.

Importantly, the MCF-7X model has consolidated the central importance of increased ERα signalling (in this instance, apparently classical genomic) in resistance to oestrogen deprivation, alongside several previous LTED models generated in the presence of serum growth factors. The data cumulatively are supportive of use of faslodex in acquired resistance to oestrogen deprivation, where in MCF-7X cells this agent depletes nuclear ERα, decreases Ser118ER phosphorylation (maintained by as yet unknown kinases triggered by residual oestrogen) and ERα transcriptional activity, and inhibits growth for a reasonably long duration in culture. Excitingly, faslodex responses following clinical acquisition of resistance to aromatase inhibitors are now being described (Johnston, 2004). The Martin/Dowsett LTED *in vitro* model (Martin *et al.*, 2003; 2005) has already inspired the SOFEA clinical trial which is comparing progression-free survival in patients who have progressed on a non-steroidal aromatase inhibitor and subsequently treated with faslodex plus anastrozole or faslodex alone. The study will also address the comparison of the steroidal aromatase inactivator exemestane versus faslodex examining biological markers of response (Johnston *et al.*, 2005) and given the promising faslodex responses noted in MCF7-X cells, the results of this clinical study are eagerly anticipated.

Deciphering of MCF-7X cells has furthermore identified a key contribution for intracellular kinase signalling, primarily PI3K/AKT rather than MAPK to the growth

of cells that have acquired resistance to oestrogen deprivation. As stated above, the identity of the upstream receptor activators of this kinase basally remains as yet unknown. Again, nuclear ERα plays a central role in this growth mechanism, with PI3K/AKT cross-talking closely with this receptor via phosphorylation of its AF-1 Ser167 residue to influence ERα transcriptional activity. The studies from Brodie/Sabnis similarly support PI3K/AKT cross-talk with ERα in their UMB-1Ca cell line. MCF-7X cells reveal the significant potential for PI3K/AKT blockade to treat resistance to oestrogen deprivation, where impact on ERα phosphorylation (in this instance the AKT-driven Ser167 site) again appears central to subsequent inhibitory effects on growth. Excitingly agents adversely influencing PI3K pathways are now emerging for experimental and clinical evaluation. Moreover, Santen/Yue have challenged their LTED model with farnesylthiosalicylic acid (FTS) which encouragingly has shown inhibition of proliferation and enhancement of apoptotic cell death. They have shown that FTS not only subverts MAPK activity but also partially blocks AKT (McMahon *et al.*, 2005; Santen *et al.*, 2006), although subsequent impact on ERα phosphorylation status remains unknown.

However, the various monotherapies examined, although having considerable merit, all proved incomplete inhibitors of MCF-7X cell growth and as such allowed subsequent emergence of resistance. Importantly, this project has revealed that the oestrogen-deprived phenotype is extremely flexible in its recruitment of signalling pathways during these various treatments, and can also maintain residual ERα phosphorylation and hence ERα function. These events provide the initial compensatory mechanism that limits therapeutic efficacy of the single agents and subsequently drive resistance. Thus, challenge with faslodex that depletes ligand/ER signalling is associated with a de-repression of EGFR/HER2 expression, maintained downstream MAPK and PI3K/AKT signalling, and ultimately significant increases in these various signalling elements culminating in resistant growth. In the case of PI3K blockade, while there is little change in expression during response, the cells again exhibit increased EGFR/HER2 (albeit more modest) by the time resistance emerges that may promote MAPK and recovery of AKT activity via RSK. Such observations indicate that growth factor receptor inhibitors such as gefitinib or MAPK inhibitors may be of some value in treating established resistance to faslodex or PI3K inhibitors, although this project has shown that combination treatment of MAPK inhibitor plus PI3K inhibitor is unable to prevent subsequent development of resistance. A

significantly more rewarding avenue has been to consider the role for ERα phosphorylation. With faslodex or PI3K inhibitor treatment, phosphorylation of ERα remains a crucial element both in limiting maximal drug response and maintaining resistance. Thus, during the responsive phase faslodex fails to inhibit AKT-driven Ser167ER activity and blockade of Ser118ER is incomplete, while PI3K inhibitors do not subvert ERα ligand-promoted Ser118ER activation. The resultant resistant growth mechanism is associated with further re-activation of ERα by kinase-driven phosphorylation (including MAPK and AKT downstream of the increased growth factor receptors), substantial recovery of ERα transcriptional activity and thereby expression of ERα regulated genes (such as the growth signalling element IGF-1R).

Encouragingly, an improved quality and longer duration of growth inhibition can be achieved by combining faslodex with PI3K signalling inhibitor in order to promote a superior depletion of the compensatory mechanism that involves residual ERα AF-1 phosphorylation. Furthermore, the resultant cells do not show substantial increases in their aggressive behaviour, in contrast to treatment with faslodex alone. However, there again remains some residual ERα phosphorylation during the responsive phase not surprisingly resistance does emerge and is associated with full ERα re-activation. Again, these events may involve recruitment of increased EGFR (and IGF-1R) that triggers downstream kinases (although in contrast HER2 remains at low levels perhaps explaining the lack of aggressiveness). Importantly, this thesis has been able to show that intelligent, simultaneous blockade of all the dominant regulators of ERα AF-1 phosphorylation can completely abrogate the compensatory cell survival mechanism that relies on functional ERα. In the MCF-7X cells, this can be achieved using a simultaneous treatment with faslodex plus PI3K/AKT inhibitor plus a MAPK inhibitor in MCF-7X cells, where the central importance of ERα knockdown is revealed by the somewhat inferior effect noted with PI3K/AKT plus MAPK inhibitor alone. The triple treatment approach not only maximises initial anti-tumour activity but also promotes cell loss, thus preventing emergence of therapeutic resistance. Clearly, therefore, the aim in designing clinical combinations treatments should be to achieve "total depletion of ERα phosphorylation" for maximal inhibitory effect to improve patient outlook. This may, of course, be difficult to achieve if we are to avoid potential unwanted side-effects of complex "cocktails" of signal transduction inhibitors. However, intelligent combination strategies of faslodex together with the upstream regulators of the various kinase activity remaining during ERα blockade

(i.e. gefitinib) could prove of future value in this regard, where such combinations are excitingly currently under clinical evaluation. In contrast, it is envisaged that sequential use of single agents following development of resistance could prove less effective, since in the case of faslodex, the drug resistant phenotype was also more aggressive (probably promoted by increased HER2), worrying observations if translated into prognostic impact in the clinic.

CHAPTER 5

∞ *REFERENCES* ∞

1. Abdul-Wahab K., Corcoran D., Perachiotti A. & Darbre P.D. (1999) Overexpression of insulin-like growth factor II (IGFII) in ZR75-71 human breast cancer cells: higher threshold levels of receptor (IGFIR) are required for a proliferative response than for effects on specific gene expression. *Cell Proliferation*, **32**:271-287.
2. Agarwal P.K., Mehrotra A., Chandra T. & Singh K. (2001) Immunohistochemical localization of transferring in human breast cancer tissue. *Indian Journal of Pathology and Microbiology*, **44**:107-111.
3. van Agthoven T., van Agthoven T.L., Portengen H., Foekens J.A. & Dorssers L.C. (1992) Ectopic expression of epidermal growth factor receptors induces hormone independence in ZR75-71 human breast cancer cells. *Cancer Research*, **52**:5082-5088.
4. Alessi D.R., Deak M., Casamayor A., Caudwell F.B., Morrice N., Norman D.G., Gaffney P., Reese C.B., MacDougall C.N., Harbison D., Ashworth A. & Bownes M. (1997) 3-Phosphoinositide-dependent protein kinase-1 (PDK1): structural and functional homology with the Drosophila DSTPK61 kinase. *Current Biology*, 7:776-789.
5. Ali S. & Coombes R.C. (2002) Endocrine-responsive breast cancer and strategies for combating resistance. *Nature Reviews Cancer*, **2**: 101-115.
6. American Cancer Society (2005-2006) Breast Cancer Facts and Figures. http/www.cancer.org/downloads/STT/CAFF2005BrF.pdf. Accessed August 4, 2005.
7. Angelopoulos N., Barbounis V., Livadas S., Kaltsas D. & Tolis G. (2004) Effects of estrogen deprivation due to breast cancer treatment. *Endocrine-Related Cancer*, **11**:523-535.
8. Arnold S.F., Obourn J.D., Jaffe H. & Notides A.C. (1994) Serine 167 is the major estradiol-induced phosphorylation site on the human estrogen receptor. *Molecular Endocrinology*, **8**:1208-1214.
9. Arnold S.F., Obourn J.D., Jaffe H. & Notides A.C. (1995) Phosphorylation of the human estrogen receptor on tyrosine 537 *in vivo* and by src family tyrosine kinases *in vitro*. *Molecular Endocrinology*, **9**:24-33.
10. ATAC Trialists' Group (2002) Anastrozole alone or in combination with tamoxifen versus tamoxifen alone for adjuvant treatment of postmenopausal women with early breast cancer: first results of the ATAC randomised trial. *Lancet*, **359**(9324): 2131-2139.
11. ATAC Trialists' Group (2005) Results of the ATAC (Arimidex, Tamoxifen, Alone or in Combination) trial after completion of 5 years' adjuvant treatment for breast cancer. *Lancet*, **365**:60-62.
12. Balana M.E., Labriola L., Salatino M., Movsichoff F., Peters G., Charreau E.H. & Elizalde P.V. (2001) Activation of ErbB-2 via a hierarchical interaction between ErbB-2 and type I insulin-like growth factor receptor in mammary tumor cells. *Oncogene*, **20**:34-47
13. Barnett J.B., Woods M.N., Lamon-Fava S., Schaefer E.J., McNamara J.R., Spiegelman D., Hertzmark E., Goldin B., Longcope C. & Gorbach S.L. (2004) Plasma lipid and lipoprotein levels during the follicular and luteal phases of the menstrual cycle. *Journal of Clinical Endocrinology and Metabolism*, **89**:776-782.
14. Baum M., Budzar A.U., Cuzick J., Forbes J., Houghton J.H., Klijn J.G. & Sahmound T. (2002) Anastrozole alone or in combination with tamoxifen versus tamoxifen alone for adjuvant treatment of postmenopausal women with early breast cancer: first results of the ATAC randomised trial. *Lancet*, **360**(9344):1520.

15. Baum M., Budzar A.U., Cuzick J., Forbes J., Houghton J.H., Klijn J.G. & Sahmound T. (2003) Anastrozole alone or in combination with tamoxifen versus tamoxifen alone for adjuvant treatment of postmenopausal women with early-stage breast cancer: results of the ATAC (Arimidex, Tamoxifen Alone or in Combination) trial efficacy and safety update analyses. *Cancer*, **98**:1802-1810.
16. Baum M., Hackshaw A., Houghton J., Rutqvist, Fornander T., Nordenskjold B., Nicolucci A. & Sainsbury R: ZIPP International Collaborators' Group. (2006) Adjuvant goserelin in premenopausal patients with early breast cancer: Results from the ZIPP study. *European Journal of Cancer*, Mar 15:Epub ahead of print.
17. Beatson G.T. (1896) On the treatment of inoperable cases of carcinoma of the mamma: suggestions for a new method of treatment, with illustrative cases. *Lancet*, **2**:104-107.
18. Benz C.C., Scott G.K., Sarup J.C., Johnson R.M., Tripathy D., Coronado E., Shepard H.M. & Osborne C.K. (1993) Estrogen-dependent, tamoxifen-resistant tumorigenic growth of MCF-7 cells transfected with HER2/neu. *Breast Cancer Research and Treatment*, **24**:85-95.
19. Bezwoda W.R., Esser J.D., Dansey R., Kessel I. & Lange M. (1991) The value of estrogen and progesterone receptor determinations in advanced breast cancer. Estrogen receptor level but not progesterone receptor correlates with response to tamoxifen. *Cancer*, **68**:867-872.
20. Blake R.A., Broome M.A., Liu X., Wu J., Gishizky M., Sun L. & Courtneidge S.A. (2000) SU6656, a selective Src family kinase inhibitor, used to probe growth factor signaling. *Molecular & Cellular Biology*, **20**:9018-9027.
21. Blobe G.C., Stribling S., Obeid L.M. & Hannun Y.A. (1996) Protein kinase C isoenzymes: regulation and function. *Cell Signalling*, **27**:213-247.
22. Bonneterre J., Thurlimann B., Robertson J.F.R., Krzakowski M., Mauriac L., Koralewski P., Vergote I., Webster A., Steinberg M. & von Euler M. (2000) Anastrozole versus tamoxifen as first-line therapy for advanced breast cancer in 668 postmenopausal women: Results of the tamoxifen or arimidex randomized group efficacy and tolerability study. *Journal of Clinical Oncology*, **18**:3748-3757.
23. Bowlin S.J., Leske M.C., Varma A., Nasca P., Weinstein A. & Caplan L. (1997) Breast cancer risk and alcohol consumption: results of a large case-control study. *International Journal of Epidemiology*, **26**:915-923.
24. Brantley D.M., Cheng N., Thompson E.J., Lin Q., Brekken R.A., Thorpe P.E., Muraoka R.S., Cerretti D.P., Pozzi A., Jackson D., Lin C. & Chen J. (2002) Soluable Eph A receptors inhibit tumor angiogenesis and progression in vivo. *Oncogene*, **21**:7011-7026.
25. Britton D.J., Hutcheson I.R., Knowlden J.M., Barrow D., Giles M., McClelland R.A., Gee J.M. & Nicholson R.I. (2006) Bidirectional cross talk between ERalpha and EGFR signalling pathways regulates tamoxifen-resistant growth. *Breast Cancer Research and Treatment*, **96**:131-146.
26. Brodie A., Jelovac D., Sabnis G., Long B., Macedo L. & Goloubeva O. (2005) Model systems: mechanisms involved in the loss of sensitivity to letrozole. *The Journal of Steroid Biochemistry & Molecular Biology*, **95**:41-48.
27. Brodie A.M., Lu Q., Liu Y. & Long B. (1999) Aromatase inhibitors and their antitumor effects in model systems. *Endocrine-Related Cancer*, **6**:205-210.
28. Brodie A.M., Lu Q., Long B.J., Fulton A., Chen T., Macpherson N., De Jong P.C., Blankenstein M.A., Nortier J.W., Slee P.H., Van De Ven J., Van Gorp J.M., Elbers J.R., Schipper M.E., Blijham G.H. & Thijssen J.H. (2001) Aromatase and COX-2 expression in human breast cancers. *The Journal of Steroid Biochemistry & Molecular Biology*, **79**:41-47.

29. Brodie A.M.H. & Njar V.C.O. (2000) Aromatase inhibitors and their application in breast cancer. *Steroids*, **65**:171-179.
30. Bross P.F., Baird A., Chen G., Jee J.M., Lostritto R.T., Morse D.E., Rosario L.A., Williams G.M., Yang P., Rahman A., Williams G. & Pazdur R. (2003) Fulvestrant in postmenopausal women with advanced breast cancer. *Clinical Cancer Research*, **9**: 4309-4317.
31. Budzar A. & Howell A. (2001) Advances in aromatase inhibition: Clinical efficacy and tolerability in the treatment of breast cancer. *Clinical Cancer Research*, **7**: 2620-2635.
32. Bulun S., Sebastian S., Takayama K., Suzuki T., Sasano H. & Shozu M. (2003) The human *CYP19* (aromatase P450) gene: update on physiologic roles and genomic organization of promoters. *The Journal of Steroid Biochemistry & Molecular Biology*, **86**: 219-224.
33. van der Burg B., Rutteman G.R., Blankenstein M.A., de Laat S.W. & van Zoelen E.J. (1988) Mitogenic stimulation of human breast cancer cells in a growth factor-defined medium: synergistic action of insulin and estrogens. *Journal of Cell Physiology*, **134**:101-118.
34. Campbell R.A., Bhat-Nakshatri P., Patel N.M., Constantinidou D., Ali S. & Nakshatri H. (2001) Phosphatidylinositol 3-kinase/ AKT-mediated activation of estrogen receptor alpha: a new model for anti-estrogen resistance. *Journal of Biological Chemistry*, **27**:9817-9824.
35. Cardone M.H., Roy N., Stennicke H.R., Salvesen G.S., Franke T.F., Stanbridge E., Frisch S. & Reed J.C. (1998) Regulation of cell death protease caspase-9 by phosphorylation. *Science*, **282**:1318-1321.
36. Casey G. (1997) The BRCA1 and BRCA2 breast cancer genes. *Current Opinions in Oncology*, **9**:88-93.
37. Castoria G., Migliaccio A., Bilancio A., Di Domenico M., de Falco A., Lombardi M., Fiorentino R., Varricchio L., Barone M.V. & Auricchio F. (2001) PI3-kinase in concert with Src promotes the S-phase entry of oestradiol-stimulated MCF-7 cells. *EMBO Journal*, **20**:6050-6059.
38. Cavanaugh P.G., Jia L., Zou Y. & Nicolson G.L. (1999) Transferrin receptor overexpression enhances transferring responsiveness and the metastatic growth of a rat mammary adenocarcinoma cell line. *Breast Cancer Research and Treatment*, **56**:203-217.
39. Chen D., Pace P.E., Coombes R.C. & Ali S. (1999) Phosphorylation of human estrogen receptor-α by protein kinase A regulates dimerization. *Molecular and Cellular Biology*, **19**:1002-1015.
40. Chen D., Riedl T., Washbrook E., Pace P.E., Coombes R.C., Egly J.M., & Ali S. (2000) Activation of estrogen receptor alpha by S118 phosphorylation involves a ligand-dependent interaction with TFIIH and participation of CDK7. *Molecular and Cellular Biology*, **6**:127-137.
41. Chen D., Washbrook E., Sarwar N., Bates G.J., Pace P.E., Thirunuvakkarasu E., Taylor J., Epstein R.J., Fuller-Pace F.V., Coombes R.C. & Ali.S. (2002) Phosphorylation of human estrogen receptor alpha at serine 118 by two distinct signal transduction pathways revealed by phosphorylation-specific antisera. *Oncogene*, **21**:4921-4931.
42. Cheung K.L., Willsher P.C., Pinder S.E., Ellis I.O., Elston C.W., Nicholson R.I., Blamey R.W. & Robertson J. F. (1997) Predictors of response to second-line endocrine therapy for breast cancer. *Breast Cancer Research and Treatment*, **45**:219-224.

43. Chisamore M.J., Ahmed Y., Bentrem D.J., Jordan V.C. & Tonetti D.A. (2001) Novel antitumor effect of estradiol in athymic mice injected with a T47D breast cancer cell line overexpressing protein kinase C alpha. *Clinical Cancer Research*, 7:3156-3165.
44. Chlebowski R.T., Hendrix S.L., Langer R.D., Stefanick M.L., Gass M., Lane D., Rodabough R.J., Gilligan M.A., Cyr M.G., Thomson C.A., Khandekar J., Petrovitch H. & McTiernan A. (2003) Influence of estrogen plus progestin on breast cancer and mammography in healthy postmenopausal women: the Women's Health Initiative Randomized Trial. *Journal of the American Medical Association*, **289**:3243-3253.
45. Chrysogelos S.A., Yarden R.I., Lauber A.H. & Murphy J.M. (1994) Mechanisms of EGF receptor regulation in breast cancer cells. *Breast Cancer Research and Treatment*, **31**:227-236.
46. Clarke R., Liu M.C., Bouker K.B., Gu Z., Lee R.Y., Zhu Y., Skaar T.C., Gomez B., O'Brien K., Wang Y. & Hilakivi-Clarke L.A. (2003) Antiestrogen resistance in breast cancer and the role of estrogen receptor signaling. *Oncogene*, **22**: 7316-7339.
47. Cole M.P., Jones C.T. & Todd I.D. (1971) A new anti-oestrogenic agent in late breast cancer. An early clinical appraisal of ICI 46474. *Br J Cancer*, **25**:270-275.
48. Collaborative Group on Hormonal Factors in Breast Cancer (1997) Collaborative reanalysis of data from 51 epidemiological studies of 52,705 women with breast cancer and 108,441 women without breast cancer. *Lancet*, **350**:1047-1059.
49. Coller H.A., Grandori C., Tamayo P., Colbert T., Lander E.S., Eisenman R.N. & Golub T.R. (2000) Expression analysis with oligonucleotide microarrays reveals that MYC regulates genes involved in growth, cell cycle, signaling, and adhesion. *Proc. Natl. Acad. Sci. USA*, **97**:3260-3265.
50. Copppla D., Ferber A., Miura M., Sell C., D'Ambrosio C., Rubin R. & Baserga R. (1994) A functional insulin-like growth factor I receptor is required for the mitogenic and transforming activities of the epidermal growth factor receptor. *Molecular and Cellular Biology*, **14**:4588-4595.
51. Coombes R.C., Hughes S.W. & Dowsett M. (1992) 4-hydroxyandrostenedione: a new treatment for postmenopausal patients with breast cancer. *European Journal of Cancer*, **28A**:1941-1945.
52. Cui X., Zhang P., Deng W., Oesterreich S., Lu Y., Mills G.B. & Lee A.V. (2003) Insulin-like growth factor-I inhibits progesterone receptor expression in breast cancer cells via the phosphatidylinositol 3-kinase/AKT/mammalian target of rapamycin pathway: progesterone receptor as a potential indicator of growth factor activity in breast cancer. *Molecular Endocrinology*, **17**:575-588.
53. Cummings S.R., Eckert S., Krueger K.A., Grady D., Powles T.J., Cauley J.A., Norton L., Nickelsen T., Bjarnson N.H., Morrow M., Lippman M.E., Black D., Glusman J.E., Costa A. & Jordan V.C. (1999) The effect of raloxifene on risk of breast cancer in postmenopausal women: results from the MORE randomized trial. *Journal of the American Medical Association*, **281**:2189-2197.
54. Cuzick J. & Baum M. (1985) Tamoxifen and contralateral breast cancer. *Lancet*, **2**(8449):282.
55. Daly R.J., Harris W.H., Wang D.Y. & Darbre P.D. (1991) Autocrine production of insulin-like growth factor II using an inducible expression system results in reduced estrogen sensitivity of MCF-7 human breast cancer cells. *Cell Growth and Differentiation*, **2**:457-464.
56. Dauvois S., White R. & Parker M.G. (1993) The anti-estrogen ICI 182,780 disrupts estrogen receptor nucleocytoplasmic shuttling. *Journal of Cell Science*, **106**:1377-1388.

57. Delaunay F., Pettersson K., Tujague M. & Gustafsson J-A. (2000) Functional differences between the amino- terminal domains of estrogen receptors α and β. *Molecular Pharmacology*, **58**:584-590.
58. De Lorenzo C., Palmer D.B., Piccoli R., Ritter M.A. & D'Alessio G. (2002) A new human antitumor immunoreagent specific for erbB2. *Clinical Cancer Research*, **8**: 1710-1719.
59. DeNardo D.G., Kim H.T., Hilsenbeck S., Cuba V., Tsimelzon A. & Brown P.H. (2005) Global gene expression analysis of estrogen receptor transcription factor cross talk in breast cancer: identification of estrogen-induced/activator protein-1-dependent genes. *Molecular Endocrinology*, **19**:362-378.
60. Delmas P.D., Bjarnason N.H., Mitlak B.H., Ravoux A.C., Shah A.S., Huster W.J., Draper M. & Christiansen C. (1997) Effects of raloxifene on bone mineral density, serum cholesterol concentrations, and uterine endometrium in postmenopausal women. *New England Journal of Medicine*, **337**:1641-1647.
61. Dixon J.M. (2004) Exemestane and aromatase inhibitors in the management of advanced breast cancer. *Expert Opinion on Pharmacotherapy*, **5**(2):307-316.
62. Dodwell D. & Vergote I. (2005) A comparison of fulvestrant and the third-generation aromatase inhibitors in the second-line treatment of postmenopausal women with advanced breast cancer. *Cancer Treatment Reviews*, **31**(4):274-282.
63. Dowsett M. (2001) Overexpression of HER-2 as a resistance mechanism to hormonal therapy for breast cancer. *Endocrine-Related Cancer*, **8**:191-195.
64. Dowsett M., Smithers D., Moore J., Trunet P.F., Coombes R.C., Powles T.J., Rubens R. & Smith I.E. (1994) Endocrine changes with the aromatase inhibitor fadrozole hydrochloride in breast cancer. *European Journal of Cancer*, **30A**:1453-1458.
65. Dumont J.A., Bitonti A.J., Wallace C.D., Baumann R.J., Cashman E.A. & Cross-Doersen D.E. (1996) Progression of MCF-7 breast cancer cells to antiestrogen-resistant phenotype is accompanied by elevated levels of AP-1 DNA-binding activity. *Cell Growth Differentiation*, **7**:351-359.
66. Dutertre M. & Smith C.L. (2003) Ligand-independent interactions of p160/steroid receptor coactivators and CREB-binding protein (CBP) with estrogen receptor-α: Regulation by protein phosphorylation sites in the A/B region depends on other receptor domains. *Molecular Endocrinology*, **17**:1296-1314.
67. Early Breast Cancer Trialists' Collaborative Group (1992) Systemic treatment of early breast cancer by hormonal, cytotoxic, or immune therapy. 133 randomised trials involving 31,000 recurrences and 24,000 deaths among 75,000 women. *Lancet*, **339**(8784):1-15.
68. Early Breast Cancer Trialists' Collaborative Group (1998) Tamoxifen for early breast cancer: an overview of the randomised trials. *Lancet*, **351**(9114):1451-1467.
69. Eiermann W., Paepke S., Appfelstaedt J., Llombart-Cussac A., Eremin J., Vinholes J., Mauriac L., Ellis M., Lassus M., Chaudi-Ross H.A., Dugan M. & Borgs M. (2001) Preoperative treatment of postmenopausal breast cancer patients with letrozole: a randomized double-blind multicenter study. *Ann Oncology*, **12**:1527-1532.
70. El-Ashry D., Miller D.L., Kharbanda S., Lippman M.E. & Kern F.G. (1997) Constitutive Raf-1 kinase activity in breast cancer cells induces both estrogen-independent growth and apoptosis. *Oncogene*, **15**:423-435.
71. Elisaf M.S., Bairaktari E.T., Nicolaides C., Kakaidi B., Tzallas C.S., Katsaraki A. & Pavlidis N.A. (2001) Effect of letrozole on the lipid profile in postmenopausal women with breast cancer. *European Journal of Cancer*, **37**:1510-1513.

72. Elliot R.L., Elliot M.C. Wang F. & Head J.F. (1993) Breast carcinoma and the role of iron metabolism. A cytochemical, tissue culture, and ultrastructural study. *Annals of the New York Academy of Sciences*, **698**:159-166.
73. Ellis M.J. (2004) Importance of correlative science in advancing hormonal therapy and a new clinical paradigm for neoadjuvant therapy. *Ann Surg Oncology*, **11**:S9-S17.
74. Endoh H., Maruyama K., Masuhiro Y., Kobayashi Y., Goto M., Tai H., Yanagisawa J., Metzger D., Hashimoto S. & Kato S. (1999) Purification and identification of p68 RNA helicase acting as a transcriptional coactivator specific for the activation function 1 of human estrogen receptor-α. *Molecular and Cellular Biology*, **19**:5363-5372.
75. Ernster V.L. & Barclay J. (1997) Increases in ductal carcinoma *in situ* (DCIS) of the breast in relation to mammography: A dilemma. *Journal of the National Cancer Institute Monographs*, **22**:151-156.
76. Fang W.B., Brantley-Sieders D.M., Parker M.A., Reith A.D. & Chen J. (2005) A kinase-dependent role for EphA2 receptor in promoting tumor growth and metastasis. *Oncogene*, **24**:7859-7868.
77. Feng W., Webb P., Ngugen P., Liu X.H., Li J. & Kushner P.J. (2001) Potentiation of estrogen receptor AF-1 by Src/JNK through a serine 118 independent pathway. *Molecular Endocrinology*, **15**:32-45.
78. Filardo E.J. (2002) Epidermal growth factor receptor (EGFR) transactivation by estrogen via the G-protein-coupled receptor, GPR30: a novel signaling pathway with potential significance for breast cancer. *The Journal of Steroid Biochemistry and Molecular Biology*, **80**:231-238.
79. Fisher B., Wolmark N., Bauer M., Redmond C. & Gebhardt M. (1981) The accuracy of clinical nodal staging and of limited axillary dissection as a determinant of histological nodal status in carcinoma of the breast. *Surg. Gynecol. Obstet.*, **152**:765-772.
80. Font de Mora J. & Brown M. (2000) AIB1 is a conduit for kinase-mediated growth factor signaling to the estrogen receptor. *Molecular and Cellular Biology*, **20**(14):5041-5047.
81. Fournier D.B., Chisamore M., Lurain J.R., Rademaker A.W., Jordan V.C. & Tonetti D.A. (2001) Protein kinase C alpha expression is inversely related to ER status in endometrial carcinoma: possible role in AP-1-mediated proliferation of ER-negative endometrial cancer. *Gynecologic Oncology*, **81**:366-372.
82. Fowler A., Solodin N., Preisler-Mashek M.T., Zhang P., Lee A.V. & Alarid E.T. (2004) Increases in estrogen receptor-α concentration in breast cancer cells promote serine 118/104/106 independent AF-1 transactivation and growth in the absence of estrogen. *The FASEB Journal*, **18**:81-93.
83. Fox B.P. & Kandpal R.P. (2004) Invasiveness of breast carcinoma cells and transcript profile: Eph receptors and ephrin ligands as molecular markers of potential diagnostic and prognostic application. *Biochem Biophys Res Commun.*, **318**:882-892.
84. Freedman O.C., Verma S. & Clemons M.J. (2005) Using aromatase inhibitors in the neoadjuvant setting: evolution or revolution? *Cancer Treatment Reviews*, **31**:1-17.
85. Fry M.J. (2001) Phosphoinositide 3-kinase signalling in breast cancer: how big a role it might play. *Breast Cancer Research*, **3**:304-312.
86. Fuqua S.A., Wiltschke C., Zhang Q.X., Borg A., Casltes C.G., Friedrichs W.E., Hopp T., Hilsenbeck S., Mohsin S., O'Connell P. & Allred D.C. (2000) A hypersensitive estrogen receptor-alpha mutation in premalignant breast lesions. *Cancer Research*, **60**:4026-4029.

87. Gee J.M., Harper M.E., Hutcheson I.R., Madden T.A., Barrow D., Knowlden J.M., McClelland R.A., Jordan N., Wakeling A.E. & Nicholson R.I. (2003) The antiepidermal growth factor receptor agent gefitinib (ZD1839/Iressa) improves antihormone response and prevents development of resistance in breast cancer in vitro. *Endocrinology*, **144**:5105-5117.
88. Gee J.M.W., Giles M.G. & Nicholson R.I. (2004) Extreme growth factor signalling can promote oestrogen receptor-α loss: therapeutic implications in breast cancer. *Breast Cancer Research*, **6**:162-163.
89. Gee J.M., Robertson J.F., Gutteridge E., Ellis I.O., Pinder S.E., Rubini M. & Nicholson R.I. (2005) Epidermal growth factor receptor/HER2/insulin-like growth factor receptor signalling and oestrogen receptor activity in clinical breast cancer. *Endocrine-Related Cancer*, **12**:S99-111.
90. Geisler J., Lien E.A., Ekse D. & Lonning P.E. (1997) Influence of aminoglutethimide on plasma levels of estrone sulphate and dehydroepiandrosterone sulphate in postmenopausal breast cancer patients. *The Journal of Steroid Biochemistry & Molecular Biology*, **63**: 53-58.
91. Geisler J. & Lonning P.E. (2005) Aromatase Inhibition: Translation into a successful therapeutic approach. *Clinical Cancer Research*, **11**(8):2809-2821.
92. Geisler J., Haynes B., Anker G., Dowsett M. & Lonning P.E. (2002) Influence of letrozole and anastrozole on total body aromatization and plasma estrogen levels in postmenopausal breast cancer patients evaluated in a randomized, cross-over study. *Journal of Clinical Oncology*, **20**:751-757.
93. Gershanovich M., Chaudri H.A., Campos D., Lurie H., Bonaventura A., Jeffrey M., Buzzi F., Bodrogi I., Ludwig H., Reichardt P., O'Higgins N., Romieu G., Friederich P. & Lassus M. (1998) Letrozole, a new oral aromatase inhibitor: randomised trial comparing 2.5 mg daily, 0.5 mg daily and aminoglutethimide in postmenopausal women with advanced breast cancer. Letrozole International Trial Group (AR/BC3). *Ann Oncology*, **9**:639-645.
94. Gomes A.L., Guimaraes M.D., Gomes C.C., Chaves I.G., Gobbi H. & Camargos A.F. (1995) A case control study of risk factors for breast cancer in Brazil, 1978-1987. *International Journal of Epidemiology*, **24**:292-299.
95. Goodwin P.J., Ennis M., Pritchard K.I., Trudeau M. & Hood N. (1999) Risk of menopause during the first year after breast cancer diagnosis. *Journal of Clinical Onocology*, **17**:2365-2370.
96. Goss P.E. (1999) Risks versus benefits in the clinical application of aromatase inhibitors. *Endocrine-Related Cancer*, **6**:325-332.
97. Goss P.E. & Strasser-Weippl K. (2004) Prevention strategies with aromatase inhibitors. *Clinical Cancer Research*, **10**(1):372S-379S.
98. Goss P.E., Ingle J.N., Martino S., Robert N.J., Muss H.B., Piccart M.J., Castiglione M., Tu D., Shepard L.E., Pritchard K.I., Livingston R.B., Davidson N.E., Norton L., Perez E.A., Abrams J.S., Therasse P., Palmer M.J. & Pater J.L. (2003) A randomized trial of letrozole in postmenopausal women after five years of tamoxifen therapy for early-stage breast cancer. *New England Journal of Medicine*, **349**:1793-1802.
99. Granville C.A., Memmott R.M., Gills J.J. & Dennis P.A. (2006) Handicapping the race to develop inhibitors of the phosphoinositide 3-kinase/Akt/mammalian target of rapamycin pathway. *Clinical Cancer Research*, **12**:679-689.
100. Gross J.M. & Yee D. (2003) The type-I insulin-like growth factor receptor tyrosine kinase and breast cancer: biology and therapeutic relevance. *Cancer and Metastasis Review*, **22**:327-336.

101. Guo P., Fang Q., Tao H-Q., Schafer C.A., Fenton B.M., Ding I., Hu B. & Cheng S-Y. (2003) Overexpression of vascular endothelial growth factor by MCF-7 breast cancer cells promotes estrogen-independent tumor growth *in vivo*. *Cancer Research*, **63**: 4684-4691.
102. Guvakova M.A. & Surmacz E. (1997) Overexpressed IGF-I receptors reduce estrogen growth requirements, enhance survival, and promote E-cadherin-mediated cell-cell adhesion in human breast cancer cells. *Experimental Cell Research*, **231**:149-162.
103. de Haes H., Olschewski M., Kaufmann M., Schumacher M., Jonat W. & Sauerbrei W. (2003) Quality of life in goserelin-treated versus cyclophosphamide + methotrexate + Fluorouracil –treated premenopausal and perimenopausal patients with node- positive, early breast cancer: The Zoladex Early Breast Cancer Research Association Trialists Group. *Journal of Clinical Oncology*, **21**:4510-4516.
104. van der Hage J.A., van den Broek L.J., Legrand C., Clahsen P.C., Bosch C.J.A., Robanus-Maandag E.C., van de Velde C.J.H. & van de Vijver M.J. (2004) Overexpression of p70 S6 kinase protein is associated with increased risk of locoregional recurrence in node-negative premenopausal early breast cancer patients. *British Journal of Cancer*, **90**:1543-1550.
105. Hall J.M., Lee M.K., Newman B., Morrow J.E., Anderson L.A., Huey B. & King M-C. (1990) Linkage of early-onset familial breast cancer to chromosome 17q21. *Science*, **250**:1684-1689.
106. Heldin C-H. (2001) Signal transduction: multiple pathways, multiple options for therapy. *Stem Cells*, **19**: 295-303.
107. Heroult M., Schaffner F. & Augustin H.G. (2006) Eph receptor and ephrin ligand-mediated interactions during angiogenesis and tumor progression. *Experimental Cell Research*, **312**:642-650.
108. Hiscox S., Morgan L., Green T.P., Barrow D., Gee J. & Nicholson R.I. (2005) Elevated Src activity promotes cellular invasion and motility in tamoxifen resistant breast cancer cells. *Breast Cancer Research and Treatment*, Dec 7: Epub ahead of print.
109. Horwitz K.B. & McGuire W.L. (1975) Specific progesterone receptors in human breast cancer. *Steroids*, **25**:497-505.
110. Horwitz K.B., Koseki Y. & McGuire W.L. (1978) Estrogen control of progesterone receptor in human breast cancer: role of estradiol and antiestrogen. *Endocrinology*, **103**:1742-1751.
111. Howe G.R., Hirohata T., Hislop T.G., Iscovich J.M., Yuan J.M., Katsouyanni K., Lubin F., Marubini E., Modan B., Rohan T., *et al.* (1990) Dietary risk factors and risk of breast cancer: combined analysis of 12 case-control studies. *Journal of the National Cancer Institute*, **82**:561-569.
112. Howell A. (2002) Selective oestrogen receptor downregulator. *European Journal of Cancer*, **6**:s61-s62.
113. Howell A., Robertson J.F., Quaresma Albano J., Aschermannova A., Mauriac L., Kleeberg U.R., Vergote I., Erikstein B., Webster A. & Morris C. (2002) Fulvestrant, formerly ICI 182,780, is as effective as ANZ in postmenopausal women with advance breast cancer progressing after prior endocrine treatment. *Journal of Clinical Oncology*, **20**:3396-3403.
114. Hu X.F., Veroni M., De Luise M., Wakeling A., Sutherland R., Watts C.K. & Zalcberg J.R. (1993) Circumvention of tamoxifen resistance by the pure anti-estrogen ICI 182,780. *International Journal of Cancer*, **55**:873-876.

115. Huang Z., Hankinson S.E., Colditz G.A., Stampfer M.J., Hunter D.J., Manson J.E., Hennekens C.H., Rosner B., Speizer F.E. & Willett W.C. (1997) Dual effects of weight and weight gain on breast cancer risk. *JAMA*, **278**:1407-1411.
116. Huggins C. & Bergenstal D.M. (1952) Inhibition of human mammary and prostatic cancers by adrenalectomy. *Cancer Research*, **12**:134-141.
117. Hutcheson I.R., Knowlden J.M., Madden T-A., Barrow D., Gee J.M.W., Wakeling A.E. & Nicholson R.I. (2003) Oestrogen receptor-mediated modulation of the EGFR/MAPK pathway in tamoxifen-resistant MCF-7 cells. *Breast Cancer Research and Treatment*, **81**: 81-93.
118. Inoue T., Cavanaugh P.G., Steck P.A., Brunner N. & Nicolson G.L. (1993) Differences in transferrin response and numbers of transferrin receptors in rat and human mammary carcinoma lines of different metastatic potentials. *Journal of Cell Physiology*, **156**:212-217.
119. Janicke F. (2004) Are all aromatase inhibitors the same? A review of the current evidence. *The Breast*, **13**:S10-S18.
120. Jankesz R., Hausmaninger H., Kubista E., Gnant M., Menzel C., Bauernhofer T., Seifert M., Haider K., Mlineritsch B., Steindorfer P., Kwasny W., Fridrik M., Steger G., Wette V. & Samonigg H. (2002) Austrian Breast and Colorectal Cancer Study Group 5. Randomized adjuvant trial of tamoxifen and goserelin versus cyclophosphamide, methotrexate and fluorouracil: evidence for the superiority of treatment with endocrine blockade in premenopausal patients with hormone- responsive breast cancer. *Journal of Clinical Oncology*, **20**: 4621-4627.
121. Jefcoate C., Liehr J.G., Santen R.J., Sutter T.R., Yager J.D., Yue W., Santner S.J., Tekmal R., Demers L., Pauley R., Naftolin F., Mor G. & Berstein L. (2000) Tissue-specific synthesis and oxidative metabolism of estrogens. *Journal of the National Cancer Institute Monographs*, **27**:95-112.
122. Jeng M-H., Yue W., Eischeid A., Wang J.P. & Santen R.J. (2000) Role of MAP kinase in the enhanced cell proliferation of long term estrogen deprived human breast cancer cells. *Breast Cancer Research and Treatment*, **62**:167-175.
123. Jensen E.V. & Jacobson H.I. (1960) Fate of steroidal estrogen in target tissues. In: Piccus G. & Voilmer E.P., editors. Biological Activities of Steroids in Relations to Cancers. New York, Academic Press:161-174.
124. Jensen E.V. & Jordan V.C. (2003) The estrogen receptor: A model for molecular medicine. *Clinical Cancer Research*, **9**: 1980-1989.
125. Jensen J., Kitlen J.W., Briand P., Labrie F. & Lykkesfeldt A.E. (2003) Effect of antiestrogens and aromatase inhibitor on basal growth of the human breast cancer cell line MCF-7 in serum-free medium. *The Journal of Steroid Biochemistry & Molecular Biology*, **84**: 469-478.
126. Jess T.J., Belham C.M., Thomson F.J., Scott P.H., Plevin R.J. & Gould G.W. (1996) Phosphatidylinisitol 3'-kinase, but not p70 ribosomal S6 kinase, is involved in membrane protein recycling: wortmannin inhibits glucose transport and down-regulates cell-surface transferring receptor numbers independently of any effect on fluid-phase endocytosis in fibroblasts. *Cellular Signalling*, **8**:297-304.
127. Joel P.B., Smith J., Sturgill T.W., Fisher T.L., Blenis J. & Lannigan D.A. (1998) $pp90^{rsk1}$ regulates estrogen receptor-mediated transcription through phosphorylation of Ser-167. *Molecular and Cellular Biology*, **18**:1978-1984.
128. Joensuu H., Ejlertsen B., Lonning P.E. & Rutqvist L-E. (2005) Aromatase inhibitors in the treatment of early and advanced breast cancer. *Acta Oncologica*, **44**:23-31.
129. Johnson D.E. & Williams L.T. (1993) Structural and functional diversity in the FGF receptor multigene family. *Advances in Cancer Research*, **60**:1-41.

130. Johnston S.R., Lu B., Scott G.K., Kushner P.J., Smith I.E., Dowsett M. & Benz C.C. (1999) Increased activator protein-1 DNA binding and c-Jun NH2-terminal kinase activity in human breast tumors with acquired tamoxifen resistance. *Clinical Cancer Research*, **5**:251-256.
131. Johnston S.R.D. & Dowsett M. (2003) Aromatase inhibitors for breast cancer: lessons from the laboratory. *Nature Reviews Cancer*, **3**: 821-831.
132. Johnston S.R.D., Head J., Pancholi S., Detre S., Martin L-A., Smith I.E. & Dowsett M. (2003) Integration of signal transduction inhibitors with endocrine therapy: An approach to overcoming hormone resistance in breast cancer. *Clinical Cancer Research*, **9**: 524s-532s.
133. Johnston S.R.D., Martin L-A., Head J., Smith I. & Dowsett M. (2005) Aromatase inhibitors: Combination with fulvestrant or signal transduction inhibitors as a strategy to overcome endocrine resistance. *The Journal of Steroid Biochemistry & Molecular Biology*, **95**:173-181.
134. Jonat W., Kaufmann M., Sauerbrei W., Blamey R., Cuzick J., Namer M., Fogelman I., de Haes J.C., de Matteis A., Stewart A., Eiermann W., Szakolczai I., Palmer M., Schumacher M., Geberth M., Lisboa B; Zoladex Early Breast Cancer Research Association Study. (2002) Goserelin versus cyclophosphamide, methotrexate, and fluorouracil as adjuvant therapy in premenopausal patients with node-positive breast cancer: The Zoladex Early Breast Cancer Research Association Study, *Journal of Clinical Onocology*, **20**:4628-4635.
135. Jones H.E., Goddard L., Gee J.M., Hiscox S., Rubini M., Barrow D., Knowlden J.M., Williams S., Wakeling A.E. & Nicholson R.I. (2004) Insulin-like growth factor-I receptor signalling and acquired resistance to gefitinib (ZD1839; Iressa) in human breast and prostate cancer cells. *Endocrine-Related Cancer*, **11**:793-814.
136. de Jong P.C., Blankenstein M.A., Nortier J.W., Slee P.H., van de Ven J., van Gorp J.M., Elbers J.R., Schipper M.E., Blijham G.H., Thijssen J.H., Lu Q., Jelovac D. & Brodie A.M. (2003) The relationship between aromatase in primary breast tumors and response to treatment with aromatase inhibitors in advanced disease. *The Journal of Steroid Biochemistry & Molecular Biology*, **87**:149-155.
137. de Jong P.C., ven de Ven J., Nortier H.W., Maitimu-Sneede I., Danker T.H., Thijssen J.H., Slee P.H. & Blankenstein R.A. (1997) Inhibition of breast cancer tissue aromatase activity and estrogen concentrations by the third-generation aromatase inhibitor varozole. *Cancer Research*, **57**:2109-2111.
138. Jordan N.J., Gee J.M., Barrow D., Wakeling A.E. & Nicholson R.I. (2004) Increased constitutive activity of PKB/AKT in tamoxifen resistant breast cancer MCF-7 cells. *Breast Cancer Research and Treatment*, **87**:167-180.
139. Kampert J.B., Whittemore A.S. & Paffenbarger R.S. Jr. (1988) Combined effect of childbearing, menstrual events, and body size on age-specific breast cancer risk. *American Journal of Epidemiology*, **128**:962-979.
140. Kandel E.S. & Hay N. (1999) The regulation and activities of the multifunctional serine/threonine kinase Akt/PKB. *Experimental Cell Research*, **253**:210-219.
141. Kasid A., Lippman M.E., Papageorge A.G., Lowy D.R. & Gelmann E.P. (1985) Transfection of v-rasH DNA into MCF-7 human breast cancer cells bypasses dependence on estrogen for tumorigenicity. *Science*, **228**:725-728.
142. Kato S., Endoh H., Masuhiro Y., Kitamoto T., Uchiyama S., Sasaki H., Masushige S., Gotoh Y., Nishida E., Kawashima H., Metzger D. & Chambon P. (1995) Activation of the estrogen receptor through phosphorylation by mitogen-activated protein kinase. *Science*, **270**:1491-1494.

143. Kiley S.C., Clark K.J., Goodnough M., Welch D.R. & Jaken S. (1999) Protein kinase C delta involvement in mammary tumor cell metastasis. *Cancer Research*, **59**:3230-3238.
144. Kim D. Cheng G.Z., Lindsley C.W., Yang H. & Cheng J.Q. (2005) Targeting the phosphatidylinositol-3 kinase/Akt pathway for the treatment of cancer. *Current Opinion in Investigational Drugs*, **6**:1250-1258.
145. Klijn J.G., Blamey R.W., Boccardo F., Tominaga T., Duchateau L. & Sylvester R. (2001) Combined Hormone Agents Trialists' Group and the European Organization for Research and Treatment of Cancer. Combined tamoxifen and luteinizing hormone-releasing hormone (LHRH) agonist versus LHRH agonist alone in premenopausal advanced breast cancer: a met-analysis of four randomized trials. *Journal of Clinical Oncology*, **19**:343-353.
146. Klint P. & Claesson-Welsh L. (1999) Signal transduction by fibroblast growth factor receptors. *Frontiers in Bioscience*, **4**:D165-177.
147. Knowlden J.M., Hutcheson I.R., Barrow D., Gee J.M.W. & Nicholson R.I. (2005) Insulin-like growth factor-I receptor signaling in Tamoxifen-resistanct breast cancer: A supporting role to the epidermal growth factor receptor. *Endocrinology*, **146**:4609-4618.
148. Knowlden J.M., Hutcheson I.R., Barrow D. & Nicholson R.I. (2003a) IGF-1R and EGFR crosstalk in tamoxifen resistant breast cancer cells. *Breast Cancer Research and Treatment*, **82**:S171.
149. Knowlden J.M., Hutcheson I.R., Jones H.E., Madden T., Gee J.M.W., Harper M.E., Barrow D., Wakeling A.E. & Nicholson R.I. (2003b) Elevated levels of epidermal growth factor receptor/c-erbB2 heterodimers mediate an autocrine growth regulatory pathway in tamoxifen-resistant MCF-7 cells. *Endocrinology*, **144**:1032-1044.
150. Koziczak M. & Hynes N.E. (2004) Cooperation between fibroblast growth factor receptor-4 and ErbB2 in regulation of cyclin D1 translation. *The Journal of Biological Chemistry*, **279**:50004-50011.
151. Kruger J.S. & Reddy K.B. (2003) Distinct mechanisms mediate the initial and sustained phases of cell migration in epidermal growth factor receptor-overexpressing cells. *Molecular Cancer Research*, **1**:801-809.
152. Kucab J.E. & Dunn S.E. (2003) Role of IGF-1R in mediating breast cancer invasion and metastasis. *Breast Disease*, **17**:41-47.
153. Kuiper G. G., Enmark E., Pelto-Huikko M., Nilsson S. & Gustafsson. (1996) Cloning of a novel estrogen receptor expressed in rat prostate and ovary. *Proceedings of the National Academy of Science USA*, **93**:5925-5930.
154. Kullander K. & Klein R. (2002) Mechanisms and functions of Eph and ephrin signalling. *Nature Reviews Molecular Cell Biology*, **3**:475-486.
155. Kushner P., Agard D.A., Greene G.L., Scanlan T.S., Shiau A.K., Uht R.M. & Webb P. (2000) Estrogen receptor pathways to AP-1. *The Journal of Steroid Biochemistry & Molecular Biology*, **74**:311-317.
156. Labrie F., Belanger A., Cusan L. & Candas B. (1997) Physiological changes in dehydroepiandrosterone are not reflected by serum levels of active androgens and estrogen but of their metabolites: intracrinology. *Journal of Clinical Endocrinology and Metabolism*, **82**:2403-2409.
157. Labrie F., Luu-The V., Labrie C., Belanger A., Simard J., Lin S-X. & Pelletier G. (2003) Endocrine and intracrine sources of androgens in women; Inhibition of breast cancer and other roles of androgens and their precursor dehydroepiandrosterone. *Endocrine Reviews*, **24**: 152-182.

158. Lahooti H., Thorsen T. & Aakvaag A. (1998) Modulation of mouse estrogen receptor transcription activity by protein kinase C delta. *Journal of Molecular Endocrinology*, **20**:245-259.
159. Langston A.A., Malone K.E., Thompson J.D., Daling J.R. & Ostrander E.A. (1996) BRCA1 mutations in a population-based sample of young women with breast cancer. *New England Journal of Medicine*, **334**:137-142.
160. Lannigan D.A. (2003) Estrogen receptor phosphorylation. *Steroids*, **68**:1-9.
161. Lash T.L. & Aschengrau A. (2000) Alcohol drinking and risk of breast cancer. *The Breast Journal*, **6**:396-399.
162. Lee A.V., Jackson J.G., Gooch J.L., Hilsenbeck S.G., Coronado-Heinsohn E., Osborne C.K. & Yee D. (1999) Enhancement of insulin-like growth factor signaling in human breast cancer: estrogen regulation of insulin receptor substrate-1 expression in vitro and in vivo. *Molecular Endocrinology*, **13**:787-796.
163. Lee A.V., Schiff R., Cui X., Sachdev D., Yee D., Gilmore A.P., Streuli C.H., Oesterrich S. & Hadsell D.L. (2003) New mechanisms of signal transduction inhibitor action: Receptor tyrosine kinase down-regulation and blockade of signal transactivation. *Clinical Cancer Research*, **9**: 516s-523s.
164. LeGoff P., Montano M.M., Schodin D.J. & Katzenellenbogen B.S. (1994) Phosphorylation of the human estrogen receptor. Identification of hormone-regulated sites and examination of their influence on transcriptional activity. *Journal of Biological Chemistry*, **269**:4458-4466.
165. Leu Y.-W., Yan P.S., Fan M., Jin V.X., Liu J.C., Curran E.M., Welshons W.V., Wei S.H., Davuluri R.V., Plass C., Nephew K.P. & Huang T.H.-M. (2004) Loss of estrogen receptor signalling triggers epigenetic silencing of downstream targets in breast cancer. *Cancer Research*, **64**:8184-8192.
166. Levin E.R. (1999) Cellular functions of plasma membrane estrogen receptor. *Trends in Endocrinology and Metabolism*, **10**:374-377.
167. Levin E.R. (2002) Cellular functions of plasma membrane estrogen receptors. *Steroids*, **67**:471-475.
168. Levin E.R. (2003) Bidirectional signaling between the estrogen receptor and the epidermal growth factor receptor. *Molecular Endocrinology*, **17**: 309-317.
169. Liao J.K. (2003) Cross-coupling between the oestrogen receptor and phosphoinositide 3-kinase. *Biochemical Society Transactions*, **31**:66-70.
170. Liu Y., El-Ashry D., Chen D., Ding I.Y. & Kern F.G. (1995) MCF-7 breast cancer cells overexpressing transfected c-erbB-2 have an *in vitro* growth advantage in estrogen-depleted conditions and reduced estrogen dependence and tamoxifen-sensitivity *in vivo*. *Breast Cancer Research and Treatment*, **34**:97-117.
171. Lobenhofer E.K., Huper G., Iglehart J.D. & Marks J.R. (2000) Inhibition of mitogen-activated protein kinase and phosphatidylinositol 3-kinase activity in MCF-7 cells prevents estrogen-induced mitogenesis. *Cell Growth & Differentiation*, **11**: 99-110.
172. Lonning P.E., Bajetta E., Murray R., Tubiana-Hulin M., Eisenberg P.D., Mickiewicz E., Celio L., Pitt P., Mita M., Aaronson N.K., Fowst C., Arkipov A., di Salle E., Polli A. & Massimini G. (2000) Activity of exemestane in metastatic breast cancer after failure of nonsteroidal aromatase inhibitors: A phase II trial. *Journal of Clinical Oncology*, **8**(11):2234-2244.
173. Lonning P.E., Dowset M & Powles T.J. (1990) Postmenopausal estrogen synthesis and metabolism: alterations caused by aromatase inhibitors used for the treatment of breast cancer. *Journal of Steroid Biochemistry*, **35**:355-366.
174. Lu Q., Liu Y., Long B.J., Grigoryev D., Gimbel M. & Brodie A. (1999) The effect of combining aromatase inhibitors with antiestrogens on tumor growth in a

nude mouse model for breast cancer. *Breast Cancer Research and Treatment*, **57**:183-192.

175. Lu Q., Yue W., Wang J., Lui Y., Long B. & Brodie A. (1998) The effects of aromatase inhibitors and antiestrogens in the nude mouse model. *Breast Cancer Research and Treatment*, **50**:63-71.
176. Luft R. & Olivecrona H. (1953) Experiences with hypophysectomy in man. *Journal of Neurosurgery*, **10**:301-316.
177. MacGregor J.I. & Jordan V.C. (1998) Basic guide to the mechanisms of antiestrogen action. *Pharmacology Reviews*, **50**:151-196.
178. McClelland R.A., Barrow D., Madden T-A., Dutkowski C.M., Pamment J., Knowlden J.M., Gee J.M.W. & Nicholson R.I. (2001) Enhanced epidermal growth factor receptor signaling in MCF-7 breast cancer cells after long-term culture in the presence of the pure antiestrogen ICI 182,780 (Faslodex). *Endocrinology*, **142**:2776-2788.
179. McClelland R.A., Gee J.M., Francis A.B., Robertson J.F., Blamey R.W., Wakeling A.E. & Nicholson R.I. (1996) Short-term effects of the pure anti-oestrogen ICI 182780 treatment on oestrogen receptor, epidermal growth factor receptor and transforming growth factor-alpha protein expression in human breast cancer. *European Journal of Cancer*, **32A**:413-416.
180. McClelland R.A., Wilson D., Leake R., Finlay P. & Nicholson R.I. (1991) A multicentre study into the reliability of steroid receptor immunocytochemical assay quantification. British Quality Control Group. *European Journal of Cancer*, **27**:711-715.
181. McKenna N.J., Lanz R.B. & O'Malley B.W. (1999) Nuclear receptor coregulators: Cellular and molecular biology. *Endocrine Reviews*, **20**(3): 321-344.
182. McMahon L.P., Yue W., Santen R.J. & Lawrence J.C. (2005) Farnesylthiosalicylic acid inhibits mammalian target of rapamycin (mTOR) activity both in cells and in vitro by promoting dissociation of the mTOR-raptor complex. *Molecular Endocrinology*, **19**:175-183.
183. McPherson K., Steel M. & Dixon J.M. (2000) ABC of breast diseases: Breast cancer- epidemiology, risk factors, and genetics. *British Medical Journal*, **321**:624-628.
184. Magnusson C., Baron J., Persson I., Wolk A., Bergstrom R., Trichopoulos D. & Adami H.O. (1998) Body size in different periods of life and breast cancer risk in post-menopausal women. *International Journal of Cancer*, **76**:29-34.
185. Mangelsdorf D.J., Thummel C., Beato M., Herrlich P., Schutz G., Umesono K., Blumberg B., Kastner P., Mark M., Chambon P. & Evans R.M. (1995) The nuclear receptor superfamily: the second decade. *Cell*, **83**:835-839.
186. Martin L-A., Farmer I., Johnston S.R.D., Ali S., Marshall C. & Dowsett M. (2003) Enhanced ERα, erbB2 and MAPK signal transduction pathways operate during the adaptation of MCF-7 cells to long term oestrogen deprivation. *The Journal of Biological Chemistry*, **278**: 30458-30468.
187. Martin L-A., Pancholi S., Chan C.M., Farmer I., Kimberley C., Dowsett M. & Johnston S.R. (2005) The anti-oestrogen ICI 182,780, but not tamoxifen, inhibits the growth of MCF-7 breast cancer cells refractory to long-term oestrogen deprivation through down-regulation of oestrogen receptor and IGF signalling. *Endocrine-Related Cancer*, **12**:1017-1036.
188. Martin M.B., Franke T.F., Stoica G.E., Chambon P., Katzenellenbogen B.S., Stoica B.A., McLemore M.S., Olivo S.E. & Stoica A. (2000) A role for AKT in mediating the estrogenic functions of epidermal growth factor and insulin-like growth factor I. *Endocrinology*, **141**:4503-4511.

189. Massarweh S.A., Jiang S., Mohsin S.K., Di Pietro M., Wakeling A.E., Osborne C.K. & Schiff R. (2003) Resistance to endocrine therapy in a xenograft model of HER2 overexpressing breast cancer is accompanied by increased HER2 but loss of IGF-1 receptor expression. *Breast Cancer Research and Treatment*, **82**:S1007.
190. Metivier R., Penot G., Flouriot G. & Pakdel F. (2001) Synergism between ERα transactivation function 1 (AF-1) and AF-2 mediated by steroid receptor coactivator protein-1: requirement for the AF-1 α-helical core and for a direct interaction between the N- and C-terminal domain. *Molecular Endocrinology*, **15**(11): 1953-1970.
191. Metivier R., Stark A., Flouriot G., Hubner M.R., Brand H., Penot G., Manu D., Denger S., Reid G., Kos M., Russell R.B., Kah O., Pakdel F. & Gannon F. (2002) A dynamic structural model for estrogen receptor-alpha activation by ligands, emphasizing the role of interactions between distant A and E domains. *Molecular Cell*, **10**:1019-1032.
192. Miao H., Burnett E., Kinch M.S., Simon E. & Wang B. (2000) EphA2 kinase associates with focal adhesion kinase upon activation, inhibits integrin-mediated cell adhesion and migration. *Nature Cell Biology*, **2**:62-69.
193. Michalides R., Griekspoor A., Balkenende A., Verwoerd D., Janssen L., Jalink K., Floore A., Velds A., van't Veer L. & Neefjes J. (2004) Tamoxifen resistance by a conformational arrest of the estrogen receptor α after PKA activation in breast cancer. *Cancer Cell*, **5**:597-605.
194. Migliaccio A., Castoria G., Di Domenico M., de Falco A., Bilancio A., Lombardi M., Barone M.V., Ametrano D., Zannini M.S., Abbondanza C. & Auricchio F. (2000) Steroid-induced androgen receptor-oestradiol receptor beta-Src complex triggers prostate cancer cell proliferation. *EMBO Journal*, **19**:5406-5417.
195. Migliaccio A., Piccolo D., Castoria G., Di Domenico M., Bilancio A., Lombardi M et al. (1998) Activation of the src-p21(Ras)/Erk pathway by progesterone receptor via cross-talk with estrogen receptor. *EMBO Journal*, **17**:2008-2018.
196. Miller W.L. (2004) P450 oxidoreductase deficiency: a new disorder of steroidogenesis with multiple clinical manifestations. *Trends in Endocrinology and Metabolism*, **15**:311-315.
197. Miller W.R. & Dixon J.M. (2000) Antiaromatase agents: preclinical data and neoadjuvant therapy. *Clinical Breast Cancer*, **1**:S9-S14.
198. Miller D.L., El-Ashry D., Cheville A.L., Liu Y., McLeskey S.W. & Kern F.G. (1994) Emergence of MCF-7 cells overexpressing a transfected epidermal growth factor receptor (EGFR) under estrogen-depleted conditions: evidence for a role of EGFR in breast cancer growth and progression. *Cell Growth and Differentiation*, **5**:1263-1274.
199. Moscat J., Sanz L., Sanchez P. & Diaz-Meco M.T. (2001) Regulation and role of the atypical PKC isoforms in cell survival during tumor transformation. *Advances in Enzyme Regulation*, **41**:99-120.
200. Moudgil V.K., Dinda S., Khattree N., Jhanwar S., Alban P. & Hurd C. (2001) Hormonal regulation of tumor suppressor proteins in breast cancer cells. *The Journal of Steroid Biochemistry & Molecular Biology*, **76**: 105-117.
201. Mouridsen H., Gershanovich M., Sun Y., Perez-Carrion R., Boni C., Monnier A., Apffelstaedt J., Smith R., Sleeboom H.P., Jaenicke F., Pluzanska A., Dank M., Becquart D., Bapsy P.P., Salminen E., Snyder R., Chaudri-Ross H., Lang R., Wyld P. & Bhatnagar A. (2003) Phase III study of letrozole versus tamoxifen as first-line therapy of advanced breast cancer in postmenopausal women: analysis of survival and update of efficacy from the International Letrozole Breast Cancer Group. *Journal of Clinical Oncology*, **21**:2101-2109.

202. Murphy L.C., Simon S.L.R., Parkes A., Leygue E., Dotzlaw H., Snell L., Troup S., Adeyinka A. & Watson P.H. (2000) Altered expression of estrogen receptor coregulators during human breast tumorigenesis. *Cancer Research*, **60**:6266-6271.
203. Nabholtz J.M., Budzar A., Pollak M., Harwin W., Burton G., Mangalik A., Steinberg M., Webster A. & von Euler M. (2000) Anastrozole is superior to tamoxifen as first-line therapy for advanced breast cancer in postmenopausal women: Results of the North American multicenter randomized trial. *Journal of Clinical Oncology*, **18**:3758-3767.
204. Nakajima T., Fukamizu A., Takahashi J., Gage F.H., Fisher T., Blenis J. & Montminy M.R. (1996) The signal-dependent coactivator CBP is a nuclear target for $pp90_{RSK}$. *Cell*, **86**:465-474.
205. Nakatani K., Thompson D.A., Barthel A., Sakaue H., Liu W., Weigel R.J. & Roth R.A. (1999) Up-regulation of Akt3 in estrogen-deficient breast cancers and androgen-independent prostate cell lines. *Journal Biol. Chem.*, **274**:21528-21532.
206. Nasi S., Ciarapica R., Jucker R., Rosati J. & Soucek L. (2001) Making decisions through Myc. *FEBS Letters*, **490**:153-162.
207. Nicholson R.I. & Gee J.M. (2000) Estrogen and growth factor cross-talk and endocrine insensitivity and acquired resistance in breast cancer. *British Journal of Cancer*, **82**:501-513.
208. Nicholson R.I., Gee J.M., Manning D.L., Wakeling A.E., Maontano M.M. & Katzenellenbogen B.S. (1995) Responses to pure antiestrogens (ICI 164384, ICI 182780) in estrogen-sensitive and –resistant experimental and clinical breast cancer. *Ann NY Acad Sci*, **761**:148-163.
209. Nicholson R.I., Hutcheson I.R., Harper M.E., Knowlden J.M., Barrow D., McClelland R.A., Jones H.E., Wakeling A.E. & Gee J.M.W. (2001) Modulation of epidermal growth factor receptor in endocrine-resistant, oestrogen receptor-positive breast cancer. *Endocrine-Related Cancer*, **8**: 175-182.
210. Nicholson R.I., Hutcheson I.R., Hiscox S.E., Knowlden J.M., Giles M., Barrow D. & Gee J.M. (2005) Growth factor signalling and resistance to selective oestrogen receptor modulators and pure anti-oestrogens: the use of anti-growth factor therapies to treat or delay endocrine resistance in breast cancer. *Endocrine-Related Cancer*, **12**:S29-36
211. Nicholson R.I., Hutcheson I.R., Knowlden J.M., Jones H.E., Harper M.E., Jordan N., Hiscox S.E., Barrow D. & Gee J.M.W. (2004a) Nonendocrine pathways and endocrine resistance: Observations with antiestrogens and signal transduction inhibitors in combination. *Clinical Cancer Research*, **10**:346s-354s.
212. Nicholson R.I., Staka C., Boyns F., Hutcheson I.R. & Gee J.M.W. (2004b) Growth factor-driven mechanisms associated with resistance to estrogen deprivation in breast cancer: new opportunities for therapy. *Endocrine-Related Cancer*, **11**:623-641.
213. Normanno N., Ciardiello F., Brandt R. & Salomon D.S. (1994) Epidermal growth factor-related peptides in the pathogenesis of human breast cancer. *Breast Cancer Research and Treatment*, **29**:11-27.
214. Nunez N.P., Jelovac D., Macedo L., Berrigan D., Perkins S.N., Hursting S.D., Barrett J.C. & Brodie A. (2004) Effects of the antiestrogen tamoxifen and the aromatase inhibitor letrozole on serum hormones and bone characteristics in a preclinical tumor model for breast cancer. *Clinical Cancer Research*, **10**:5375-5380.
215. Oesterreich S., Zhang P., Guler R.L., Sun X., Curran E.M., Welshons W.V., Osborne C.K. & Lee A.V. (2001) Re-expression of estrogen receptor alpha in estrogen receptor alpha-negative MCF-7 cells restores both estrogen and insulin-

like growth factor-mediated signaling and growth. *Cancer Research*, **61**:5771-5777.

216. Oh A.S., Lorant L.A., Holloway J.N., Miller D.L., Kern F.G. & El-Ashry D. (2001) Hyperactivation of MAPK induces loss of ERalpha expression in breast cancer cells. *Endocrinology*, **15**:1344-1359.
217. Osborne C.K., Bardou V., Hopp T.A., Chamness G.C., Hilsenbeck S.G., Fuqua S.A., Wong J., Allred D.C., Clark G.M. & Schiff R. (2003) Role of the estrogen receptor coactivator AIB1 (SRC-3) and HER-2/neu in tamoxifen resistance in breast cancer. *Journal of the National Cancer Institute*, **95**:353-361.
218. Osborne C.K., Coronado-Heinsohn E.B., Hilsenbeck S.G., McCue B.L., Wakeling A.E., McCelland R.A., Manning D.L. & Nicholson R.I. (1995) Comparison of the effects of a pure steroidal antiestrogen with those of tamoxifen in a model of human breast cancer. *Journal of the National Cancer Institute*, **87**:746-750.
219. Osborne C.K. & Fuqua S.A. (1994) Mechanisms of tamoxifen resistance. *Breast Cancer Research and Treatment*, **32**:49-55.
220. Osborne C.K. & Schiff R. (2003) Growth factor receptor cross-talk with estrogen receptor as a mechanism for tamoxifen resistance in breast cancer. *Breast*, **12**:362-367.
221. Osborne C.K., Schiff R., Arpino G., Lee A.S. & Hisenbeck V.G. (2005) Endocrine responsiveness: understanding how progesterone receptor can be used to select endocrine therapy. *Breast*, **14**:458-465.
222. Osborne C.K., Wakeling A. & Nicholson R.I. (2004) Fulvestrant: an oestrogen receptor antagonist with a novel mechanism of action. *British Journal of Cancer*, **90**:S52-56.
223. Ottman R., King M.C., Pike M.C. & Henderson B.E. (1983) Practical guide for estimating risk for familial breast cancer. *Lancet*, **2**:556-558.
224. Paine T.M., Soule H.D., Pauley R.J. & Dawson P.J. (1992) Characterization of epithelial phenotypes in mortal and immortal human breast cells. *International Journal of Cancer*, **50**:463-473.
225. Pandey A., Lazar D.F., Saltiel A.R. & Dixit V.M. (1994) Activation of the Eck receptor protein tyrosine kinase stimulates phosphatidylinositol 3-kinase activity. *Journal of Biological Chemistry*, **269**:30154-30157.
226. Paridaens R., Dirix L., Beex L., Nooij M., Cufer T., Lohrisch C., Biganzoli L., Van Hoorebeeck I., Duchateau L., Lobelle J.P. & Piccart M. (2000) Promising results with exemestane in the first-line treatment of metastatic breast cancer: a randomized phase II EORTC trial with a tamoxifen control. *Clinical Breast Cancer*, **1**:S19-S21.
227. Paridaens R., Therasse P., Dirix L., Beex L., Piccart M., Cameron D., Cufer T., Roozendeal K., Nooij M. & Mattiacci M.-R. (2004) First line hormonal treatment (HT) for metastatic breast cancer (MBC) with exemestane (E) or tamoxifen (T) in postmenopausal patients- a randomized phase III trial of the EORTC Breast Group. *Proceedings of the American Society of Clinical Oncology*, **23**:6 [Abstract 515].
228. Pasapera Limon A.M., Herrera-Munoz J., Gutierrez-Sagal R. & Ulloa-Aguirre A. (2003) The phosphatidylinositol 3-kinase inhibitor LY294002 binds the estrogen receptor and inhibits 17beta-estradiol-induced transcriptional activity of an estrogen sensitive reporter gene. *Molecular Cellular Endocrinology*, **200**:199-202.
229. Pasqualini J.R., Chetrite G., Blaker C., Feinstein M.C., Delalonde L., Talbi M. & Maloche C. (1996) Concentrations of estrone, estradiol, and estrone sulfate and evaluation of sulfatase and aromatase activities in pre- and postmenopausal breast

cancer patients. *Journal of Clinical Endocrinology and Metabolism*, **81**:1460-1464.

230. Patrick D.R. & Heimbrook D.C. (1996) Protein kinase inhibitors for the treatment of cancer. *Therapeutic Focus Reviews*, **1**:325-330.
231. Pauley R.J., Soule H.D., Tait L., Miller F.R. Wolman S.R., Dawson P.J. & Heppner G.H. (1993) The MCF10 family of spontaneously immortalized human breast epithelial cell lines: models of neoplastic progression. *European Journal of Cancer Prevention*, **2**:S67-76.
232. Pearce S.T., Liu H. & Jordan V.C. (2003) Modulation of estrogen receptor-α function and stability by tamoxifen and a critical amino acid (Asp-538) in helix 12. *The Journal of Biological Chemistry*, **278**:7630-7638.
233. Peekhaus N.T., Chang T., Hayes E.C., Wilkinson H.A., Mitra S.W., Schaeffer J.M. & Rohrer. (2004) Distinct effects of the antiestrogen Faslodex on the stability of estrogen receptors-α and -β in the breast cancer cell line MCF-7. *Journal of Molecular Endocrinology*, **32**:987-995.
234. Penault-Llorca F., Bertucci F., Adelaide J., Parc P., Coulier F., Jacquemier J., Birnbaum D. & de Lapeyriere O. (1995) Expression of FGF and FGF receptor genes in human breast cancer. *International Journal of Cancer*, **61**:170-176.
235. Perez-Tenorio G. & Stal O.; Southwest Sweden Breast Cancer Group. (2002) Activation of AKT/PKB in breast cancer predicts a worse outcome among endocrine treated patients. *British Journal of Cancer*, **86**:540-545.
236. Pierce L.J., Hutchins L.F., Green S.R., Lew D.L., Gralow J.R., Livingston R.B., Osborne C.K. & Albain K.S. (2005) Sequencing of tamoxifen and radiotherapy after breast-conserving surgery in early-stage breast cancer. *Journal of Clinical Oncology*, **23**:24-29.
237. Pietras R. & Szego C.M. (1977) Specific binding sites for oestrogen at the outer surfaces of isolated endometrial cells. *Nature*, **265**:69-72.
238. Pietras R.J., Arboleda J., Reese D.M., Wongvipat N., Pegram M.D., Ramos L., Gorman C.M., Parker M.G., Sliwkowski M.X. & Slamon D.J. (1995) HER-2 tyrosine kinase pathway targets estrogen receptor and promotes hormone-independent growth in human breast cancer cells. *Oncogene*, **10**:2435-2446.
239. Planas-Silva M.D., Shang Y., Donaher J.L., Brown M. & Weinberg R.A. (2001) AIB1 enhances estrogen-dependent induction of cyclin D1 expression. *Cancer Research*, **61**:3858-3862.
240. Prall O.W., Rogan E.M. & Sutherland R.L. (1998) Estrogen regulation of cell cycle progression in breast cancer cells. *The Journal of Steroid Biochemistry and Molecular Biology*, **65**:169-174.
241. Preston-Martin S., Pike M.C., Ross R.K. & Henderson B.E. (1993) Epidemiologic evidence for the increased cell proliferation model of carcinogenesis. *Environmental Health Perspective*, **101**(5):137-138.
242. Price J.E. (1996) Metastasis from human breast cancer cell lines. *Breast Cancer Research and Treatment*, **39**:93-102.
243. Prowell T.M. & Davidson N.E. (2004) What is the role of ovarian ablation in the management of primary and metastatic breast cancer today? *The Oncologist*, **9**:507-517.
244. Rajah T.T., Dunn S.T. & Pento J.T. (1996) The influence of anti-estrogens on pS2 and cathepsin D mRNA induction in MCF-7 breast cancer cells. *Anticancer Research*, **16**:837-842.
245. Ron D., Reich R., Chedid M., Lengel C., Cohen O.E., Chan A.M., Neufeld G., Miki T.& Tronick S.R. (1993) Fibroblast growth factor receptor-4 is a high affinity receptor for both acidic and basic fibroblast growth factor but not for keratinocyte growth factor. *The Journal of Biological Chemistry*, **268**:5388-5394.

246. Rubini M., D'Ambrosio C., Carturan S., Yumet G., Catalano E., Shan S., Huang Z., Criscuolo M., Pifferi M. & Baserga R. (1999) Characterization of an antibody that can select an activated IGF-1 receptor in human cancers. *Experimental Cell Research*, **251**:22-32.
247. Sabnis G.J., Jelovac D., Long B. & Brodie A. (2005) The role of growth factor receptor pathways in human breast cancer cells adapted to long-term estrogen deprivation. *Cancer Research*, **65**:3903-3910.
248. Sachdev D. & Yee D. (2001) The IGF system and breast cancer. *Endocrine-Related Cancer*, **8**:197-209.
249. Sainsbury R. (2004) Aromatase inhibition in the treatment of advanced breast cancer: is there a relationship between potency and clinical efficacy? *British Journal of Cancer*, **90**:1733-1739.
250. Santen R., Jeng M.H., Wang J.P., Song R., Masamura S., McPherson R., Santner S., Yue W. & Shim W.S. (2001) Adaptive hypersensitivity to estradiol: potential mechanism for secondary hormonal responses in breast cancer patients. *Journal of Steroid Biochemistry & Molecular Biology*, **79**:115-125.
251. Santen R.J., Lynch A.R., Neal L.R., McPherson R.A. & Yue W. (2006) Farnesylthiosaliclic acid: inhibition of proliferation and enhancement of apoptosis of hormone-dependent breast cancer cells. *Anti-Cancer Drugs*, **17**:33-40.
252. Santen R.J., Demers L.M., Lynch J., Harvey H., Lipton A., Mulagha M., Hanagan J., Garber J.E., Henderson I.C., Navari R.M. & Miller A.A. (1991) Specificity of low dose fadrozole hydrochloride (CGS 16949A) as an aromatase inhibitor. *Journal of Clinical Endocrinology and Metabolism*, **73**:99-106.
253. Santen R. J., Santner S., Davis B., Veldhuis J., Samojlik E. & Ruby E. (1978) Aminoglutethimide inhibits extraglandular estrogen production in postmenopausal women with breast carcinoma. *Journal of Clinical Endocrinology and Metabolism*, **47**:1257-1265.
254. Santen R.J., Song R.X., Zhang Z., Yue W. & Kumar R. (2004a) Adaptive hypersensitivity to estrogen: Mechanism for sequential responses to hormonal therapy in breast cancer. *Clinical Cancer Research*, **10**: 337s-345s.
255. Santen R.J., Song R.X., Zhang Z., Kumar R., Jeng M-H., Masamura S., Yue W. & Berstein L. (2003) Adaptive hypersensitivity to estrogen: mechanism for superiority of aromatase inhibitors over selective estrogen receptor modulators for breast cancer treatment and prevention. *Endocrine-Related Cancer*, **10**:111-130.
256. Santen R.J., Yue W., Bocchinfuso W., Korach K., Wang J-P., Rogan E.G., Li Y., Cavalieri E., Russo J., Devanesan P. & Verderame M. (2004b) Estradiol-induced carcinogensis via formation of genotoxic metabolites. In: Ingle J.N. & Dowsett M., editors. Advances in endocrine therapy of breast cancer. New York, Summit Communications LLC:163-177.
257. Schiff R., Massarweh S., Shou J. & Osbourne C.K. (2003) Breast cancer endocrine resistance: How growth factor signaling and estrogen receptor coregulators modulate response. *Clinical Cancer Research*, **9**: 447s-454s.
258. Schiff R. & Osborne C.K. (2005) Endocrinology and hormone therapy in breast cancer: new insight into estrogen receptor-alpha function and its implication for endocrine therapy resistance in breast cancer. *Breast Cancer Research*, 7:205-211.
259. Schiff R., Reddy P., Ahotupa M., Coronado-Heinsohn E., Grim M., Hilsenbeck S.G., Lawrence R., Deneke S., Herrera R., Chamness G.C., Fuqua S.A., Brown P.H. & Osborne C.K. (2000) Oxidative stress and AP-1 activity in tamoxifen-

resistant breast tumors in vivo. *Journal of the National Cancer Institute*, **92**:1926-1934.

260. Shaulian E. & Karin M. (2001) AP-1 in cell proliferation and survival. *Oncogene*, **20**:2390-2400.
261. Shiau A.K., Barstad D., Loria P.M., Cheng L., Kushner P.J., Agard D.A. & Greene G.L. (1998) The structural basis of estrogen receptor/ coactivator recognition and the antagonism of this interaction by tamoxifen. *Cell*, **95**(7):927-937.
262. Shim W.S., Conaway M., Masamura S., Yue W., Wang J.P., Kumar R. & Santen R.J. (2000) Estradiol hypersensitivity and mitogen-activated protein kinase expression in long-term estrogen deprived human breast cancer cells *in vivo*. *Endocrinology*, **141**:396-405.
263. Shou J., Massarweh S., Osborne C.K., Wakeling A.E., Ali S., Weiss H & Schiff R. (2004) Mechanisms of tamoxifen resistance: Increased estrogen receptor-HER2/neu cross-talk in ER/HER2-positive breast cancer. *Journal of the National Institute*, **96**:926-935.
264. Shupnik M.A. (2004) Crosstalk between steroid receptors and the c-Src-receptor tyrosine kinase pathways: implications for cell proliferation. *Oncogene*, **23**:7979-7989.
265. Simoncini T. & Genazzani A.R. (2003) Non-genomic actions of sex steroid hormones. *European Journal of Endocrinology*, **148**: 281-292.
266. Simoncini T., Fornari L., Mannella P., Varone G., Caruso A., Liao J.K. & Genazzani A.R. (2002) Novel non-transcriptional mechanisms for estrogen receptor signaling in the cardiovascular system: Interaction of estrogen receptor-α with phosphatidylinositol 3-OH kinase. *Steroids*, **67**:935-939.
267. Simpson E.R. (2003) Sources of estrogen and their importance. *The Journal of Steroid Biochemistry and Molecular Biology*, **86**:225-230.
268. Simpson E.R. & Davis S.R. (2001) Minireview: Aromatase and the regulation of estrogen biosynthesis - some new perspectives. *Endocrinology*, **142**(11): 4589-4594.
269. Simpson E., Rubin G., Clyne C., Robertson K., O'Donnell L., Jones M. & Davis S. (2000) The role of local estrogen biosynthesis in males and females. *Trends in Endocrinology and Metabolism*, **11**(5):184-188.
270. Smith C.L., Nawaz Z. & O'Malley B.W. (1997) Coactivator and corepressor regulation of the agonist/antagonist activity of the mixed antiestrogen, 4-hydroxytamoxifen. *Molecular Endocrinology*, **11**:657-666.
271. Smith I.E. & Dowsett M. (2003) Aromatase inhibitors in breast cancer. *New England Journal of Medicine*, **348**:2431-2442.
272. Song R.X., Barnes C.J., Zhang Z., Bao Y., Kumar R. & Santen R.J. (2004) The role of Shc and insulin-like growth factor 1 receptor in mediating the translocation of estrogen receptor α to the plasma membrane. *PNAS*, **101**:2076-2081.
273. Song R.X., McPherson R.A., Adam L., Bao Y., Shupnik M., Kumar R. & Santen R.J. (2002) Linkage of rapid estrogen action to MAPK activation by ERalpha-Shc association and Shc pathway activation. *Molecular Endocrinology*, **16**:116-127.
274. Stephen R.L., Shaw L.E., Larsen C., Corcoran D. & Darbre P.D. (2001) Insulin-like growth factor receptor levels are regulated by cell density and by long term estrogen deprivation in MCF-7 human breast cancer cells. *The Journal of Biological Chemistry*, **276**:40080-40086.
275. Stimpfl M., Tong D., Fasching B., Schuster E., Obermair A., Leodolter S. & Zeillinger R. (2002) Vascular endothelial growth factor splice variants and their

prognostic value in breast cancer and ovarian cancer. *Clinical Cancer Research*, **8**: 2253-2259.

276. Sun M., Paciga J.E., Feldman R.I., Yuan Z-Q., Coppola D., Lu Y-Y., Shelley S.A., Nicosia S.V. & Cheng J.Q. (2001) Phosphatidylinositol-3-OH kinase (PI3K)/AKT2, activated in breast cancer, regulates and is induced by estrogen receptor-α (ERα) via interaction between ERα and PI3K. *Cancer Research*, **61**: 5985-5991.
277. Taetle R., Castagnola J. & Mendelsohn J. (1986) Mechanisms of growth inhibition by anti-transferrin receptor monoclonal antibodies. *Cancer Research*, **46**: 1759-1763.
278. Tang C.K., Perez C., Grunt T., Waibel C., Cho C. & Lupu R. (1996) Involvement of heregulin-beta2 in the acquisition of the hormone-independent phenotype of breast cancer cells. *Cancer Research*, **56**:3350-3358.
279. Thomas D.B. & Karagas M.R. (1987) Cancer in first and second generation Americans. *Cancer Research*, **47**:5771-5776.
280. Thompson E.A. Jr. & Siiteri P.K. (1974) The involvement of human placental microsomal cytochrome P-450 in aromatization. *The Journal of Biological Chemistry*, **249**(17):5373-5378.
281. Tidow N., Boecker A., Schmidt H., Agelopoulos K., Boecker W., Buerger H. & Brandt B. (2003) Distinct amplification of an untranslated regulatory sequence in the egfr gene contributes to early steps in breast cancer development. *Cancer Research*, **63**:1172-1178.
282. Toft D. & Gorski J. (1966) A receptor molecule for estrogens: isolation from the rat uterus and preliminary characterization. *Proceedings of the National Academy of Science*, **55**:1574-1581.
283. Tsuda H. (2001) Prognostic and predictive value of c-erbB-2 (HER-2/neu) gene amplification in human breast cancer. *Breast Cancer*, **8**:34-44.
284. Valentinis B. & Baserga R. (2001) IGF-1 receptor signalling in transformation and differentiation. *Molecular Pathology*, **54**:133-137.
285. Vandewalle B., Hornez L., Revillion F. & Lefebvre J. (1989) Secretion of transferring by human breast cancer cells. *Biochemical and Biophysocal Research Communications*, **163**:149-154.
286. Vandewalle B. & Lefebvre J. (1989) Opposite effects of estrogen and catecholestrogen on hormone-sensitive breast cancer cell growth and differentiation. *Molecular Cell Endocrinology*, **61**:239-246.
287. Vivanco I & Sawyers C.L. (2002) The phosphatidylinositol 3-Kinase-AKT pathway in human cancer. *Nature Reviews Cancer*, **2**:489-501.
288. Vyhlidal C., Li X. & Safe S. (2002) Estrogen regulation of transferrin gene expression in MCF-7 human breast cancer cells. *Journal of Molecular Endocrinology*, **29**: 305-317.
289. Wakeling A.E. (1991) A potent specific pure antiestrogen with clinical potential. *Cancer Research*, **51**:3867-3873.
290. Wang R., Mazumdar A., Vadlamudi R.K. & Kumar R. (2002) P21-activated kinase-1 phosphorylates and transactivates estrogen receptor-α and promotes hyperplasia in mammary epithelium. *EMBO Journal*, **20**:5437-5447.
291. Watanabe M., Yanagisawa J., Kitagawa H., Takeyama K-I., Ogawa S., Arao Y., Suzawa M., Kobayashi Y., Yano T., Yoshikawa H., Mashuhiro Y. & Kato S. (2001) A subfamily of RNA-binding DEAD-box proteins acts as an estrogen receptor-α coactivator through the N-terminal activation domain (AF-1) with an RNA coactivator, SRA. *EMBO Journal*, **20**:1341-1352.
292. Webb P., Nguyen P., Shinsako J., Anderson C.M., Nguyen M.P., Feng W-J., Chen D., Huang S-M., Subramanian S., McKinerney E., Katzenellenbogen B.S.,

Stallcup M. & Kushner P.J. (1998) Estrogen receptor activation function 1 works by binding to p160 coactivator proteins. *Molecular Endocrinology*, **14**:3741-3751.

293. Webb P., Nguyen P., Valentine C., Lopez G., Kwok G.R., McInerney E., Katzenellenbogen B.S., Enmark E., Gustafsson J.A., Nilsson S. & Kushner P.J. (1999) The estrogen receptor enhances AP-1 activity by two distinct mechanisms with different requirements for receptor transactivation functions. *Molecular Endocrinology*, **13**:1672-1685.
294. Wells S.A. Jr., Santen R.J., Lipton A., Haagensen D.E. Jr., Ruby E.J., Harvey H. & Dilley W.G. (1978) Medical adrenalectomy with aminoglutethimide: studies in postmenopausal patients with metastatic breast carcinoma. *Annals of Surgery*, **187**:475-484.
295. Wessler S., Otto C., Wilck N., Stangl V. & Fritzemeier K.H. (2006) Identification of estrogen receptor ligands leading to activation of non-genomic signaling pathways while exhibiting only weak transcriptional activity. *The Journal of Steroid Biochemistry & Molecular Biology*, **98**:25-35.
296. White E. (1987) Projected changes in breast cancer incidence due to the trend toward delayed childbearing. *American Journal of Public Health*, **77**:495-497.
297. Williams M.R., Arthur S.C., Balendran A., van der Kaay J., Poli V., Cohen P. & Alessi D.R. (2000) The role of 3-phosphonositide-dependent protein kinase 1 in activation AGC kinases defined in embryonic stem cells. *Current Biology*, **10**:439-448.
298. Witters L.M., Kumar R., Chinchilli V.M. & Lipton A. (1997) Enhanced anti-proliferative activity of the combination of tamoxifen plus HER-2-neu antibody. *Breast Cancer Research and Treatment*, **42**:1-5.
299. Wong Z-W & Ellis M.J. (2004) First-line endocrine treatment of breast cancer: aromatase inhibitor or antioestrogen? *British Journal of Cancer*, **90**:20-25.
300. Wooster R., Bignell G., Lancaster J., Swift S., Seal S., Mangion J., Collins N., Gregory S., Gumbs C., Micklem G., Barfoot R., Hamoudi R., Patel S., Rice C., Biggs P., Hashim Y., Smith A., Connor F., Arason A., Gudmundsson J., Ficenec D., Kelsell D., Ford D., Tonin P., Bishop D.T., Spurr N.K., Ponder B.A.J., Eeles R., Peto J., Devilee P., Cornelisse C., Lynch H., Narod S., Lenoir G., Egilsson V., Barkadottir R.B., Easton D.F., Bentley D.R., Futreal P.A., Ashworth A. & Stratton M.R. (1995) Identification of the breast cancer susceptibility gene BRCA2. *Nature*, **378**:789-792.
301. Wooster R., Neuhausen S.L., Mangion J., Quirk Y., Ford D., Collins N., Nguyen K., Seal S., Tran T., Averill D., Fields P., Marshall G., Narod S., Lenoir G.M., Lynch H., Feunteum J., Deville P., Cornelisse C.J., Menko F.H., Daly P.A., Ormiston W., McManus R., Pye C., Lewis C.M., Cannon-Albright L.A., Peto J., Ponder B.A.J., Skolnick M.H., Easton D.F., Goldgar D.E. & Stratton M.R. (1994) Localization of a breast cancer susceptibility gene, BRCA2, to chromosome 13q12-13. *Science*, **265**:2088-2090.
302. Wrba F., Chott A., Reiner A., Reiner G., Markis-Ritzinger E. & Holzner J.H. (1989) Ki-67 immunoreactivity in breast carcinomas in relation to transferring receptor expression, estrogen receptor status and morphological criteria. An immunohistochemical study. *Oncology*, **46**:255-259.
303. Yager J.D. (2000) Chapter 3: Endogenous estrogens as carcinogens through metabolic activation. *JNCI Monographs*, **27**:67-73.
304. Yang D.C., Jiang X.P., Elliott R.L. & Head J.F. (2001) Inhibition of growth of human breast carcinoma cells by an antisense oligonucleotide targeted to the transferrin receptor gene. *Anticancer Research*, **21**:1777-1787.

305. Yang S-P., Song S-T. & Song H-F. (2003) Advancement of antisense oligonucleotides in treatment of breast cancer. *Acta Pharmacologica Sinica*, 24, **4**: 289-295.
306. Yarden R.I., Wilson M.A. & Chrysogelos S.A. (2001) Estrogen suppression of EGFR expression in breast cancer cells: A possible mechanism to modulate growth. *Journal of Cellular Biochemistry*, **81**:232-246.
307. Yee D. & Lee A.V. (2000) Crosstalk between the insulin-like growth factors and estrogens in breast cancer. *Journal of Mammary Gland Biol Neoplasia*, **5**:107-115.
308. Yu Y. & Feig L.A. (2002) Involvement of R-Ras and Ral GTPases in estrogen-independent proliferation of breast cancer cells. *Oncogene*, **21**:7557-7568.
309. Yue W., Berstein L.M., Wang J.P. Clark G.M., Hamilton C.J., Demers L.M. & Santen R.J. (2001) The potential role of estrogen in aromatase regulation in the breast. *The Journal of Steroid Biochemistry & Molecular Biology*, **79**:157-164.
310. Yue W., Wang J-P., Conaway M., Masamura S., Li Y. & Santen R.J. (2002) Activation of the MAPK pathway enhances sensitivity of MCF-7 breast cancer cells to the mitogenic effect of estradiol. *Endocrinology*, **143**: 3221-3229.
311. Yue W., Wang J-P., Conaway M. R., Li Y. & Santen R.J. (2003) Adaptive hypersensitivity following long-term estrogen deprivation: involvement of multiple signal pathways. *Journal of Steroid Biochemistry & Molecular Biology*, **86**:265-274.
312. Yue W., Wang J-P., Li Y., Fan P. & Santen R.J. (2005) Farnesylthiosalicylic acid blocks mammalian target of rapamycin signaling in breast cancer cells. *International Journal of Cancer*, **117**:746-754.
313. Yue W., Zhou D., Chen S. & Brodie A. (1994) A new nude mouse model for postmenopausal breast cancer using MCF-7 cells transfected with the human aromatase gene. *Cancer Research*, **54**:5092-5095.
314. Zantek N.D., Azimi M., Fedor-Chaiken M., Wang B., Brackenbury R. & Kinch M.S. (1999) E-Cadherin regulates the function of the EphA2 receptor tyrosine kinase. *Cell Growth & Differentiation*, **10**:629-638.
315. Zelanski D.P., Zantek N.D., Stewart J.C., Irizarry A.R. & Kinch M.S. (2001) EphA2 overexpression causes tumorigenesis of mammary epithelial cells. *Cancer Research*, **61**:2301-2306.
316. Zelanski D.P., Zantek N.D., Walker-Daniels J., Peters M.A., Taparowsky E.J. & Kinch M.S. (2002) Estrogen and Myc negatively regulate expression of the EphA2 tyrosine kinase. *Journal of Cell Biochemistry*, **85**:714-720.
317. Zhao Y., Agarwal V.R., Mendelson C.R. & Simpson E.R. (1996) Estrogen biosynthesis proximal to a breast tumor is stimulated by PGE_2 via cyclic AMP, leading to activation of promoter II of the *CYP19* (aromatase gene). *Endocrinology*, **137**:5739-5742.
318. Zhou Y., Eppenberger-Castori S., Eppenberger U. & Benz C.C. (2005) The NFkappaB pathway and endocrine-resistant breast cancer. *Endocrine-Related Cancer*, **12**:S37-46.
319. Zinda M.J., Johnson M.A., Paul J.D., Horn C., Konicek B.W., Lu Z.H., Sandusky G., Thomas J.E., Neubauer B.L., Lai M. T. & Graff J.R. (2001) AKT-1, -2, and –3 are expressed in both normal and tumor tissues of the lung, breast, prostate, and colon. *Clinical Cancer Research*, 7:2475-2479.

CHAPTER 6

∞ *APPENDIX* ∞

2.2.3 (pg. 45) MCF-7 Resistant Sub-lines Culture Conditions and Maintenance: TAM-R, FAS-R and TAM/TKI-R

The TAM-R (tamoxifen resistant), FAS-R (faslodex resistant), and TAM/TKI-R (tamoxifen and gefitinib resistant) cell lines are all derivatives of the MCF-7 hormone sensitive breast cancer cell line and have been established within the Tenovus Centre for Cancer Research. The TAM-R is an acquired resistant stable cell line that evolved from the MCF-7 cells following a long-term exposure to tamoxifen (10^{-7} M). These cells were continually cultured in the presence of tamoxifen (10^{-7} M). After an initial inhibition of 50-60% the cells developed a resistant phenotype and log phase growth began after 4 months.

The FAS-R cell line was acquired in a similar fashion to the TAM-R cell line. MCF-7 cells were routinely cultured in the presence of the pure anti-oestrogen faslodex (10^{-7} M) with 60-70% initial inhibition for 5 months, before log phase growth resumed.

The TAM/TKI-R cells were TAM-R (6 months) cells exposed to subsequent treatment with the tyrosine kinase inhibitor, gefitinib (TKI, 1 μM) followed by an initial sensitivity to the compound of about 60%. Approximately 3 months later the cells, in the continued presence of both tamoxifen (10^{-7} M) and gefitinib (1 μM) began log phase growth as a 'double' resistant cell line.

2.2.4 (pg. 46) Experimental MCF-7 Culture Medium

For experimental purposes MCF-7 cells were seeded into phenol-red-free RPMI (wRPMI) + 5% charcoal stripped fetal calf serum (SFCS). In order to charcoal strip serum a charcoal solution was first made containing: 18 ml distilled H_2O, 2 g Norit A, 0.01 g Dextran T-70. This solution was set to stir for at least 1 hour. The FCS (100 ml) was pH adjusted to 4.2 with 5 M HCl and allowed to equilibrate for 30 minutes at 4°C. The charcoal solution (5 ml) was added to the FCS and incubated for approximately 16 hours at 4°C with gentle agitation. The charcoal was removed by centrifugation at 12,000 x g for 40 minutes, followed by coarse filtration (Whatman filter paper grade, 4). The pH was readjusted to 7.2 followed by sterile filtration (0.2 μm sterile vacuum cap filter), and stored at –20°C until utilised.

2.3.2 (pg. 49) RNA and PCR Product Loading Buffer and TAE Running Buffer

Loading buffer was stored at 4°C until use and contained: 6 g sucrose in 10 ml of sterile H_2O. A very small amount of bromophenol blue was added prior to filtration (0.2 μm filter paper) of the buffer followed by storage.

A stock 50X TAE running buffer contains:

242 g Tris base

57.1 ml glacial acetic acid

18.6 g EDTA

1 L distilled H_2O

When making a 2% agarose gel or running a gel the stock 50X TAE was diluted to 1X.

2.3.3 (pg. 50) RT Master Mix

The RT master mix was made up immediately before reverse transcription on ice (wet). For each sample subject to reverse transcription, an 11 μl aliquot of RT master mix was placed in a thin wall PCR tube.

5 μl dNTP's (2.5 mM)

2 μl PCR Buffer (10X)*

2 μl DTT (0.1M)

2 μl Random Hexamers (100 μM)

* PCR Buffer (10X): 100 mM Tris-HCl pH 8.3, 500 mM KCl, 15 mM $MgCl_2$, 0.01% w/v gelatin.

2.3.4 (pg. 51) PCR master mix

The PCR master mix was made up immediately before PCR reaction on ice (wet). The master mix was made according to the number of samples being run. For each sample subject to PCR, a 24.5 µl aliquot of the PCR master mix was placed in a thin wall PCR tube:

18.625 µl Sterile H_2O

2.5 µl PCR Buffer (10X)

2.0 µl dNTP's (2.5 mM)

0.2 µl BIOTAQ DNA Polymerase

0.625 µl Primer set of target sequence (20 µM)

0.156 µl β-Actin primer set (20 µM) NB: only if PCR is being run as a co-amp.

0.5 µl cDNA equivalent to 0.025 µg starting material

2.4.4 (pg. 55) X-gal Staining Solution

The staining solution was made prior to 0.5% glutaraldehyde fixation of the β-Galactosidase transfected cells.

Solution A contained:

1.0% potassium ferricyanide (300 mM/ 130 mM $MgCl_2$ in PBS) and

1.0% potassium ferrocyanide (300 mM/ 130 mM $MgCl_2$ in PBS) in PBS.

Solution B (X-gal solution) contained:

3.125 µl of X-gal (40 mg/ml) /ml of solution A

These solutions were made and kept in the dark to avoid degradation.

2.5.2 (pg. 56) Protein Lysis Buffer (pH 7.5)

A stock solution containing the following was stored at 4°C until protein lysis buffer was needed: 50 mM Trizma HCl, 5 mM EGTA, 150 mM Sodium Chloride, 1% Triton X-100. Prior to lysis the following reagents were added to the stock protein lysis buffer solution: 2 mM Sodium Vanadate, 50mM Sodium Fluoride, 1 mM Phenylmethylsulphonyl Fluoride, 20 µM Phenylarsine Oxide, 10 mM Sodium Molybdate, 10 µg/ml Leupeptin, 2 mg/ml Aprotinin.

2.5.3 (pg. 56) Protein Concentration Assay Reagents

DC BioRad protein assay reagents contain:

Reagent A- 1-5% Sodium Hydroxide, 1% sodium tartrate and less than 0.1% copper sulfate.

Reagent S- 5-10% Sodium dodecyl sulfate (SDS)

Reagent B- a diluted FOLIN reagent containing less than 1% of each the following, lithium sulfate, tungstic acid sodium salt, molybolic acid sodium salt, hydrochloric acid and phosphoric acid.

2.5.4 (pg. 56) Separating Gel, Stacking Gel, Running Buffer 1X

The separating gel was made according to the molecular size of the target protein:

7.5% gel for protein range 70-200 (kDa)- 30% Acrylamide (2.5 ml), distilled H_2O (4.8 ml), 1.5 M Tris-HCl (pH 8.8, 2.5 ml), 10% SDS (0.1 ml), 10% APS (0.1 ml), Temed (10 µl).

10% gel for protein range 20-100 (kDa)- 30% Acrylamide (3.3 ml), distilled H_2O (4.0 ml), 1.5 M Tris-HCl (pH 8.8, 2.5 ml), 10% SDS (0.1 ml), 10% APS (0.1 ml), Temed (10 µl).

The 5% stacking gel contained: 30% Acrylamide (1.7 ml), distilled H_2O (5.8 ml), 1.5 M Tris-HCl (pH 6.8, 2.5 ml), 10% SDS (0.1 ml), 10% APS (0.1 ml), Temed (10 µl).

A stock solution of 10X running buffer (pH 8.3) was stored at room temperature until SDS-PAGE was performed: 0.23 M Trizma Base, 1.92 M Glycine, 0.1% SDS. A 1X dilution of this solution was utilised for SDS-PAGE.

Protein sample loading buffer contains: 10% SDS (4 ml), Glycerol (2 ml), 0.5 M Tris (2.4 ml, pH 6.8 upper buffer), H_2O (1.6 ml) and Bromophenol Blue (~1 mg). Prior to use DTT (15.5 mg/ml) was added.

2.5.5 (pg. 57) Transfer Buffer and TBS-T Solution

Transfer buffer was made up fresh just before the transferring procedure and contained: 0.25 M Trizma Base, 1.92 M Glycine, 20% Methanol

A stock solution of 10X TBS-T contains: 12.1 g Trizma base, 58 g NaCl, 5 ml Tween 20, and 15 ml 5M HCl.

A 1X dilution of this solution is utilized as the antibody diluent and washing buffer.

2.6.2.1 (pg. 60) Sucrose Storage Medium

Sucrose storage medium (SSM) was made and stored at –20°C until utilized. SSM contained: 42.8 g sucrose, 0.33 g $MgCl_2$ dissolved in 250 ml PBS, followed by the addition of 250 ml glycerol.

2.6.2.2 (pg. 60) Formal Saline (FS) Solution

Formal saline solution was stored at room temperature contained the following: 4.5 g NaCl, 450 ml H_2O, 50 ml Formaldehyde.

2.6.2.3 (pg. 60) 2.5% Phenol Formal Saline (pFS) Solution

Phenol formal saline was made on the day of fixation and contained: 0.5 g phenol in 20 ml formal saline.

2.6.2.4 (pg. 61) 2% Paraformaldehyde Vanadate (PFV) Solution

The 2% paraformaldehyde vanadate (vanadate maintains integrity of phosphorylation site) solution was made fresh on the day of cell fixation. Paraformaldehyde (0.25 g) was weighed out into a glass beaker and a small volume of PBS (3 ml) was added. With gentle agitation the mixture was heated to 60°C, until the solid paraformaldehyde had dissolved. In order to clear the solution, 1M NaOH (10 µl) was added, followed by the remaining volume of PBS (9.5 ml). After adding 1 M HCl (10 µl), the pH was checked to verify the solution was approximately 7.4. Just before fixation 2% sodium orthovanadate ($NaVO_4$, 100 mM) was added.

2.6.2.5 (pg. 61) Methanol Vanadate Solution

The methanol vanadate solution was made fresh on the day of cell fixation. 2% sodium orthovanadate ($NaVO_4$, 100 mM) was added to cooled methanol (–10 to –30°C, on dry ice).